

UNCLASSIFIED

AD NUMBER

AD847706

LIMITATION CHANGES

TO:

Approved for public release; distribution is unlimited.

FROM:

Distribution authorized to U.S. Gov't. agencies and their contractors; Critical Technology; JUN 1968. Other requests shall be referred to Air Force Flight Dynamics Laboratory, Attn: FDD, Wright-Patterson AFB, OH 45433. This document contains export-controlled technical data.

AUTHORITY

AFFDL ltr, 10 May 1976

THIS PAGE IS UNCLASSIFIED

THIS REPORT HAS BEEN DELIMITED
AND CLEARED FOR PUBLIC RELEASE
UNDER DOD DIRECTIVE 5200.20 AND
NO RESTRICTIONS ARE IMPOSED UPON
ITS USE AND DISCLOSURE.

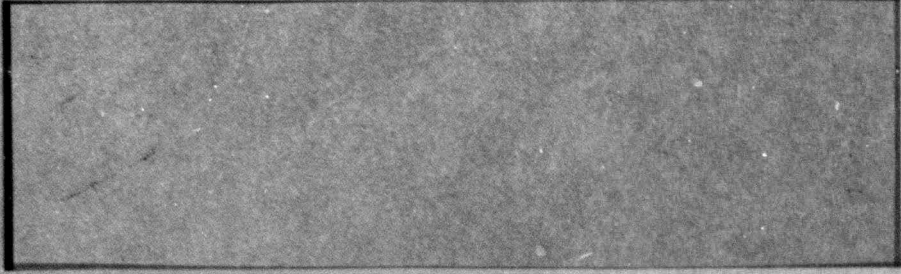
DISTRIBUTION STATEMENT A

APPROVED FOR PUBLIC RELEASE;
DISTRIBUTION UNLIMITED.

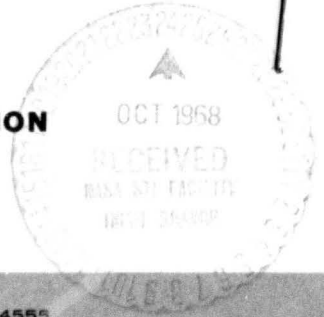
AD847706



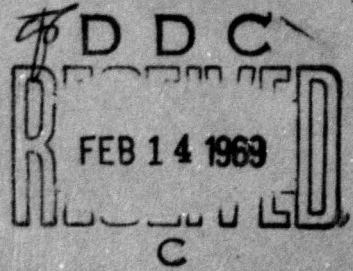
cb



MEASUREMENT ANALYSIS CORPORATION



10960 SANTA MONICA BLVD • LOS ANGELES, CALIFORNIA 90025 • TELEPHONE 477-4555



AFFDL-TR-68-92

AD847706

STATISTICAL ANALYSIS OF
FLIGHT VIBRATION AND ACOUSTIC DATA

ALLAN G. PIERSOL
W. F. van der LAAN

TECHNICAL REPORT AFFDL-TR-68-92

JUNE 1968

This document is subject to special export controls and each transmittal to foreign governments or foreign nationals may be made only with prior approval of AFFDL (FDD).

↓
AIR FORCE FLIGHT DYNAMICS LABORATORY
AIR FORCE SYSTEMS COMMAND
WRIGHT-PATTERSON AIR FORCE BASE, OHIO 45433

NOTICE

When Government drawings, specifications, or other data are used for any purpose other than in connection with a definitely related Government procurement operation, the United States Government thereby incurs no responsibility nor any obligation whatsoever; and the fact that the Government may have formulated, furnished, or in any way supplied the said drawings, specifications, or other data, is not to be regarded by implication or otherwise as in any manner licensing the holder or any other person or corporation, or conveying any rights or permission to manufacture, use, or sell any patented invention that may in any way be related thereto.

This document is subject to special export controls and each transmittal to foreign governments or foreign nationals may be made only with prior approval of AFFDL (FDD).

The distribution of this report is limited because it contains data related to current operational weapon systems.

Copies of this report should not be returned unless return is required by security considerations, contractual obligations, or notice on a specific document.

**STATISTICAL ANALYSIS OF
FLIGHT VIBRATION AND ACOUSTIC DATA**

**ALLAN G. PIERSOL
W. F. van der LAAN**



This document is subject to special export controls and each transmittal to foreign governments or foreign nationals may be made only with prior approval of AFFDL (FDD).

FOREWORD

This report and its Appendices were prepared by the Measurement Analysis Corporation (MAC), Los Angeles, California, for the Air Force Flight Dynamics Laboratory (AFFDL), Wright-Patterson Air Force Base, Ohio, under Contract No. F33615-67-C-1118. The performance period for the reported work was from 1 November 1966 to 1 May 1968. The work was conducted under Project 1472, "Dynamic Measurement and Analysis Technology," Task 147204, "Optimization of Dynamics Data Analysis." Technical administration by AFFDL was provided by Mr. Charles E. Thomas and Mrs. Phyllis Bolds (FDDS).

The work was performed by MAC personnel under the direction of Mr. Allan G. Piersol with the assistance of Mr. W. Frank van der Laan. Principal contributors included Dr. Richard L. Barnoski (structural dynamics), Dr. Sung C. Choi (statistics), Mr. Loren D. Enochson (digital computing), Mr. Ronald D. Kelly (analog data analysis), and Dr. Prichard H. White (vibroacoustics). The contractor's report number is MAC Report No. 616-05.

Manuscript released by the authors, Mr. Allan G. Piersol and Mr. W. Frank van der Laan, for publication as an AFFDL Technical Report.

This report has been reviewed and approved.

WALTER J. MYKYTOW
Asst. for Research and Technology
Vehicle Dynamics Division
AF Flight Dynamics Laboratory

ABSTRACT

Techniques for predicting the vibration environments of future aircraft based upon statistical extrapolations from data measured on past aircraft are investigated. As a first step, principal sources of aircraft vibration are identified, and analytical relationships for the resulting vibration environment are approximated. Available AFFDL data are then summarized and evaluated. Extensive statistical studies are performed on the available data to investigate the average properties of aircraft vibration among the three orthogonal directions, various structural zones, various aircraft models, and various aircraft groups. The available data are also used to study the spatial distribution of vibration levels within a given structural zone. Specific prediction models are then suggested and regression analysis procedures to arrive at conservative prediction levels are detailed. The suggested techniques are illustrated using available AFFDL data. Procedures for deriving vibration test specifications based upon environmental vibration predictions are suggested. Finally, possible extension of the techniques to the prediction of internal acoustic noise are discussed.

This abstract is subject to special export controls and each transmittal to foreign governments or foreign nationals may be made only with prior approval of the Air Force Flight Dynamics Laboratory, Wright-Patterson AFB, Ohio.

CONTENTS

1.	Introduction	1
2.	Problem Formulation and Approach	7
2.1	Selection of Variables	8
2.2	Determination of Weights	9
2.3	Statistical Considerations	12
2.4	Outline of Suggested Approach	15
3.	Development of Vibration Relationships	19
3.1	Identification of Vibration Sources	19
3.2	Analytical Description of Structural Vibration	31
3.3	Analytical Description of Primary Sources	39
3.3.1	Jet Acoustic Noise	40
3.3.2	Aerodynamic Boundary Layer Noise	43
3.3.3	Wake Turbulence	44
3.3.4	Propeller (or Rotor) Blade Passage	45
3.3.5	Helicopter Rotor Rotation	47
3.3.6	Jet Engine Turbine Shaft Rotation	47
3.3.7	Reciprocating Engine Exhaust	48
3.3.8	Engine Accessory Equipment	48
3.3.9	Helicopter Gear Box Noise	49
3.3.10	Gunfire	49
4.	Review of Available Data	51
4.1	Summary of Aircraft	51
4.2	Data Acquisition Equipment and Procedures	57
4.2.1	Velocity Transducer System	57
4.2.2	Acceleration Transducer System	59
4.2.3	Microphone Transducer System	61

CONTENTS (Continued)

4.3	Data Processing Procedures	62
4.3.1	Analysis Procedures for Velocity Data	62
4.3.2	Analysis Procedures for Acceleration Data	63
4.3.3	Analysis Procedures for Microphone Data	64
5.	Preliminary Data Evaluation	65
5.1	Summary of Data Limitations	66
5.1.1	Use of Velocity Transducers	66
5.1.2	Frequency Response for Velocity Transducers	68
5.1.3	Use of Fixed Sensitivity into All Channels of the Recorder	69
5.1.4	Data Analysis and Presentation Procedures	69
5.2	Limitations Imposed on Data Evaluation	70
6.	Homogeneity Studies	73
6.1	Development of Testing Procedures	74
6.1.1	Chi-Square Test	74
6.1.2	Multiple Rank Test	79
6.2	Application to AFFDL Vibration Data	85
6.2.1	Comparisons of the Three Orthogonal Directions	85
6.2.2	Comparisons of the Various Structural Zones	101
6.2.3	Comparisons of the Various Aircraft Models and Groups	119
7.	Spatial Distribution Studies	135
7.1	Construction of a Distribution Function Model	135
7.1.1	Definition of the Lognormal Distribution	136
7.1.2	Applications to Aircraft Vibration Environments	139

CONTENTS (Continued)

7.2	Development of Testing Procedures	143
7.3	Application to AFFDL Vibration Data	146
8.	Prediction Model Studies	157
8.1	Model Formulation for Jet Bombers and Fighters . . .	160
8.1.1	Jet Noise Contribution	162
8.1.2	Aerodynamic Noise Contribution	165
8.1.3	Wake Turbulence Contribution	166
8.1.4	Jet Engine Shaft Rotation Contribution	168
8.1.5	Gunfire Contribution	171
8.1.6	Suggested Data Reduction Procedures	172
8.2	Model Formulation for Helicopters	175
8.3	Regression Analysis Procedures	180
8.3.1	Evaluation of Model Linearity	182
8.3.2	Evaluation of Model Efficiency	183
8.3.3	Selection of Prediction Limits	183
8.4	Illustration of Regression Analysis Procedures	184
8.5	Statistical Considerations in the Selection of Prediction Limits	189
9.	Selection of Vibration Test Levels and Durations	193
9.1	Failure Criteria	194
9.1.1	Fatigue Damage Criterion	195
9.1.2	Peak Value Criterion	198
9.2	Application to Component Model	199
9.2.1	Application of Fatigue Damage Criterion	201
9.2.2	Application of Peak Value Criterion	203

CONTENTS (Continued)

9.3	Relationships Between Vibration Level and Exposure Time	203
9.3.1	Fatigue Damage Criterion	203
9.3.2	Peak Value Criterion	205
9.3.3	Comparison of Fatigue Damage and Peak Value Criteria	208
9.4	Application to Nonstationary Environments	208
9.5	Development of Vibration Profile Data	212
9.6	Selection of Test Level Percentage Points	219
9.7	Concluding Comments on Vibration Test Specifications	222
9.7.1	Endurance Limit Problem	223
9.7.2	Structural Nonlinearity Problem	223
9.7.3	Equipment Loading Problem	224
9.7.4	Environmental Simulation Problem	225
10.	Extensions to Acoustic Environments	227
11.	Conclusions	229
	References	231
	Appendix A - Tabulated Computer Results (under separate cover)	
	Appendix B - Documentation Report for Computer Program to Compute Power Spectral Density Functions (MAC-PSD) (under separate cover)	

LIST OF FIGURES

Figure 1.	Illustration of Scatter About Prediction Model	14
Figure 2.	Relative Contribution of Off-Diagonal Terms to Vibration Response Power Spectrum	37
Figure 3.	Spectrum for Jet Acoustic Noise	41
Figure 4.	Spectrum for Aerodynamic Boundary Layer Noise . . .	43
Figure 5.	Frequency Response of MB Type 124 Velocity Pickup	59
Figure 6.	Frequency Response of Piezoelectric Crystal Accelerometers	60
Figure 7.	Velocity and Acceleration Spectra of Vibration Data for Zone 2 of Aircraft Group 5	67
Figure 8.	Illustration of Spectrum for Sine Wave and Random Signals in Noise	71
Figure 9a.	Mean Values and Standard Deviations for the Vibration in the Three Orthogonal Directions for Aircraft Group 1	89
Figure 9b.	Mean Values and Standard Deviations for the Vibration in the Three Orthogonal Directions for Aircraft Group 2	90
Figure 9c.	Mean Values and Standard Deviations for the Vibration in the Three Orthogonal Directions for Aircraft Group 3	91
Figure 9d.	Mean Values and Standard Deviations for the Vibration in the Three Orthogonal Directions for Aircraft Group 5	92

LIST OF FIGURES (Continued)

Figure 9e.	Mean Values and Standard Deviations for the Vibration in the Three Orthogonal Directions for Aircraft Group 10	93
Figure 10a.	Summary of Average Vibration in the Three Orthogonal Directions for Aircraft Group 1	95
Figure 10b.	Summary of Average Vibration in the Three Orthogonal Directions for Aircraft Group 2	96
Figure 10c.	Summary of Average Vibration in the Three Orthogonal Directions for Aircraft Group 3	97
Figure 10d.	Summary of Average Vibration in the Three Orthogonal Directions for Aircraft Group 5	98
Figure 10e.	Summary of Average Vibration in the Three Orthogonal Directions for Aircraft Group 10	99
Figure 11a.	Mean Values and Standard Deviations for the Vibration in Various Structural Zones of Aircraft Group 1	104
Figure 11b.	Mean Values and Standard Deviations for the Vibration in Various Structural Zones of Aircraft Group 2	106
Figure 11c.	Mean Values and Standard Deviations for the Vibration in Various Structural Zones of Aircraft Group 3	108
Figure 11d.	Mean Values and Standard Deviations for the Vibration in Various Structural Zones of Aircraft Group 5	110
Figure 11e.	Mean Values and Standard Deviations for the Vibration in Various Structural Zones of Aircraft Group 10	112

LIST OF FIGURES (Continued)

Figure 12a.	Summary of Average Vibration for Various Structural Zones of Aircraft Group 1	113
Figure 12b.	Summary of Average Vibration for Various Structural Zones of Aircraft Group 2	114
Figure 12c.	Summary of Average Vibration for Various Structural Zones of Aircraft Group 3	115
Figure 12d.	Summary of Average Vibration for Various Structural Zones of Aircraft Group 5	116
Figure 12e.	Summary of Average Vibration for Various Structural Zones of Aircraft Group 10	117
Figure 13a.	Mean Values and Standard Deviations for the Vibration in Various Aircraft of Group 1	121
Figure 13b.	Mean Values and Standard Deviations for the Vibration in Various Aircraft of Group 2	122
Figure 13c.	Mean Values and Standard Deviations for the Vibration in Various Aircraft of Group 3	123
Figure 13d.	Mean Values and Standard Deviations for the Vibration in Various Aircraft of Group 5	124
Figure 13e.	Mean Values and Standard Deviations for the Vibration in Various Aircraft of Group 10	126
Figure 14a.	Summary of Average Vibration for Various Aircraft in Group 2	127
Figure 14b.	Summary of Average Vibration for Various Aircraft in Group 3	128
Figure 14c.	Summary of Average Vibration for Various Aircraft in Group 5	129

LIST OF FIGURES (Continued)

Figure 15.	Mean Values and Standard Deviations for the Vibration in Various Aircraft Groups	131
Figure 16.	Summary of Average Vibration for the Five Aircraft Groups	133
Figure 17.	Illustration of Spatial Distribution for Vibration Data	154
Figure 18.	Illustration of Random Data Analysis Procedures .	174
Figure 19.	97.5% Prediction Limits for Helicopter Vibration Levels	179
Figure 20.	97.5% Prediction Limits Calculated from RF-4C Vibration Data	190
Figure 21.	First Order Approximation for a S - N Curve . . .	197
Figure 22.	Mechanical Oscillator with Foundation Motion . . .	200
Figure 23.	Test Level and Duration Tradeoffs for Fatigue Damage and Peak Criteria	206
Figure 24.	Illustration of Distribution Function for Aircraft Service Vibration Environment	209
Figure 25.	Illustration of Density Function for Aircraft Service Vibration Environment	210
Figure 26.	Illustration of Flight Vibration Profile	212
Figure 27.	Flow Chart for Statistical Analysis of AFFDL Flight Vibration and Acoustic Data	228

LIST OF TABLES

Table 1.	Environmental Sources for Reciprocating Engine Transports (Group 1)	20
Table 2.	Environmental Sources for Turboprop Transports (Group 2)	21
Table 3.	Environmental Sources for Jet Bombers (Group 3) and Century Jet Fighters (Group 5)	22
Table 4.	Environmental Sources for Helicopters (Group 10) . .	23
Table 5.	Summary of Environmental Sources of Vibration	24
Table 6.	Classification of Sources for Each Aircraft Group . . .	30
Table 7.	Summary of Aircraft	52
Table 8.	Summary of Structural Zones	53
Table 9.	Summary of Flight Conditions	54
Table 10.	Illustration of Data Format for Chi-Square Test	75
Table 11.	Illustration of Chi-Square Test for Homogeneity	78
Table 12.	Illustration of Rank Sum Test	83
Table 13.	Summary of Data Codes for Homogeneity Tests	86
Table 14.	Rank Sum Test Results for Direction Comparisons . .	88
Table 15.	Rank Sum Test Results for Zone Comparisons	102
Table 16.	Rank Sum Test Results for Aircraft Comparisons . . .	120

LIST OF TABLES (Continued)

Table 17.	Summary of Fuselage Vibration Data for Aircraft Group 5 Cruise	147
Table 18.	Mean Square Value Intervals for Lognormality Test . .	149
Table 19.	Means, Standard Deviations, and Sample Sizes for Lognormality Test	150
Table 20.	Illustration of Calculations for Lognormality Test . . .	151
Table 21.	Summary of Results for Lognormality Test	152
Table 22.	Comparison of Vibration Induced by Jet Engine Shaft Rotation for Various Flight Conditions	170
Table 23.	Comparison of Average Helicopter Vibration Levels for Various Flight Conditions	177
Table 24.	Measurement Locations for RF-4C Vibration Data . . .	185
Table 25.	Average Power Spectra for RF-4C Vibration Data . . .	186
Table 26.	Summary of Regression Analysis Results	188
Table 27.	Estimated Flight Condition Profile for B-58, F-101A, and H-37 Aircraft	215

LIST OF SYMBOLS

a	acceleration
A	area, regression coefficient, material constant
A(f)	regression coefficient versus frequency
b	material constant
c	viscous damping coefficient, speed of sound
c_e	local speed of sound
C	constant
d	diameter of jet exit nozzle, difference
D	diameter of propeller
E[]	expected value of []
f	cyclical frequency
f_n	undamped natural frequency
F	F distribution variable
g	acceleration due to gravity
G(f)	power spectral density function
G(x, x', f)	spatial cross spectral density function
H(f)	frequency response function
i	index

j	$\sqrt{-1}$
$J^2(f)$	joint acceptance function
k	spring constant, index
K	tolerance factor, ratio of peak to rms value
L	limit
m	median value, mass density
M	generalized mass
n	sample size
$p(x)$	probability density function
$P(x)$	probability distribution function
P	pressure, probability
<i>p</i>	standardized normal distribution function
q	dynamic pressure ($\rho V^2/2$)
Q	quality factor ($1/2\zeta$)
R_t	temperature in degrees Rankine
s	sample standard deviation, number of data sets
t	time variable, student's t distribution variable
T	observation time, sum of ranks
V	aircraft velocity
V_e	jet exhaust gas velocity
w	surface weight density

x, y	general variables
$1/\bar{x}$	sample mean value
X	independent variable
X^2	chi-square test statistic
z_α	α percentage point of standardized normal distribution
Z	Fisher Z transformation
α	small probability, level of significance
γ	correlation coefficient
δ^*	boundary layer thickness
ζ	damping ratio
ρ	atmospheric density
$\phi(x)$	mode shape
Φ	linearity test statistic
σ^2	variance, mean square value when $\mu = 0$
σ	standard deviation, rms value when $\mu = 0$
τ	time delay
μ	mean value
Ω	dimensionless frequency, π times number of crossings per second
χ^2	chi-square distribution variable

1. INTRODUCTION

The most critical step in the derivation of vibration and acoustic design criteria and/or test specifications for modern aircraft is the prediction of the anticipated flight vibration and acoustic environments. This usually involves the prediction of power spectra (or some other measure of frequency composition) for the environments. Consider first the problem of predicting flight vibration environments.

There are two fundamental ways to approach the vibration prediction problem. For the purpose here, these two ways will be referred to as (1) analytical prediction procedures and (2) empirical extrapolation prediction procedures. Analytical prediction procedures include all those techniques for predicting flight vibration environments which are based upon calculating or measuring the response of a derived structural model to an assumed excitation function. Such prediction procedures have been classified by Gray and Piersol [1] into four categories, as follows:

1. Classical (mathematical model) approach
2. Multiple input model approach
3. Physical model approach
4. Statistical energy approach

Analytical prediction procedures have been used with varying degrees of success in the past. They all have the common characteristic, however, of requiring detailed information about the structural design of the aircraft in question, and the excitation functions to which it will be subjected. Unfortunately, such information is rarely available in the

necessary detail at the time when vibration predictions are most desired (early in the design phase).

Empirical extrapolation prediction procedures include those techniques which are based upon studies of data collected during flight tests of previous aircraft. There are two basic types of extrapolation techniques. The predictions may be based upon data from a single vehicle of similar design (specific extrapolation), or they may be based upon pooled data from one or more general vehicles (general extrapolation). The most commonly used specific extrapolation procedures are those suggested by Condos and Butler [2], Barrett [3], and Winter [4]. All three procedures employ a scaling formula to extrapolate vibration data measured on a previous vehicle to predict the vibration of a new vehicle of similar design based upon differences in the excitation pressure levels and structural surface weight densities.

General extrapolation procedures are based upon empirically derived correlations between the average vibration response characteristics for a general class of structure and one or more parameters related to the excitation forces, structural properties, and/or flight conditions for the aircraft of interest. A number of such procedures have been proposed in recent years for missiles and spacecraft, as well as aircraft. One of the earliest to appear in the literature was the method suggested by Mahaffey and Smith [5], which is based upon observed correlations between structural vibration and jet engine acoustic noise for data collected from the B-58 aircraft. These same data were modified by Brust and Himelblau [6] to develop a prediction rule for the SKYBOLT missile. Similar studies were performed by Eldred, Roberts, and White [7] using data collected from the SNARK missile. Curtis [8] developed an empirical prediction rule by observing correlations between aircraft

structural vibration and free stream dynamic pressure using data collected from the F-AU, B-59, F-101, and F-106 aircraft. From JUPITER and TITAN I missile vibration and acoustic data collected during static firings, Franken [9] developed a procedure which predicts radial skin vibration for missiles as a function of rocket engine acoustic noise and skin surface weight density. A similar technique was developed by Winter [4] for predicting ring frame and stringer vibration for missiles and spacecraft based upon JUPITER, TITAN, MINUTEMAN, SKYBOLT, and GEMINI vibration and acoustic measurements.

All of the above general extrapolation procedures are similar in that they permit the prediction of structural vibration levels in a future flight vehicle without a detailed knowledge of the specific structural design, or the need for detailed data from a previous vehicle of similar design. The advantage of such procedures is clear. They can be readily applied to anticipated flight vehicles even at the preliminary design stage before the detailed structural design has been established. The fundamental disadvantage is equally clear. Since the procedures do not use detailed structural information for the flight vehicle design in question, or specific data for a similar vehicle, they do not provide the potential accuracy which an analytical procedure or a specific extrapolation procedure could theoretically produce under ideal conditions. In the opinion of many contemporary environmental engineers, however, the fundamental advantage of general extrapolation prediction procedures far outweighs their disadvantage. This fact is clearly established by the current widespread use of such procedures.

Noting the current availability of previously developed general extrapolation procedures, an obvious question arises at this point; namely, is there a need for an improved general extrapolation procedure

for predicting aircraft vibration environments? It is believed that the answer to this question is yes. A recent survey of the better known flight vehicle vibration prediction techniques [4] indicates that all of the general extrapolation procedures reviewed have limitations and deficiencies of one form or another. The principal deficiencies are as follows:

1. All of the procedures (with the notable exception of the Curtis procedure [5]) require predictions for the excitation environment. The resulting vibration predictions can be no better than the excitation predictions.
2. All of the procedures (again excluding the Curtis procedure) were developed using acoustic induced vibration data. Such procedures are fully useful only for the prediction of takeoff (or liftoff) vibration environments.
3. Most of the procedures were developed from data for only a few (in some cases, only one) flight vehicles. This clearly limits the generality of the procedures.
4. None of the procedures include provisions for predicting periodic contributions to the vibration environment from the rotation of jet engine shafts and/or auxiliary equipment.
5. The statistical techniques used in the development of the procedures were not always as thorough as would appear to be warranted by the importance of the problem.

The above deficiencies, along with others, have tended to limit the effectiveness of the various procedures in practice. Available comparisons between predictions and actual measured data [4] indicate that errors in the predicted power spectra of 20 dB or more are common.

In light of the above discussions, it is believed that the development of an improved and more efficient general extrapolation prediction procedure is a worthwhile task. For the case of aircraft vibration predictions, AFFDL is in a unique position to pursue such a task because of their large and ever growing library of aircraft vibration data.

Now consider the problem of predicting flight acoustic environments (inside the aircraft). Considerable attention has been given in recent years to the prediction of the external acoustic noise generated by jet and rocket engines, as well as the aerodynamic noise generated by boundary layer turbulence during flight [10]. As previously noted, such information is needed as an intermediate step in the prediction of flight vibration environments. Except for the case of commercial aircraft, however, somewhat less attention has been given to the problem of predicting internal acoustic noise environments. This relative lack of interest is unquestionably due in large part to the widespread (and in most cases, accurate) belief that the internal acoustic noise environment in aircraft is far less damaging to equipment than the vibration environment. Furthermore, since the crew of noncommercial aircraft generally wear protective head gear, relatively high acoustic noise levels can be permitted inside the aircraft without posing a serious hazard to the crew members.

For the case of commercial aircraft, internal acoustic predictions are usually based upon calculations for the attenuation of aeroacoustic loads by the aircraft structure and sound proofing, combined with estimates for the noise generated by the airconditioning system and other noise producing equipment. Because of the stringent competitive requirements for passenger comfort, the predictions must be relatively accurate. For the case of noncommercial aircraft, however, it appears

that acoustic predictions with the accuracy provided by a general extrapolation procedure might be adequate. The statistical techniques required to develop an extrapolation procedure for acoustic predictions would be basically the same as those required to develop a procedure for vibration predictions. Hence, it is believed that this constitutes a worthwhile task to pursue along with the development of a general extrapolation procedure for aircraft vibration predictions.

The primary purpose of the studies reported herein is to formulate a well defined program for the development of an improved extrapolation procedure for the prediction of aircraft flight vibration environments. The intent is that AFFDL will implement the program using AFFDL collected flight vibration data and computer facilities. Secondary objectives of the studies include (a) a general evaluation of currently available AFFDL aircraft vibration data and (b) the investigation of improved techniques for converting aircraft flight vibration predictions into appropriate test levels and durations for aircraft component vibration test specifications.

In order to establish proper statistical procedures and illustrate their use, it was necessary during the course of these studies to perform a considerable amount of data analysis. For convenience and clarity, only summaries of pertinent results are included in this report. The detailed results of the analysis are presented under separate cover in Appendix A. Also as part of the work reported herein, a digital computer program for the efficient computation of power spectra using fast Fourier transform techniques was developed and delivered to AFFDL. The documentation for this fast Fourier transform power spectrum program is also presented under separate cover in Appendix B.

2. PROBLEM FORMULATION AND APPROACH

The basic approach to be pursued herein centers around the development of a linear model for the power spectrum of aircraft flight vibration. In general terms, the model will be of the form

$$\begin{aligned} G(f) &= A_0(f) + A_1(f) X_1 + A_2(f) X_2 + \dots + A_N(f) X_N \\ &= A_0(f) + \sum_{i=1}^N A_i(f) X_i \end{aligned} \tag{1}$$

where

$G(f)$ = the power spectral density for the vibration response

X_i = the i th independent variable

$A_i(f)$ = the weighting factor for the i th independent variable

$A_0(f)$ = the power spectral density for the residual vibration (if any) when all independent variables equal zero

The variables, X_i ($i = 1, 2, 3, \dots, N$), ideally would cover all factors which influence the flight vibration environment. Included would be pertinent descriptive parameters of the aircraft structure, the engine operating conditions, and/or the aircraft flight conditions. For example, the X_i variables might be X_1 = structural weight density (w), X_2 = engine exhaust gas velocity (V_e), and X_3 = dynamic pressure (q). Note

that a single variable might be a power, product, and/or quotient of several parameters. For example, $X_1 = (q/w)^2$ and $X_2 = V_e^8$. Hence, although Eq. (1) is a linear model, it can be applied to nonlinear relationships as long as they are anticipated and properly incorporated into the independent variables.

The weights, $A_i(f)$ ($i = 1, 2, 3, \dots, N$), establish the relative contribution of each variable to the vibration power spectrum. For example, if $X_1 = w$ and $A_1(f) = 0$, this would mean that the structural weight density has no influence on the vibration power spectrum at frequency f . The $A_0(f)$ weight accounts for any contributions to the vibration power spectrum which occur when $X_i = 0$ ($i = 1, 2, 3, \dots, N$).

The development of a model of the form given in Eq. (1) involves two general problems. The first is to select the variables to be used in the model, and the second is to determine appropriate values for the weights. These two problems along with statistical considerations and the specific approach which hopefully will solve them are now discussed.

2.1 SELECTION OF VARIABLES

The selection of appropriate independent variables could be approached by purely empirical procedures. This would be done by simply guessing at all possible factors which might influence structural vibration. Those factors which are actually related to structural vibration in a statistically significant way would then be determined through a multiple correlation study of all available vibration data. Such an approach, however, is considered unsuitable for the problem of concern here.

It is believed that a superior approach is to select the variables based principally upon theoretical knowledge and well-established experience. This second approach provides important advantages. First, assuming sufficient theoretical and experimental information is available, it increases the likelihood of selecting only those variables which are relevant to the vibration environment. Second, it permits nonlinear relationships, as well as product and quotient relationships, for various factors to be anticipated and properly included into Eq. (1) as a single variable in the linear model. The elimination of irrelevant variables and nonlinear relationships in Eq. (1) will greatly increase the statistical significance of the regression analyses required to calculate the $A_i(f)$ weights. Of course, there is the possibility that relevant variables may be omitted or that nonlinear relationships for various factors may be improperly interpreted. These risks, however, should be minimal for two reasons. First, theoretical and experimental definitions for aircraft vibration sources and, hence, the factors which influence flight vibration, are readily available and quite thorough. Second, special tests for significant correlation and linearity of all selected variables can and will be performed as part of the regression analysis to establish the $A_i(f)$ weights.

2.2 DETERMINATION OF WEIGHTS

The $A_i(f)$ weights in Eq. (1) will be determined using a conventional regression analysis procedure. The general procedure is as follows. Assume that M different aircraft flight vibration measurements are available for various different combinations of structural locations, engine operating conditions, and/or flight conditions. Hence, M power spectra can be computed, and each can be considered an estimate of the power

spectrum, $G(f)$, given by Eq. (1). That is, the k th measured spectrum, $\hat{G}_k(f)$ ($k = 1, 2, 3, \dots, M$) can be considered an estimate (denoted by the hat $\hat{}$) for

$$\begin{aligned}
 G_k(f) &= A_0(f) + A_1(f) X_{1k} + A_2(f) X_{2k} + \dots + A_N(f) X_{Nk} \\
 &= A_0(f) + \sum_{i=1}^N A_i(f) X_{ik} \quad ; \quad k = 1, 2, 3, \dots, M
 \end{aligned}
 \tag{2}$$

where X_{ik} is the value of the i th variable for the k th measurement. The problem is to solve for values of $A_i(f)$ which will minimize the variance of the measured values $\hat{G}_k(f)$ about the model values $G_k(f)$.

Assume that the spectral density measurements, $\hat{G}_k(f)$, are normally distributed with a mean value of $G_k(f)$, as given in Eq. (2). Under this assumption, the best minimum variance unbiased estimates for the weights $A_i(f)$ are determined as follows. Let $Q(f)$ denote the sum of the squared deviations at a given frequency, as follows.

$$Q(f) = \sum_{k=1}^M \left[\hat{G}_k(f) - G_k(f) \right]^2
 \tag{3}$$

Using Eq. (2) and dropping the (f) notation for clarity, it follows that

$$Q = \sum_{k=1}^M \left(\hat{G}_k - A_0 - A_1 X_{1k} - A_2 X_{2k} - \dots - A_N X_{Nk} \right)^2
 \tag{4}$$

Excluding the first equation and the first column from each equation, Eq. (5) may now be written in matrix form, as follows.

$$\begin{bmatrix} \hat{A}_1 \\ \hat{A}_2 \\ \vdots \\ \hat{A}_N \end{bmatrix} = \begin{bmatrix} B_{11} & B_{12} & \cdots & B_{1N} \\ B_{21} & B_{22} & \cdots & B_{2N} \\ \vdots & \vdots & \ddots & \vdots \\ B_{N1} & B_{N2} & & B_{NN} \end{bmatrix}^{-1} \begin{bmatrix} \sum X_{1k} \hat{G}_k \\ \sum X_{2k} \hat{G}_k \\ \vdots \\ \sum X_{Nk} \hat{G}_k \end{bmatrix} \quad (7)$$

Equation (7) solves for the A_i weight for $i = 1, 2, 3, \dots, N$. The weight A_0 can be solved for using the first equation in Eq. (6) after the other weights have been determined. Computer programs for performing multiple regression analyses are widely available.

2.3 STATISTICAL CONSIDERATIONS

Having estimated the weights for the N selected variables, a prediction model for the power spectrum of aircraft flight vibration can now be written, as follows.

$$\tilde{G}(f) = \hat{A}_0(f) = \sum_{i=1}^N \hat{A}_i(f) X_i \quad (8)$$

At this point, it should be made clear that the development of a "perfect" prediction model for aircraft vibration is beyond practicality. There are certain factors (particularly those related to structural characteristics) which significantly influence vibration, but which cannot be conveniently defined in terms of simple variables. In other words, there will be some pertinent X_i terms missing in Eq. (8). This will appear as scatter in the actual power spectra about the predicted power spectra determined using Eq. (8).

To illustrate this point, assume the model consists of only one variable, such that

$$\tilde{G}(f) = \hat{A}(f) X \quad (9)$$

where the regression equation used to estimate the weight $\hat{A}(f)$ is

$$\hat{A}(f) = \frac{\sum_{k=1}^M X_k \hat{G}_k(f)}{\sum_{k=1}^M X_k^2} \quad (10)$$

Now assume the M power spectra measured for the various values of X are compared to the prediction model given by Eq. (9). The results at a specific frequency might be as shown in Figure 1. The scatter in Figure 1 may be thought of as an indication of the "efficiency" of the prediction model. If X were the only variable relevant to the vibration

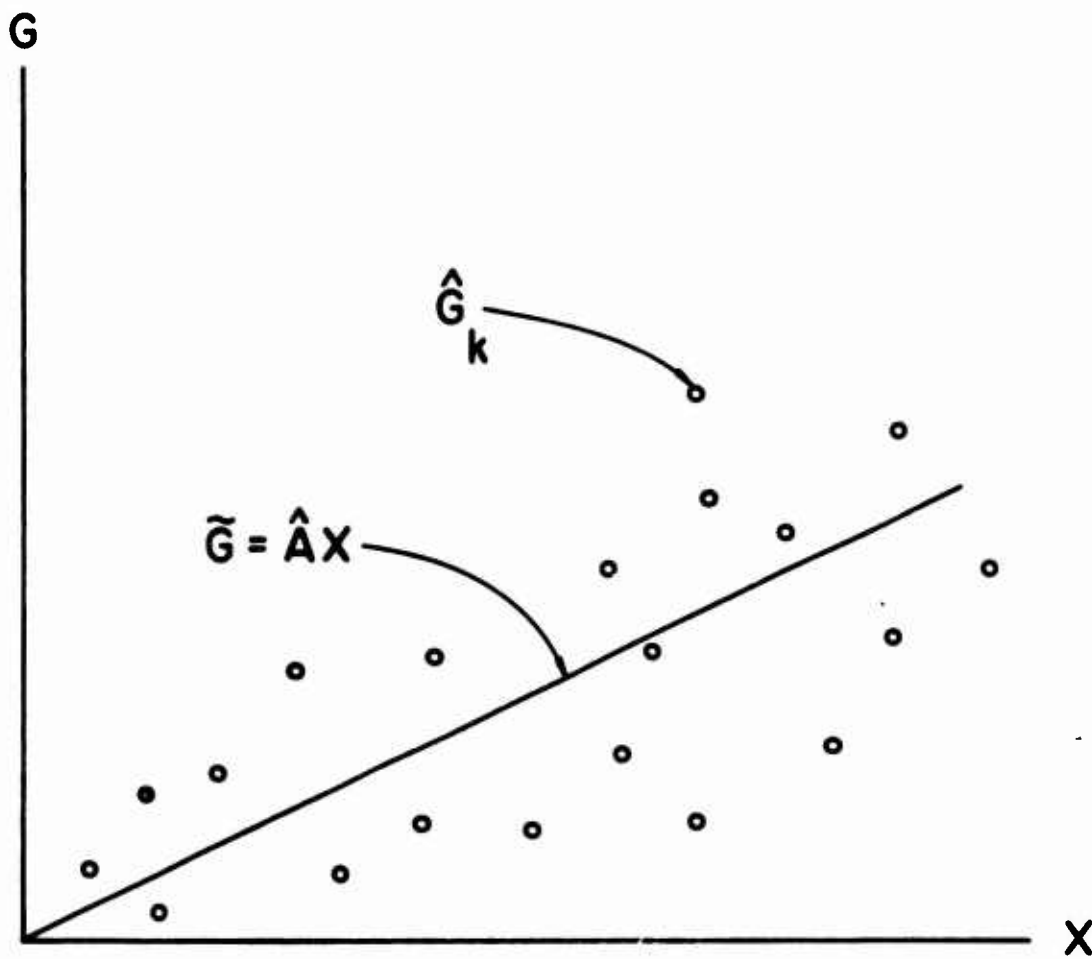


Figure 1. Illustration of Scatter About Prediction Model

environment, there would be no scatter; that is, all measurements would fall on the prediction line (assuming no measurement error is present). This would constitute a perfectly efficient model.

A convenient measure for the efficiency of the prediction model is given by the "correlation coefficient," γ , for the regression analysis. The correlation coefficient is a number bounded by zero and unity, ($0 \leq \gamma \leq 1$), where unity indicates a perfect model. The quantity $1 - \gamma^2$ is a measure of the "power" contributed to the observed vibration by variables which have not been included in the model. For correlation coefficients of less than unity, the scatter of the measured data about the model can be described by a standard deviation for the measured \hat{G} values at various values of X . Assuming some specific distribution function for this scatter, prediction limits for future measurements of the vibration environment at any value of X can be determined. For the case of a flight vehicle vibration model, conservative estimates are required. Hence, some upper limit with a relatively large probability of exceeding future vibration levels will be required in practice.

Other analyses which should be performed during the regression study include a test for significance of the calculated correlation coefficients and a test for linearity of the model. The former can be performed using a Fisher "Z" transformation and the latter using an analysis of variance test.

These various statistical analysis procedures will be outlined and illustrated in Section 8.

2.4 OUTLINE OF SUGGESTED APPROACH

The specific steps which will be pursued to develop a prediction model for aircraft vibration using AFFDL data are as follows.

1. Development of Vibration Relationships — This initial step involves three requirements. The first is to identify the various sources of aircraft vibration and assess their relative importance. The second is to provide a preliminary definition of the structural excitation parameters which theoretically influence aircraft vibration environments. The third is to analytically relate the primary sources of vibration to basic flight and/or engine performance parameters. Section 3 covers this subject.

2. Summary of Available Data — The flight vibration and acoustic data currently available for study must now be defined and collected. Fortunately, AFFDL has carefully documented and published the results of all flight vibration surveys performed by their activity. Hence, this first step requires only a summary of this documentation, which is presented in Section 4.

3. Preliminary Evaluation of Available Data — The final procedure to be recommended in this report will require no small amount of digital computer computations by AFFDL. Hence, a careful editing and evaluation of all available data to eliminate unrepresentative data and/or data of questionable quality is warranted. This evaluation is summarized in Section 5.

4. Homogeneity Studies — This step is needed to reduce the redundancy of the available data and the resulting prediction model. For example, there is no point in deriving separate prediction models for the vibration environment of different types of aircraft if, in fact, the vibration environments are not significantly different. It follows that careful investigations of the available data for homogeneity (equivalence) should be performed. Of particular interest are possible differences in the vibration environment among the three orthogonal axes, the various structural zones of the aircraft, the various aircraft in a given aircraft group, and the various aircraft groups. These homogeneity tests are developed and illustrated in Section 6.

5. Spatial Distribution Studies — In some cases, it may not be feasible to include variables in the prediction model which will account for differences in the vibration from one location to another on the aircraft structure. For such cases, the predictions must be based upon some conservative upper limit determined using the distribution function for the variation of the vibration over the structure. The determination of this spatial distribution function is the subject of Section 7.

6. Prediction Model Studies — Based upon the material developed in Sections 3 through 7, the next step is to select the variables for the regression analysis, and to illustrate the analysis procedures on properly edited data. This is done in Section 8.

7. Test Level and Duration Selection Studies — Having established an empirical procedure for predicting structural vibration, the next logical step is to formulate specific techniques for converting the resulting vibration predictions into appropriate test specifications. This problem is not straightforward for the case of aircraft vibration environments for two reasons. First, the vibration service life of many aircraft is measured in terms of thousands of hours. However, laboratory vibration tests must be performed in much shorter periods of time, preferably in terms of minutes. This means that techniques must be employed to compress the long service life into short test durations. The second problem relates to the basic nonstationary character of the aircraft flight vibration environment. The vibration levels experienced by the aircraft during takeoff are considerably different from those which occur during cruise. It is desirable, however, that the vibration tests be specified in terms of only one vibration level (at least for a given structural zone). Hence, it is necessary to convert the various different vibration levels which occur during the service life to a single vibration level for the vibration tests. These matters are pursued in Section 9.

8. Applications to Acoustic Predictions — A final step is to investigate how the techniques for arriving at a vibration prediction procedure might be modified to develop a procedure for predicting internal acoustic noise. This subject is considered in Section 10.

3. DEVELOPMENT OF VIBRATION RELATIONSHIPS

3.1 IDENTIFICATION OF VIBRATION SOURCES

The sources of aircraft vibration may be broadly divided into two classifications, random and deterministic. From various references including [11-28], the principal random and deterministic sources of vibration which might occur for various types of aircraft are as summarized in Tables 1 through 4. All vibration sources taken together are summarized in Table 5. Note that the aircraft are divided into five types, where each type is identified by a "group" number consistent with designations used by AFFDL. Also note that fixed wing propeller aircraft (Groups 1 and 2) are included in the summary only for completeness. The development of prediction models for these aircraft groups is probably not warranted since the future design of such aircraft is unlikely.

From Table 5, there are eight principal sources of random vibration and twelve principal sources of deterministic vibration in aircraft. Each of these sources will now be briefly reviewed in terms of their relative importance to the overall vibration environment, and their suitability for consideration in the development of a general extrapolation procedure for the prediction of aircraft vibration.

R-1. Jet Acoustic Noise — The operation of turbo-jet engines is accompanied by intense random acoustic noise caused by the mixing of the high velocity exhaust gases with the ambient air. This acoustic noise is a major source of vibration in jet powered aircraft during take-off and early climb, particularly for those aircraft with wing mounted engines (Group 3). It becomes less significant as the aircraft speed increases.

Table 1. Environmental Sources for Reciprocating Engine Transports
(Group 1)

Sources of Random Vibration	Sources of Deterministic Vibration
<ul style="list-style-type: none"> ● Aerodynamic boundary layer noise ● Propeller blade vortex noise ● Atmospheric turbulence (gust loads) ● Runway roughness ● Wake turbulence caused by auxiliary lift devices, drag devices, and spoilers ● Airconditioning noise 	<ul style="list-style-type: none"> ● Propeller blade passage ● Engine exhaust ● Propeller rotation ● Engine shaft rotation ● Engine accessory equipment ● Auxiliary rotating equipment ● Acoustical cavity resonances ● Unstable aerodynamic conditions

Table 2. Environmental Sources for Turboprop Transports (Group 2)

Source of Random Vibration	Source of Deterministic Vibration
<ul style="list-style-type: none"> ● Jet acoustic noise ● Aerodynamic boundary layer noise ● Propeller blade vortex noise ● Atmospheric turbulence (gust loads) ● Runway roughness ● Wake turbulence caused by auxiliary lift devices, drag devices, and spoilers ● Airconditioning noise 	<ul style="list-style-type: none"> ● Propeller blade passage ● Propeller rotation ● Turbine shaft rotation and blade passage ● Engine accessory equipment ● Auxiliary rotating equipment ● Gear box noise ● Acoustic cavity resonances ● Unstable aerodynamic conditions

Table 3. Environmental Sources for Jet Bombers (Group 3) and Century Jet Fighters (Group 5)

Sources of Random Vibration	Sources of Deterministic Vibration
<ul style="list-style-type: none"> ● Jet acoustic noise ● Aerodynamic boundary layer noise ● Atmospheric turbulence (gust loads) ● Runway roughness ● Wake turbulence caused by auxiliary lift devices, drag devices, and spoilers ● Transonic shock wave-boundary layer interaction ● Airconditioning noise 	<ul style="list-style-type: none"> ● Turbine shaft rotation and blade passage ● Engine accessory equipment ● Auxiliary rotating equipment ● Gunfire ● Acoustic cavity resonances ● Unstable aerodynamic conditions

Table 4. Environmental Sources for Helicopters (Group 10)

Source of Random Vibration	Source of Deterministic Vibration
<ul style="list-style-type: none"> ● Jet acoustic noise * ● Rotor blade vortex noise ● Atmospheric turbulence ● Airconditioning noise 	<ul style="list-style-type: none"> ● Rotor blade passage (main and tail) ● Rotor rotation ● Jet engine turbine shaft rotation and blade passage * ● Reciprocating engine exhaust ** ● Reciprocating engine shaft rotation ** ● Engine accessory equipment ● Auxiliary rotating equipment ● Gear box noise ● Rotor blade slope ● Gunfire

* Jet engine powered helicopters only

** Reciprocating engine powered helicopters only

Table 5. Summary of Environmental Sources of Vibration

Code	Sources of Random Vibration	Code	Sources of Deterministic Vibration
R-1	Jet acoustic noise	D-1	Propeller (or rotor) blade passage
R-2	Aerodynamic boundary layer noise	D-2	Propeller (or rotor) rotation
R-3	Propeller (or rotor) blade vortex noise	D-3	Jet engine turbine shaft rotation and blade passage
R-4	Atmospheric turbulence	D-4	Reciprocating engine exhaust
R-5	Runway roughness	D-5	Reciprocating engine shaft rotation
R-6	Wake turbulence caused by auxiliary lift devices, drag devices, and spoilers	D-6	Engine accessory equipment
R-7	Transonic shock wave-boundary layer interaction	D-7	Auxiliary rotating equipment
R-8	Airconditioning noise	D-8	Gear box noise
		D-9	Rotor blade slap
		D-10	Gunfire
		D-11	Acoustic cavity resonances
		D-12	Unstable aerodynamic conditions

R-2. Aerodynamic Boundary Layer Noise — The flight of aircraft at high speeds produces a turbulent boundary layer at the interface between the aircraft and the atmosphere. This turbulence produces vibration which increases in severity as dynamic pressure increases. For high speed aircraft (Groups 3 and 5), it is a major source of vibration during cruise and other high speed flight conditions.

R-3. Propeller (or Rotor) Blade Vortex Noise — Fixed wing aircraft propellers and helicopter rotors are responsible for two types of acoustic excitation. The first is a periodic excitation related to propeller or rotor blade passage, which is discussed later. The second is a random excitation produced by vortex shedding from the propeller or rotor blades. Vortex noise may be quite pronounced when propellers or rotors are operated at high rpm with low pitch (high rpm but low power). For the more interesting case where flight power is delivered to the propellers and rotors, the vortex noise is generally not significant compared to the vibration induced by blade passage and other sources.

R-4. Atmospheric Turbulence — Atmospheric turbulence is a principal source of low frequency vibration in aircraft. However, it is not a continuous source of vibration. Its occurrence is a function only of atmospheric conditions and not of aircraft flight parameters. Hence, there is no way to generally predict the vibration induced by atmospheric turbulence based upon parameters of the aircraft structure, engine operating conditions, and/or aircraft flight conditions. Of course, given the knowledge that atmospheric turbulence will occur, one can calculate the aircraft response to the turbulence, as outlined in [12]. Predictions of this type should be handled separately and should not be included in a general prediction procedure of the type being studied here.

R-5. Runway Roughness — Runway roughness is a source of low frequency vibration during takeoff, landing and taxi. The resulting vibration is a function of the specific runway condition and aircraft. Hence, like atmospheric turbulence, the runway roughness problem should be handled separately and should not be included in a general prediction procedure.

R-6. Wake Turbulence — Wake turbulence caused by auxiliary lift devices, drag devices and spoilers can be a significant source of aircraft vibration, particularly during landing approaches. It should be considered in a vibration prediction model for any type of aircraft for those flight conditions where such devices are used.

R-7. Transonic Vibration — For missiles and spacecraft, the interaction of shock waves and boundary layer pressures during transonic flight is often the predominate source of flight vibration. The relatively clean geometry of modern aircraft, however, greatly restricts the influence of transonic shock wave-boundary layer interaction. Any significant vibration induced by transonic flight would probably be very localized and a function of the detailed geometry of the aircraft. Hence, such vibration should not be included in a general prediction procedure.

R-8. Airconditioning Noise — Airconditioning noise is usually more of an acoustical comfort problem than a structural vibration problem. The vibration produced by airconditioning noise is generally local and high frequency in nature. It is rarely a significant contributor to the overall vibration environment of aircraft, except perhaps in very restricted structural areas. It is, however, a major source of cabin acoustic noise.

D-1. Propeller (or Rotor) Blade Passage — As discussed under R-3, fixed wing aircraft propellers and helicopter rotors are responsible for two types of acoustic excitation. One type is due to vortex shedding from the propeller or rotor blades, as discussed previously. The other type is caused by the periodic pressure pulses emitted from the propeller or rotor blades. This second type of excitation is most severe for the case of fixed wing aircraft with wing mounted engines, where the primary aircraft structure is outside the cylinder of blade rotation. For this type of aircraft (Groups 1 and 2), propeller blade passage is the major source of vibration. For helicopters (Group 10), rotor blade passage is a less severe source relative to other vibration sources, but still may be significant.

D-2. Propeller (or Rotor) Rotation — The vibration induced by propeller rotation on fixed wing aircraft, or rotor rotation on helicopters, is a direct function of the magnitude of propeller or rotor unbalance and RPM. For fixed wing aircraft, propeller rotation is a negligible source of vibration under normal conditions, and can be ignored in the prediction procedure being studied here. For helicopters, however, the main rotor rotation may be a significant source of low frequency vibration.

D-3. Jet Engine Shaft Rotation and Blade Passage — Periodic vibration due to jet engine shaft unbalance may be quite significant in jet powered aircraft, particularly those with fuselage incorporated engines (Group 5). The vibration occurs at the rotational frequency of the shaft (or shafts) and all harmonics thereof. Some vibration may also occur at frequencies corresponding to the rate at which turbine and compressor blades pass the engine stator blades. This latter excitation, however, is usually more of an acoustical comfort problem than a structural vibration problem.

D-4. Reciprocating Engine Exhaust — For reciprocating engine type aircraft (Groups 1 and 10), the engine ignition contributes to the aircraft vibration environment in two ways. First, the actual ignition explosions produce engine vibration which transmits in part through the engine mounts into the airframe. Second, the acoustical pressure pulses from the exhaust induce vibration much like the propeller blade passage does. The first source is usually negligible under normal conditions, but the second source can be significant.

D-5, D-6, D-7, D-8. Reciprocating Engine Shaft Rotation, Engine Accessory Equipment, Auxiliary Rotating Equipment, Gear Box Noise — These various periodic contributions are usually negligible sources of vibration in fixed wing aircraft, but may be significant sources in helicopters. In particular, gear box noise is often a major source of vibration in helicopters.

D-9. Rotor Blade Slap — When helicopters perform sharp turn maneuvers or approach limiting forward speeds, the main rotor blades moving aft (in the direction of air flow) may experience a partial stall condition. This repetitive quasi-stall of the blades induces a momentary flow separation called blade slap. This condition can be a significant source of low frequency vibration, as well as acoustic noise. Since it occurs only under special conditions, however, it should be handled separately and should not be included in a general prediction procedure.

D-10. Gunfire — Gunfire can produce considerable vibration, particularly in the structural regions near the gun locations. It should be considered in the prediction model for those aircraft which are equipped with guns.

D-11, D-12. Acoustic Cavity Resonances and Unstable Aerodynamic Conditions — These two sources of periodic vibration will hopefully not be present since they imply a poor design. If they are present, they constitute a special problem which must be dealt with by special techniques. The inclusion of such techniques in a general prediction model is clearly not feasible.

In summary, the various sources of random and deterministic vibration may be classified into four categories as follows.

- A. Sources which are considered sufficiently significant to include in the prediction model
- B. Sources which are considered significant, but which should be treated separately and not as part of the prediction model
- C. Sources which are not considered sufficiently significant to include in the prediction model
- D. Sources which do not apply to the aircraft group in question.

The classification of sources for each aircraft group is summarized in Table 6. Note that these classifications are tentative and may be altered by later data studies.

Table 6. Classification of Sources for Each Aircraft Group

Aircraft Group	Classifications for Random (R) and Deterministic (D) Sources									
	A		B		C		D		D	
	R	D	R	D	R	D	R	D	R	D
1	6	1, 4	4, 5	11, 12	2, 3, 8	2, 5, 6, 7, 8	1, 7	3, 9, 10		
2	2, 6	1	4, 5	11, 12	1, 3, 8	2, 3, 6, 7, 8	7	4, 5, 9, 10		
3 and 5	1, 2, 6	3, 10	4, 5	11, 12	7, 8	6, 7, 8	3	1, 2, 4, 5, 9		
10 (Reciprocating Engines)		1, 2, 4, 6, 8, 10	4	9, 11, 12	2, 3, 6, 8	5, 7	1, 5, 7	3		
10 (Jet Engines)		1, 2, 3, 6, 8, 10	4	9, 11, 12	1, 2, 3, 6, 8	7	5, 7	4, 5		

3.2 ANALYTICAL DESCRIPTION OF STRUCTURAL VIBRATION

All of the significant random sources of aircraft vibration summarized in Table 6 are pressure field type sources. Hence, as a preliminary step to establishing relationships between these sources and the resulting structural vibration, a review of the theory for structural response to random pressure excitations is in order.

Consider an arbitrary structure which is subjected to a random pressure field, $p(x, t)$. The pressure field may be described by a spatial cross spectral density function, as follows.

$$G_p(x, x', f) = E \left[\lim_{T \rightarrow \infty} \frac{1}{T} P_T^*(x, f) P_T(x', f) \right] \quad (11)$$

where

$$P_T(x, f) = \int_{-\infty}^{\infty} p(x, t) e^{-j2\pi ft} dt$$

x, x' = two different vector points on the structure

$$P_T^*(x, f) = \text{complex conjugate of } P_T(x, f)$$

Note that the spatial cross spectrum can also be defined as

$$G_p(x, x', f) = \int_{-\infty}^{\infty} R_p(x, x', \tau) e^{-j2\pi f\tau} d\tau \quad (12)$$

where

$$R_p(x, x', \tau) = \lim_{T \rightarrow \infty} \frac{1}{2T} \int_{-T}^T p(x, t) p(x', t + \tau) dt$$

From [13], the power spectrum for the acceleration response of the structure at any point x induced by this pressure field is given by

$$G_a(x, f) = \sum_i \sum_k \phi_i(x) \phi_k(x) \frac{H_i(f) H_k^*(f)}{M_i M_k f_i^2 f_k^2} f^4 G_{ik}(f) \quad (13)$$

where

$$G_{ik}(f) = \int_0^A \int_0^A \phi_i(x) \phi_k(x') G_p(x, x', f) dx dx' \quad (\text{modal cross spectrum})$$

$$M_i = \int_0^A m(x) \phi_i^2(x) dx \quad (\text{modal mass})$$

$\phi_i(x)$ = mode shape for i th normal mode

$H_i(f)$ = frequency response function for i th normal mode

f_i = undamped natural frequency for i th normal mode

$m(x)$ = surface mass density

A = surface area

The modal cross spectrum in Eq. (13) can be reduced to a more convenient form, as follows.

$$G_{ik}(f) = A^2 G_p(x_0, f) J_{ik}^2(f) \quad (14)$$

where

$$J_{ik}^2(f) = \frac{1}{A^2} \int_0^a \int_0^a \phi_i(x) \phi_k(x') \mathcal{G}_p(x, x', f) dx dx' \quad (\text{cross joint acceptance})$$

$$\mathcal{G}_p(x, x', f) = \frac{G_p(x, x', f)}{G_p(x_0, f)}$$

The acceleration power spectrum in Eq. (13) may be separated into the $i = k$ terms and the $i \neq k$ terms, as follows.

$$G_a(x, f) = \sum_i \phi_i^2(x) \frac{|H_i(f)|^2}{M_i^2 f_i^4} f^4 G_i(f) + \sum_i \sum_{k \neq i} \phi_i(x) \phi_k(x) \frac{H_i(f) H_k^*(f)}{M_i M_k f_i^2 f_k^2} f^4 G_{ik}(f) \quad (15)$$

Now consider the ratio of any $i \neq k$ term to the $i = k$ term.

$$\begin{aligned}
R &= \frac{\phi_i(x) \phi_k(x)}{M_i M_k f_i^2 f_k^2} \cdot \frac{M_i^2 f_i^4}{\phi_i^2(x)} \cdot \frac{f^4 H_i(f) H_k^*(f) G_{ik}(f)}{f^4 H_i(f) H_i^*(f) G_i(f)} \\
&= \frac{\phi_k(x)}{\phi_i(x)} \cdot \frac{M_i f_i^2}{M_k f_k^2} \cdot \frac{H_k^*(f)}{H_i^*(f)} \cdot \frac{J_{ik}^2(f)}{J_i^2(f)} \quad (16)
\end{aligned}$$

By averaging over the structure,

$$\langle R \rangle = \frac{\int_0^A \phi_k(x) dx}{\int_0^A \phi_i(x) dx} \cdot \frac{K_i}{K_k} \cdot \frac{H_k^*(f)}{H_i^*(f)} \cdot \frac{J_{ik}^2(f)}{J_i^2(f)} \quad (17)$$

where $K_i = M_i f_i^2$. Assuming that the frequency response functions are given by

$$H_i(f) = \frac{1}{1 - (f/f_i)^2 + j 2 \zeta_i f/f_i} \quad (18)$$

where ζ_i is the damping ratio for the i th mode, it follows that the absolute value of the average ratio is

$$|\langle R \rangle| = \frac{\int_0^A \phi_k(x) dx}{\int_0^A \phi_i(x) dx} \cdot \frac{K_i}{K_k} \cdot \sqrt{\frac{[1 - (f/f_i)^2]^2 + [2\zeta_i f/f_i]^2}{[1 - (f/f_k)^2]^2 + [2\zeta_k f/f_k]^2}} \cdot \frac{J_{ik}^2(f)}{J_i^2(f)} \quad (19)$$

To simplify the development, assume the mode shapes are sinusoidal and normalized such that

$$M_i = m \int_0^A \phi_i^2(x) dx = mA \quad (20)$$

That is, $\phi_i(x) = \sqrt{2} \sin \beta_i x$ where $\beta_i = i\pi/A$. Hence, the average value will be

$$\begin{aligned} \sqrt{2} \int_0^A \sin \beta_i x dx &= \frac{\sqrt{2}}{\beta_i} \left| \cos \beta_i x \right|_0^A \\ &= \frac{\sqrt{2A}}{i\pi} (1 - \cos i\pi) = \begin{cases} 1 & (i = 1, 3, 5, \dots) \\ 0 & (i = 2, 4, 6, \dots) \end{cases} \quad (21) \end{aligned}$$

Further assume that the cross point acceptances are such that $J_{ik}^2(f)/J_i^2(f) = 1$. Then,

$$|\langle R \rangle| = \left(\frac{i}{k}\right) \left(\frac{f_i}{f_k}\right)^2 \sqrt{\frac{\left[1 - (f/f_i)^2\right]^2 + \left[2\zeta_i f/f_i\right]^2}{\left[1 - (f/f_k)^2\right]^2 + \left[2\zeta_k f/f_k\right]^2}} \quad (22)$$

The power spectrum values of principal concern are those at frequencies near normal mode frequencies, since these frequencies will be the peak values in the spectrum. Letting $f = f_i$, Eq. (22) becomes

$$|\langle R \rangle| = \left(\frac{i}{k}\right) \left(\frac{f_i}{f_k}\right)^2 \frac{1}{Q_i \sqrt{\left[1 - (f_i/f_k)^2\right]^2 + \left[2\zeta_k f_i/f_k\right]^2}} \quad (23)$$

where $Q_i = 1/(2\zeta_i)$.

The quantity $(k/i) |\langle R \rangle|$ is plotted against the frequency ratio f_k/f_i for various values of damping in Figure 2. It is clear from Figure 2 that, on the average, the contribution of the $i \neq k$ terms in Eq. (13) falls off very rapidly with normal mode frequency ratio for small damping. For example, if $\zeta = 0.01$ ($Q = 50$), the contribution of the k th mode to the power spectrum at the i th normal mode frequency is less than 10% when the k th mode is only 10% from the i th mode frequency. Since the damping ratio for most aircraft structures is relatively small, it appears justified as a first order of approximation to ignore the $i \neq k$ terms in Eq. (13). With this approximation, the power spectrum for the acceleration response of a structure may be written as

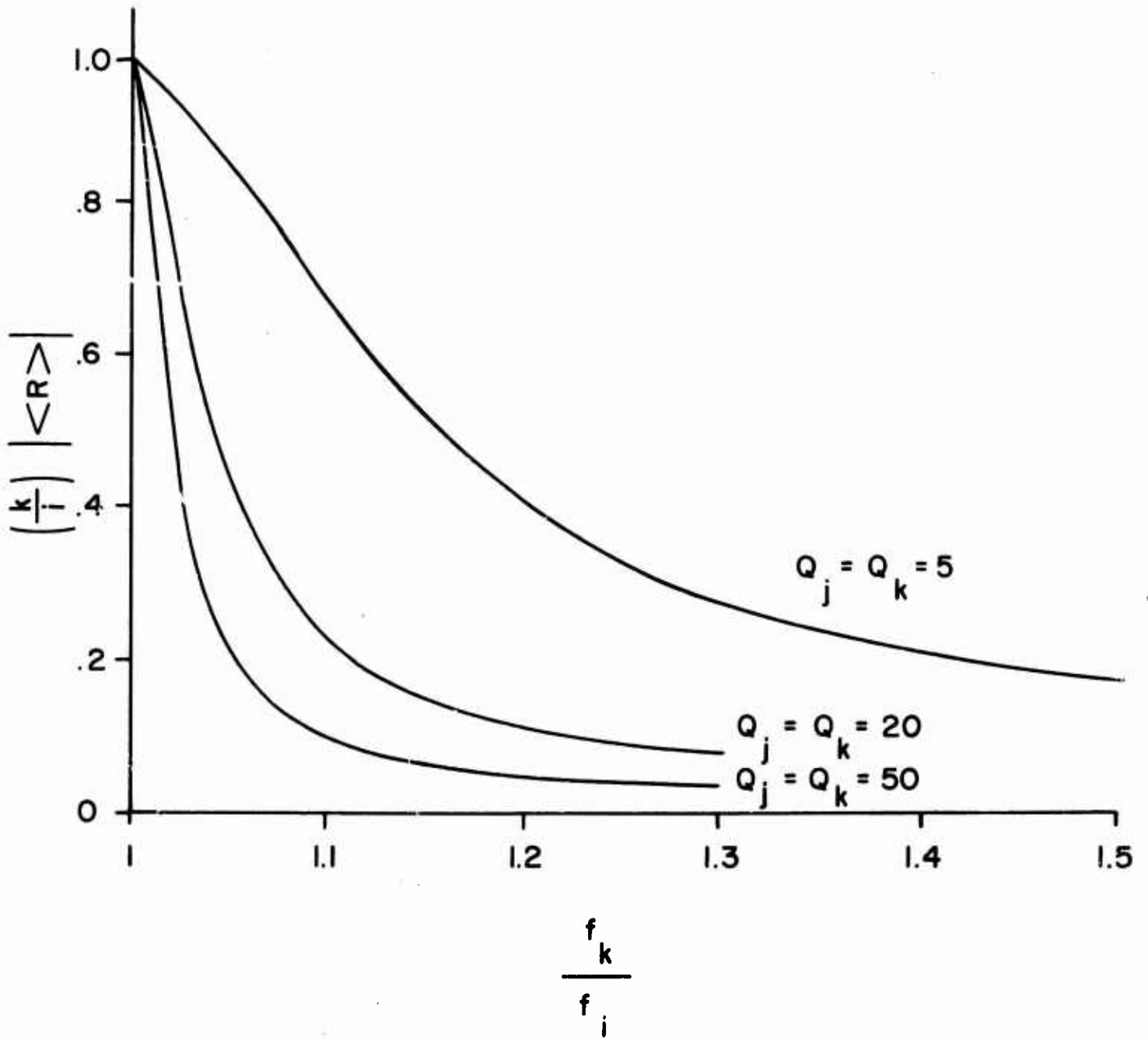


Figure 2. Relative Contribution of Off-Diagonal Terms to Vibration Response Power Spectrum

$$G_a(x, f) \approx \sum_i \phi_i^2(x) \frac{|H_i(f)|^2}{M_i^2 f_i^4} f^4 G_i(f) \quad (24)$$

By further assuming that the generalized masses and joint acceptances are constants $[M_i = mA = (w/g) A$ and $J_i^2(f) = J_a^2]$, Eq. (24) can be further reduced to

$$G_a(x, f) = A^2 J_a^2 G_p(x_0, f) \sum_i \left(\frac{\phi_i(x) Q_i}{w/g} \right)^2 \quad (25)$$

On the average, the quantities $A^2 J_a^2$ and $[\phi_i(x) Q_i]^2$ should not vary sharply for similar types of structures. Hence, as a first order of approximation, it appears reasonable to assume that the power spectrum for the acceleration response of a structure is proportional to the average power spectrum of the excitation over the structure divided by the square of the surface weight density for the structure. That is,

$$G_a(x, f) \sim \frac{G_p(x_0, f)}{w^2} \quad (26)$$

3.3 ANALYTICAL DESCRIPTION OF PRIMARY SOURCES

From Table 6, there are three random and seven deterministic sources of vibration which are considered sufficiently significant and otherwise suitable to include in the vibration prediction model. These significant sources are:

- R-1* Jet acoustic noise
- R-2* Aerodynamic boundary layer noise
- R-6* Wake turbulence caused by auxiliary lift devices, drag devices, and spoilers
- D-1* Propeller (or rotor) blade passage
- D-2 Helicopter rotor rotation
- D-3 Jet engine turbine shaft rotation
- D-4* Reciprocating engine exhaust
- D-6 Engine accessory equipment
- D-8 Gear box noise
- D-10 Gunfire

Five of the ten sources listed above (those marked with an asterisk) are basically pressure field type sources; that is, they induce vibration by generating fluctuating pressure fields which impinge over the structural surface. In Section 3.2, it was established that, as a first order of approximation, the resulting structural vibration may be considered proportional to the power spectrum of the generated pressure field. Hence, for the purposes of a vibration prediction model, it is desirable to define the power spectrum for these seven sources in terms of engine operating conditions and/or aircraft flight conditions, where possible.

The remaining five sources (D-2, D-3, D-6, D-8, and D-10) are basically mechanical type sources which induce vibration by direct mechanical transmission of energy through the structure. The definition of vibration as a function of operational parameters is more difficult for these sources since the mechanical impedance of the structure is the primary factor which controls the resulting vibration intensity. The use of detailed impedance information is not appropriate for the type of general vibration model of interest here. Hence, it will be necessary to use more general statistic techniques to describe these mechanical sources.

Each of the ten significant sources of aircraft vibration will now be discussed in terms of their relationships to various descriptive parameters of engine operating conditions and flight conditions.

3.3.1 Jet Acoustic Noise

From [14], the total acoustic power radiated by a jet engine at rest is related to various engine and atmospheric parameters by

$$P \sim \rho A V_e^8 / c^5 \quad (27)$$

where

- ρ = air density
- A = jet exit area
- V_e = exhaust gas velocity
- c = speed of sound

Furthermore, the power spectrum for the noise is approximately as shown in Figure 3.

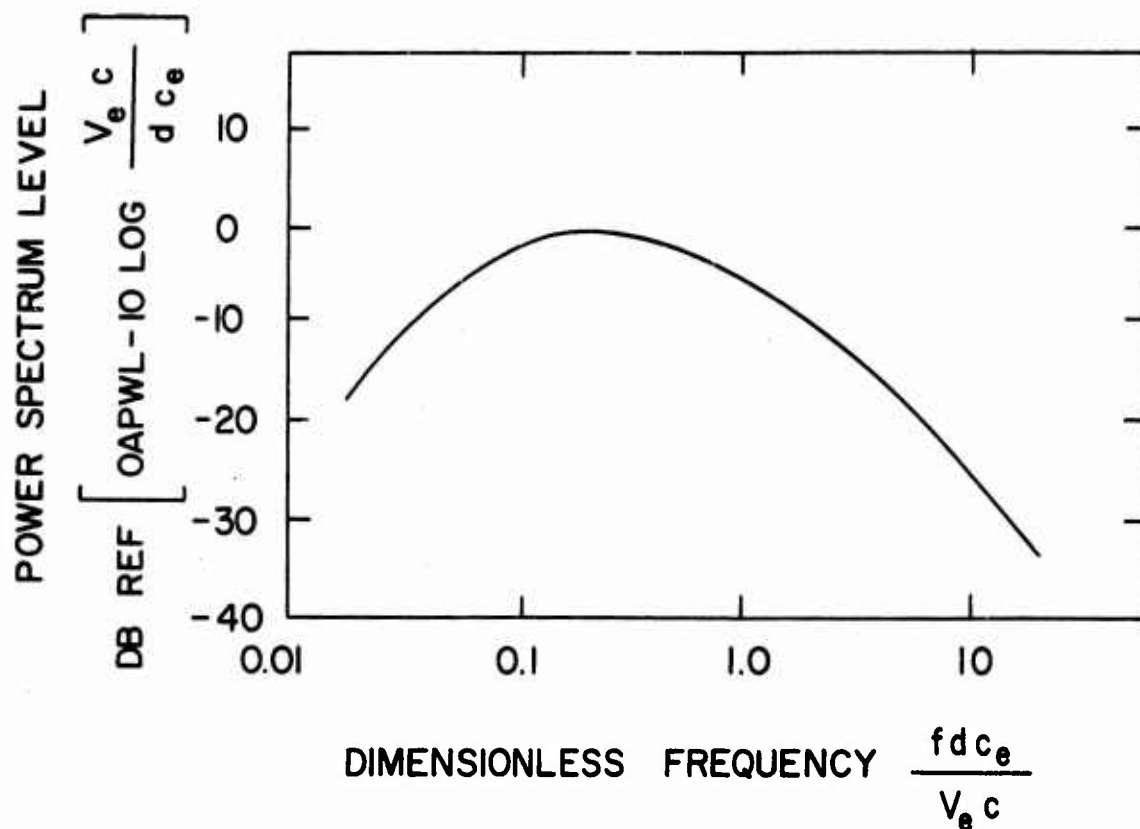


Figure 3. Spectrum for Jet Acoustic Noise

In Figure 3, f = frequency in cps, d = jet exit diameter, and c_e = local speed of sound. Note that for typical jet engines at takeoff conditions, the spectral peak usually occurs at a frequency between 100 and 300 cps, but because of the shallow slope of the spectrum, significant acoustical power exists over the entire audio frequency range.

The power spectrum for the acoustic pressure at any point on the aircraft structure due to jet noise is a function of the directivity pattern of the noise as well as the structural location relative to the jet engine, the aircraft velocity, wind conditions, and the presence of reflecting surfaces. For the problem at hand, it will be necessary to ignore variations in the directivity pattern, wind conditions, and reflecting surfaces; that is, these factors will be permitted to appear as variability in the resulting prediction model. Structural location relative to the jet engine and aircraft velocity, however, cannot be ignored. The variation of sound pressure level with structural location can be dealt with by deriving a different set of $A_{ij}(f)$ weights for each of several different structural regions or zones. The variation of sound pressure level with airspeed could be dealt with in a similar way, but it appears more appropriate to simply restrict attention to a single airspeed; namely zero. This should be adequate for the desired prediction model since the jet noise impinging on the structure is greatest when the engine is at maximum thrust, and maximum thrust occurs during the takeoff roll when the airspeed is near zero. Furthermore, as the airspeed increases, the directivity pattern of the jet noise shifts aft, rapidly reducing the contribution of jet noise to the vibration environment.

In conclusion, for a given structural zone of an aircraft at zero airspeed, the power spectrum for the acoustic noise impinging on the structure is related, as a first order of approximation, to engine and atmospheric parameters by

$$G(\Omega) \sim \rho A V_e^n / c^5 \quad (28)$$

where Ω is dimensionless frequency ($fd c_e / V_e c$), and n is some number probably between 6 and 8. A suitable value for n should be determined by optimizing the correlation coefficient for the vibration model during the regression studies.

3.3.2 Aerodynamic Boundary Layer Noise

From [16], for Mach numbers less than 2.5, the mean square value of the pressure generated by boundary layer turbulence for relatively "clean" structures is approximated by

$$\sigma_p^2 \approx (0.006 q)^2 \quad (29)$$

where q is the free stream dynamic pressure ($q = \rho V^2 / 2$). Furthermore, the power spectrum for the noise is approximately as shown in Figure 4.

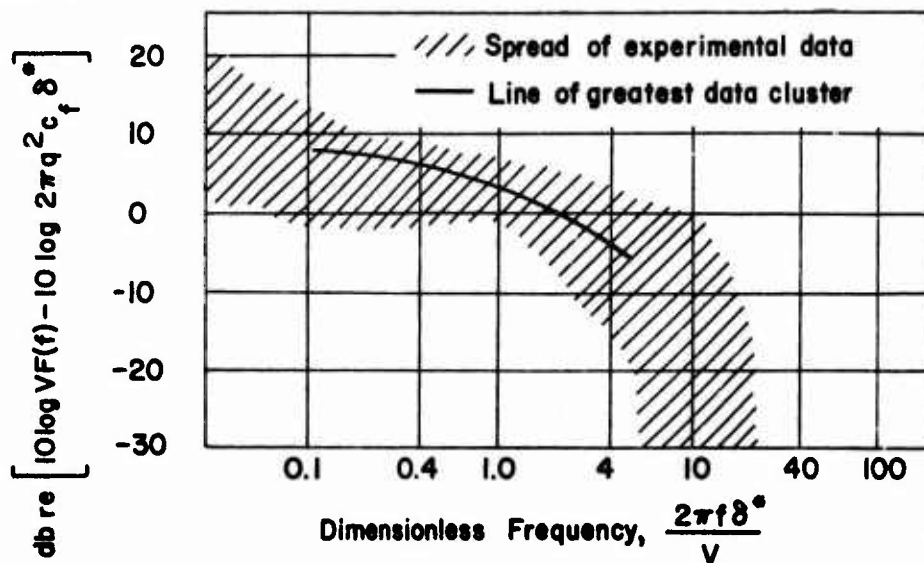


Figure 4. Spectrum for Aerodynamic Boundary Layer Noise

In Figure 4, δ^* is the boundary layer thickness, and is given by $\delta^* \approx 0.0026 x$ for "clean" structures where x is the distance from the front of the structure.

The power spectrum for the boundary layer pressures, as shown in Figure 4, is relatively uniform for dimensionless frequencies up to $f\delta^*/V \approx 0.2$. Beyond this frequency, the spectrum falls off gradually until $f\delta^*/V \approx 2.0$, where the spectrum cuts off sharply. For a 50 ft long airplane traveling at 1000 ft/sec (about 700 mph), this means that the spectrum starts falling off at about 3000 cps for a point halfway back on the airplane, and at about 1500 cps for a point at the rear of the airplane. In practice, it can probably be assumed that the power spectrum of the boundary layer pressures is white noise in the frequency range of usual interest (0 to 2000 cps). Hence, as a first order of approximation, the power spectrum for the boundary layer noise pressure on the structure is related to flight conditions by

$$G(f) \sim q^2 \quad (30)$$

3.3.3 Wake Turbulence

Wake turbulence caused by auxiliary lift devices, drag devices, and spoilers is no doubt a function of aircraft flight parameters such as airspeed and density. However, the actual geometry of the devices involved is a more significant influencing factor. Furthermore, the problem generally arises for a limited range of flight parameters, since such devices are used only for special conditions such as landing

and takeoff. This means that an effort to correlate wake turbulence induced vibration and aircraft flight conditions may not be very profitable. Perhaps a better approach is to consider the wake turbulence induced vibration as a separate environment which will be predicted using a general statistical evaluation of all data taken in each of various structural zones when the various turbulence inducing devices are deployed. For the case of speed break deployment, the possibility of a relationship between vibration and dynamic pressure might be investigated. Fortunately, such studies are easy to accomplish because AFFDL identifies and separates all data taken with and without the deployment of such devices.

3.3.4 Propeller (or Rotor) Blade Passage

Consider first the case of fixed wing aircraft with wing mounted propeller engines (Groups 1 and 2). From [12], the overall sound power level generated by a propeller in the near field is proportional to

$$P \sim \frac{P_p^2 \cdot 3.66M_t}{v^2 D^4 (z/D) \cdot 3.34 + 2.44M_t^2 (R_t/528)} \quad (31)$$

where

P_p = mechanical power to propeller

M_t = propeller tip Mach number

v = number of propeller blades

z = clearance between propeller blade tip and fuselage

D = propeller diameter

R_t = absolute temperature in degrees Rankine (degrees F + 460)

The power spectrum for the propeller noise (neglecting vortex noise) will be a series of harmonic components with frequencies of

$$f_i = \frac{iv \text{ (RPM)}}{60} \quad ; \quad i = 1, 2, 3, \dots \quad (32)$$

For the propeller aircraft of concern to AFFDL, the fundamental frequency, f_1 , is approximately 50 cps for normal cruise conditions. The amount of power in the various harmonics is a function of M_t . For $M_t < 0.8$, over 50% of the power occurs at the fundamental frequency (f_1). As $M_t \rightarrow 1.0$, the power in the harmonics increases relative to the power of the fundamental.

As for jet acoustic noise, the power spectrum for the propeller acoustic pressures at any point on the aircraft structure is a function of the directivity pattern of the blade passage noise as well as the structural location relative to the propeller, the aircraft velocity, wind conditions, and the presence of reflecting surfaces. Hence, it will be necessary to deal with the propeller noise problem in the same manner as suggested for the jet noise problem in Section 3.3.1. Specifically, a prediction model for propeller induced vibration should be developed by deriving a different set of $A_{ij}(f)$ weights for each of several different structural zones at zero airspeed only. If this is done, the power spectrum for the propeller noise impinging on the structure will be a series of harmonically related delta functions at the frequencies given in Eq. (32), and with a total mean square value proportional to P in Eq. (31).

Now consider the case of helicopters. There is a similar problem of vibration induced by the tail rotor blade passage, and Eq. (31) applies to this problem. For the case of the main rotor, however, the problem is somewhat different. Equation (31) applies only to structure outside the cylinder of rotation for the propeller or rotor. Most of the structure for helicopters is inside the cylinder of rotation for the main rotor. A model for this vibration is not known to be available. Hence, it will be necessary to establish a prediction model for the helicopter vibration induced by main rotor blade passage by careful inspection of past data.

3.3.5 Helicopter Rotor Rotation

The vibration induced by rotor rotation on helicopters is a direct function of the magnitude of the rotor unbalance and rotor RPM, as well as the mechanical impedance of the supporting structure. The frequency of the rotor rotation induced vibration is generally below 10 cps. It is unlikely that a strong correlation would be obtained with flight conditions and engine operating conditions, other than RPM. Since the RPM for helicopter rotors is relatively constant for most flight conditions and rotor unbalance is usually unknown, it is suggested that rotor rotation induced vibration be predicted using a general statistical evaluation of all data taken in each of various structural zones.

3.3.6 Jet Engine Turbine Shaft Rotation

The problem of vibration induced by the jet engine turbine shaft rotation is similar to the problem of helicopter rotor vibration discussed in Section 3.3.5, and should be handled in a similar way. Specifically, shaft rotation induced vibration should be predicted using a general

statistical evaluation of all data taken in each of various structural zones. The fundamental frequency of shaft rotation induced vibration is generally between 50 cps and 150 cps for most jet engine operating conditions.

3.3.7 Reciprocating Engine Exhaust

From [12], the overall sound power level generated by the exhaust of a reciprocating engine is proportional to the total horsepower delivered by the engine. Furthermore, the spectrum for the exhaust noise is basically periodic with a fundamental frequency equal to the ignition firing frequency (from 100 cps to 200 cps for most engines and operating conditions). The power content of the harmonics falls off at a rate of about 3:1 per octave. The vibration induced by the exhaust is a function of the directivity pattern, structural location, etc., as discussed for jet noise in Section 3.3.1. Hence, it will be necessary to derive a different set of $A_{ij}(f)$ weights for each of several different structural zones for various different flight conditions.

3.3.8 Engine Accessory Equipment

The vibration induced by engine accessory equipment tends to be localized and relatively independent of flight conditions. It may occur at frequencies up to 1000 cps. The most important factors influencing the magnitude of the vibration are the details of the equipment and the mounting point impedance of the supporting structure. It is suggested that accessory equipment induced vibration be predicted using a general statistical evaluation of all data collected in each of several structural zones.

3.3.9 Helicopter Gear Box Noise

The vibration generated by helicopter gear box noise is quite complex and may occur over a wide frequency range. Although the magnitude of the vibration is unquestionably related to engine operating conditions and perhaps flight conditions, the relationships are not well defined. It is suggested that gear box induced vibration be predicted using a general statistical evaluation of all data collected at the frequencies corresponding to anticipated gear box frequencies.

3.3.10 Gunfire

The vibration induced by gunfire is clearly not related to engine operating conditions or flight conditions. Hence, the contribution of gunfire to the vibration environment should be predicted based upon a general statistical evaluation of data collected when guns are fired.

4. REVIEW OF AVAILABLE DATA

The flight acoustic and vibration data available to AFFDL, and the acquisition and analysis procedures used to obtain the data are summarized in this section.

4.1 SUMMARY OF AIRCRAFT

As of 1 January 1968, AFFDL has documented flight vibration data collected on a total of 13 different aircraft. Flight acoustic data were also collected and documented for two of those aircraft. The 13 aircraft are classified into 5 different groups depending upon their basic mission and configuration. In Table 7, the specific aircraft in each of the 5 groups are presented along with the AFFDL aircraft code number and report number which summarizes the results of the acoustic and vibration surveys for each of the aircraft.

For the purposes of test specifications and design criteria, AFFDL considers an aircraft to be composed of a possible 27 different structural zones. Each of these structural zones and the code number used to identify the zone are presented in Table 8. The data measured in each zone of each aircraft are further classified in terms of the aircraft flight condition at the time of measurement. Each flight condition and the code number used for its identification are summarized in Table 9.

Using the code numbers in Tables 7 through 9, the general location and flight condition for any vibration measurement can be readily identified. For example, a measurement in zone 03 of aircraft 46 for flight condition 07 would be a measurement in the aft quarter of the fuselage of an F-102A during normal cruise. Note that the exact location for each vibration measurement is detailed in the various documentation reports.

Table 7. Summary of Aircraft

Group Code Number	Group Description	Aircraft Code Number	Aircraft	Report Number	Reference Number
1	Reciprocating Engine Transports	38	C-123	ASD-TDR-62-235	[16]
2	Turboprop Transports	40 47	C-130 C-133	ASD-TDR-62-267 ASD-TDR-62-383	[17] [18]
3	Jet Bombers	36 37 52	JRB-52 JRB-66 B-58	ASD-TR-61-507 ASD-TR ASD-TDR-62-384	[19] [20] [21]
5	Century Series Jet Fighters	42 44 46 53 63*	F-100C F-101A F-102A F-106A RF-4C	ASD-TN-61-61 ASD-TN-61-60 ASD-TDR-62-37 ASD-TDR-62-504 AFFDL-FDDS-TM-65-53	[22] [23] [24] [25] [26]
10	Helicopters	49 62*	H-37 UH-1F	WADD-TN-60-170 AFFDL-DDR-FDD-66-3	[27] [28]

* Flight acoustic data as well as vibration data were collected on aircraft code numbers 62 and 63.

Table 8. Summary of Structural Zones

Description of Structural Zone	Code Number
Forward quarter of fuselage	01
Center half of fuselage	02
Aft quarter of fuselage	03
Vertical and horizontal stabilizer, including rudder and elevators	04
Outer one-third of wing	05
Inner two-thirds of wing	06
Engine	07
Rigidly mounted equipment in zone 01	08
Rigidly mounted equipment in zone 02	09
Rigidly mounted equipment in zone 03	10
Rigidly mounted equipment in zone 04	11
Rigidly mounted equipment in zone 05	12
Rigidly mounted equipment in zone 06	13
Rigidly mounted equipment in zone 07	14
Shock mounted equipment in zone 01	15
Shock mounted equipment in zone 02	16
Shock mounted equipment in zone 03	17
Shock mounted equipment in zone 04	18
Shock mounted equipment in zone 05	19
Shock mounted equipment in zone 06	20
Shock mounted equipment in zone 07	21
Accessory section	22
Helicopter section	23
Rigidly mounted equipment in zone 22	24
Rigidly mounted equipment in zone 23	25
Shock mounted equipment in zone 22	26
Shock mounted equipment in zone 23	27

Table 9. Summary of Flight Conditions

Description of Flight Conditions	Code Number
Taxi	01
Ground Runup (clean)	02
Takeoff Roll	03
Takeoff	04
Takeoff (assisted i. e. A/B, jato, etc.)	05
Climb (normal)	06
Cruise (normal)	07
Cruise (speed brakes extended)	08
Cruise (rocket pod extended, missile launcher extended, gunfire or test item operating)	09
Cruise (09 + speed brakes)	10
Vertical Dive (clean)	11
Vertical Dive (w/09)	12
Vertical Dive (w/speed brake)	13
Vertical Dive (w/10)	14
Cruise (flaps extended)	15
Cruise (gear extended)	16
Cruise (refueling doors open)	17
Inverted Flight	18
Standard Pursuit Curve (clean)	19
Standard Pursuit Curve (w/gunfire)	20
Normal Descent (clean)	21
Normal Descent (speed brakes extended)	22
Normal Approach	23
Normal Approach (w/flaps, gear, etc.)	24

Table 9 (continued)

Description of Flight Conditions	Code Number
Touchdown	25
Landing Roll	26
Drag Chute or Reverse Thrust (or both)	27
Bomb Bay Open, Camera Doors Open or Troop Doors Open	28
Cruise (turbulent air)	29
Cruise (one or more engines out)	30
Turn (1.5 g or less)	31
Turn (more than 1.5 g)	32
Auto-Rotation — Engine at Idle % RPM = Rotor RPM (helicopter)	33
Auto-Rotation Stop — as above (helicopter)	34
Hover (helicopter)	35
Rearward Flight (helicopter)	36
Side Flight (helicopter)	37
Emergency or High Speed Stop (helicopter)	38
Test Stand Runup (w/mech. or man. gov.)	39
Test Stand Runup (w/elec. (auto) gov.)	40
Windup During Start (before eng. fires)	41
Windup During Start (after eng. fires and before idle speed is reached)	42
Cruise (unpressurized — abnormal cond.)	43
Ground Runup (w/one or more eng. out)	44
Ground Runup (w/flaps extended)	45
Stall (high or low speed)	46
Climb (w/after burner)	47

Table 9 (continued)

Description of Flight Conditions	Code Number
Cruise (A/B, clean)	48
Cruise (A/B, speed brakes extended)	49
Cruise (A/B, flaps extended)	50
Ground Runup (A/B or water injections)	51
Ground Runup (A/B, water inject., with flaps extended)	52
Cruise (flaps and gear extended)	53
Cruise (flaps and speed brakes)	54
Cruise (speed brakes and gear extended)	55
Cruise (speed brakes, flaps and gear extended)	56
Cruise (A/B, with gear extended)	57
Cruise (A/B, flaps, gear extended)	58
Cruise (A/B, flaps, and speed brakes)	59
Cruise (A/B, speed brakes and gear extended)	60
Cruise (A/B, speed brakes and flaps extended)	61
Descent (with gear extended)	62
Descent (with flaps extended)	63
Descent (with gear and flaps extended)	64
Descent (with gear and speed brakes extended)	65
Descent (with flaps and speed brakes extended)	66

4.2 DATA ACQUISITION EQUIPMENT AND PROCEDURES

Data acquisition procedures and techniques often have a profound impact on the quality of the resulting data. Hence, it is important to review and clarify the various data acquisition instruments and procedures used by AFFDL to acquire the data summarized in Table 7. Fortunately, AFFDL has been quite consistent in the instrumentation and procedures used to acquire flight acoustic and vibration data. The same basic procedures were used to acquire data in all the aircraft listed in Table 7, with the exception of aircraft Code Nos. 62 and 63 (UH-1F and RF-4C). At a point in history just prior to the flight surveys of aircraft Code Nos. 62 and 63, a basic change was made in the vibration data acquisition system, and acoustic data acquisition was introduced. Further changes in the data acquisition system are currently being contemplated. For the case of currently available data, however, the vibration data acquisition systems used for all flight vibration surveys may be divided into two categories. The principal change in the vibration data acquisition system was from velocity transducers to acceleration transducers. Hence, the two different vibration data acquisition systems will be referred to as the velocity transducer system and the acceleration transducer system.

4.2.1 Velocity Transducer System

The flight vibration surveys of all aircraft in Table 7, excluding aircraft Code Nos. 62 and 63, were performed using velocity transducers. CEC Model 4-102A-MD velocity pickups were used in aircraft Code No. 49, and MB type 124 velocity pickups were used for the other

aircraft. The pickups were mounted at various locations on the aircraft structure, generally in clusters of three so that vibration along the three orthogonal axes would be sensed. The output signals from the pickups were recorded 12 at a time on a Davies Model 501 14-channel magnetic tape recorder. Since there were usually more than 12 pickups installed for any given flight, it was necessary to restrict the vibration measurements at any given time to 12 or less pickups. By using a selector switch, data from all pickups were recorded in a grouped sequential manner. The length for each sample record was fixed at 5 seconds. The exact time of each vibration measurement was recorded along with pertinent flight parameters including engine speed, indicated airspeed, altitude, manifold pressure or power lever angle, percent of rated horsepower or percent of rated thrust, and flight condition (takeoff, cruise, etc.).

The MB Type 124 velocity pickup is a velocity signal generating device with a nominal sensitivity of 96.4 millivolts per inch per second, a usable frequency range of 5 to 2000 cps, and a usable temperature range of -65° to 250° F. A typical frequency response curve is shown in Figure 5. The CEC Model 4-102A-MP has somewhat similar characteristics.

The Davies Model 501 recorder is an FM type magnetic type tape recorder with a carrier frequency of 10 kc, a usable frequency range of 3 to 2000 cps, a nominal dynamic range of 45 dB, and a tape speed of 15 inches per second. The frequency response is relatively flat over the usable frequency range.

Further information on both the vibration transducers and the magnetic tape recorder are available in any of the documents referenced in Table 7, excluding the reports for aircraft Code Nos. 62 and 63.

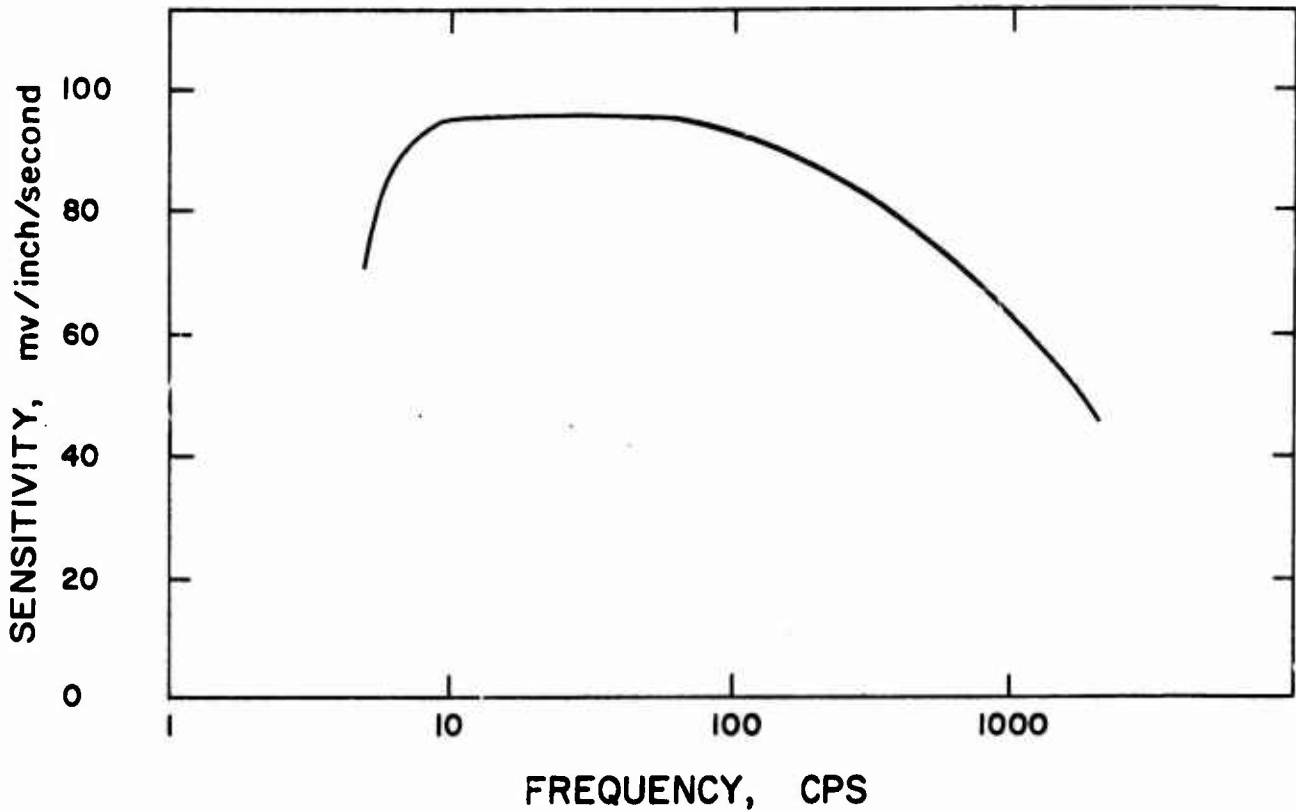


Figure 5. Frequency Response of MB Type 124 Velocity Pickup

4.2.2 Acceleration Transducer System

The flight vibration surveys on aircraft Code Nos. 62 and 63 were performed using Columbia Research Laboratories Model 902-H accelerometers and/or Endevco Model 2215, 2215C and 2245B accelerometers. The accelerometers were used in conjunction with Endevco Model 2617 amplifiers. As for the velocity pickups, the accelerometers were mounted at various locations in the aircraft, usually in clusters of three, to sense vibration along the three orthogonal axes. The output signals from the accelerometer amplifiers were sequentially recorded

in groups of 13 or less on a Honeywell Model MTR-7200 14-channel magnetic tape recorder. Record lengths were 6 seconds or longer, and the time of each measurement along with pertinent flight parameters were recorded.

The various Columbia Research Laboratories and Endevco accelerometers are piezoelectric crystal devices with a nominal sensitivity of 8 to 17 millivolts per g, a usable frequency range of 2 to 6000 cps, and a usable temperature range of -65° to 700° F. The Model 2617 amplifiers are ac voltage type amplifiers. A typical frequency response curve for an accelerometer and amplifier is shown in Figure 6.

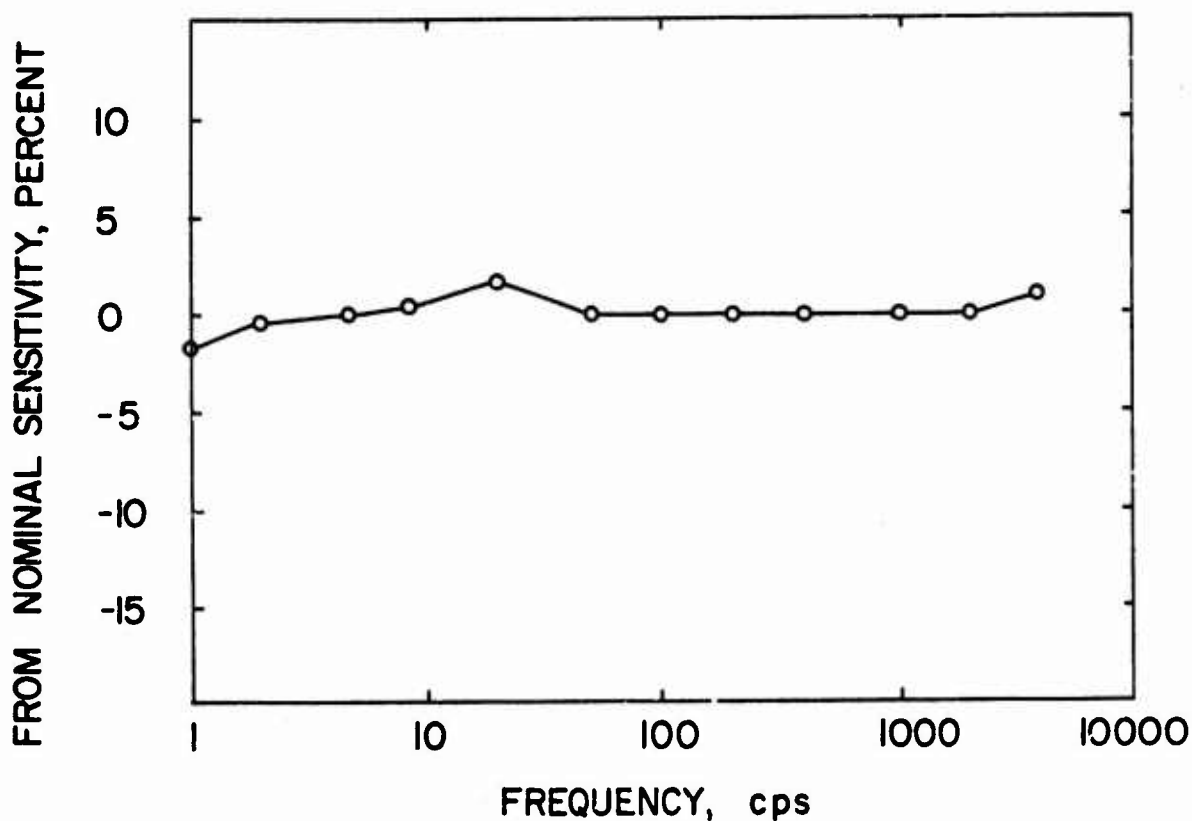


Figure 6. Frequency Response of Piezoelectric Crystal Accelerometers

The Honeywell Model MTR-7200 recorder is an FM type magnetic tape recorder with a carrier frequency of 54 kc, a usable frequency range of dc to 10,000 cps, a nominal dynamic range of 45 μ B, and a tape speed of 60 inches per second. The frequency response is relatively flat over the usable frequency range.

Further information on both the acceleration transducers and the magnetic tape recorder are presented in [26], [28].

4.2.3 Microphone Transducer System

The flight acoustic surveys on aircraft Code Nos. 62 and 63 were performed using Gulton Model MA 299501 microphones, in conjunction with Endevco Model 2617 amplifiers. The microphones were mounted in various compartments of interest to sense the acoustic noise environment in those compartments. The output signals from the microphone amplifiers were recorded on a Honeywell Model MTR-7200 14-channel magnetic tape recorder (the same instrument used to record the output of the acceleration transducers). Record lengths were 5 seconds or longer, and the time of each measurement along with pertinent flight conditions were recorded.

The Gulton microphones are piezoelectric crystal devices with an upper sound pressure level limit of 190 dB. They have a minimum open circuit sensitivity of 1.6 millivolts for 120 dB sound pressure level, a usable frequency range of 2 to 6000 cps, and a vibration sensitivity of 90 dB sound pressure level per 1 g (rms) vibration. The Model 2617 amplifiers are ac voltage type amplifiers. The frequency response for the microphones is flat to within ± 2 dB over the usable frequency range.

The Honeywell Model MRT-7200 recorder is as described in Section 3.2.2. Further information on the microphones is presented in [26], [28].

4.3 DATA PROCESSING PROCEDURES

As for the case of the data acquisition equipment and procedures, the data processing instruments and procedures have a considerable influence on the final quality of the data. The procedures used by AFFDL to reduce vibration data have been consistent for that data collected using velocity transducers. Specifically, that vibration data collected for all aircraft flight vibration surveys, excluding the surveys of aircraft Code Nos. 62 and 63, were performed using procedures detailed in WADC Technical Note 59-44 [29]. Different instruments and somewhat different data reduction procedures were introduced at a time prior to the flight vibration surveys on aircraft Code Nos. 62 and 63. Furthermore, data reduction for acoustic data were introduced at that time.

4.3.1 Analysis Procedures for Velocity Data

For the case of data collected using velocity transducers, the reels of recorded data were first edited in the laboratory and then spliced into endless loops. Each loop was placed on a Davies Model 502 Tape Playback System and continuously recirculated for analysis. A frequency analysis was performed on the data using a 6-channel Davies Model 510 heterodyne type wave analyzer. The bandwidths for the analysis were approximately 10 cps in the frequency range below 500 cps, and 30 cps in the frequency range above 500 cps. The averaging time constant for the analyzer detector circuit was approximately 1 second. A plot of vibration amplitude versus frequency was recorded on a Brown strip chart recorder for each channel of vibration data. The resulting frequency spectra were converted into discrete data points for handling by digital processing. To accomplish this, each significant peak observed in each

measured frequency spectrum was considered to be a data point. Personal judgment was used to define a significant peak. The resulting data points were punched onto IBM cards. Additional cards were punched to furnish tie-in data which described the pickup locations, the aircraft, the flight conditions, and other pertinent information. All information was then handled automatically on a computer. The value of each spectral peak was converted from a velocity to a double amplitude (peak-to-peak displacement) in inches, using calibrations which would be appropriate if the spectral peak represented a sine wave. The resulting data were then presented as scatter plots of double amplitude in inches versus frequency in cps. These data are presented in the applicable references listed in Table 7, [16] - [25], [27]. Further descriptions of the procedures are also given in these references, as well as [29].

4.3.2 Analysis Procedures for Acceleration Data

For the case of aircraft Code No. 62, the acceleration data recordings were edited in the laboratory and then spliced into endless loops. Each loop was placed on a Honeywell Model 3170 Tape Reproducer System and continuously recirculated for analysis. The data were analyzed using a 6-channel Honeywell Model 9050 Automatic Wave Analyzer. The analyses were performed using bandwidths of 10 cps in the frequency range from 3 to 300 cps, 30 cps in the frequency range from 300 to 1000 cps, and 100 cps in the frequency range from 1000 to 10,000 cps. The averaging time constant for the analyzer detector circuit was 1 second in all cases. The resulting data were reduced, processed, and plotted exactly as was done for the velocity data discussed in Section 4.3.1 (see [28] for further details).

For the case of the acceleration data acquired for aircraft Code No. 63, the data were edited, spliced into endless loops, and recirculated for analysis. The data were analyzed using the Honeywell Model 9050 Wave Analyzer and a Bruel & Kjaer Type 2111 Audio Frequency 1/3-octave spectrometer.

For the analysis performed using the wave analyzer, the analysis bandwidths were 10 cps in the frequency range from 3 to 500 cps, and 40 cps in the frequency range from 500 to 2400 cps. The averaging time constant for the wave analyzer detector circuit was approximately 3 seconds. The resulting frequency spectra were converted to discrete data points as before, where each observed peak in the spectrum was considered a data point. However, in this case, the resulting data points were converted to acceleration power spectral density levels in g^2/cps , using calibrations which would be appropriate if the spectral peaks represented narrowband Gaussian random noise. No effort was made to distinguish between those spectral peaks due to sine waves and those due to narrowband random vibrations.

For the analysis performed using the 1/3-octave band analyzer, the data were analyzed in the 21 1/3 octaves between 25 and 2500 cps. A true rms detector circuit was used. The resulting frequency spectra were presented as rms g's versus 1/3-octave center frequencies (see [28] for further details).

4.3.3 Analysis Procedures for Microphone Data

For the case of aircraft Code No. 62, the acoustic data recordings were processed and presented exactly like the vibration data, as discussed in Section 4.3.2. For the case of aircraft Co. No. 63, the acoustic data were processed and presented exactly like that vibration data analyzed using the 1/3-octave analyzer, as discussed in Section 4.3.2 (see [26], [28] for further details).

5. PRELIMINARY DATA EVALUATION

The preliminary evaluation of the available AFFDL flight vehicle vibration data immediately led to an important conclusion. Specifically, with the exception of the RF-4C survey [26], the data as acquired, analyzed and presented by AFFDL tends to accentuate the contribution of periodic vibration sources and obscure the contributions of random vibration sources. In other words, the data may present a reasonable measure of periodic vibrations, but they definitely provide a poor measure of random vibrations. The reasons for this evolve principally from the data analysis procedures, although the data acquisition procedures also contribute.

The facts which led to the above conclusion were first discovered during initial efforts to perform regression analysis on data for jet bombers and fighters [19] to [25]. These initial regression studies failed to indicate a correlation between structural vibration and dynamic pressure (q). It is interesting to note that this result was observed during a previous study of the same data [30], but the investigator in that case chose to accept the result. The result was not accepted here since past studies of data for other aircraft [8], as well as studies of the RF-4C data [31], clearly revealed a correlation between structural vibration and dynamic pressure. Furthermore, the theoretical arguments supporting the existence of this correlation, as developed in Section 3, are quite compelling. Hence, a detailed study of the basic quality of the AFFDL vibration data was pursued. This study, in turn, led to the noted conclusion. Since this conclusion is profoundly important to the determination of appropriate data evaluation and statistical analysis procedures discussed later, it is desirable to clearly present all of the related facts.

5.1 SUMMARY OF DATA LIMITATIONS

There are a number of factors in the data acquisition and analysis equipment and procedures which individually tend to exaggerate the importance of periodic contributions relative to random contributions in the vibration environment for all aircraft surveyed by AFFDL, except for the RF-4C [26]. They may be summarized as follows.

1. Use of velocity signal generators
2. Frequency response function for velocity signal generators
3. Use of common sensitivity for all recorder inputs
4. Reduction of data in terms of the amplitude and frequency for spectral peaks

Each of these contributing factors is now discussed.

5.1.1 Use of Velocity Transducers

As noted in Section 4.2, most of the AFFDL flight vehicle vibration data have been acquired using velocity type transducers. However, acceleration type transducers would have been more appropriate for the following reason. There is a general tendency for aircraft vibration data to have velocity spectra which decrease with increasing frequency. On the other hand, the acceleration spectra often increase with increasing frequency over much of the frequency range of the data. This fact is clearly illustrated in Figure 7 which summarizes data for Zone 02 of aircraft Group 5. Figure 7 covers data only in the frequency range below 500 cps, but data from [21] indicate the trend continues up to at least 2000 cps. These data support the conclusion that velocity transducers

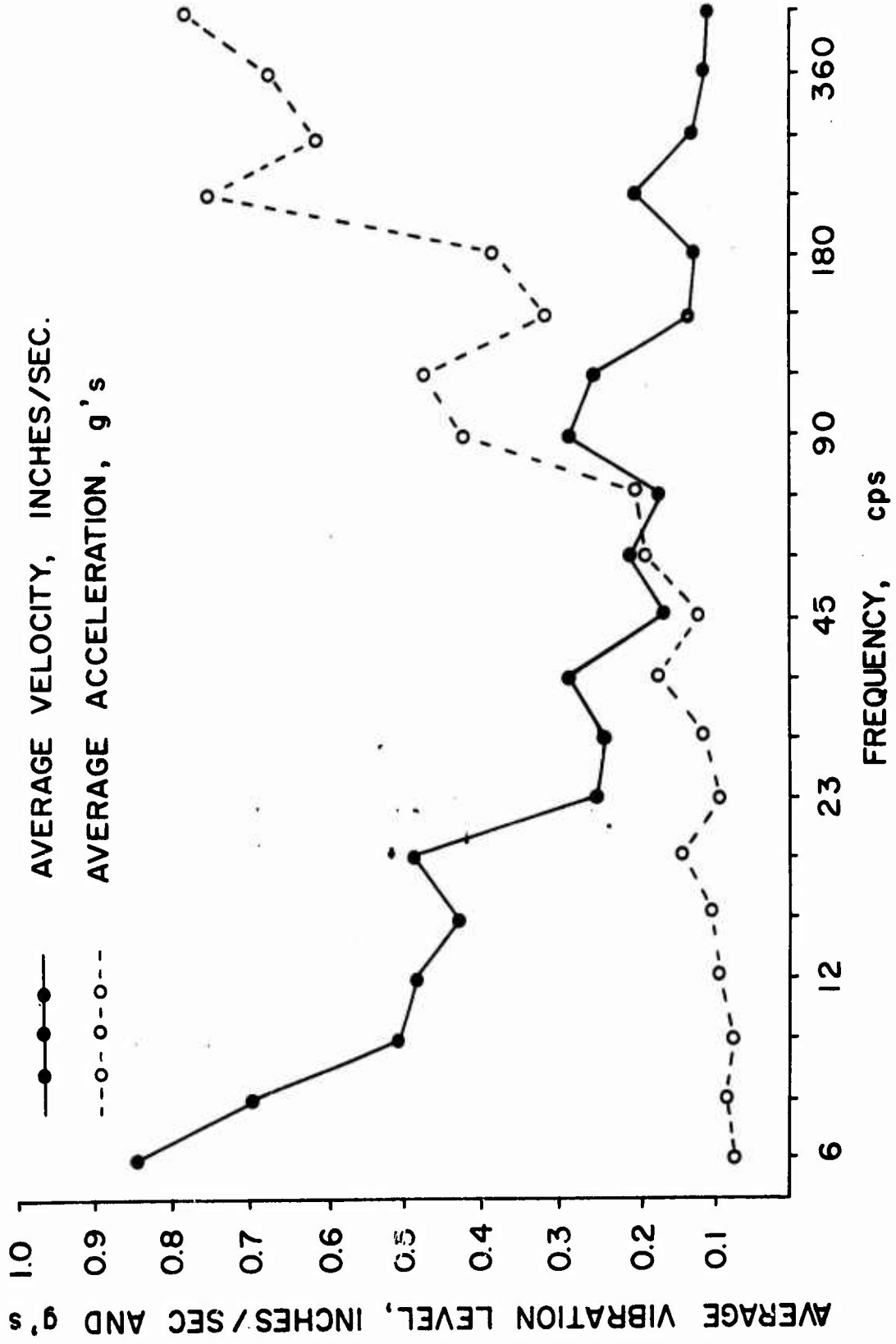


Figure 7. Velocity and Acceleration Spectra of Vibration Data for Zone 2 of Aircraft Group 5

produce data with a better signal-to-noise ratio at the lower frequencies and a poorer signal-to-noise ratio at the higher frequencies than would be obtained using acceleration transducers. From the developments in Section 3, the periodic contributions in aircraft vibration data occur principally in the frequency range below 300 cps, while the random contributions are prevalent in the frequencies above this range. Hence, the use of velocity transducers favors the periodic contributions over the random contributions. The use of accelerometers will generally produce the reverse situation. This is more desirable since periodic components can be retrieved by narrow bandwidth frequency analysis, even when they are well down into the data acquisition system noise. The random portions of the data, however, cannot be retrieved from the noise. Random signals can be extracted from random noise only by cross-correlation analysis with a noise-free replica of the random data.

5.1.2 Frequency Response for Velocity Transducers

The problem discussed in Section 5.1 is compounded by the frequency response characteristics of the velocity transducers. Referring to Figure 5, it is clear that the velocity transducer attenuates the signal being measured with increasing severity as the frequency increases above 100 cps. For example, at 2000 cps, the signal has been attenuated by more than 6 dB. However, the data acquisition system noise is not attenuated. Hence, the signal-to-noise ratio is further reduced at the higher frequencies where the random contributions in the data are prevalent.

5. 1. 3 Use of Fixed Sensitivity into all Channels of the Recorder

For all flight vehicle vibration surveys with velocity transducers, the sensitivities for the inputs to the 14-channel magnetic tape recorder were the same for all channels. Hence, the recorder sensitivities were established to measure the maximum signal level to be expected for any flight condition from any transducer mounted on the aircraft. This means that flight conditions and transducer locations of relatively low vibration severity resulted in transducer signals which were recorded well down from the maximum input level to the recorder. Since the recorder has a usable dynamic range of only 45 dB, these lower level signals were often recorded near or even below the noise level of the recorder. In such cases, the random portions of the signal were lost in the recorder noise. On the other hand, the periodic components were probably retrieved by the narrow bandwidth frequency analysis, as discussed in Section 5. 1. 1.

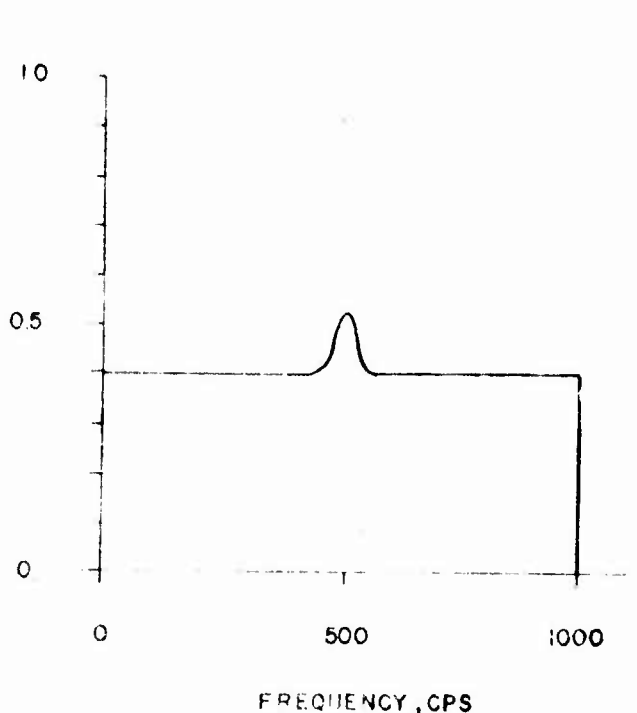
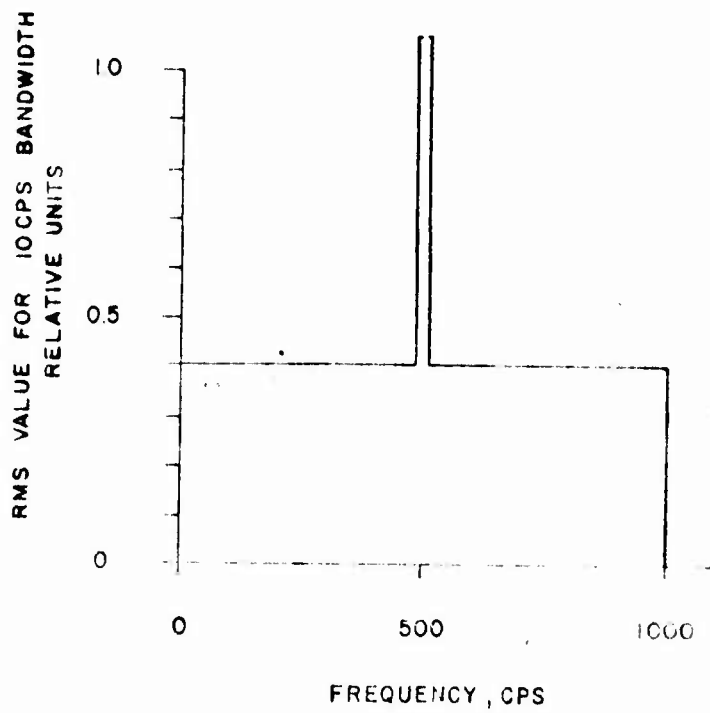
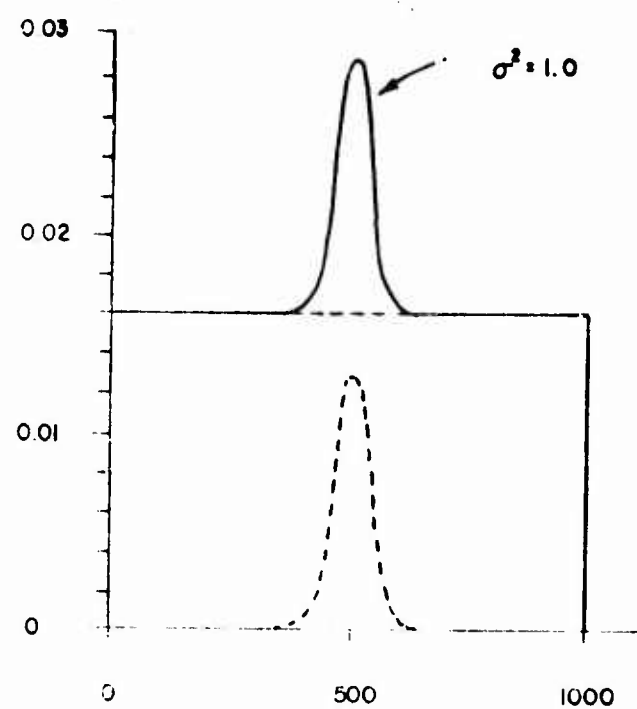
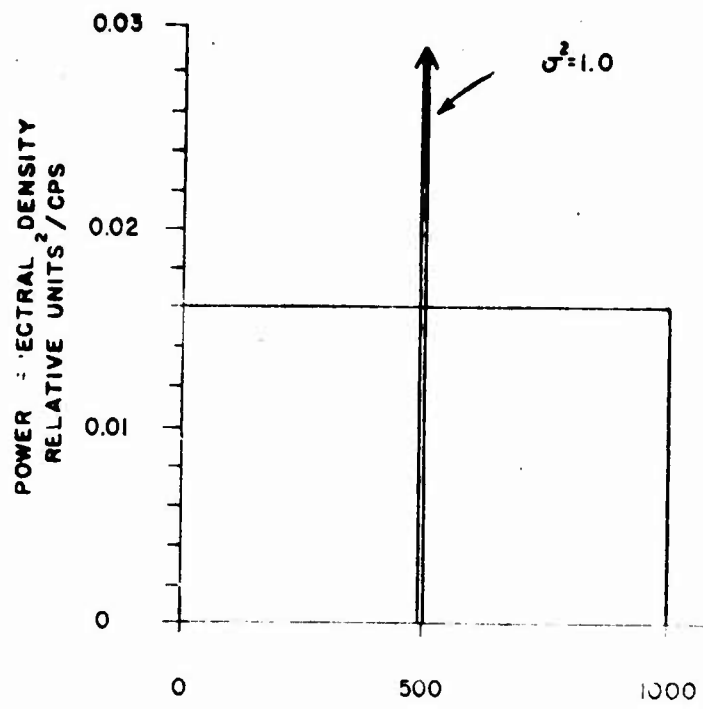
5. 1. 4 Data Analysis and Presentation Procedures

The principal problem is introduced by the procedure of reducing the data into discrete values for the significant observed spectral peaks. When a spectrum analysis is performed on any mixed signal consisting of random and periodic components, the periodic components tend to be more pronounced in the spectrum. This is due to the fact that the periodic components constitute finite amounts of energy in infinitesimally narrow bandwidths. Hence, when an analysis is performed using a narrow bandpass filter, the full magnitude of a periodic component will be passed by the filter, no matter how narrow the bandwidth may be. For random components, the mean square output of the narrow bandpass filter will be proportional to the bandwidth of the filter. Theoretically, the

periodic components in a mixed random and periodic signal will have infinite power spectral density at the frequency of the periodic components. In practice, the periodic components will not appear with infinite density, but they will appear with a very high density relative to the random components, assuming the analysis bandwidth is relatively narrow. This point is illustrated in Figure 8, which compares the analysis of a sine wave signal to that of a narrowband random signal of equal rms value and center frequency. The narrowband random signal represents the response of a 5% damped structural resonance to random excitation. In both cases, the signals are superimposed on band-limited white noise representing independent instrument noise. When these data are analyzed with a 10 cps wide filter (as was used for data analysis by AFFDL), the indicated spectral peak for the sine wave signal is 2.7 times (8.6 dB) higher than the background noise, while the spectral peak for the random signal is only 1.35 times (2.6 dB) higher than the background noise. Since the data reduction procedure requires a subjective opinion as to what constitutes a significant spectral peak, it is clear that peaks due to sine wave signals are more likely to be noted than peaks due to random signals.

5.2 LIMITATIONS IMPOSED ON DATA EVALUATION

At first glance, the discussions in Section 5.1 might imply that vibration data collected by AFFDL prior to the flight vibration survey of aircraft Code No. 63 (to be called the "previous data") are not usable for the statistical evaluations proposed herein. This conclusion, however, is not completely warranted. It certainly is true that the previous data are not suitable for the ultimate goal of developing a general prediction model for aircraft vibration, as described in Section 2. Nevertheless, the



(d) SINE WAVE SIGNAL IN NOISE

(e) NARROWBAND RANDOM SIGNAL IN NOISE

Figure 8. Illustration of Spectrum for Sine Wave and Random Signals in Noise

previous data are usable for estimating the periodic portions of the environment. Furthermore, they are useful for illustrating the various statistic evaluation techniques to be developed.

In light of the above discussions, the previously reduced data will be used to perform the homogeneity tests and spatial variation studies in Sections 6 and 7, where it is understood that the results are, at best, applicable only to the periodic portions of the aircraft vibration environment. Results for the random portion of the vibration environment must be determined from future data collected and analyzed using current equipment and procedures (similar to those employed for aircraft Code No. 63). The statistical procedures needed for the development of a general prediction model, covered in Section 8, will be illustrated using data from aircraft Code No. 63, only. The final development of a useful vibration prediction model will require considerable data from future aircraft vibration surveys.

6. HOMOGENEITY STUDIES

For simplicity, it would be desirable to have a single vibration prediction model apply to all structural locations of all aircraft. On the other hand, greater accuracy can usually be achieved by developing a separate model for various different structural locations and different aircraft. Clearly, a compromise is required. One method of approaching this compromise is to start with vibration data divided among the various structural locations and aircraft for which data have been obtained. These data can then be investigated for homogeneity (equivalence) to determine which structural locations and/or aircraft produce similar vibration. In this manner, the total number of classifications of data hopefully can be reduced to the minimum number needed to describe significant variations in the vibration environment. For the case of AFFDL, flight vibration data are initially classified by direction (vertical, lateral, and longitudinal), structural zone (see Table 8), and aircraft model and group (see Table 7). Hence, the homogeneity studies will start with the data divided among these various classifications.

Determining whether or not two sets of data are homogeneous is not as straightforward as it might appear at first glance. Remembering that the available data represent only finite samples of the vibration environment, it is not likely that two sets of data would be identical even if the data represented the same vibration environment. Some type of statistical hypothesis test is needed to determine if observed differences between two sets of data are actually significant, or simply the result of sampling errors. Such statistical tests are described and illustrated in Section 6.1. These tests are applied to all previous AFFDL vibration data in Section 6.2.

Note that the data used for these homogeneity studies do not properly describe the random portion of the aircraft vibration environment, as discussed in Section 5. Hence, at best, the conclusions will apply only to the periodic portion of aircraft vibration.

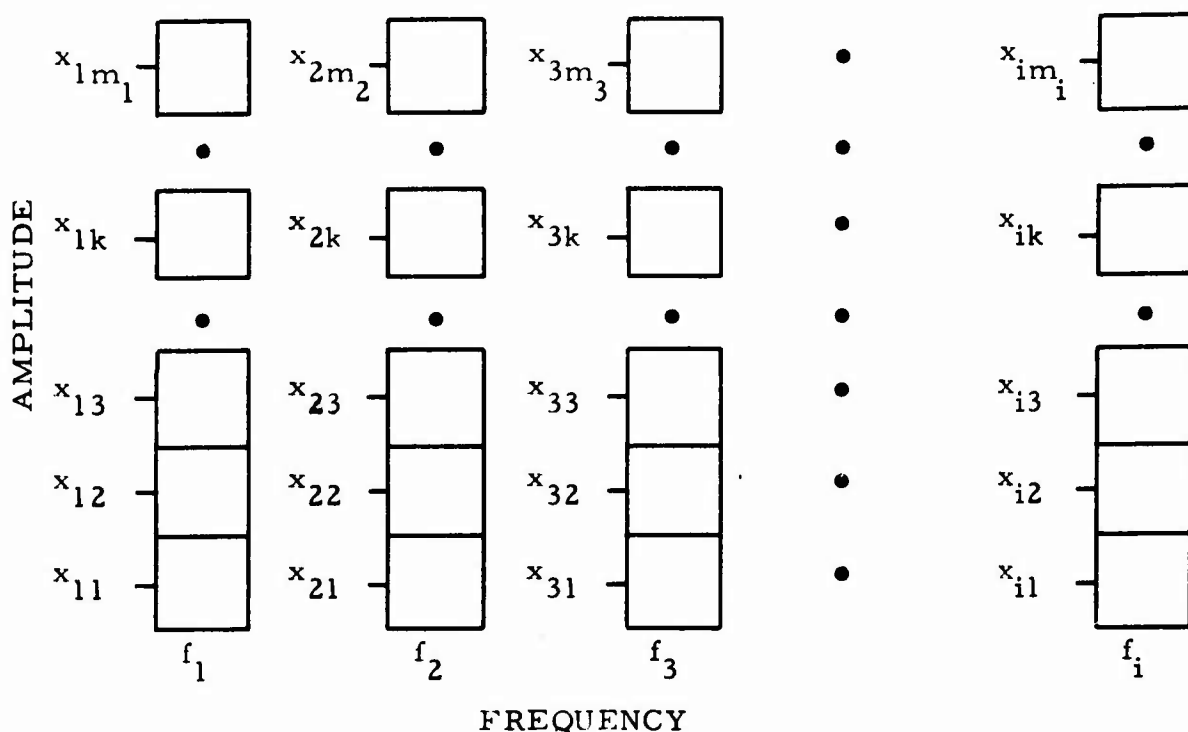
6.1 DEVELOPMENT OF TESTING PROCEDURES

There are numerous possible ways to test the homogeneity of sample data, but two specific procedures appear appropriate for the problem at hand. These procedures are (1) the chi-square test, and (2) the multiple rank test. Both of these testing procedures are now described and illustrated using AFFDL vibration data.

6.1.1 Chi-Square Test

Assume two or more sets of sample data are available which represent the structural vibration for two or more different situations of interest (different orthogonal directions, different zones, different aircraft within a group, or different aircraft groups). It is now desired to test the hypothesis that the two or more sets of sample data are from the same population. Let the data in the i th frequency interval be divided into m_i amplitude intervals, as illustrated in Table 10a. Furthermore, for any given frequency interval, let n_{jk} be the number of amplitude values in the k th amplitude interval for the j th set of data, as shown in Table 10b.

Table 10. Illustration of Data Format for Chi-Square Test



10a. Amplitude and Frequency Intervals for One Set of Data

Data Sets	Amplitude Intervals							Totals
	1	2	3	•	k	•	m	
1	n_{11}	n_{12}	n_{13}	•	n_{1k}	•	n_{1m}	n_1
2	n_{21}	n_{22}	n_{23}	•	n_{2k}	•	n_{2m}	n_2
3	n_{31}	n_{32}	n_{33}	•	n_{zk}	•	n_{3m}	n_3
•	•	•	•	•	•	•	•	•
j	n_{j1}	n_{j2}	n_{j3}	•	n_{jk}	•	n_{jm}	n_j
•	•	•	•	•	•	•	•	•
s	n_{s1}	n_{s2}	n_{s3}	•	n_{sk}	•	n_{sm}	n_s
Totals	$n_{.1}$	$n_{.2}$	$n_{.3}$	•	$n_{.k}$	•	$n_{.m}$	n

10b. Observed Number of Amplitude Values in One Frequency Interval for s Sets of Data

Now let P_{jk} be the true probability for an amplitude in the k th interval for the j th set of data. The maximum likelihood estimator for P_{jk} is given by

$$\hat{P}_{jk} = n_{jk}/n_j \quad (33)$$

The s sets of data will be homogeneous if $P_{1k} = P_{2k} = P_{3k} = \dots = P_{sk}$; $k = 1, 2, 3, \dots, m$.

For simplicity, consider the case where $s = 2$ (two sets of data are available). The homogeneity hypothesis is $P_{1k} = P_{2k}$; $k = 1, 2, 3, \dots, m$. Under this null hypothesis, the estimate of a common value for P_{1k} and P_{2k} , denoted by P_k , is

$$\hat{P}_k = n_{\cdot k}/n \quad (34)$$

where the notation $n_{\cdot k}$ means n_{jk} summed over j , $\left(n_{\cdot k} = \sum_{j=1}^2 n_{jk} \right)$.

The appropriate test statistic is then

$$\begin{aligned} X^2 &= \sum_{k=1}^m \frac{(n_{1k} - n_1 n_{\cdot k}/n)^2}{n_1 n_{\cdot k}/n} + \sum_{k=1}^m \frac{(n_{2k} - n_2 n_{\cdot k}/n)^2}{n_2 n_{\cdot k}/n} \\ &= \frac{1}{P(1-P)} \left(\sum_{k=1}^m n_{1k}^2/n_{\cdot k} - n_1 P \right) \end{aligned} \quad (35)$$

where $P = n_1/n$.

The X^2 statistic defined in Eq. (35) has a χ^2 distribution with $(m - 1)$ degrees-of-freedom for large n_1 and n_2 .

For the general case where s sets of sample data are to be compared, an overall test statistic is given by

$$X^2 = \sum_{j=1}^s \sum_{k=1}^m \frac{(n_{jk} - n_j n_{\cdot k}/n)^2}{n_j n_{\cdot k}/n} \quad (36)$$

The X^2 statistic now has a χ^2 distribution with $s(m - 1)$ degrees-of-freedom if n is large and $n_j n_{\cdot k}/n \geq 2$ for all j and k .

Example

Suppose that it is desired to test whether or not the distribution of vibration levels in Zone 01 is the same as that in Zone 02 in 400-499 cps frequency interval for Group 5 type aircraft. The results are presented in Table 11a. In order to satisfy the condition that $n_j n_{\cdot k}/n \geq 2$, it is necessary to pool classes 10, 11, and 12 together. Then the results in Table 11b are obtained.

From Table 11, $P = 266/328 = 0.811$. Hence, using Eq. (35),

$$X^2 = \frac{1}{P(1 - P)} \left(9 \frac{9}{17} + 21 \frac{21}{31} + \dots + 20 \frac{20}{20} - 266 P \right)$$

$$= (6.524)(6.413) = 41.88$$

Table 11. Illustration of Chi-Square Test for Homogeneity

Table 11a. Data for Group 5 Aircraft

Sets (Zones)	Amplitude Intervals, 10^{-5} inches												Total
	4	5	$\frac{6}{7}$	$\frac{8}{9}$	$\frac{10}{12}$	$\frac{13}{19}$	$\frac{20}{24}$	$\frac{25}{31}$	$\frac{32}{39}$	$\frac{40}{50}$	$\frac{51}{63}$	$\frac{64}{80}$	
01	9	21	53	30	41	42	17	12	21	15	3	2	266
02	8	10	25	8	8	2	1						62
$n_{\cdot k}$	17	31	78	38	49	44	18	12	21	15	3	2	328

Table 11b. Pooled Data for Group 5 Aircraft

Sets (Zones)	Amplitude Intervals, 10^{-5} inches											Total
	4	5	$\frac{6}{7}$	$\frac{8}{9}$	$\frac{10}{12}$	$\frac{13}{19}$	$\frac{20}{24}$	$\frac{25}{31}$	$\frac{32}{39}$	$\frac{40}{50}$		
01	9	21	53	30	41	42	17	12	21	20	266	
02	8	10	25	8	8	2	1				62	
$n_{\cdot k}$	17	31	78	38	49	44	18	12	21	20	328	

The 5th percentage point (95th percentile) of the χ^2 distribution with 9 degrees of freedom equals 16.9. Since $41.88 > 16.9$, the hypothesis that Zone 01 and Zone 02 of aircraft Group 5 have the same distribution in the 400-499 cps frequency interval would be rejected at the 5% level of significance.

6.1.2 Multiple Rank Test

The χ^2 test discussed in Section 6.1.1 can be used to simultaneously test more than two sets of data for homogeneity. The result of the test, however, is a simple "yes" or "no." For the case of a "no" answer (rejection of the homogeneity hypothesis), there is no information provided as to which set or sets of data are nonhomogeneous. This problem could be overcome by performing individual χ^2 tests on combinations of sets taken two at a time. Another approach which is considered more suitable is to use a nonparametric rank test. A rank test will reveal not only an overall lack of homogeneity among s sets of data, but also which of the sets are nonhomogeneous with the others. On the other hand, it should be noted that a rank test is less "powerful" than a χ^2 test; that is, the rank test involves a greater risk of accepting a false hypothesis.

Consider the case where $s \geq 2$ sets of sample data are to be compared. Let the sample size for the j th set be n_j . Now, take all of the sample values as a whole and arrange them in order of increasing numerical value (rank), as illustrated on the next page. When two samples have the same numerical value (a tie), the average rank is assigned to both values.

Rank	1	2	3	4	5	6	7	8	9	...	n_j
Value	x_9	x_5	y_2	x_7	z_1	z_8	x_2	x_1	y_7	...	z_4

x = numerical values from set 1
 y = numerical values from set 2
 z = numerical values from set 3

Let T_j be the sum of the ranks for the sample values of the j th set of data. Any two sets of data can be compared using the statistic

$$d = T_j/n_j - T_u/n_u \quad ; \quad j \neq u \quad (37)$$

To be more general, assume s_1 sets of data are to be compared to s_2 different sets of data. The desired statistic is now

$$\begin{aligned}
 d = & \left(T_1 + \dots + T_{s_1} \right) / \left(n_1 + \dots + n_{s_1} \right) \\
 & - \left(T_{1'} + \dots + T_{s_2'} \right) / \left(n_{1'} + \dots + n_{s_2'} \right) \quad (38)
 \end{aligned}$$

From [32], the statistic d has a normal distribution with a mean value of zero and a variance of

$$\sigma_d^2 = \left(\frac{n(n+1)}{12} - \frac{\sum_{v=1}^r t_v^3 - \sum_{v=1}^r t_v}{12(n-1)} \right) \left(\frac{1}{\sum_{j=1}^{s_1} n_j} + \frac{1}{\sum_{u=1}^{s_2} n_u} \right) \quad (39)$$

where $n = \sum_{j=1}^{s_1} n_j + \sum_{u=1}^{s_2} n_u$, and t_v is the number of tied scores in the v th rank. For example, the variance of d given by Eq. (37) is

$$\sigma_d^2 = \left(\frac{n(n+1)}{12} - \frac{\sum_{v=1}^r t_v^3 - \sum_{v=1}^r t_v}{12(n-1)} \right) \left(\frac{1}{n_j} + \frac{1}{n_u} \right) \quad (40)$$

Hence, a null hypothesis of homogeneity can be tested using standard normal distribution tables where the critical region is given by

$$\left| d/\sigma_d \right| > z_{\alpha/2p} \quad (41)$$

Here, $z_{\alpha/2p}$ is $\alpha/2p$ percentage point of the standardized normal distribution and p is the number of (multiple) comparisons.

To illustrate these ideas, assume there are three sets of data to be compared. Further assume it is desired to compare the first set of data with the second and third combined, the first and the third with the second, and the first with the third. The statistics to be calculated are then

$$d_1 = T_1/n_1 - (T_2 + T_3)/(n_2 + n_3)$$

$$d_2 = (T_1 + T_3)/(n_1 + n_3) - T_2/n_2$$

$$d_3 = T_1/n_1 - T_3/n_3$$

Example

The Rank Sum Test is now illustrated using the same data used to illustrate the χ^2 test in Section 6.1.1. Here, $s = 2$ and $p = 1$. The necessary calculations are summarized in Table 12.

Table 12. Illustration of Rank Sum Test

Amplitude Intervals 10 ⁻⁵ inches	Number of Observed Sampled Values		Total Number (t _v)	Cumulative Number	Average Rank*	Rank Number	
	Zone 01	Zone 02				Zone 01	Zone 02
4	9	8	17	17	9.0	81	72
5	21	10	31	48	33.0	693	330
6-7	53	25	78	126	87.5	4637.5	2187.5
8-9	30	8	38	164	145.5	4365	1164
10-12	41	8	49	213	189.0	7749	1512
13-19	42	2	44	257	235.5	9891	471
20-24	17	1	18	275	266.5	4530.5	266.5
25-31	12		12	287	281.5	3378	0
32-39	21		21	308	298.0	6258	0
40-50	15		15	323	316.0	4740	0
51-63	3		3	326	325.0	975	0
64-80	2		2	328	327.5	655	0
	<u>266</u>	<u>62</u>	<u>328</u>			<u>47953</u>	<u>6003</u>

*Computed as follows:

$$(17 + 1)/2 = 9.0; 17 + (48 - 17 + 1)/2 = 33.0; 48 + (126 - 48 + 1)/2 = 87.5, \text{ etc.}$$

From Table 12, it follows that

$$d = 47953/266 - 6003/62 = 180.27 - 96.82 = 83.45$$

$$\sigma_d^2 = \left[\frac{(328)(329)}{12} - \frac{787,192-328}{(12)(327)} \right] \left[\frac{1}{266} + \frac{1}{62} \right] = 174.86$$

and hence

$$d/\sigma_d = 83.45/13.22 = 6.31$$

Since $6.31 > 1.645$, the hypothesis that the vibration in Zones 01 and 02 of aircraft Group V have the same distribution in 400 to 499 cps frequency interval is rejected at the 5% level of significance.

6.2 APPLICATION TO AFFDL VIBRATION DATA

As previously mentioned, the aircraft vibration data collected by AFFDL is initially classified in terms of direction, structural zone, and aircraft model and group. These various classifications will be used as the basis for homogeneity studies. The rank sum test described in Section 6.1.2 will be used for the desired comparisons, as required. To assure consistency in the data used for the comparisons, only that data obtained from velocity transducers will be employed. This eliminates all data collected on aircraft Code Nos. 62 and 63. Furthermore, only data in the first six structural zones (Zone Code Nos. 01 through 06) will be used. These six zones cover the basic aircraft structure, which is of principal interest. Separate tests will be performed on the data in each of 20 contiguous frequency increments which together cover the frequency range from 5 to 500 cps. For simplicity in later presentations, these various frequency increments, as well as the different directions, aircraft, and structural zones, will be identified by a code number. These code numbers are summarized in Table 13.

6.2.1 Comparisons of the Three Orthogonal Directions

Consider first the vibration levels measured along the three orthogonal axes. The question of interest is as follows. Are there significant differences among the vibration levels measured in aircraft along the vertical, lateral, and longitudinal directions? To answer this question, rank sum tests are applied to the data segregated among the three orthogonal directions. Separate tests are performed on the data for each frequency increment and for each aircraft group. The

Table 13. Summary of Data Codes for Homogeneity Tests

Frequency Codes		Direction Codes		Aircraft Codes*			Structural Zone Codes*	
Frequency Interval cps	Code Number	Direction	Code Number	Group Number	Aircraft	Code Number	Structural Zone	Code Number
5-6	1	Vertical	1	1	C-123	38	Forward quarter of fuselage	01
7-8	2	Lateral	2	2	C-130	40	Center half of fuselage	02
9-10	3							
11-13	4	Longitudinal	3	2	C-133	47	Aft quarter of fuselage	03
14-16	5							
17-20	6							
21-25	7	Stabilizers, rudder, and elevators	3	3	JRB-52	36	Outer one-third of wing	04
26-32	8							
33-39	9							
40-49	10							
50-64	11							
65-79	12							
80-99	13							
100-129	14							
130-159	15							
160-199	16							
200-249	17	Inner two-thirds of wing	5	5	F-100C	42	Outer one-third of wing	05
250-319	18							
320-399	19							
400-499	20							
				10	H-37	49		

* The aircraft and structural zone code numbers are AFFDL designations summarized previously in Tables 7 and 8.

data for the different structural zones, different aircraft within a group, and different flight conditions are pooled together for the tests to maximize the sample size. This pooling is considered appropriate since vertical, lateral, and longitudinal measurements were made in all zones of all aircraft for all flight conditions. Note that only data from tri-axial measurement locations are used to avoid possible bias in the results.

The detailed results of the homogeneity tests are presented in Section 1 of Appendix A, and summarized in Table 14. The results are presented in terms of relative severity (A, B, C) versus frequency for the vibration measured in the three directions for each aircraft group. A common level of severity is assigned to those data which are found to be homogeneous at the 1% level of significance. For example, if the vibration in the vertical and lateral directions are found to be equivalent at the 1% level of significance, and the vibration in the longitudinal direction is found to be significantly lower, then the vertical and lateral vibration are identified as A and the longitudinal vibration is identified as B.

The rank sum tests establish only the relative severity of the data and not their absolute value. An absolute measure of the data severity is given by the mean value and standard deviation versus frequency for the vibration measured in the three directions for each aircraft group. These statistical measures are calculated in Section 4 of Appendix A, and summarized in Figure 9. Note that the results in Figure 9 do not consider possible homogeneity. The sample sizes for the mean value and standard deviation calculations vary from 4 to 4800, depending upon the direction, frequency increment, and aircraft group. Hence, a large indicated difference in two mean values may not be significant in some

Table 14. Rank Sum Test Results for Direction Comparisons

Frequency Increment	Aircraft Group 1			Aircraft Group 2			Aircraft Group 3			Aircraft Group 5			Aircraft Group 10		
	Direction			Direction			Direction			Direction			Direction		
	1	2	3	1	2	3	1	2	3	1	2	3	1	2	3
1	A	C	B	A	B	B	A	A	B	A	A	B	A	A	A
2	A	B	A	A	B	B	A	A	B	B	A	C	A	A	A
3	A	A	A	A	B	B	A	A	B	B	B	B	A	A	A
4	A	A	A	A	B	B	A	A	B	B	B	B	A	A	A
5	A	A	A	A	B	B	A	A	B	B	B	B	A	A	A
6	A	B	A	A	C	B	A	A	A	A	A	A	B	A	B
7	A	A	A	A	A	B	A	A	A	A	A	A	A	A	C
8	A	A	A	A	A	B	A	A	A	A	A	A	A	A	A
9	A	A	A	A	A	B	A	A	A	A	A	A	A	A	A
10	A	A	A	A	A	B	A	A	A	A	A	A	A	A	A
11	A	B	A	A	A	B	A	A	A	A	A	A	A	A	A
12	A	B	A	A	A	B	A	A	A	A	A	A	A	A	A
13	A	A	A	A	A	B	A	A	A	A	A	A	A	A	A
14	A	B	A	A	A	B	A	A	A	A	A	A	A	A	A
15	B	C	A	A	A	B	A	A	A	A	A	A	A	A	A
16	B	B	A	A	A	B	A	A	A	A	A	A	A	A	A
17	B	A	B	A	A	B	A	A	A	A	A	A	A	A	A
18	A	A	A	A	A	B	A	A	A	A	A	A	A	A	A
19	A	A	A	A	A	B	A	A	A	A	A	A	A	A	A
20	A	A	A	A	A	B	A	A	A	A	A	A	A	A	A

Direction 1 — Vertical
 Direction 2 — Lateral
 Direction 3 — Longitudinal

A — most severe
 B — next most severe
 C — least severe

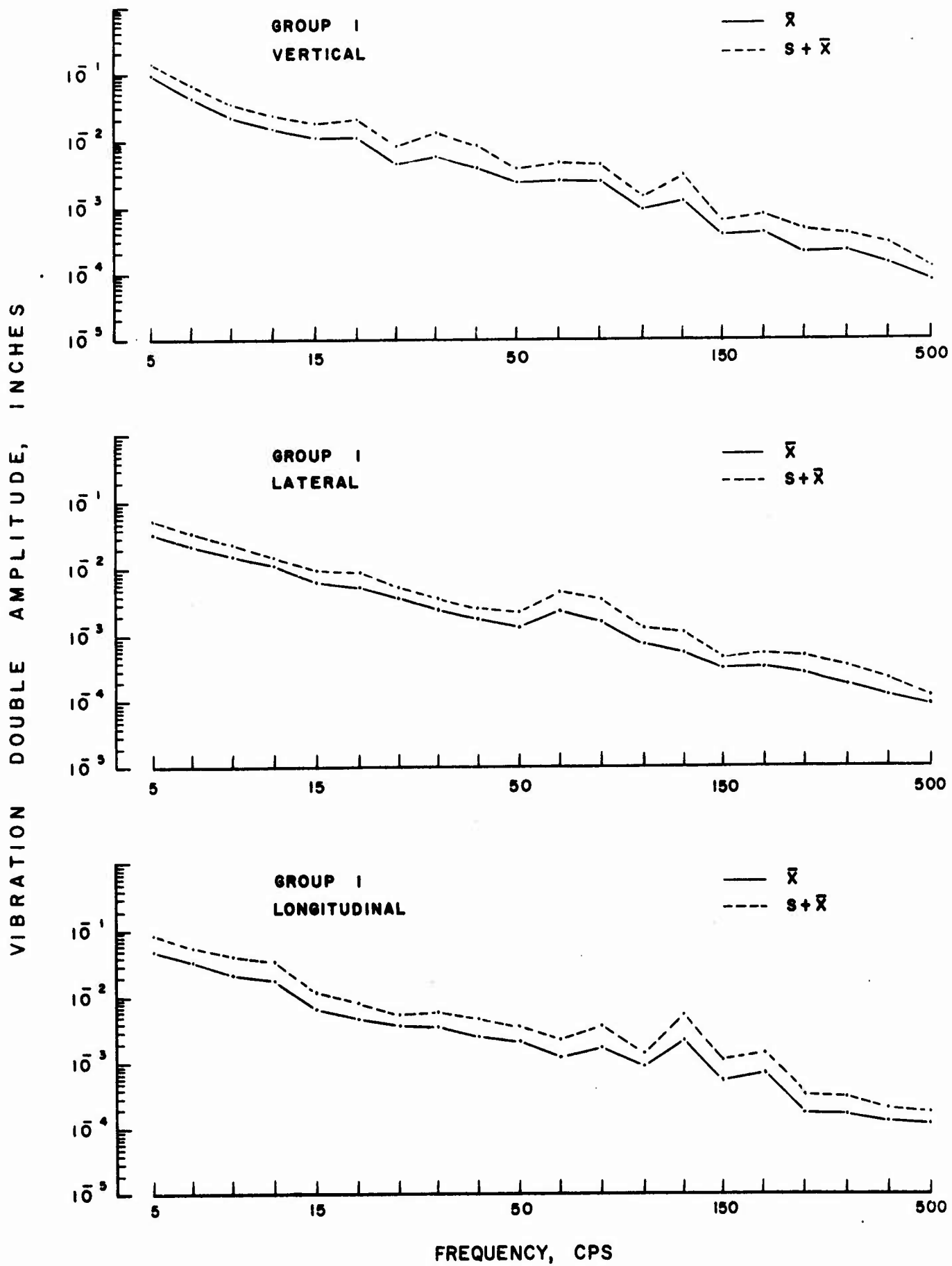


Figure 9a. Mean Values and Standard Deviations for the Vibration in the Three Orthogonal Directions for Aircraft Group 1

VIBRATION DOUBLE AMPLITUDE, INCHES

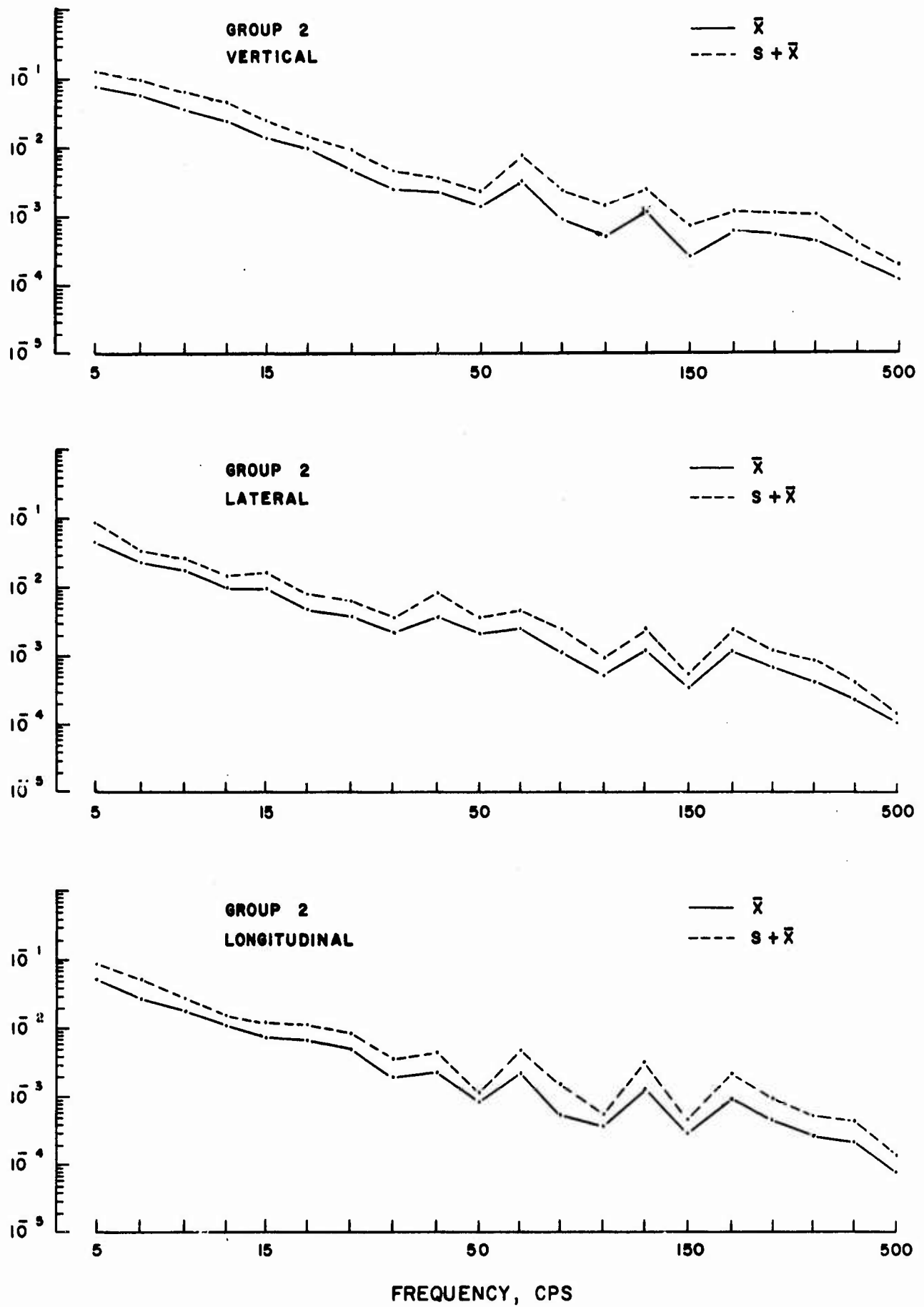


Figure 9b. Mean Values and Standard Deviations for the Vibration in the Three Orthogonal Directions for Aircraft Group 2

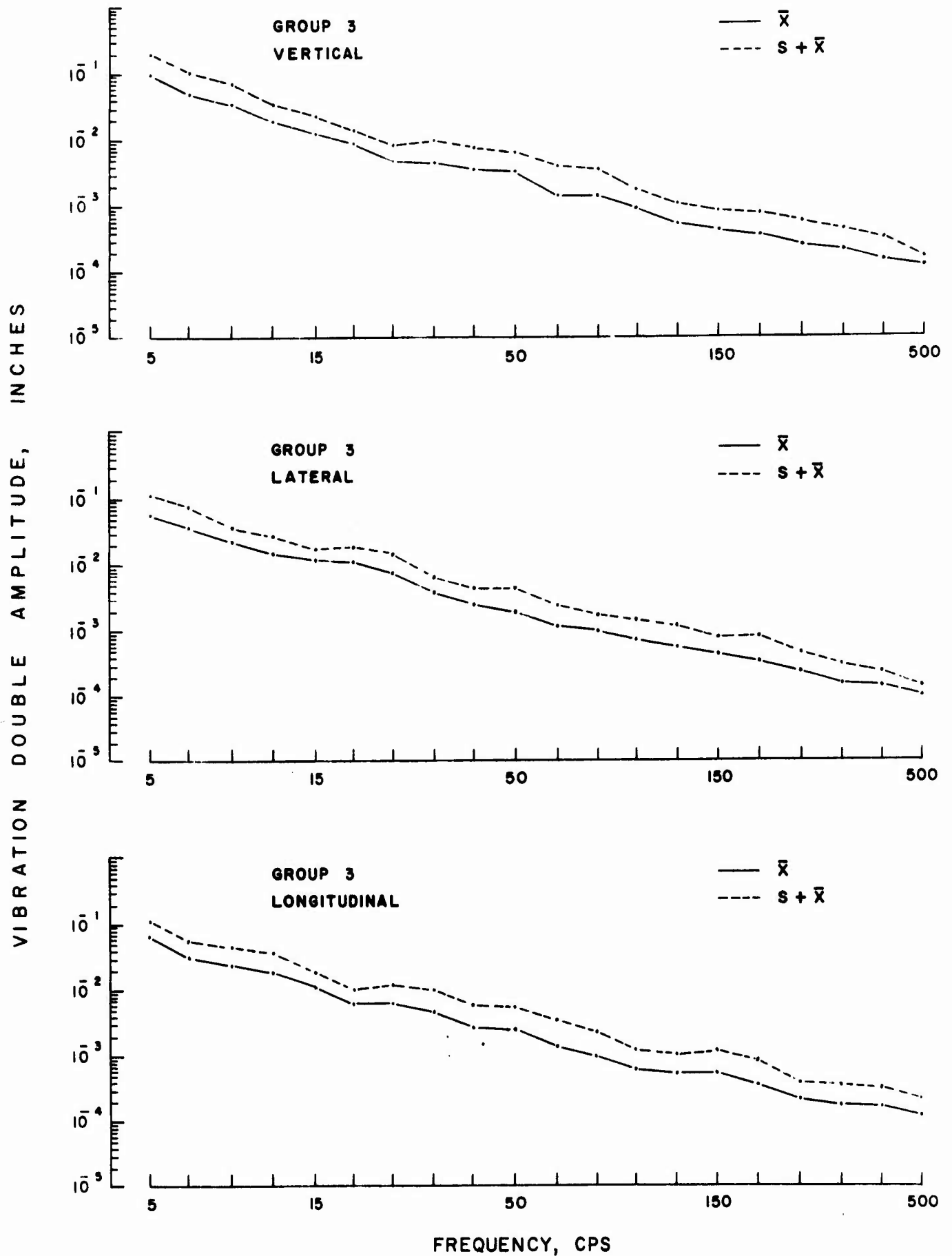


Figure 9c. Mean Values and Standard Deviations for the Vibration in the Three Orthogonal Directions for Aircraft Group 3

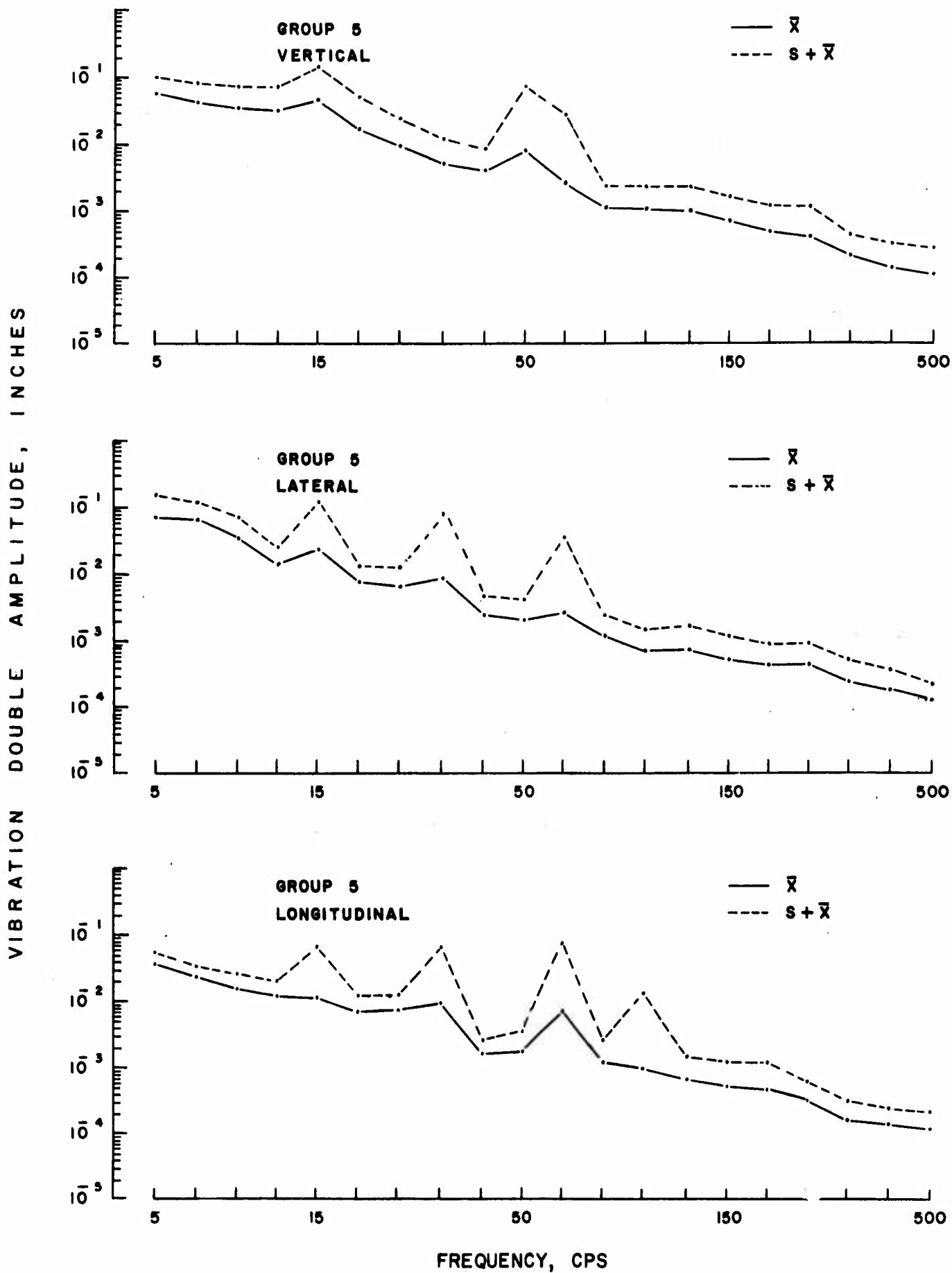


Figure 9d. Mean Values and Standard Deviations for the Vibration in the Three Orthogonal Directions for Aircraft Group 5

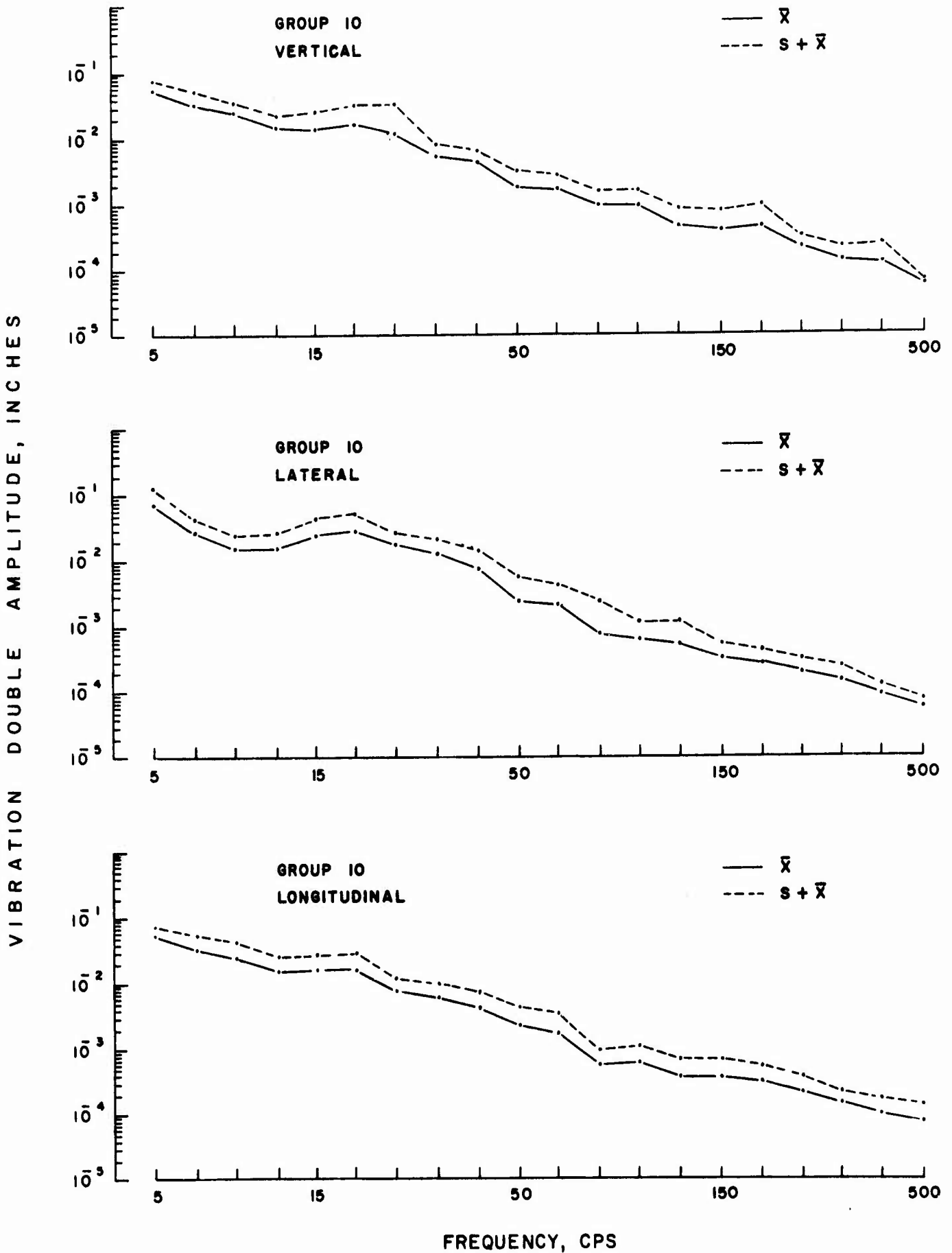


Figure 9e. Mean Values and Standard Deviations for the Vibration in the Three Orthogonal Directions for Aircraft Group 10

cases, while a small indicated difference might be significant in other cases. The results in Figure 9 can only be interpreted based upon the conclusions in Table 14. This is done in Figure 10.

Figure 10 summarizes the mean value versus frequency for the vibration measured in the three directions for each aircraft group, where homogeneous data are pooled and identified by a single mean value. Hence, all differences indicated in Figure 10 are significant differences in the statistical sense.

Inspection of the results in Figure 10 immediately reveals an important conclusion. Specifically, aircraft vibration levels measured along the three orthogonal axes appear to be quite similar on the average. From Figure 10a, for aircraft Group 1 (reciprocating engine transports), the vibration in the vertical direction is somewhat higher than in the lateral and longitudinal directions for frequencies between 50 and 80 cps. This is the frequency range for blade passage excitation. On the other hand, the longitudinal vibration appears to be the highest between 100 and 200 cps. From Figure 10b, for aircraft Group 2 (turboprop transports), the vertical vibration is consistently higher for frequencies below 20 cps, while the lateral vibration is usually the most severe for frequencies above 50 cps. From Figure 10c, for aircraft Group 3 (jet bombers), the vibration levels are surprisingly similar in all three directions over the entire frequency range. From Figure 10d, for aircraft Group 5 (century series fighters), there is a clear tendency for the most severe vibration to be in the vertical direction for frequencies below 200 cps, and in the lateral direction for frequencies above 200 cps. From Figure 10e, for aircraft Group 10 (helicopters), the vibration is most intense in the lateral direction for frequencies from 14 to 40 cps, and in the

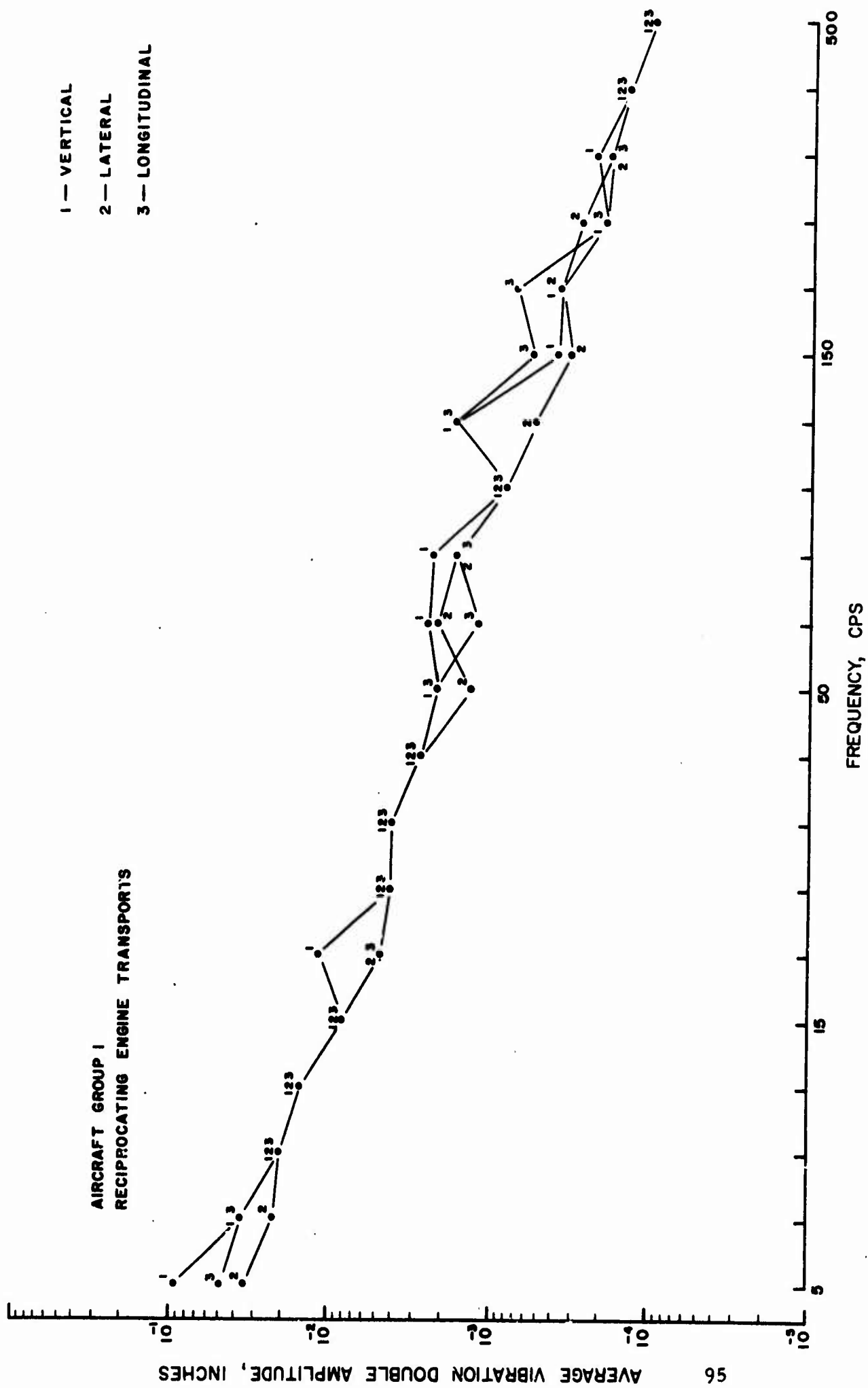


Figure 10a. Summary of Average Vibration in the Three Orthogonal Directions for Aircraft Group 1

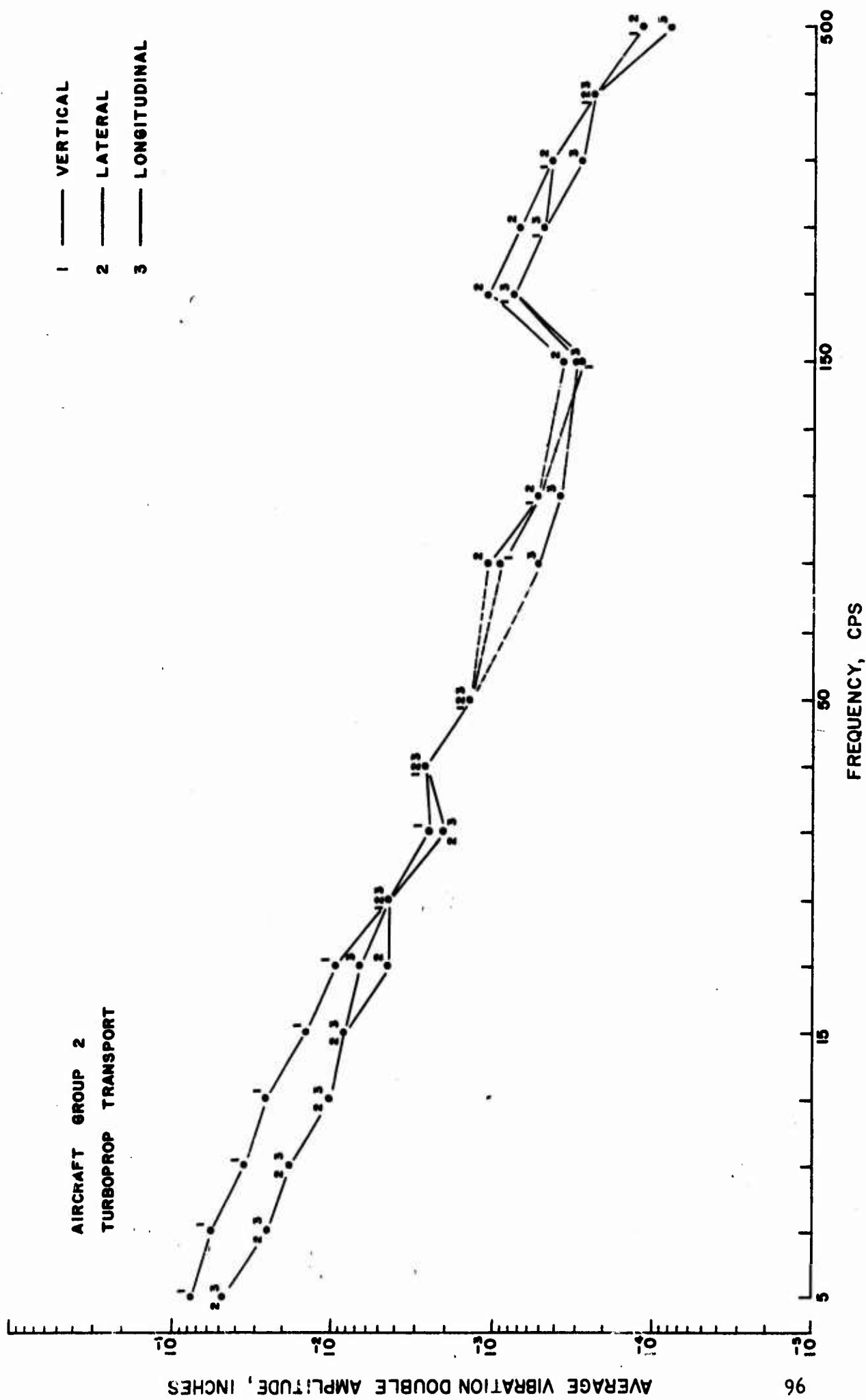


Figure 10b. Summary of Average Vibration in the Three Orthogonal Directions for Aircraft Group 2



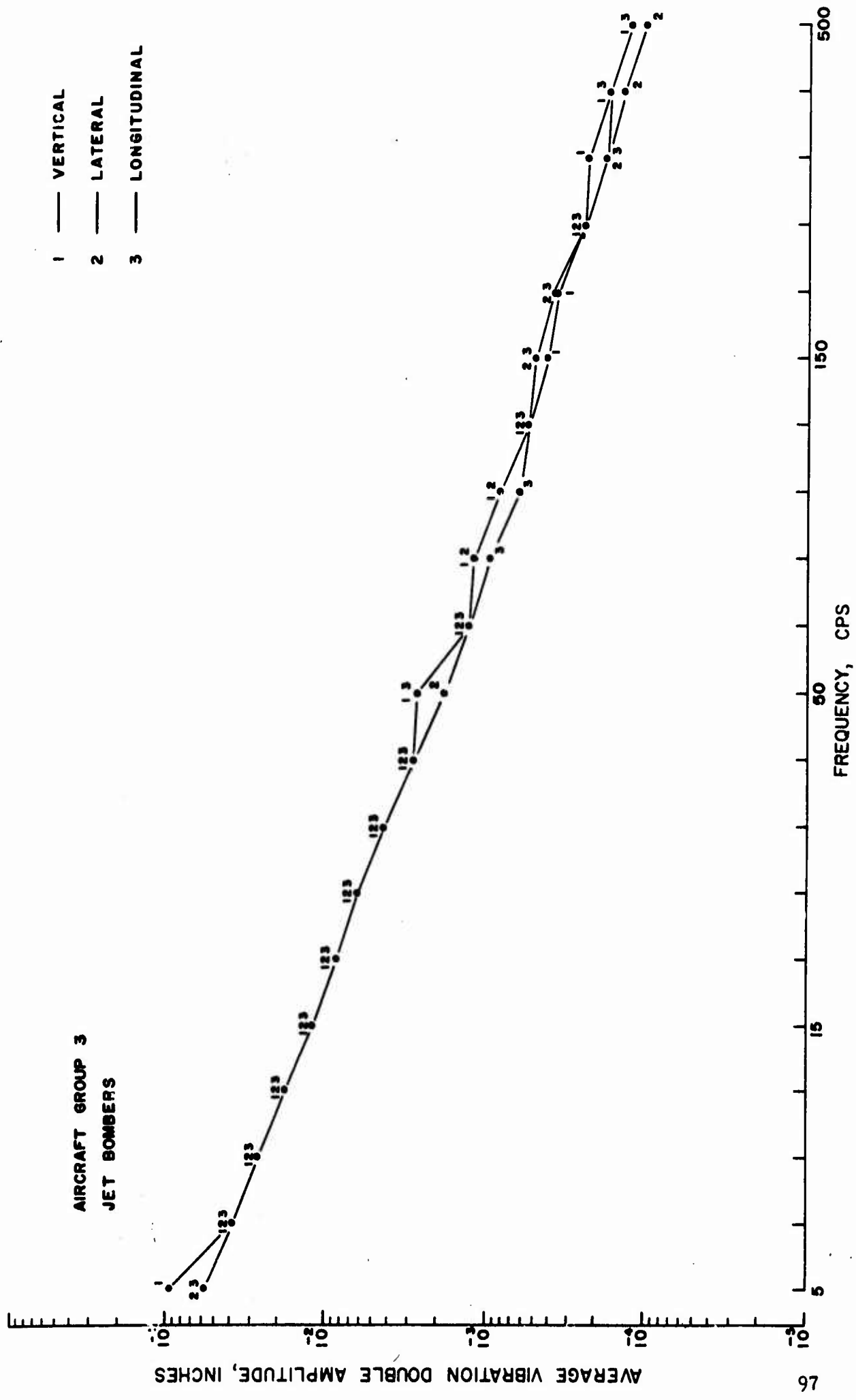


Figure 10c. Summary of Average Vibration in the Three Orthogonal Directions for Aircraft Group 3

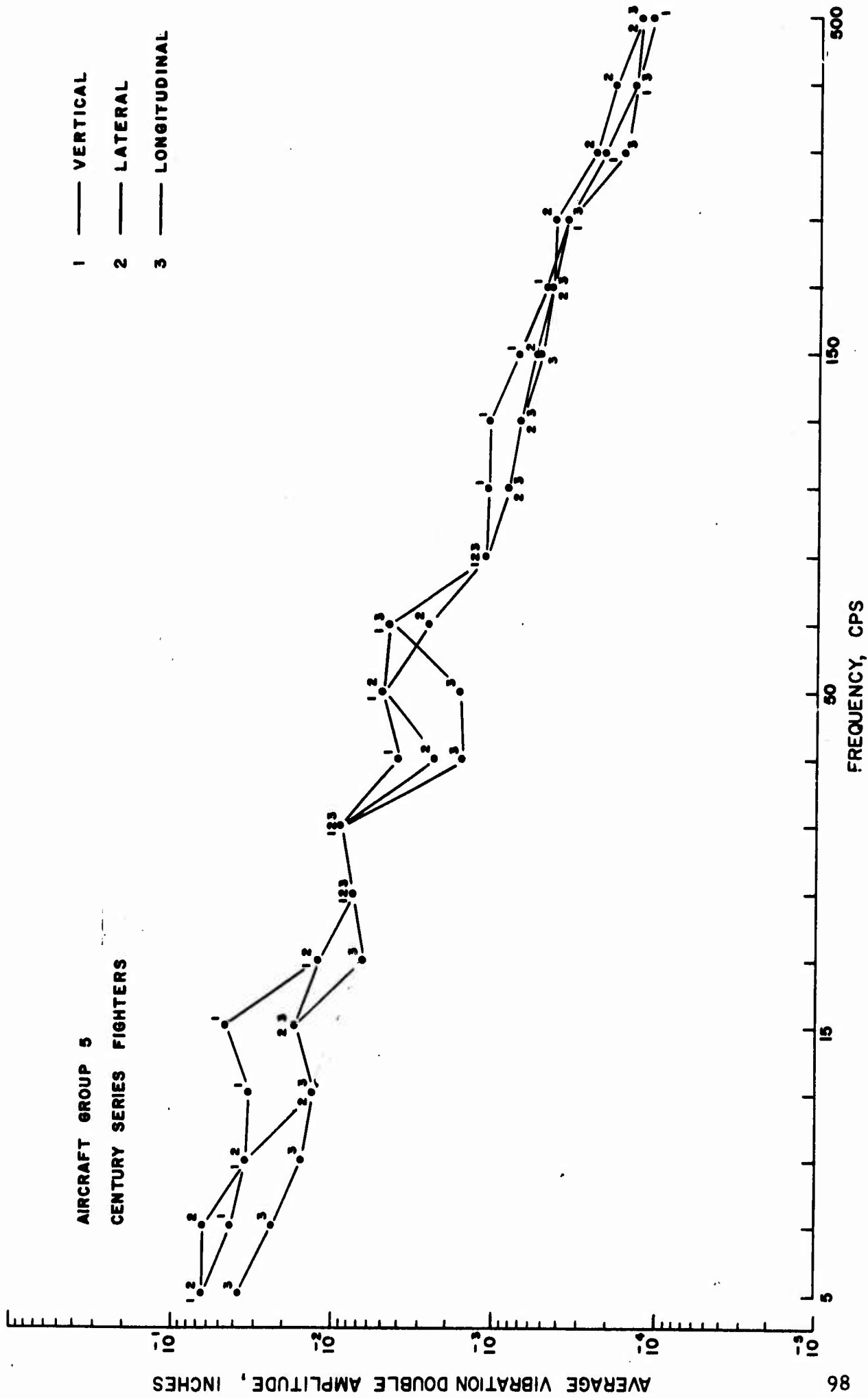


Figure 10d. Summary of Average Vibration in Three Orthogonal Directions for Aircraft Group 5

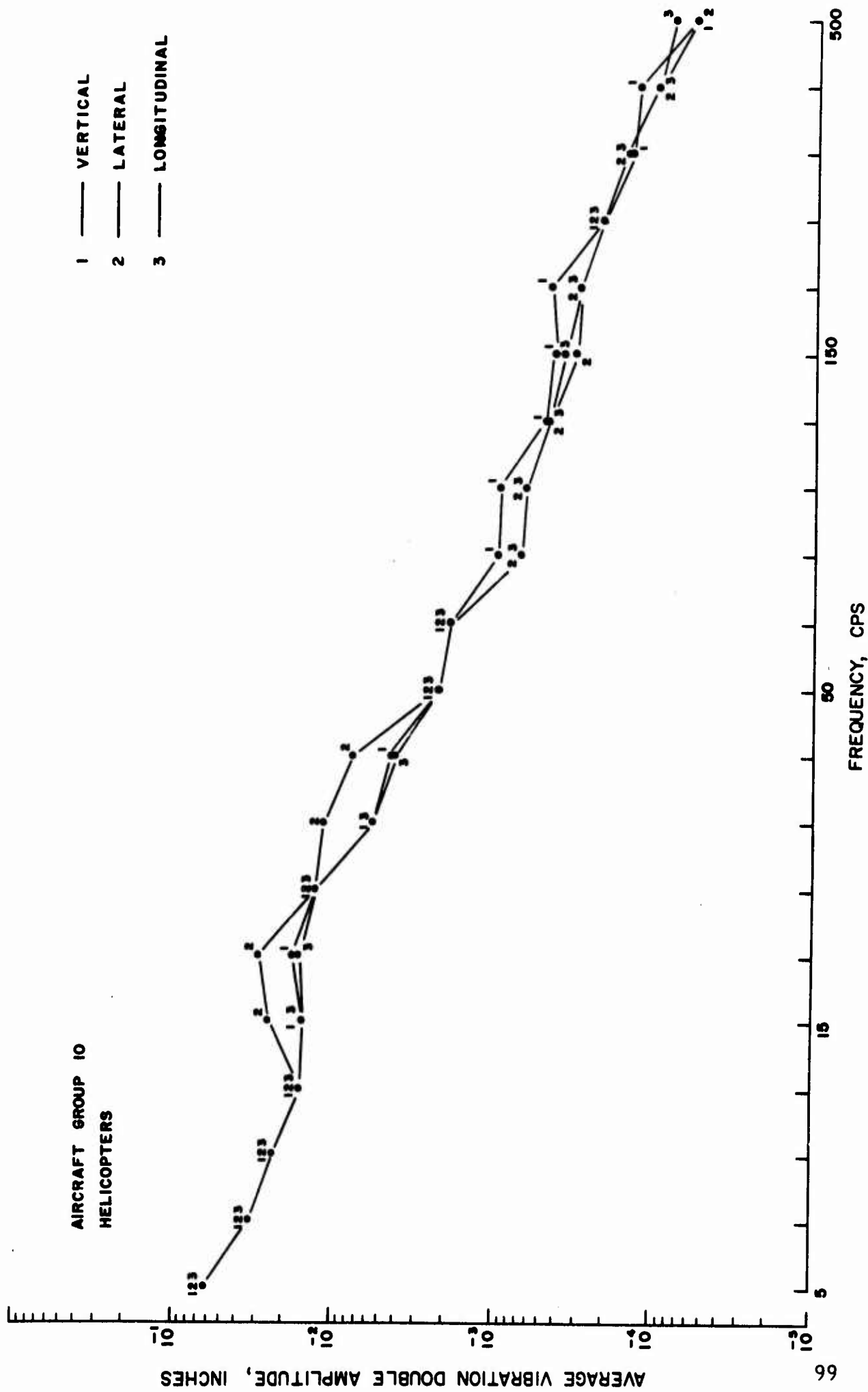


Figure 10e. Summary of Average Vibration in Three Orthogonal Directions for Aircraft Group 10

vertical direction for most frequencies above 65 cps. For all aircraft groups, however, the differences from lowest to highest average levels at any frequency are usually less than two to one (6 dB).

The results in Figure 10 have definite implications to the data acquisition problem, as well as to the test specification design problem. First, AFFDL customarily collects triaxial measurements at most measurement locations during a flight vibration survey. Since the vibration in the three orthogonal directions is so similar on the average, it appears that a more appropriate procedure might be to collect single direction measurements at three times as many locations. The measurement locations would be divided equally on a random basis, among vertical, lateral, and longitudinal measurements. This should greatly increase the amount of significant data obtained from a given survey. Second, the vibration test specifications in MIL STD 810B do not differentiate among the three orthogonal directions (the test levels are the same for vertical, lateral, and longitudinal vibration). Since the average differences in the vibration along the three directions are probably small relative to other uncertainties in the test specification, it appears that this is an acceptable procedure for testing aircraft components.

It should be emphasized that the above conclusions apply to the periodic portion of the vibration environments on the basic aircraft structure (Zones 01 through 06). The extension of these conclusions to the random portion of the environment will require a similar analysis of future data which properly represent the random contributions in the environment.

One final point should be noted. For the analyses in this section, the vibration data were divided among the three orthogonal directions relative to the aircraft reference frame. This is considered proper since

vibration tests are performed using excitation applied sequentially in these three directions. Another method of direction classification, however, would be in terms of two directions; namely, perpendicular to the structure and tangential to the structure. For example, a vertical measurement on the bottom of the aircraft fuselage would be perpendicular, while a vertical measurement on the sidewall of the aircraft fuselage would be tangential. If the AFFDL data were classified in terms of perpendicular and tangential directions, it is quite likely that different results would be obtained. Specifically, the perpendicular measurements would probably be substantially higher than the tangential measurements.

6.2.2 Comparisons of the Various Structural Zones

Now consider the vibration levels measured in the basic structural zones (Zones 01 through 06). The question of interest is as follows. Are there significant differences among the vibration levels measured in the basic structural zones of aircraft as defined by AFFDL? The answer to this question is pursued using procedures similar to those employed in Section 6.2.1. Rank sum tests are applied to the data segregated among the various structural zones. Separate tests are performed on the data for each frequency increment and for each aircraft group. The data for different orthogonal directions, different aircraft within a group, and different flight conditions are pooled together for the tests to maximize the sample size.

The detailed results of the homogeneity tests are presented in Section 2 of Appendix A, and summarized in Table 15. As before, the results are presented in terms of relative severity versus frequency for the various structural zones in each aircraft group. A common level of

Table 15. Rank Sum Test Results for Zone Comparisons

Frequency	Aircraft Group 1						Aircraft Group 2						Aircraft Group 3						Aircraft Group 5						Aircraft Group 10		
	Zone						Zone						Zone						Zone						Zone		
	01	02	03	05	06		01	02	03	05		01	02	03	04	05	06	01	02	03	04	05	06	01	02	03	
1	B	A	A	A	B	B	A	A	A	A	B	A	A	A	A	A	A	A	A	A	A	A	B	A			
2	A	A	A	A	A	B	A	A	A	A	A	A	A	A	A	A	A	A	A	A	A	A	A	A	A		
3	A	A	A	A	A	B	A	A	A	A	A	A	A	A	A	A	A	A	A	A	A	A	A	A	A		
4	A	A	A	A	A	B	A	A	A	A	A	A	A	A	A	A	A	A	A	A	A	A	A	A	A		
5	B	A	A	A	B	A	A	A	A	A	A	A	A	A	A	A	A	A	A	A	A	A	A	A	A		
6	A	A	A	A	A	C	B	A	A	A	A	A	A	A	A	A	A	A	A	A	A	A	A	A	A		
7	A	A	A	A	A	C	B	A	A	A	A	A	A	A	A	A	A	A	A	A	A	A	A	A	A		
8	B	A	A	A	B	A	A	A	A	A	A	A	A	A	A	A	A	A	A	A	A	A	A	A	A		
9	B	A	A	A	C	A	A	A	A	A	A	A	A	A	A	A	A	A	A	A	A	A	A	A	A		
10	B	A	A	A	C	A	A	A	A	A	A	A	A	A	A	A	A	A	A	A	A	A	A	A	A		
11	A	A	A	A	A	B	A	A	A	A	A	A	A	A	A	A	A	A	A	A	A	A	A	A	A		
12	A	A	A	A	B	A	A	A	A	A	A	A	A	A	A	A	A	A	A	A	A	A	A	A	A		
13	A	A	A	A	C	A	A	A	A	A	A	A	A	A	A	A	A	A	A	A	A	A	A	A	A		
14	A	A	A	A	C	A	A	A	A	A	A	A	A	A	A	A	A	A	A	A	A	A	A	A	A		
15	A	A	A	A	A	C	A	A	A	A	A	A	A	A	A	A	A	A	A	A	A	A	A	A	A		
16	A	A	A	A	A	B	A	A	A	A	A	A	A	A	A	A	A	A	A	A	A	A	A	A	A		
17	A	A	A	A	A	B	A	A	A	A	A	A	A	A	A	A	A	A	A	A	A	A	A	A	A		
18	B	A	A	A	A	C	A	A	A	A	A	A	A	A	A	A	A	A	A	A	A	A	A	A	A		
19	A	A	A	A	A	B	A	A	A	A	A	A	A	A	A	A	A	A	A	A	A	A	A	A	A		
20	A	A	A	A	A	A	A	A	A	A	A	A	A	A	A	A	A	A	A	A	A	A	A	A	A		

Zone 01 — forward quarter of fuselage
 Zone 02 — middle half of fuselage
 Zone 03 — aft quarter of fuselage
 Zone 04 — stabilizers, rudder, and elevators
 Zone 05 — outer one-third of wing
 Zone 06 — inner two-thirds of wing
 A — most severe
 B — second most severe
 C — third most severe
 D — least severe

severity is assigned to those data which are found to be homogeneous at the 1% level of significance. The mean value and standard deviation versus frequency for the vibration measured in each aircraft group are calculated in Section 4 of Appendix A, and summarized in Figure 11. The sample sizes for the mean value and standard deviation calculations vary from 2 to over 4000, depending upon the aircraft and frequency increment. Combining the information in Table 15 and Figure 11 leads to the final presentation in Figure 12.

Figure 12 summarizes the mean value versus frequency for the vibration measured in the various zones of each aircraft group, where homogeneous data are pooled and identified by a single mean value. Hence, all differences indicated in Figure 12 are significant differences in the statistical sense.

From Figure 12a, for aircraft Group 1 (reciprocating engine transports), the vibration levels in the forward quarter of the fuselage tend to be more severe than in other zones for frequencies above 50 cps. The levels are also high in the center half of the fuselage for frequencies between 50 and 100 cps. This would be expected since the propeller blade passage frequency, which is a principal source of fuselage vibration, falls within this frequency range. From Figure 12b, for aircraft Group 2 (turboprop transports), the middle half of the fuselage again displays high vibration levels at the frequencies of propeller blade passage and its harmonics. The outer one-third of the wing also displays high vibration levels at these frequencies. From Figure 12c, for aircraft Group 3 (jet bombers), the vibration does not differ widely among the basic structural zones, except for the inner two-thirds of the wing where the levels are substantially lower at some frequencies above 50 cps. The results for aircraft Group 5 (Century series fighters) in Figure 12d are similar.

VIBRATION DOUBLE AMPLITUDE, INCHES

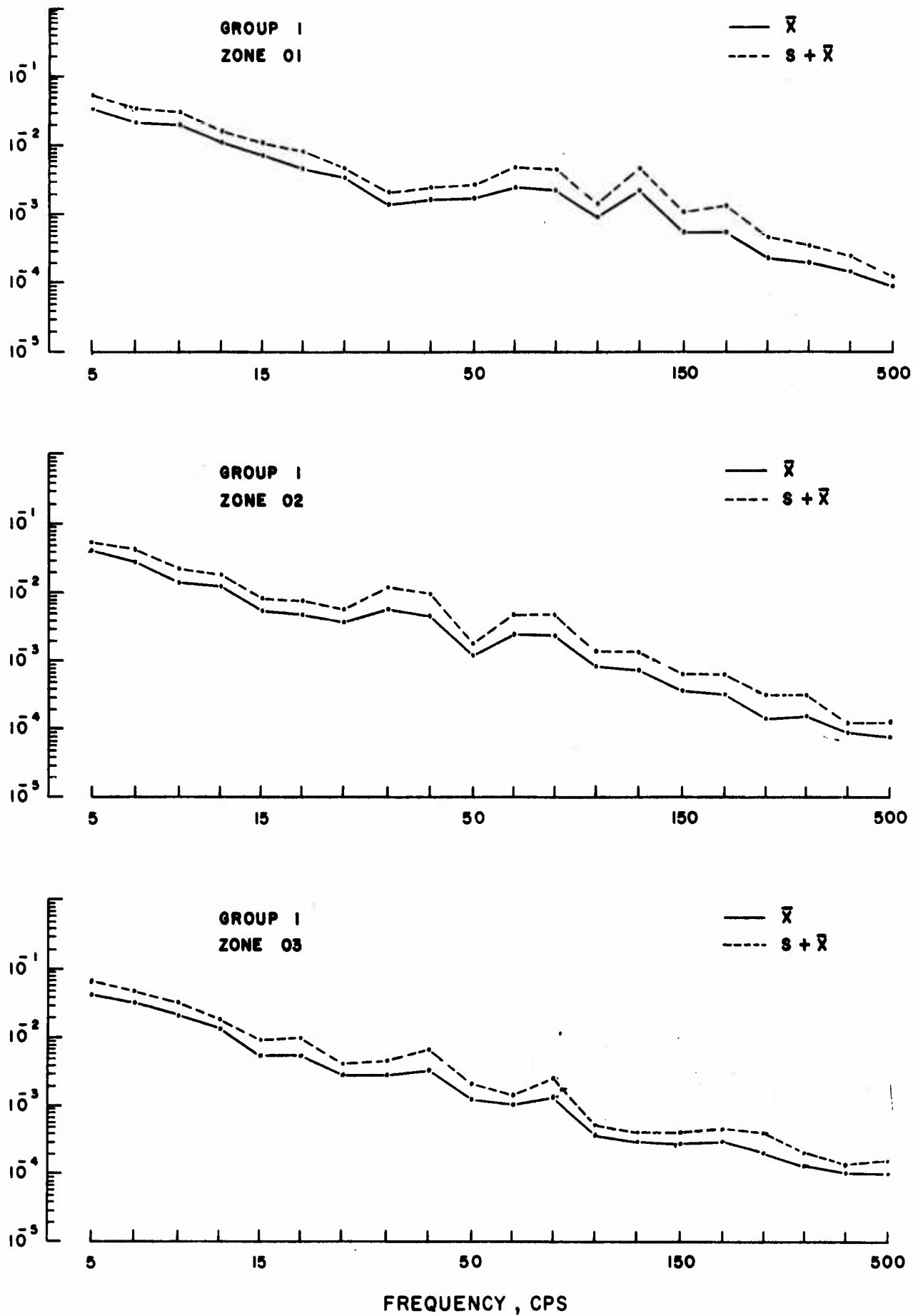


Figure 11a. Mean Values and Standard Deviations for the Vibration in Various Structural Zones of Aircraft Group 1

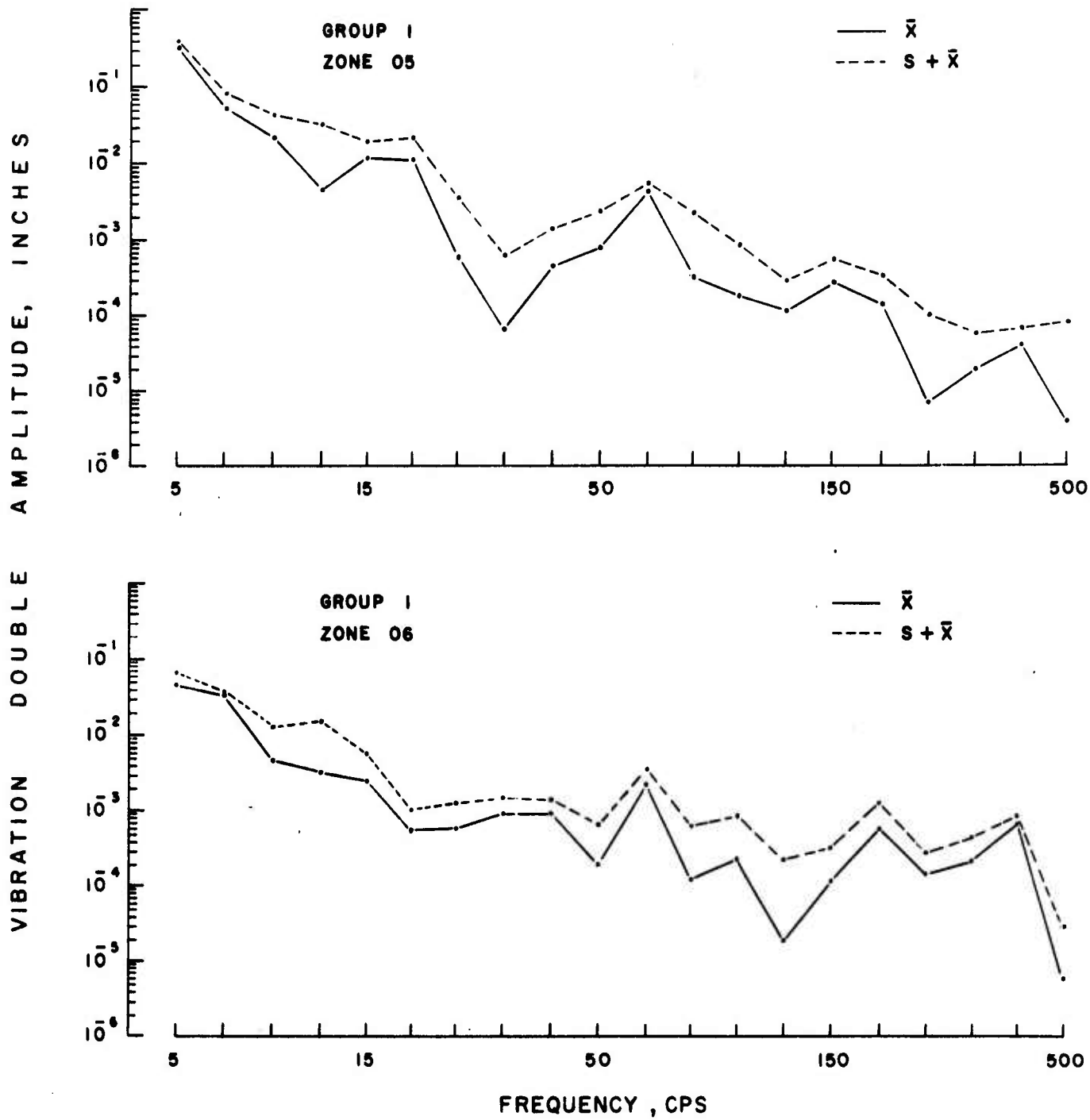


Figure 11a (Continued)

VIBRATION DOUBLE AMPLITUDE, INCHES

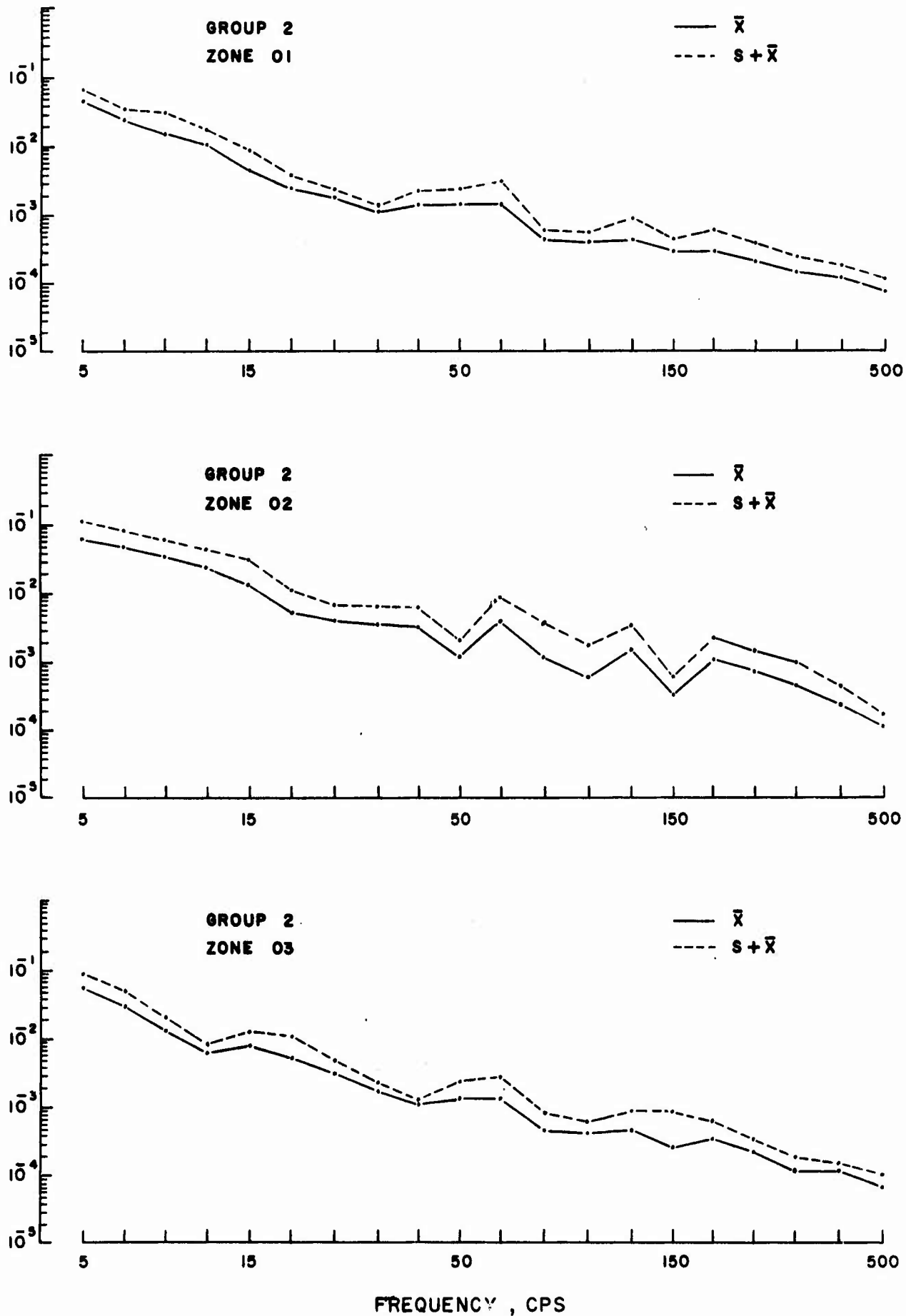


Figure 11b. Mean Values and Standard Deviations for the Vibration in Various Structural Zones of Aircraft Group 2

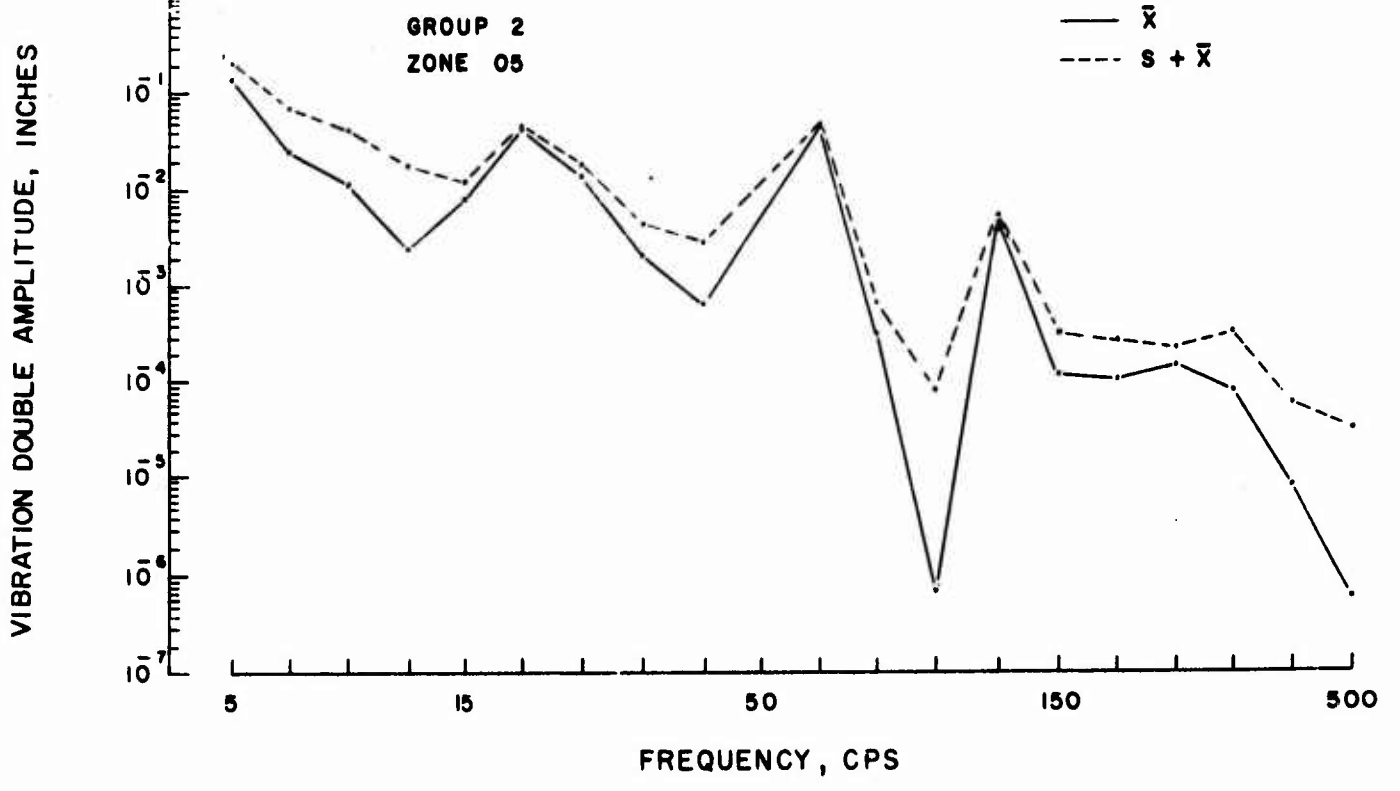


Figure 11b (Continued)

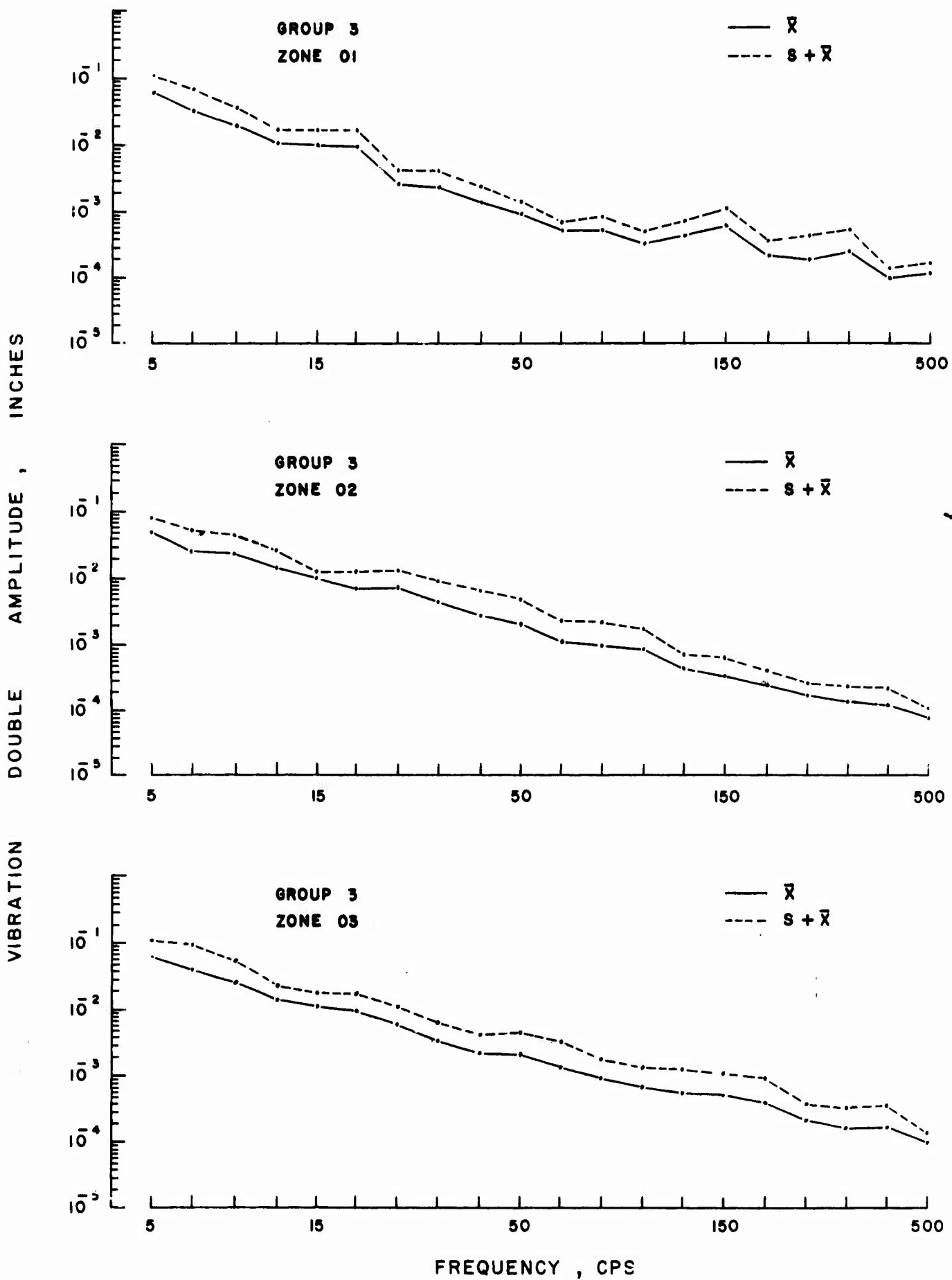


Figure 11c. Mean Values and Standard Deviations for the Vibration in Various Structural Zones of Aircraft Group 3

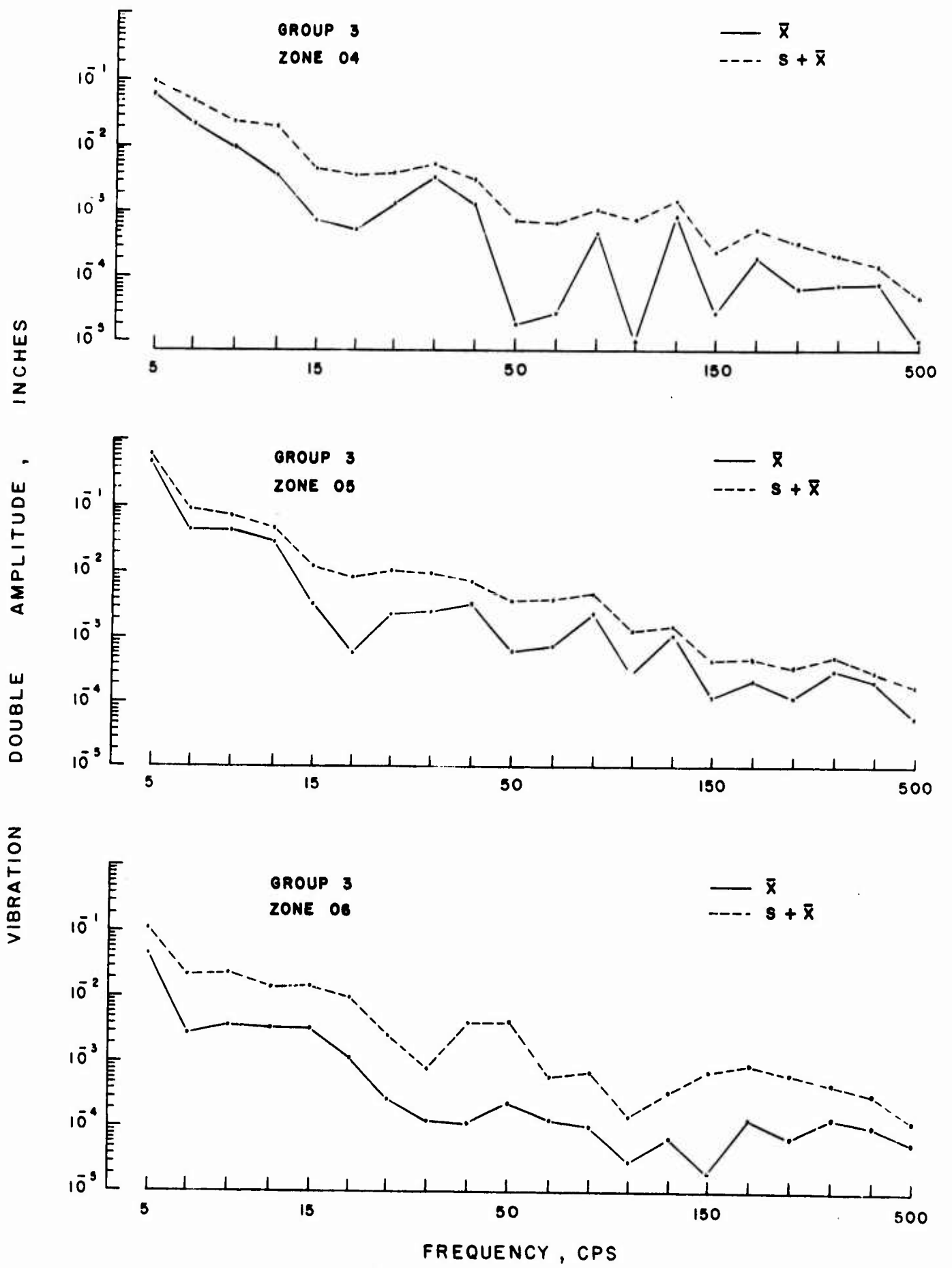


Figure 11c (Continued)

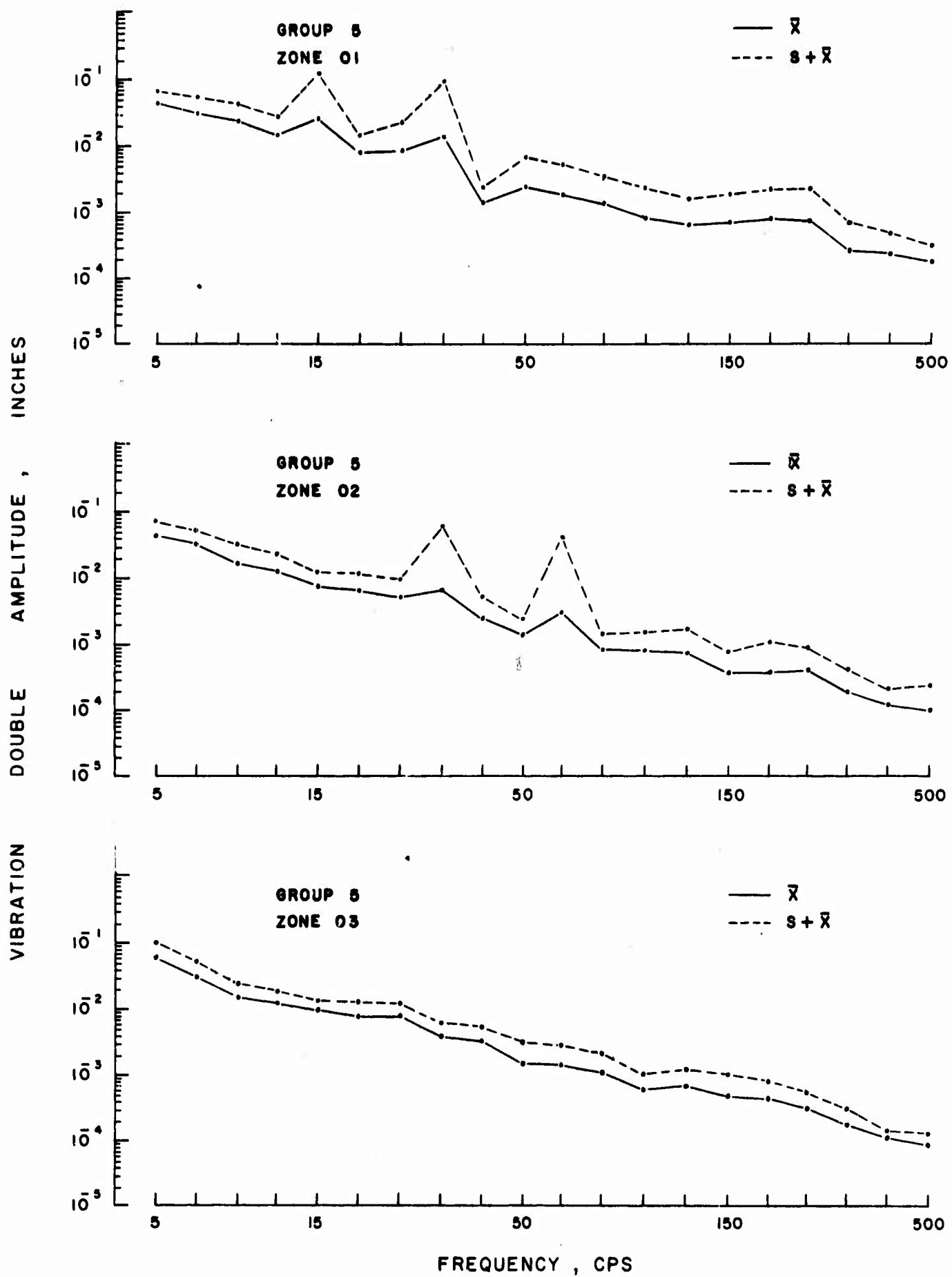


Figure 11d. Mean Values and Standard Deviations for the Vibration in Various Structural Zones of Aircraft Group 5

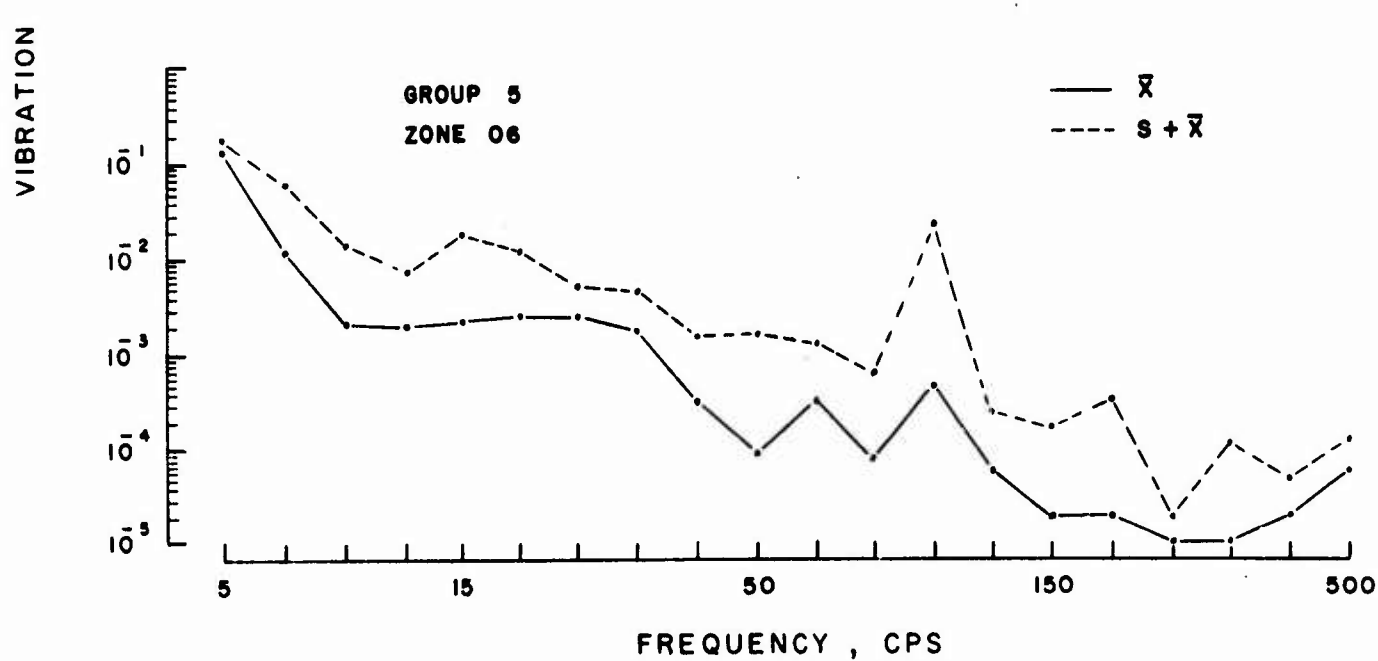
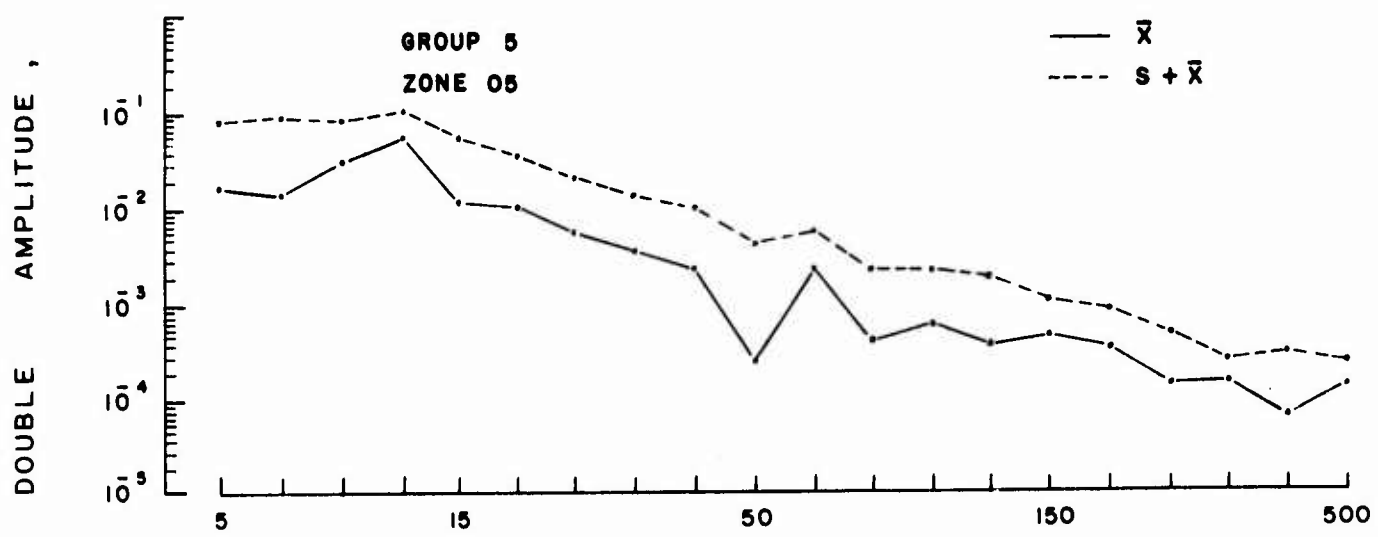
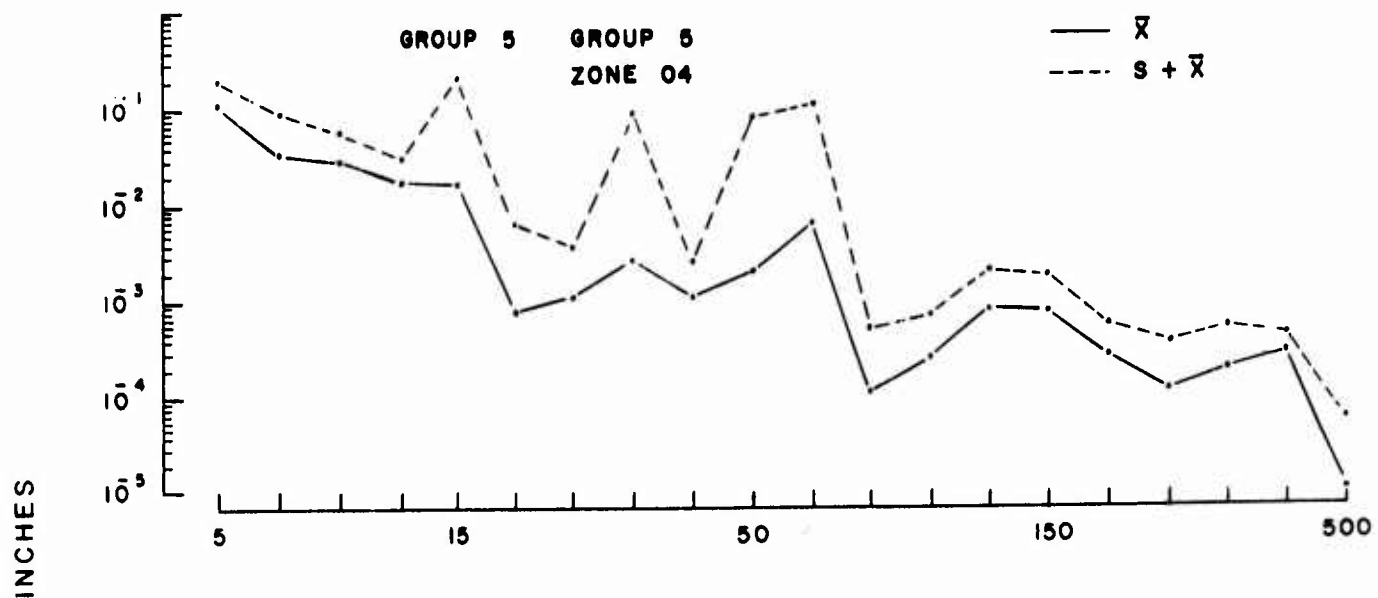


Figure 11d (Continued)

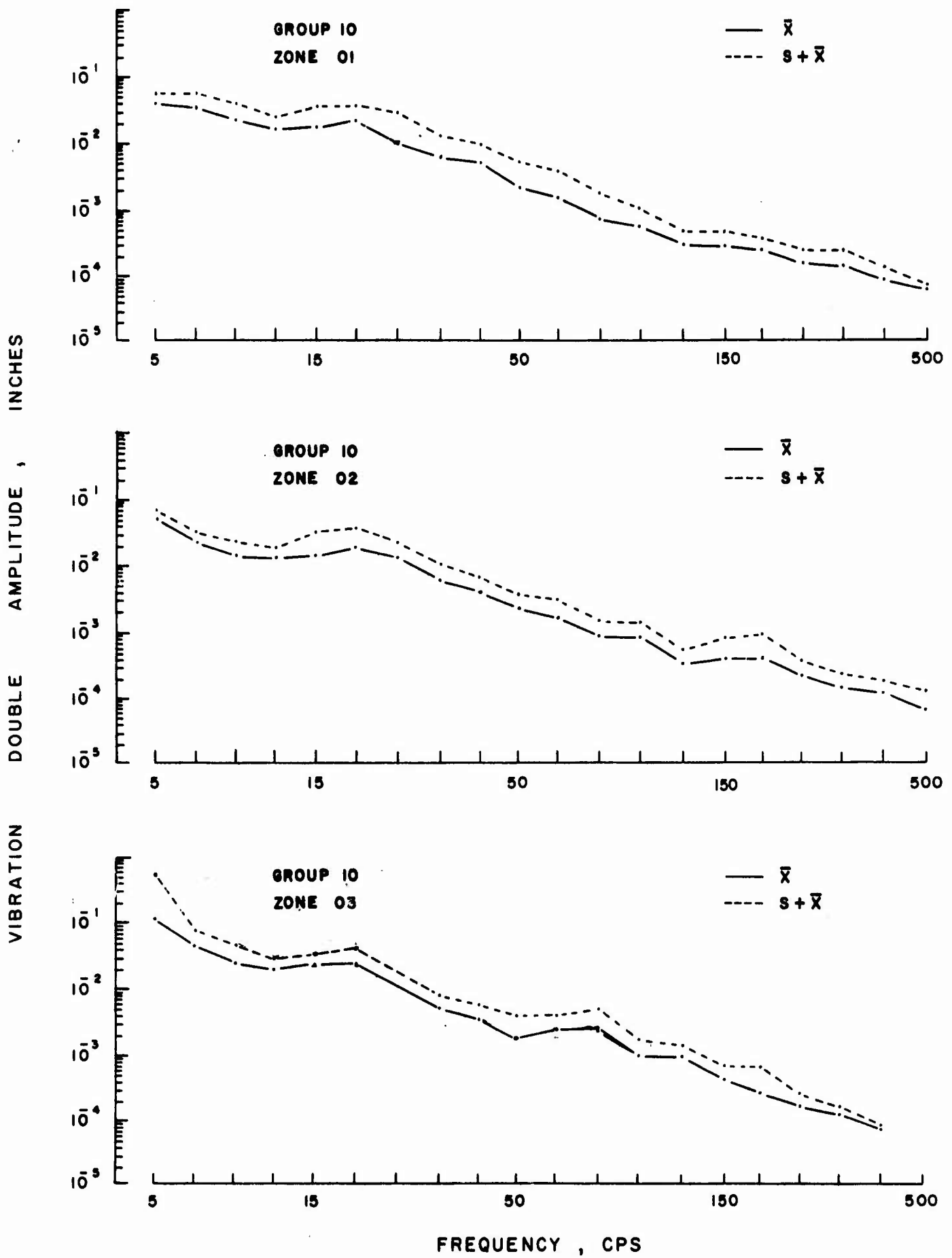


Figure 11e. Mean Values and Standard Deviations for the Vibration in Various Structural Zones of Aircraft Group 10

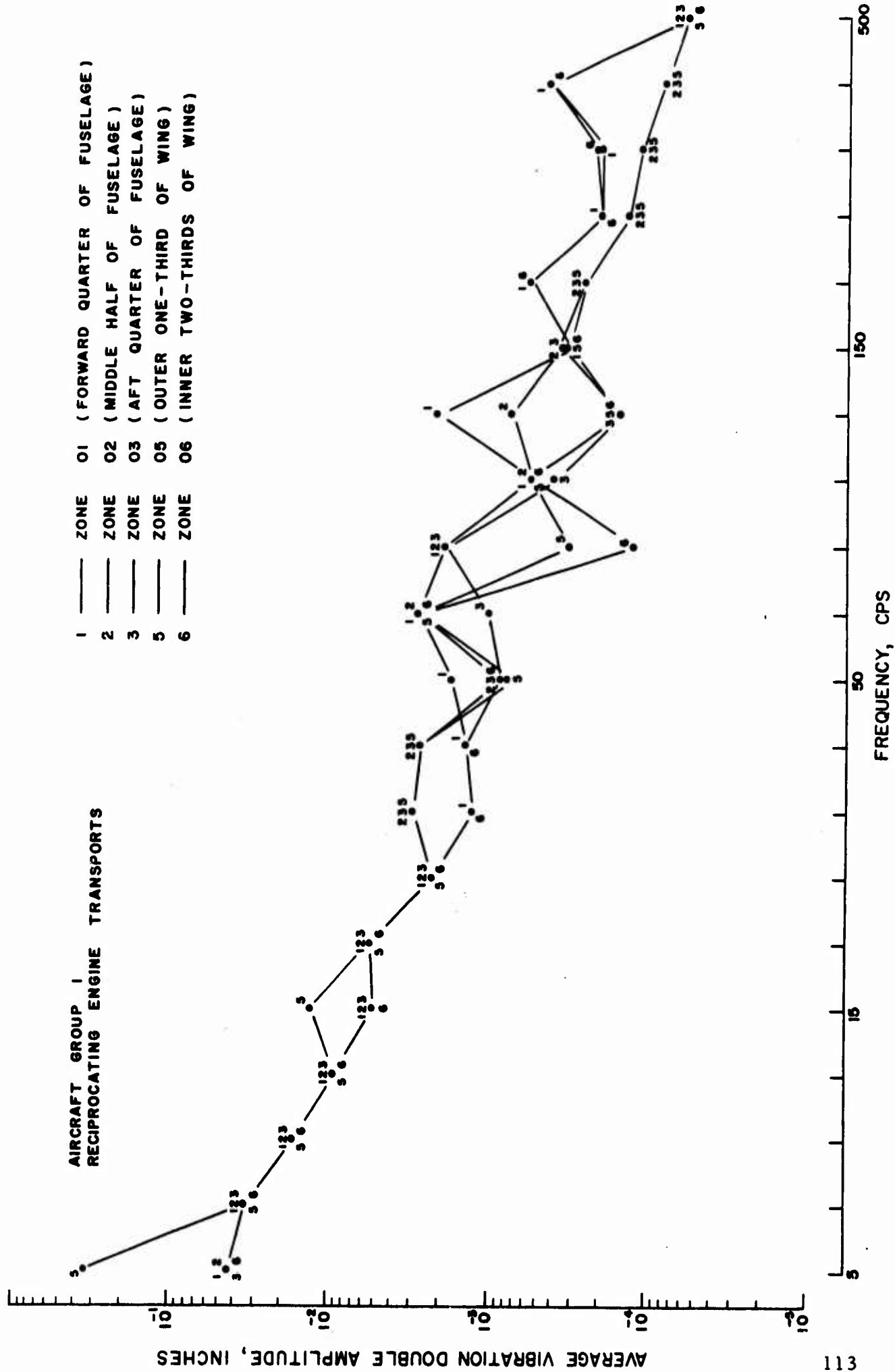


Figure 12a. Summary of Average Vibration for Various Structural Zones of Aircraft Group 1

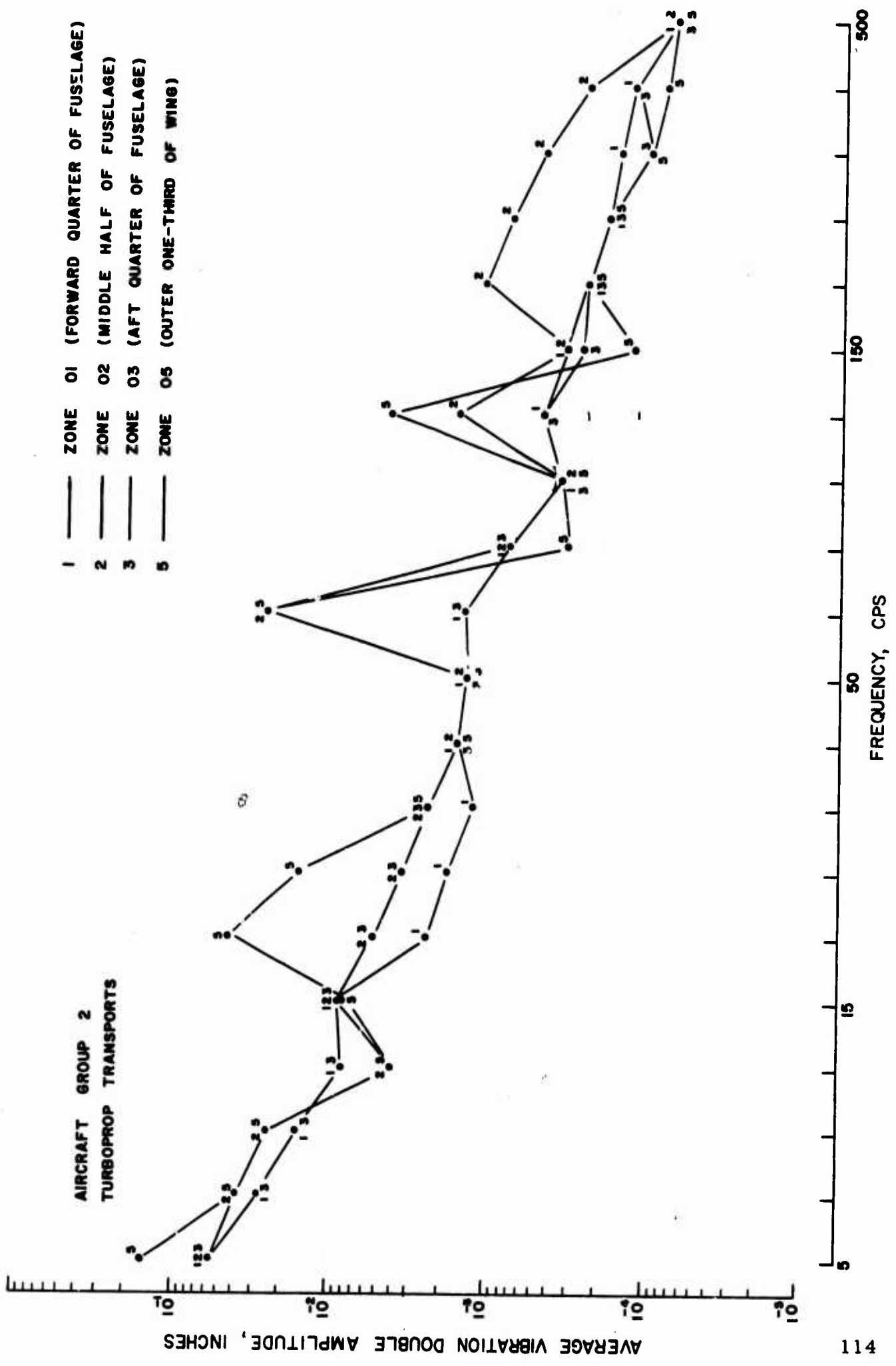


Figure 12b. Summary of Average Vibration for Various Structural Zones of Aircraft Group 2

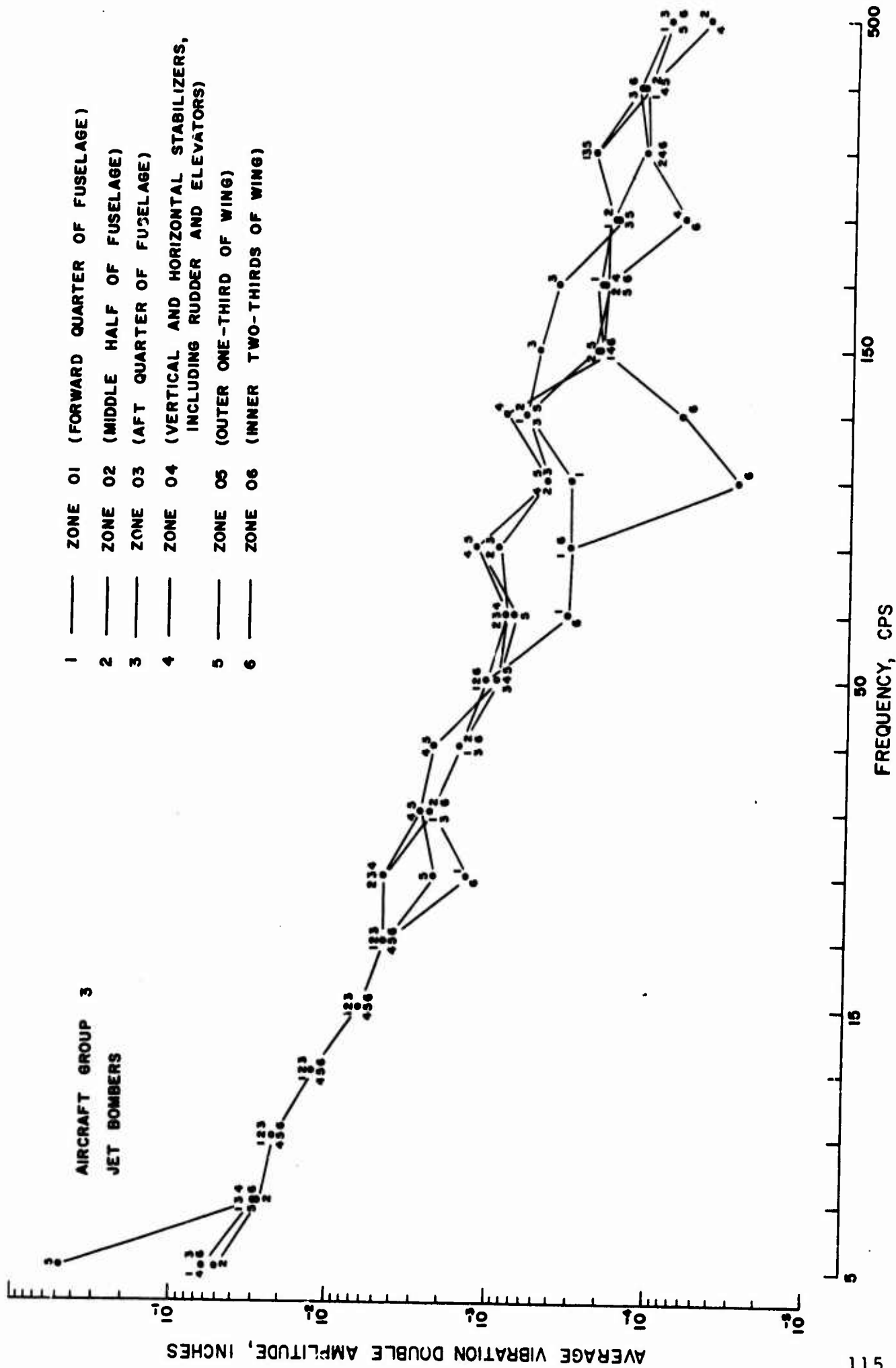


Figure 12c. Summary of Average Vibration for Various Structural Zones of Aircraft Group 3

**AIRCRAFT GROUP 5
CENTURY SERIES FIGHTERS**

- 1 — ZONE 01 (FORWARD QUARTER OF FUSELAGE)
- 2 — ZONE 02 (MIDDLE HALF OF FUSELAGE)
- 3 — ZONE 03 (AFT QUARTER OF FUSELAGE)
- 4 — ZONE 04 (VERTICAL AND HORIZONTAL STABILIZERS,
INCLUDING RUDDER AND ELEVATORS)
- 5 — ZONE 05 (OUTER ONE-THIRD OF WING)
- 6 — ZONE 06 (INNER TWO-THIRDS OF WING)

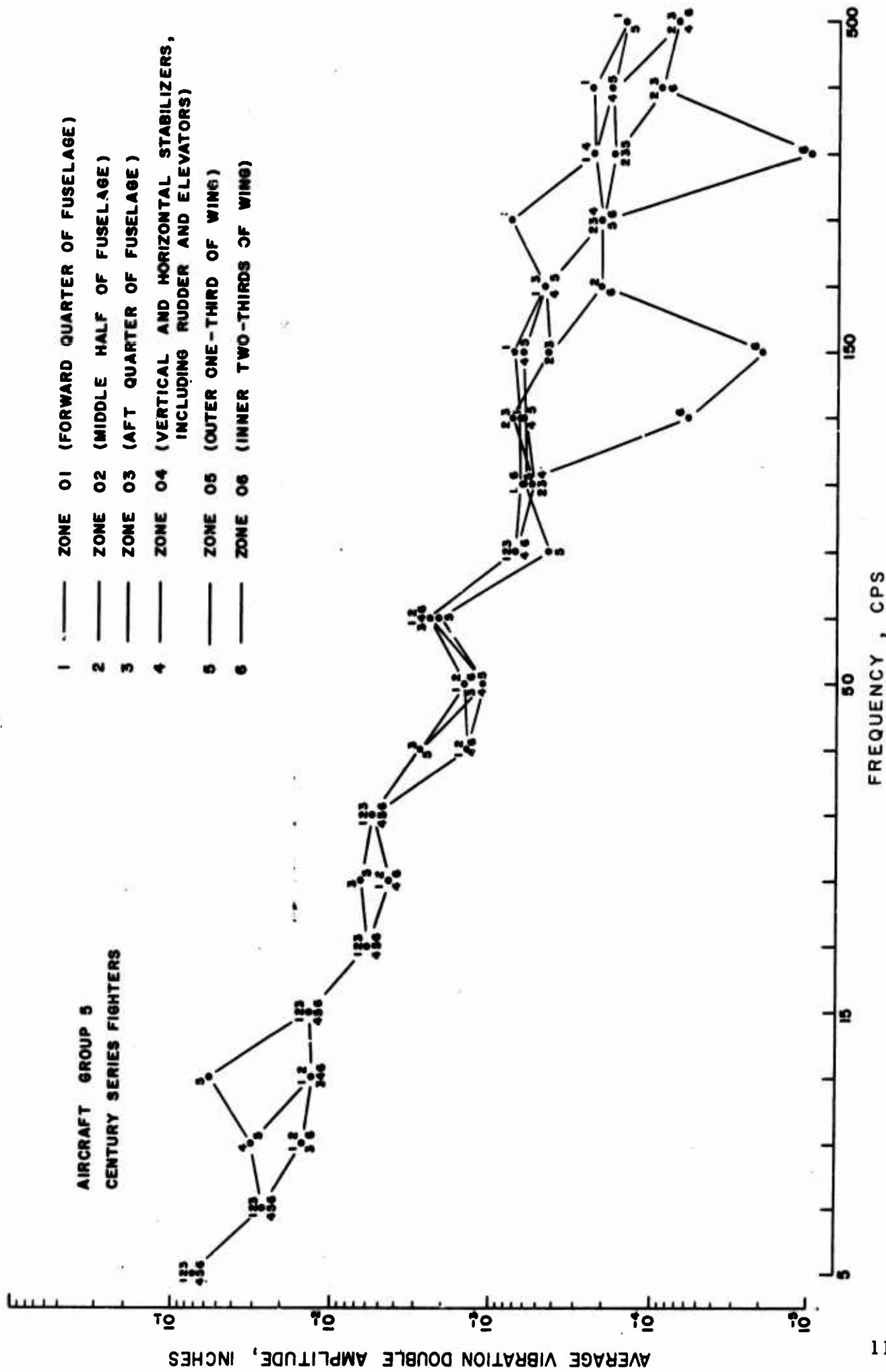


Figure 12d. Summary of Average Vibration for Various Structural Zones of Aircraft Group 5

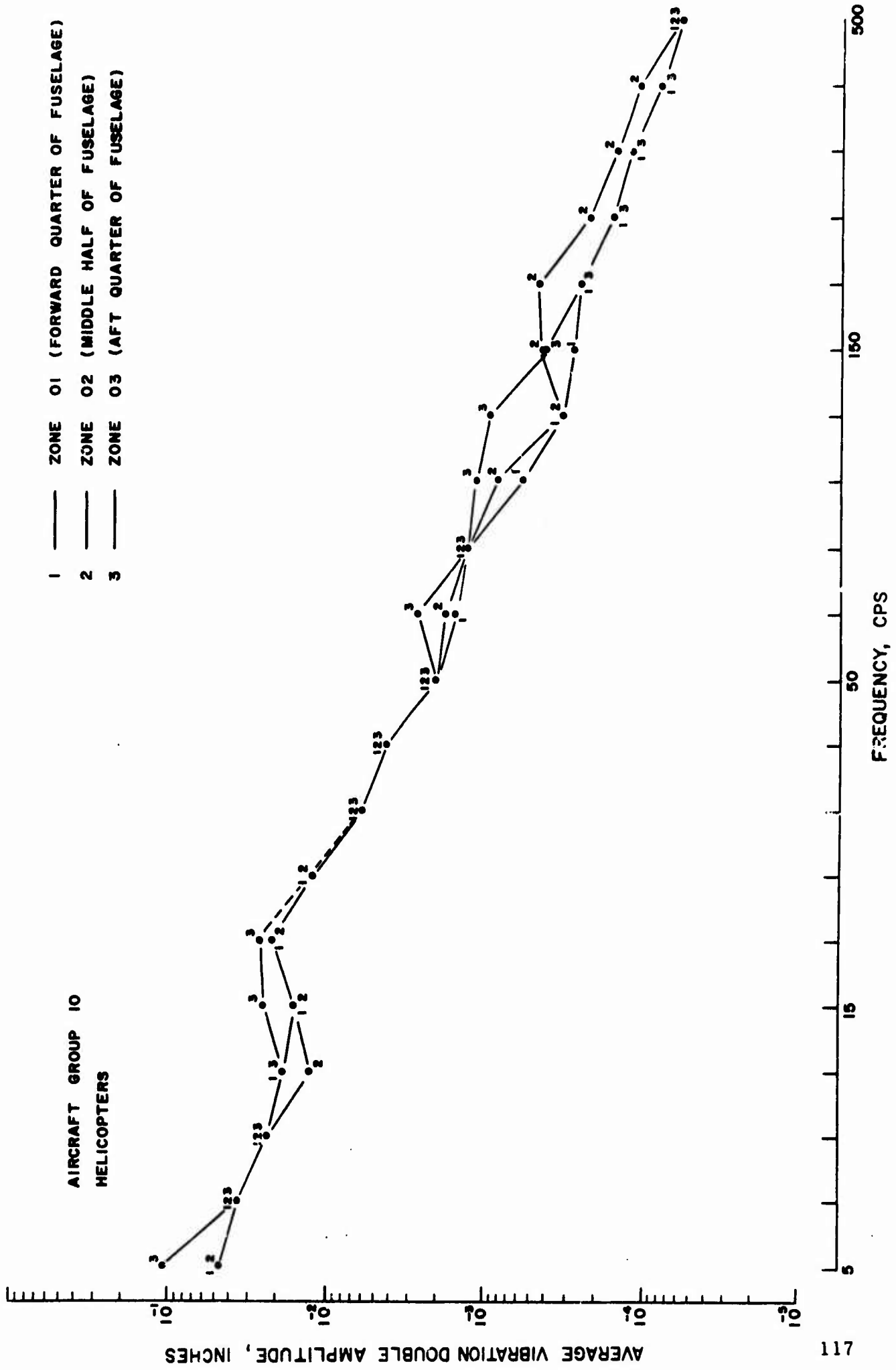


Figure 12e. Summary of Average Vibration for Various Structural Zones of Aircraft Group 10

From Figure 12e, for aircraft Group 10 (helicopters), the differences among the average vibration in the three zones are less than 10 dB at all frequencies.

The principal purpose of zoning is to segregate the aircraft structure into categories where the vibration levels in each category are similar. For example, assume an aircraft structure is to be divided into three zones. Further assume that the vibration levels over the structure vary on an arbitrary scale between 1 and 10 units. Then an optimum zoning procedure would segregate the structure such that the vibration levels vary from 1 to 4 units in Zone 1, 4 to 7 units in Zone 2, and 7 to 10 units in Zone 3. Conversely, a completely inefficient zoning procedure would segregate the structure such that the vibration levels vary from 1 to 10 in all three zones.

Inspection of the results in Figure 12 suggests that the zones used by AFFDL to segregate the basic aircraft structure are not very efficient, particularly for aircraft Groups 3, 5, and 10. It must be remembered, however, that the data used to prepare Figure 12 do not properly represent the random portion of the vibration environment. If random contributions were accurately reflected in the data, it is believed that more striking differences would be seen among the various zones, at least for aircraft Groups 3 and 5. For jet bombers and fighters, the random vibration induced by jet noise tends to be more severe towards the aft end of the fuselage. Furthermore, the boundary layer induced vibration varies in spectral composition over the fuselage length. Hence, significant differences would be expected between the vibration in the forward quarter and the aft quarter of the fuselage for these aircraft. Based upon these considerations, no change in the current zoning procedure is suggested until further studies are performed on future data which include a proper representation of the random portion of the environment.

6. 2. 3 Comparisons of the Various Aircraft Models and Groups

Attention is now directed to the average vibration environment for each of the 11 aircraft models divided among the five aircraft groups, as detailed in Table 13. The question of interest is as follows. Are there significant differences among the vibration environments for the aircraft within a given group, and for the five different groups?

For the case of aircraft comparisons within a given group, rank sum tests are applied to the data segregated among the various aircraft within each group covering two or more aircraft (Groups 2, 3, and 5). Separate tests are performed on the data for each frequency increment. The data for the different orthogonal directions, different structural zones, and different flight conditions are pooled together for the tests to maximize the sample size.

The detailed results of the homogeneity tests are presented in Section 3 of Appendix A, and summarized in Table 16. The results are presented in terms of relative severity versus frequency for the various aircraft in each aircraft group, where a common level of severity is assigned to those data which are found to be homogeneous at the 1% level of significance. The mean value and standard deviation versus frequency for the vibration measured in each aircraft of each group are calculated in Section 4 of Appendix A, and summarized in Figure 13. The sample sizes for the mean value and standard deviation calculations vary from 3 to 12, 250, depending upon the aircraft and frequency increment. Combining the information in Table 16 and Figure 13 leads to the final presentation in Figure 14.

Figure 14 summarizes the mean value versus frequency for the vibration measured in each aircraft of each group, where homogeneous

Table 16. Rank Sum Test Results for Aircraft Comparisons

Req. Increment	Aircraft Group 2		Aircraft Group 3			Aircraft Group 5				
	40	47	36	37	52	42	44	46	53	
1	A	A	A	A	B	A	A	B	B	
2	A	A	A	A	B	B	A	B	B	
3	A	A	A	A	A	B	A	B	B	
4	A	A	A	B	B	A	A	B	B	
5	A	A	A	A	A	A	A	B	A	
6	A	A	A	A	A	A	A	B	A	
7	A	A	B	A	B	A	A	B	A	
8	A	A	B	A	B	A	A	B	A	
9	A	B	A	A	A	A	A	A	A	
10	A	A	A	A	A	A	A	B	B	
11	A	A	C	B	A	A	C	C	B	
12	A	B	B	A	A	A	B	C	B	
13	A	A	B	B	A	A	C	D	B	
14	A	A	B	A	A	A	D	C	B	
15	A	B	B	C	A	A	B	B	A	
16	A	B	B	B	A	B	C	A	B	
17	A	B	C	B	A	B	C	A	C	
18	A	B	B	C	A	B	C	B	C	
19	A	B	B	C	A	A	C	A	A	
20	A	B	B	C	A	A	A	A	A	

Aircraft 40-C-130 Aircraft 37-JRB-66 Aircraft 44-F-101A
 Aircraft 47-C-133 Aircraft 52-B-58 Aircraft 46-F-102A
 Aircraft 36-JRB-52 Aircraft 42-F-100C Aircraft 53-F-106A

A — most severe
 B — second most severe
 C — third most severe
 D — least severe

VIBRATION DOUBLE AMPLITUDE, INCHES

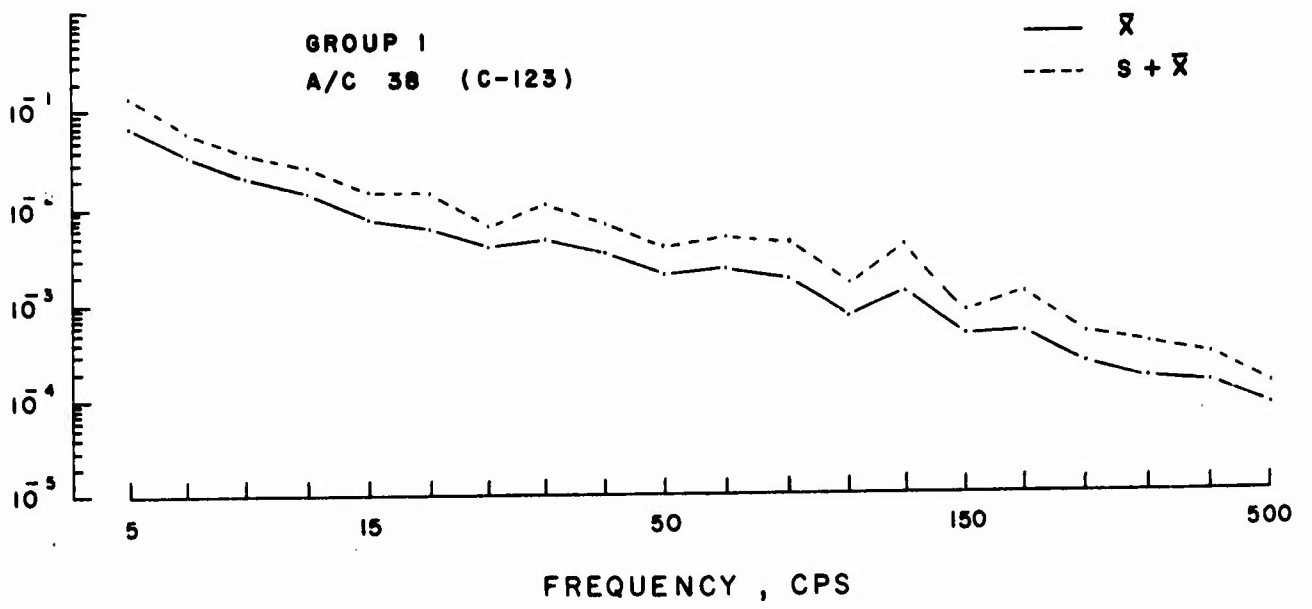


Figure 13a. Mean Values and Standard Deviations for the Vibration in Various Aircraft of Group 1

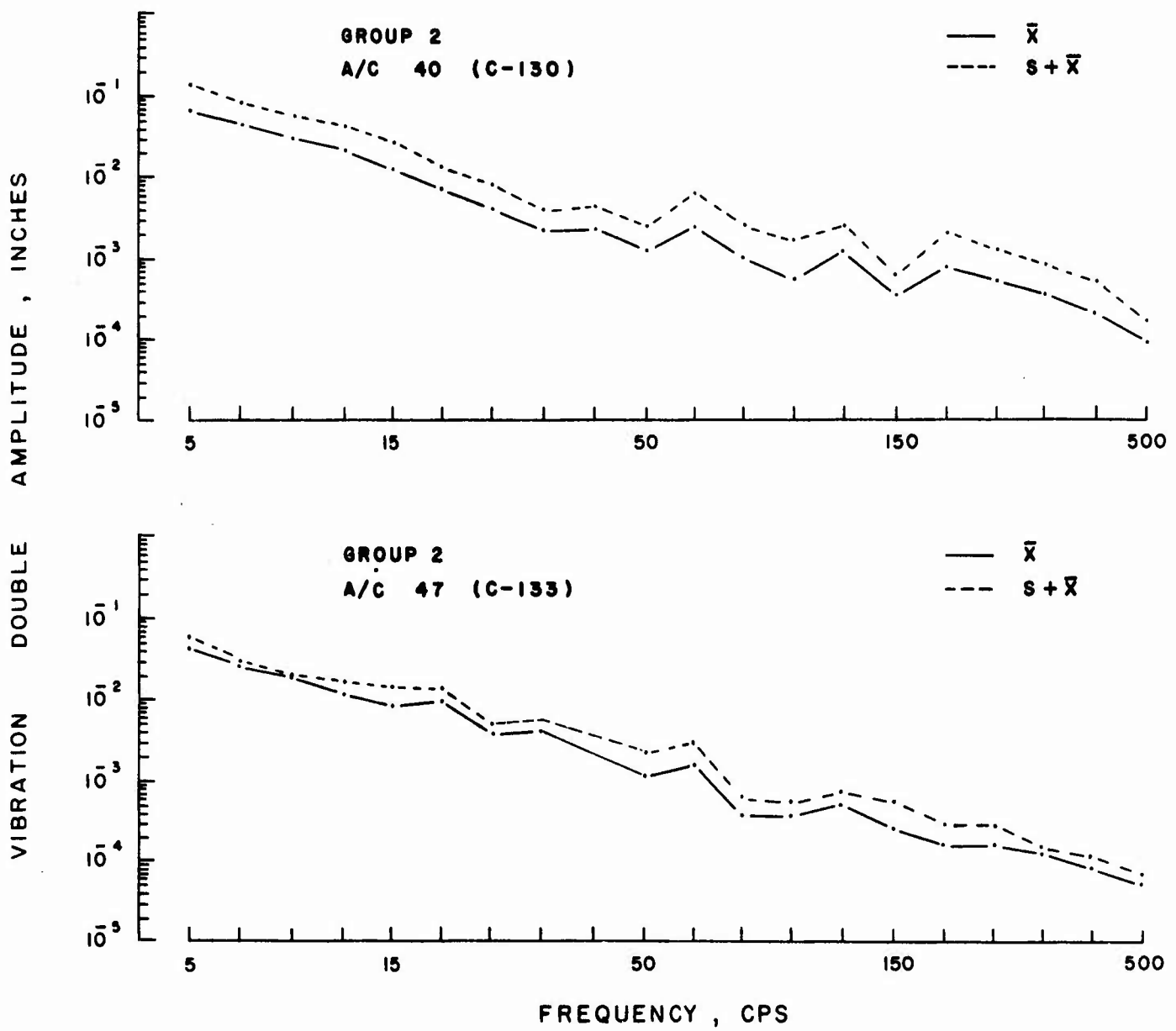


Figure 13b. Mean Values and Standard Deviations for the Vibration in Various Aircraft of Group 2

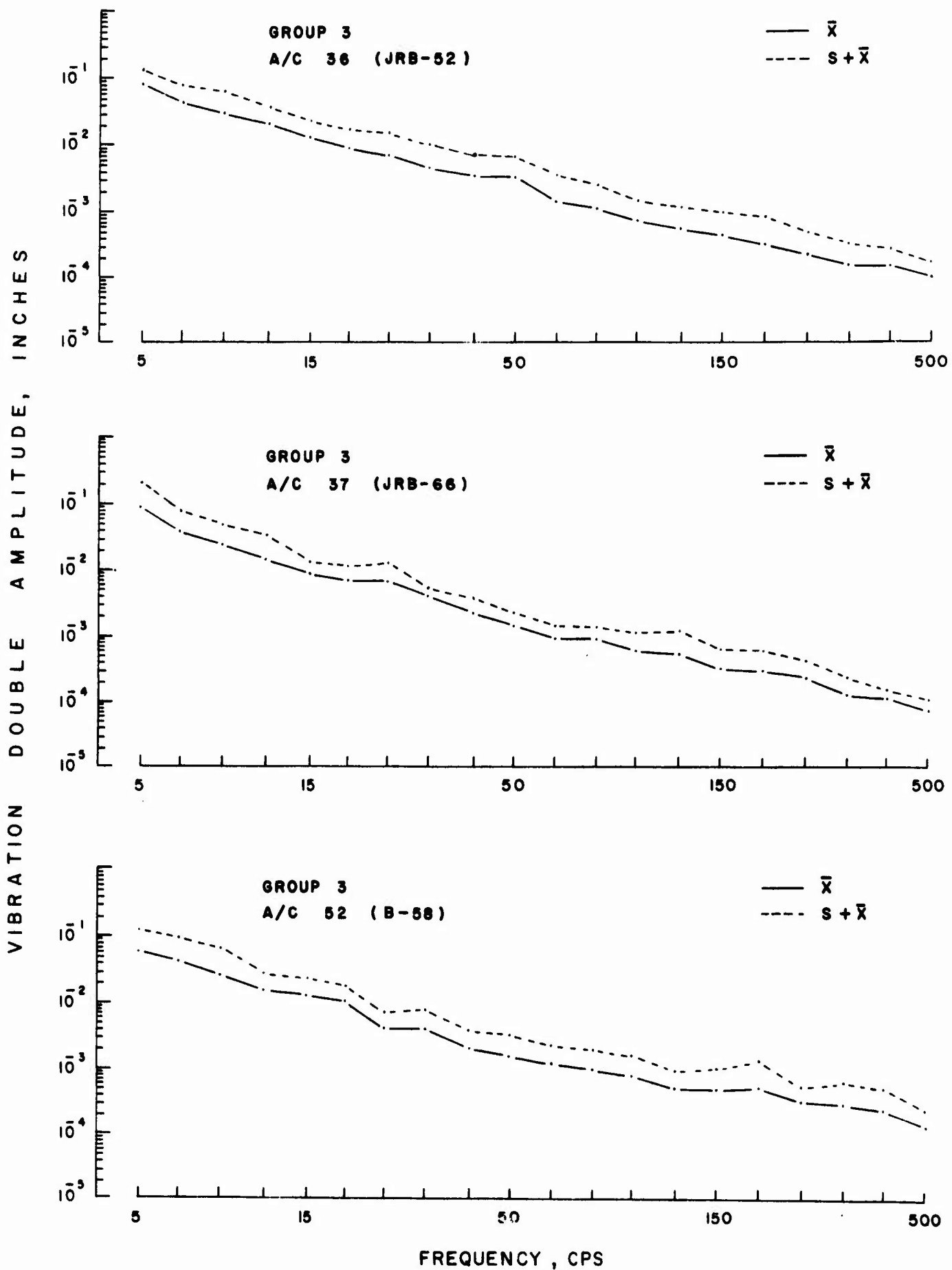


Figure 13c. Mean Values and Standard Deviations for the Vibration in Various Aircraft of Group 3

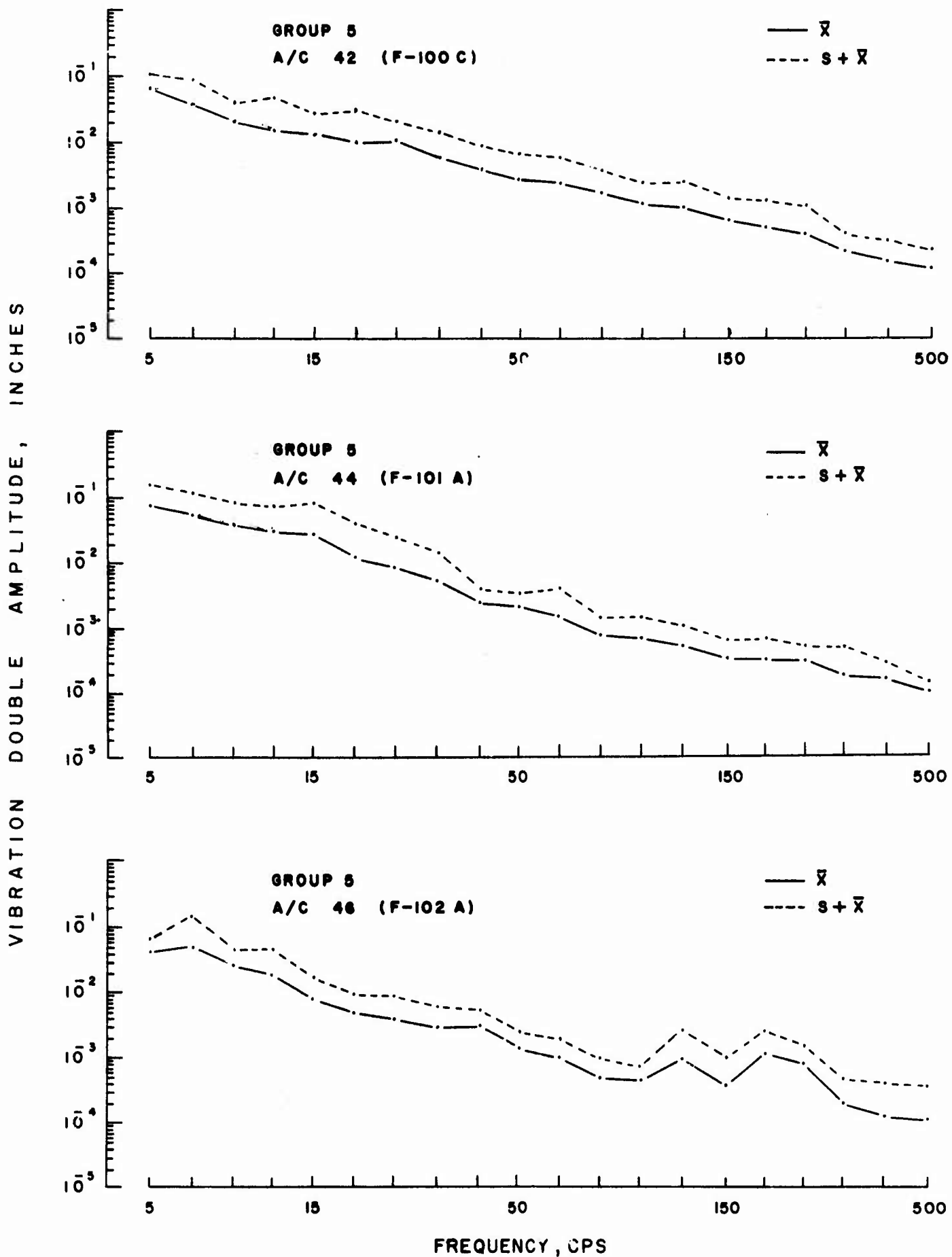


Figure 13d. Mean Values and Standard Deviations for the Vibration in Various Aircraft of Group 5

VIBRATION DOUBLE AMPLITUDE, INCHES

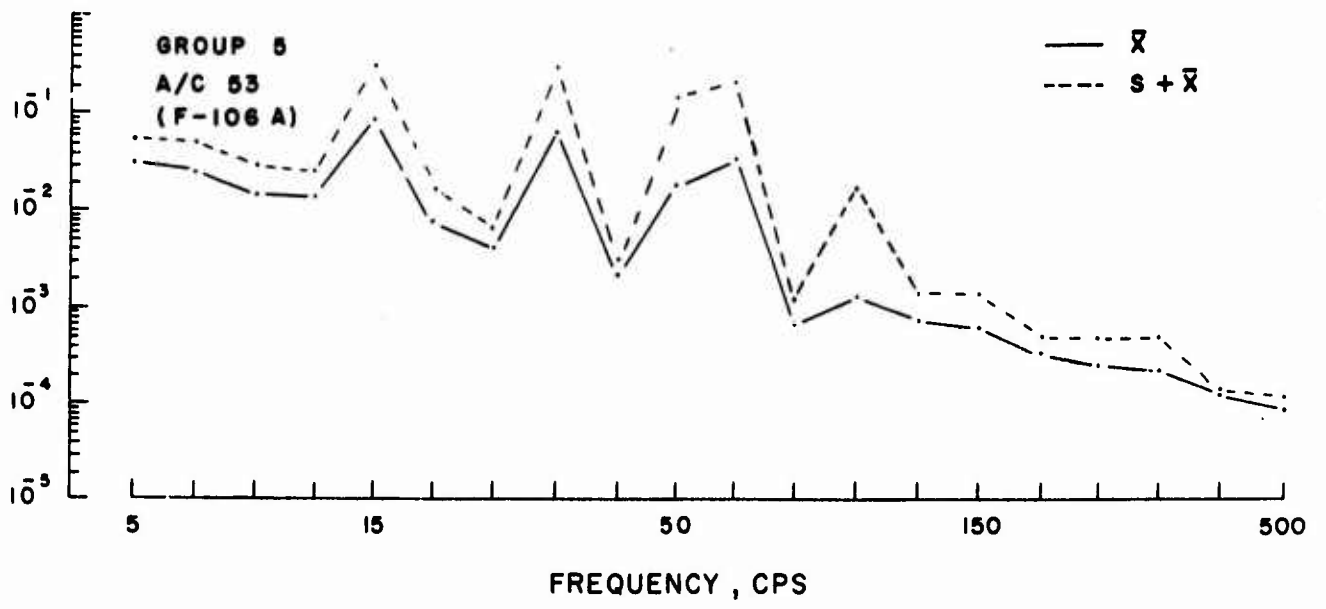


Figure 13d (Continued)

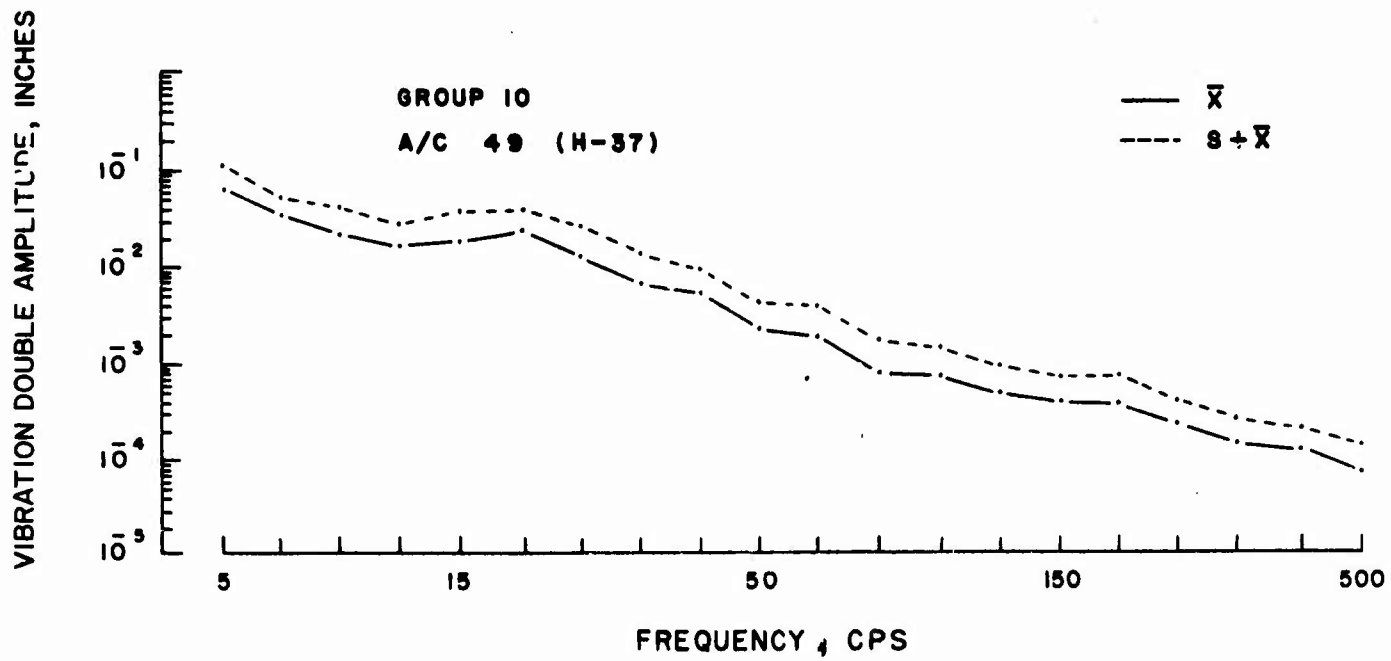


Figure 13e. Mean Values and Standard Deviations for the Vibration in Various Aircraft of Group 10

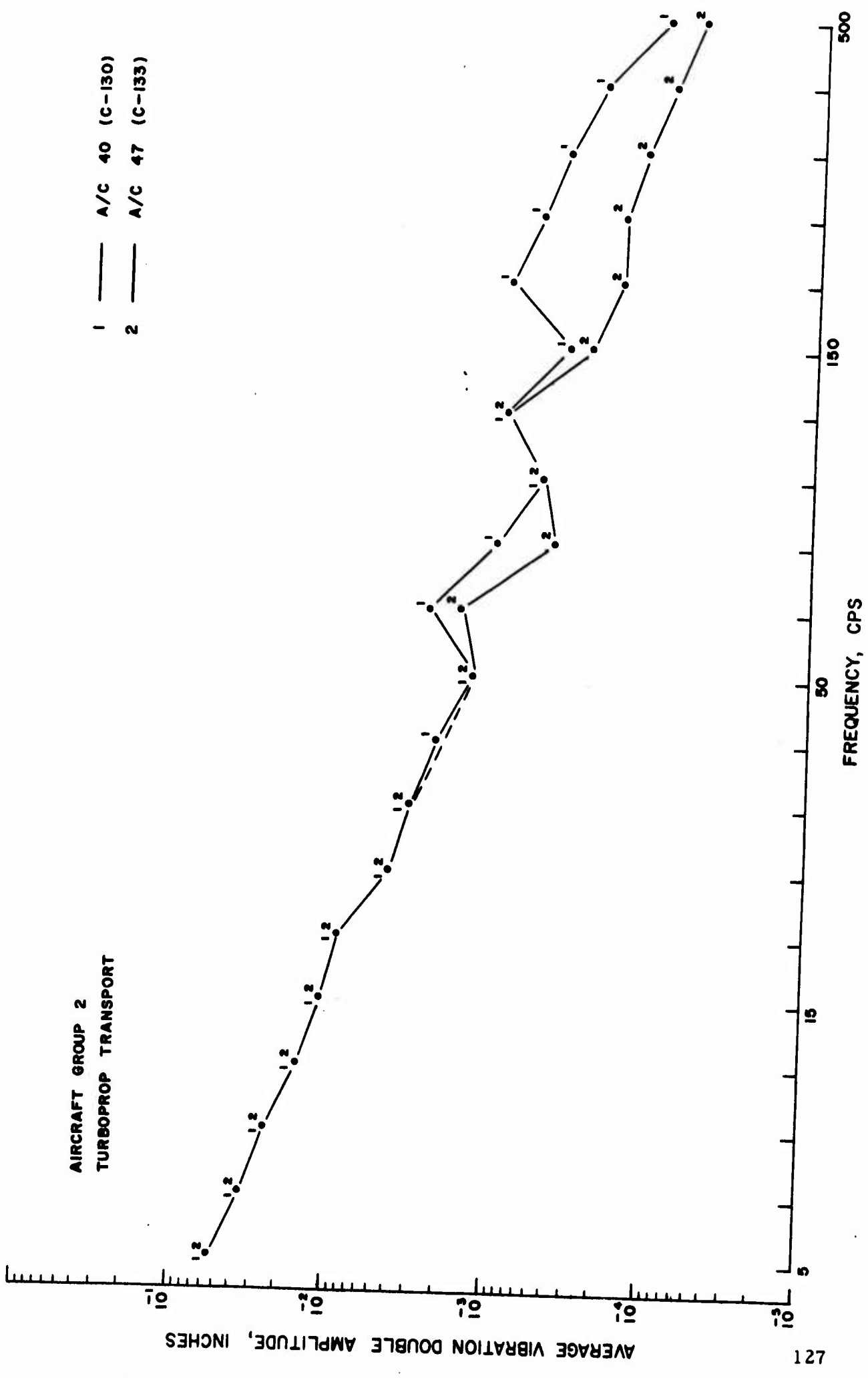


Figure 14a. Summary of Average Vibration for Various Aircraft in Group 2

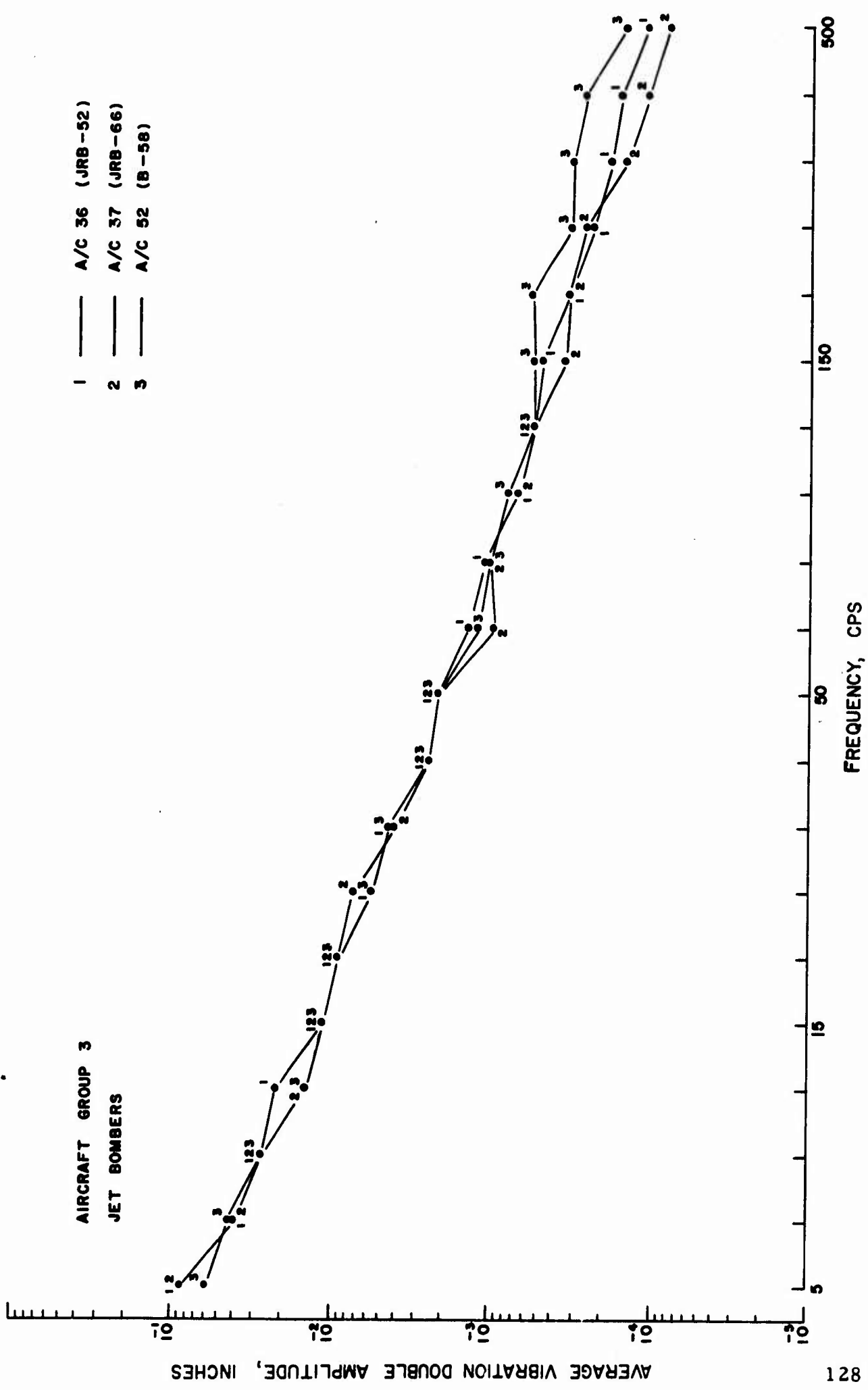


Figure 14b. Summary of Average Vibration for Various Aircraft in Group 3

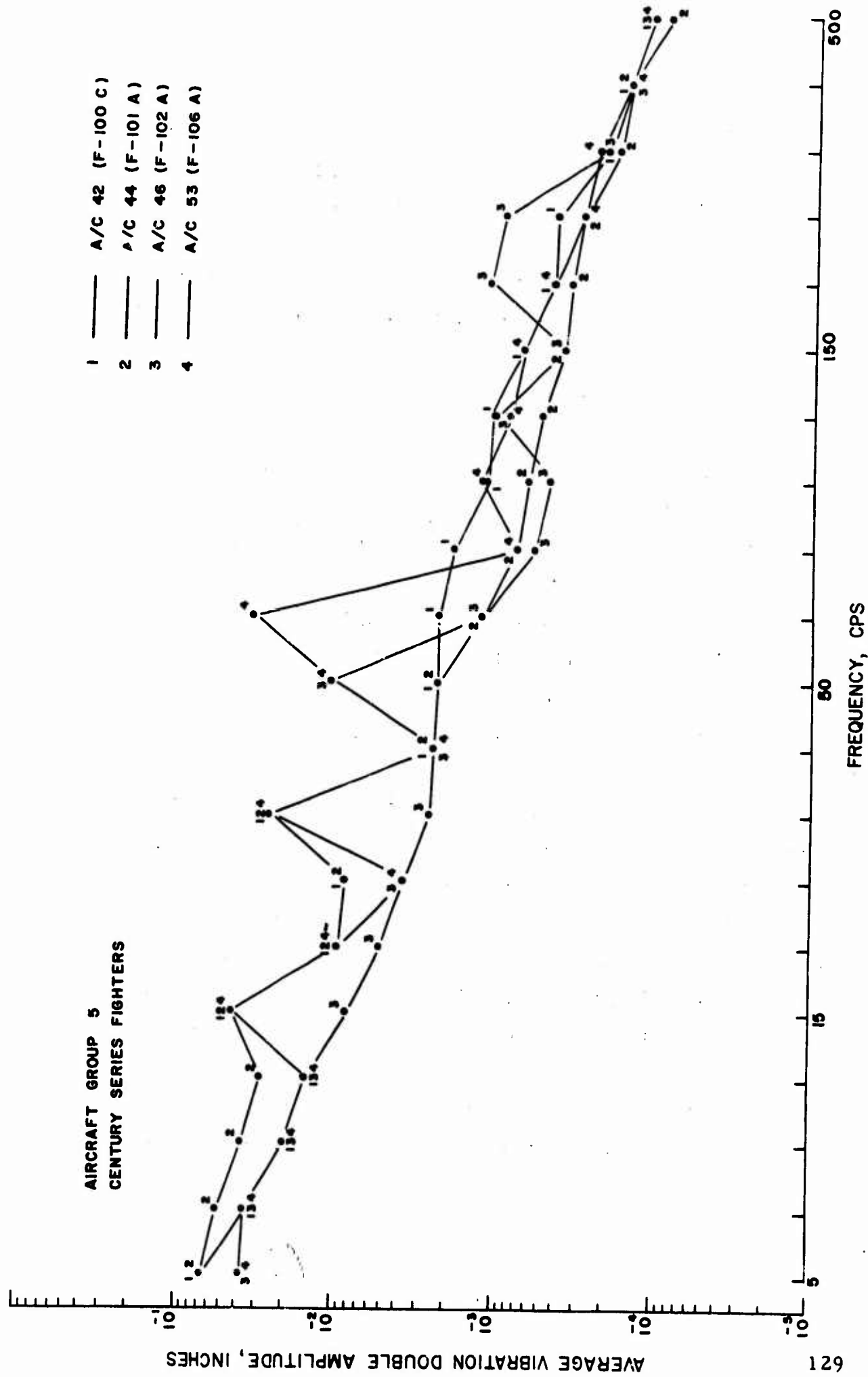


Figure 14c. Summary of Average Vibration for Various Aircraft in Group 5

data are pooled and identified by a single mean value. Hence, all differences indicated in Figure 14 are significant differences. Note that no summaries are presented for aircraft Groups 1 and 10 since data from only one aircraft are available for these two groups.

Referring to Figure 14a, which summarizes aircraft Group 2 (turboprop transports), it is seen that the average vibration levels in the C-130 are up to 5 times (14 dB) higher than in the C-133 in the frequency range above 40 cps. Below 40 cps, the vibration environments are similar in the two aircraft. From Figure 14b, for aircraft Group 3 (jet bombers), the vibration environments for the three aircraft are quite similar up to about 150 cps. Above this frequency, the vibration levels in the B-58 are somewhat higher than in the JRB-52 and JRB-66. From Figure 14c, for aircraft Group 5 (Century series fighters), the vibration environments for the four aircraft differ widely in some frequency increments, with the F-106 levels being generally the most severe. In the frequency range above 65 cps, however, the average vibration levels in the four aircraft differ by less than three to one (10 dB).

Now consider the average vibration environments for each of the five aircraft groups. Homogeneity tests are not required here since the sample size of the data within each group is quite large (over 500 in most frequency increments). The mean value and standard deviation versus frequency for the vibration measured in each aircraft group are calculated in Section 4 of Appendix A, and summarized in Figure 15. A comparison of the mean value versus frequency for the five groups is presented in Figure 16.

The results in Figure 16 must be interpreted with caution. Noting that the maximum difference in average vibration among the five groups

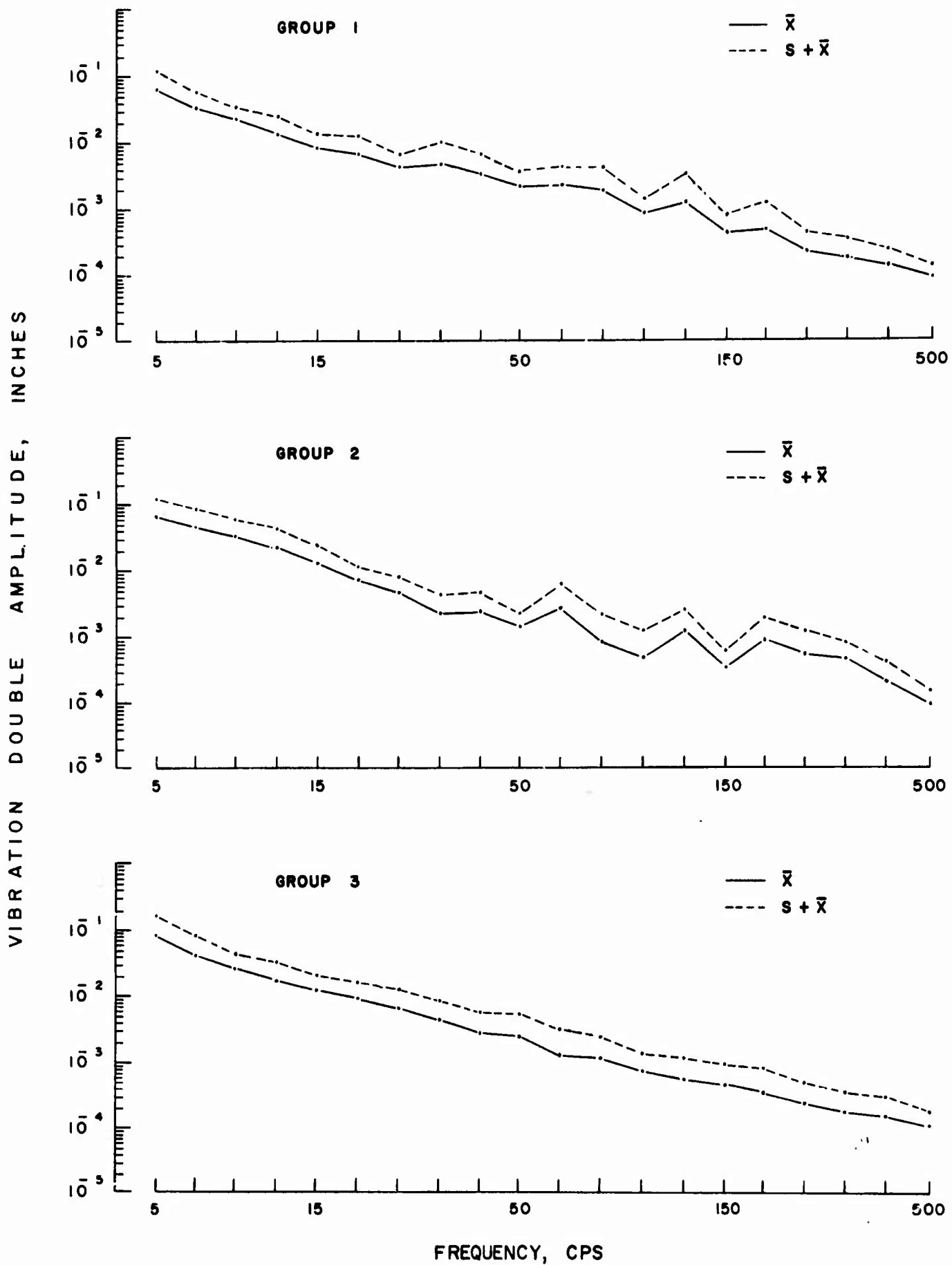


Figure 15. Mean Values and Standard Deviations for the Vibration in Various Aircraft Groups

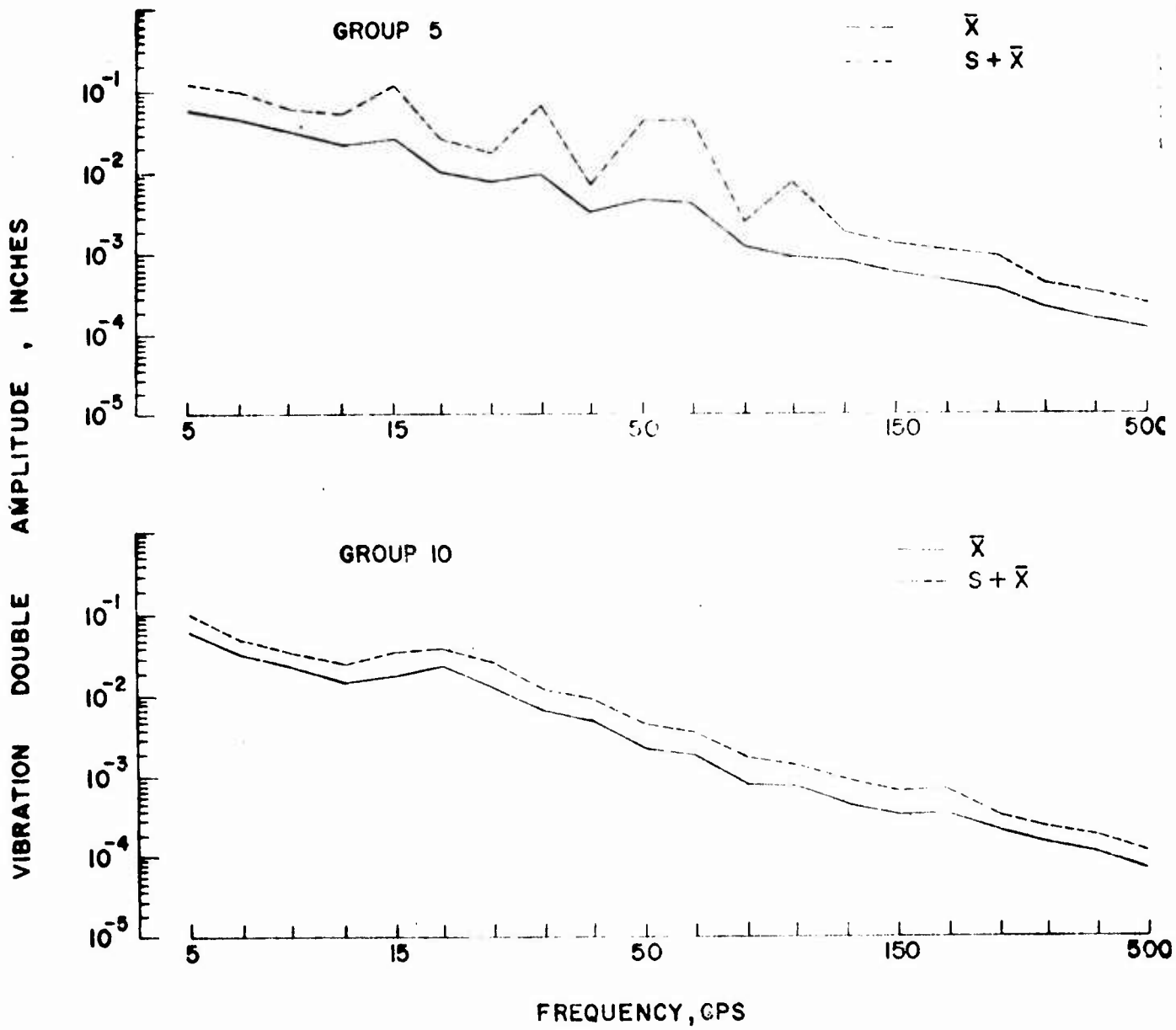


Figure 15 (Continued)

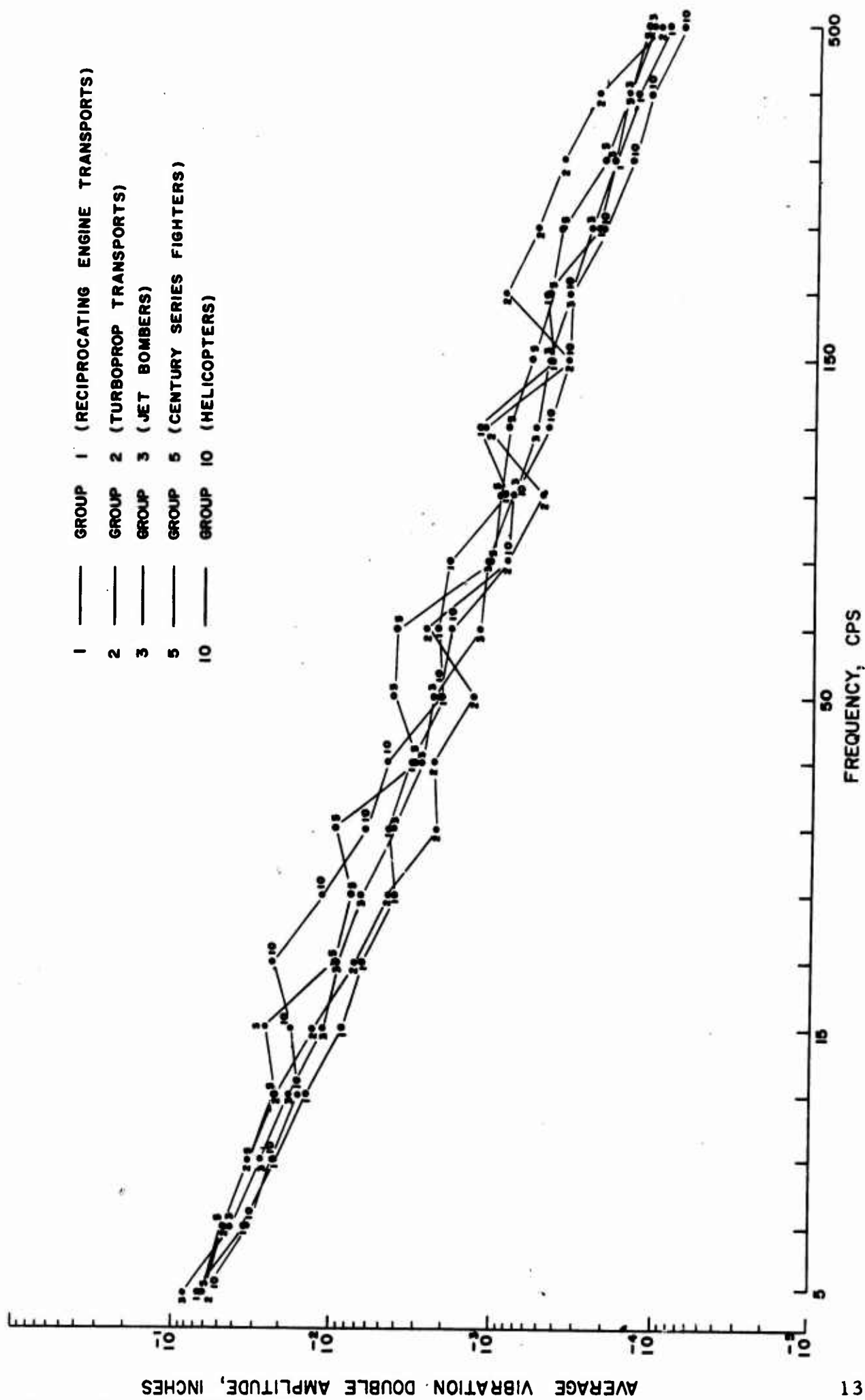


Figure 16. Summary of Average Vibration for the Five Aircraft Groups

is less than 10 dB at all frequencies, the first inclination might be to conclude that the vibration environments for propeller transports, jet bombers and fighters, and helicopters are not strikingly different. Figure 16 indeed suggests that this may be true on a gross average basis, at least for the periodic portions of the environments below 500 cps. However, it certainly is not true on a detailed basis. For example, consider the vibration levels in the frequency increment from 50 to 64 cps for turboprop transports and jet bombers. From Figure 15, the average vibration in turboprop transports is less than 2 times (6 dB) higher than in jet bombers. Now restrict attention to the center half of the fuselage. From Figure 12, for the same frequency increment, it is seen that the average vibration in the center half of the fuselage for turboprop transports is 30 times (30 dB) higher than in the same zone for jet bombers. If the comparison were further reduced to an individual turboprop transport versus an individual jet bomber, even greater differences might be observed. In purely statistical terms, the above argument is supported by the relatively large standard deviations for the data in each group, as illustrated in Figure 15. In conclusion, the results in Figure 16 serve only to prove that nearly all pertinent information in any data can be obscured if sufficient averaging is performed. One is reminded at this point of the story about the man who drowned in a lake with an average depth of 3 feet.

7. SPATIAL DISTRIBUTION STUDIES

The mean values and standard deviations for various classifications of past AFFDL vibration data have been calculated and evaluated in Section 6. Such information, however, is not sufficient to arrive at test specifications and design criteria. Specifications and criteria must be based upon an extreme vibration level as opposed to an average level. To establish an extreme level, it is necessary to determine a distribution function for the vibration levels within each structural zone to be covered by the specification or criteria. It would be most convenient if a single type of distribution function could be found which would fit the spatial variation of vibration levels in all zones. It would be further convenient if the distribution function in question were of a classic form which is well tabulated.

7.1 CONSTRUCTION OF A DISTRIBUTION FUNCTION MODEL

In the past, various models have been used to describe the spatial distribution of flight vehicle vibration levels. In some cases, a classical function is assumed and fitted to the data. Examples of functions which have been assumed include the lognormal distribution function [2] and the Rayleigh distribution function [8]. In other cases, an empirical function is developed by analysis of actual data [33]. The most common of these techniques is to assume the power spectra of the vibration data fit a lognormal distribution function. It appears logical that the first approach to the problem should be to establish whether or not the lognormal distribution is an appropriate fit to the spatial distribution of aircraft vibration data collected by AFFDL.

7.1.1 Definition of the Lognormal Distribution

The random variable x is said to have a lognormal distribution if $y = \log x$ is normally distributed. That is, if y is normal, then $x = e^y$ has a lognormal distribution.

The probability density function of x is given by

$$\begin{aligned} p(x) &= \frac{d}{dx} P(x) = \frac{d}{dx} P(y) = \frac{1}{x} p(\log x) \\ &= \frac{1}{x\sigma\sqrt{2\pi}} e^{-\frac{1}{2} \frac{(\log x - \mu)^2}{\sigma^2}} \quad \text{for } x \geq 0 \\ &= 0 \quad \text{for } x < 0 \end{aligned} \tag{42}$$

where $P(y)$ denotes the normal distribution function.

The lognormal density function has positive skewness, and is defined by two parameters. The mean of x , denoted by μ_x , is defined in terms of the mean and standard deviation of y , denoted by μ and σ , respectively, as follows.

$$\begin{aligned}
\mu_x &= \int_{-\infty}^{\infty} x p(x) dx \\
&= \int_{-\infty}^{\infty} e^y p(y) dy \\
&= \frac{1}{\sqrt{2\pi\sigma}} \int_{-\infty}^{\infty} e^{y - \frac{(y-\mu)^2}{2\sigma^2}} dy = e^{\mu + \frac{\sigma^2}{2}} \frac{1}{\sqrt{2\pi\sigma}} \int_{-\infty}^{\infty} e^{-\frac{(y-\mu-\sigma^2)^2}{2\sigma^2}} dy \\
&= e^{\mu + \sigma^2/2} \tag{43}
\end{aligned}$$

Correspondingly, the variance of x , denoted by σ_x^2 , is defined in terms of the mean and standard deviation for y , as follows.

$$\begin{aligned}
\sigma_x^2 &= E(x^2) - \mu_x^2 \\
&= \int_{-\infty}^{\infty} x^2 p(x) dx - e^{2\mu + \sigma^2} \\
&= \int_{-\infty}^{\infty} e^{2y} p(y) dy - e^{2\mu + \sigma^2} = e^{2\mu + 2\sigma^2} - e^{2\mu + \sigma^2} \\
&= e^{2\mu + \sigma^2} (e^{\sigma^2} - 1) \tag{44}
\end{aligned}$$

It is important to note that the transformation e^y transforms the mean as well as the variance.

If the median of x is denoted by m_x , then

$$P(x \leq m_x) = P(e^y \leq m_x) = P(y \leq \log m_x) = \frac{1}{2}$$

Thus

$$\log m_x = \mu \quad \text{or} \quad m_x = e^\mu \quad (45)$$

Using the invariance property of the maximum likelihood estimate, the maximum likelihood estimate of μ_x , σ_x^2 and m_x can be shown to be

$$\begin{aligned} \hat{\mu}_x &= e^{\bar{y} + s^2/2} \\ \hat{\sigma}_x^2 &= e^{2\bar{y} + s^2} (e^{s^2} - 1) \\ \hat{m}_x &= e^{\bar{y}} \end{aligned} \quad (46)$$

where \bar{y} and s^2 denote the sample mean and variance of the normal distribution of $y = \log x$. The above estimates are not unbiased.

A convenient method of computing

$$P(a < x \leq b)$$

is to observe the following.

$$\begin{aligned}
P(a < x \leq b) &= P(\log a < \log x \leq \log b) \\
&= P\left(\frac{\log a - \mu}{\sigma} < \frac{\log x - \mu}{\sigma} \leq \frac{\log b - \mu}{\sigma}\right) \\
&= P\left(\frac{\log b - \mu}{\sigma}\right) - P\left(\frac{\log a - \mu}{\sigma}\right)
\end{aligned} \tag{47}$$

where μ and σ are the mean and standard deviation of the normally distributed random variable, $y = \log x$, and $P(z)$ denotes the standardized normal distribution. For example, if $\sigma = 1$ and $\mu = 0$, then

$$\begin{aligned}
P\left(x \leq e^{\mu + \sigma^2/2}\right) &= P(\log x \leq \mu + \sigma^2/2) \\
&= P\left(\frac{1}{2}\right) \doteq 0.6915
\end{aligned}$$

7.1.2 Applications to Aircraft Vibration Environments

Consider a given structural zone of a particular aircraft group. Assume the vibration data have been reduced into the form of mean square values (or average power spectra) in contiguous narrow frequency intervals. Let f_i be the midpoint of the i th frequency interval. Let the data in the i th frequency interval be divided into m_i mean square value intervals, where x_{ik} is the midpoint of the k th mean square value interval for the data in the i th frequency interval. Hence, the segregation of the

data is as illustrated previously in Figure 10a, except there x is a mean square value rather than a peak value.

Now let $p(x_i)$ denote the probability density for the number of mean square values in the i th frequency interval. If the mean square values in the i th frequency interval are lognormally distributed, then $p(x_i)$ is given by (42) as

$$p_i(x_i) = \frac{1}{x_i \sigma_i \sqrt{2\pi}} e^{-(y_i - \mu_i)^2 / 2\sigma_i^2} \quad \text{for } x_i \geq 0$$

$$= 0 \quad \text{for } x_i < 0$$
(48)

where μ_i and σ_i are the mean value and standard deviation, respectively, for the random variable $y_i = \log x_i$.

Let n_i be the sample size in the i th frequency interval, and n_{ik} be observed number of values in the k th mean square value interval of the i th frequency interval. The maximum likelihood estimates of μ_i and σ_i^2 are given by

$$\hat{\mu}_i = \sum_{k=1}^{n_i} n_{ik} y_{ik} / n_i$$
(49)

$$\hat{\sigma}_i^2 = \frac{\sum_{k=1}^{n_i} n_{ik} y_{ik}^2 - \left(\sum_{k=1}^{n_i} n_{ik} y_{ik} \right)^2 / n_i}{n_i - 1}$$
(50)

where $y_{ik} = \log x_{ik}$. Substituting Eqs. (49) and (50) into Eq. (48) gives an estimate for the probability density function, $\hat{p}(x_i)$.

Various statistical inferences can now be made about the vibration environment from which the data were taken. First, the 100α percentage point of the spatial distribution function for the vibration is given by x_α , which satisfies

$$P(x_\alpha) = \int_0^{x_\alpha} \hat{p}(x_i) dx_i = 1 - \alpha \quad (51)$$

It follows that

$$\begin{aligned} P(x_\alpha) &= P(x_i \leq x_\alpha) = P(\log x_i \leq \log x_\alpha) \\ &= P\left(\frac{\log x_\alpha - \hat{\mu}_i}{\hat{\sigma}_i}\right) = 1 - \alpha \end{aligned} \quad (52)$$

where $P(z)$ is the standardized normal distribution function. Let z_α denote the 100α percentage point of the standardized normal distribution. Then it follows that

$$\frac{\log x_\alpha - \hat{\mu}_i}{\hat{\sigma}_i} = z_\alpha \quad (53)$$

Hence, the 100α percentage point of $\hat{p}(x_i)$ is given by

$$x_\alpha = e^{z_\alpha \hat{\sigma}_i + \hat{\mu}_i} \quad (54)$$

Because of the functional dependence of a lognormal variable on a normal random variable, various pertinent problems of statistical inference for a lognormal probability model may be solved using the properties of a normal distribution. For example, $100(1 - \alpha)\%$ tolerance limits with probability γ for the lognormal variable x_i can be constructed as follows.

$$\left(e^{\hat{\mu}_i - K\hat{\sigma}_i}, e^{\hat{\mu}_i + K\hat{\sigma}_i} \right) \quad (55)$$

where K is the same constant appropriate for the corresponding tolerance limits for the normal variable y_i ; that is,

$$\left(\hat{\mu}_i - K\hat{\sigma}_i, \hat{\mu}_i + K\hat{\sigma}_i \right)$$

Eq. (55) is deduced from the following relation

$$P \left[P \left(e^{\hat{\mu}_i - K\hat{\sigma}_i} < x_i < e^{\hat{\mu}_i + K\hat{\sigma}_i} \right) > 1 - \alpha \right] \quad (56)$$

$$= P \left[P \left(\hat{\mu}_i - K\hat{\sigma}_i < y_i < \hat{\mu}_i + K\hat{\sigma}_i \right) > 1 - \alpha \right] = \gamma$$

7.2 DEVELOPMENT OF TESTING PROCEDURES

The degree to which the distribution of vibration data fits an assumed distribution function model can be tested by the classical χ^2 goodness-of-fit test, as follows. Assume the mean square values of the data in the i th frequency interval are divided into m_i mutually exclusive intervals, where the number of mean square values in each of the intervals is n_{ik} ; $k = 1, 2, 3, \dots, m_i$. Let the corresponding probability of a mean square value being in each of the intervals be $P_{ik}(\theta_1, \theta_2, \dots, \theta_u)$; $k = 1, 2, 3, \dots, m_i$, where P_{ik} is determined from an empirical distribution function with a set of $\{\theta\}$ parameters. If the true values of $\{\theta\}$ are unknown, the statistic for a χ^2 test is given by

$$X_i^2 = \sum_{k=1}^{m_i} \frac{[n_{ik} - n_i P_{ik}(\theta_1, \dots, \theta_u)]^2}{n_i P_{ik}(\hat{\theta}_1, \dots, \hat{\theta}_u)} \quad (57)$$

where X_i^2 is asymptotically distributed as χ^2 with $m_i - u - 1$ degrees-of-freedom. Note that u number of degrees-of-freedom are lost because u parameters are estimated.

The adequacy of the fit to vibration data provided by the log-normal distribution defined in Eq. (48) can be tested by the χ^2 test given in Eq. (57). For the i th frequency interval, the statistic used is

$$X_i^2 = \sum_{k=1}^{m_i} \frac{(n_{ik} - n_i \hat{P}_{ik})^2}{n_i \hat{P}_{ik}} \quad (58)$$

where \hat{P}_{ik} is an estimate given by

$$\hat{P}_{ik} = \int_{a_{ik}}^{b_{ik}} \hat{p}(x_i) dx_i \quad (59)$$

The term $\hat{p}(x_i)$ is an estimate of $p_i(x_i)$ as described in Section 7.1.2, and a_{ik} , b_{ik} are the lower and upper limits of the k th mean square value interval. The statistic X_i^2 given by Eq. (58) has an asymptotic chi-square distribution with $m - 3$ degrees-of-freedom. Evaluation of Eq. (58) can be performed conveniently as follows.

$$\begin{aligned} \hat{P}_{ik} &= P(a_{ik} < x_i \leq b_{ik}) = P(\log a_{ik} < y_i \leq \log b_{ik}) \\ &= \mathcal{P}\left(\frac{\log b_{ik} - \hat{\mu}_i}{\hat{\sigma}_i}\right) - \mathcal{P}\left(\frac{\log a_{ik} - \hat{\mu}_i}{\hat{\sigma}_i}\right) \end{aligned} \quad (60)$$

where $\mathcal{P}(z)$ denotes the standardized normal distribution function, and $\hat{\mu}_i$ and $\hat{\sigma}_i$ are given by Eqs. (49) and (50).

The χ^2 test described above can be implemented to perform an overall test for the fit of c sets of empirical distributions. For example, it may be desired to test the overall goodness-of-fit of the log-normal probability model for all frequency intervals in a particular zone. The desired statistic is given by

$$X_t^2 = \sum_{i=1}^c X_i^2 = \sum_{i=1}^c \sum_{k=1}^{m_i} \frac{(n_{ik} - n_i \hat{P}_{ik})^2}{n_i \hat{P}_{ik}} \quad (61)$$

The variable X_t^2 has a χ^2 distribution with degrees-of-freedom given by

$$\text{d. f.} = \sum_{i=1}^c m_i - 2c - c \quad (62)$$

7.3 APPLICATION TO AFFDL VIBRATION DATA

The procedures developed in Section 7.1 are now applied to test a lognormality hypothesis for the spatial distribution of aircraft vibration using AFFDL data. The structural zone selected for the test is Zone 02 (middle half of fuselage) of Aircraft Group 5 (Century series fighters). As for the homogeneity tests in Section 6.2, data for aircraft Code No. 63 is omitted to assure consistency in the measurements. This particular zone was selected because (1) it provides a relatively large sample of data, and (2) it represents a basic structural region and aircraft group of considerable interest. Since only spatial variations in the vibration levels are of concern, data for a single flight condition are used to minimize variations due to different excitation characteristics. The flight condition selected for the test is Condition 07 (normal cruise).

The flight vibration levels during normal cruise for Zone 02 of Aircraft Group 5 are summarized in Table 17. A total of 4273 data values are given. Before proceeding, it should be noted that a critical assumption must be made concerning these data. Specifically, if the data in Table 17 are to represent the spatial distribution of vibration levels in Zone 02, it must be assumed that each value represents a sample of the vibration at a randomly selected location in that zone. In reality, this assumption is not totally valid for two reasons. First, the selection of transducer locations for the measurements was unquestionably influenced by such nonrandom practical considerations as physical accessibility and proximity to equipment locations of interest. Second, some of the data values represent repeated measurements at the same point on the same aircraft. In spite of these possible biasing effects, however, the randomness assumption is considered sufficiently acceptable to produce adequate results.

The data in Table 17 are presented in terms of double amplitude histograms for each of 20 frequency increments. To be consistent with the development in Section 7.1, those double amplitude intervals which include data are converted to mean square value intervals in Table 18. This step is not actually necessary since a lognormal distribution for double amplitude values would imply a lognormal distribution for mean square values as well. Nevertheless, the step is made to fully illustrate the testing procedure as it should be applied to later data which include an accurate representation of random contributions. Such data would normally be presented in terms of power spectra (normalized mean square values versus frequency). Also included in Table 18 are the natural logarithms of the mean square value interval limits (a_k, b_k) and midpoints (y_k).

The mean values and standard deviations, μ_i and σ_i , for the logarithms of the data in each frequency increment are given in Table 19. These values are calculated using Eqs. (49) and (50). With this information, the values of X_i^2 are calculated for each frequency increment using Eq. (58). An illustration of these calculations for the $i = 13$ th frequency increment (80-99 cps) is outlined in Table 20. The final results for the X_i^2 calculations in all frequency increments are summarized in Table 21. Note that the calculations were performed with the end intervals pooled as required to make the expected number of samples, $n\hat{P}_k$, at least 3. Also note that five frequency increments ($i = 3, 4, 5, 6$ and 9) are omitted from the final results because the sample size for these increments is not considered sufficient for the χ^2 test. Actually, the sample size for many of the frequency increments is less than would normally be desired for a χ^2 test (at least 200). Furthermore, the number of mean square value intervals, m_i , for the various frequency increments is not always

Table 18. Mean Square Value Intervals for Lognormality Test

b_k^*	$\log [b_k \times 10^{10}]$	y_k^{**}	b_k^*	$\log [b_k \times 10^{10}]$	y_k^{**}
51.0×10^{-4}	17.75	17.48	80.0×10^{-8}	8.98	8.76
32.0×10^{-4}	17.22	17.01	51.0×10^{-8}	8.54	8.31
20.2×10^{-4}	16.81	16.58	32.0×10^{-8}	8.08	7.84
12.5×10^{-4}	16.35	16.12	20.2×10^{-8}	7.60	7.36
8.14×10^{-4}	15.90	15.67	12.5×10^{-8}	7.12	6.91
5.12×10^{-4}	15.44	15.21	8.14×10^{-8}	6.70	6.47
3.21×10^{-4}	14.98	14.75	5.12×10^{-8}	6.24	6.01
2.02×10^{-4}	14.52	14.29	3.25×10^{-8}	5.78	5.54
1.28×10^{-4}	14.06	13.82	2.00×10^{-8}	5.30	5.08
80.0×10^{-6}	13.58	13.36	1.28×10^{-8}	4.85	4.60
51.0×10^{-6}	13.14	12.90	78.1×10^{-10}	4.36	4.08
32.0×10^{-6}	12.66	12.43	50.0×10^{-10}	3.80	3.42
20.2×10^{-6}	12.20	11.97	21.1×10^{-10}	3.05	2.78
12.5×10^{-6}	11.74	11.52	12.5×10^{-10}	2.52	2.30
8.14×10^{-6}	11.30	11.07	8.0×10^{-10}	2.08	1.79
5.12×10^{-6}	10.84	10.61	4.5×10^{-10}	1.50	1.32
3.21×10^{-6}	10.38	10.15	3.12×10^{-10}	1.14	0.92
2.02×10^{-6}	9.92	9.69	2.00×10^{-10}	0.69	0.40
1.28×10^{-6}	9.46	9.22	1.12×10^{-10}	0.11	

* b_k = upper limit of kth interval; $a_k = b_{k-1}$ = lower limit of kth interval

** $y = \frac{\log [b_k \times 10^{10}] + \log [b_{k-1} \times 10^{10}]}{2}$ = midpoint of kth log interval

Table 19. Means, Standard Deviations, and Sample Sizes for Lognormality Test

Frequency Increments by Code Number and Range in cps										
	1	2	3	4	5	6	7	8	9	10
	5-6	7-8	9-10	11-13	14-16	17-20	21-25	26-32	33-39	40-49
Sample Size, n_i	137	34	19	13	10	9	46	51	16	40
Mean Value, μ_i	14.48	13.72	12.18	11.44	11.64	10.38	9.74	9.04	7.52	7.52
Standard Deviation, σ_i	0.962	1.014	0.948	1.296	1.592	1.064	1.220	1.410	0.604	1.260
	11	12	13	14	15	16	17	18	19	20
	50-64	65-79	80-99	100-129	130-159	160-199	200-249	250-319	320-399	400-459
Sample Size, n_i	333	302	845	642	592	366	213	286	180	139
Mean Value, μ_i	6.78	6.30	6.03	5.50	4.78	4.62	4.34	3.32	2.84	2.22
Standard Deviation, σ_i	1.250	1.212	1.316	1.064	1.034	1.294	1.208	1.064	0.938	0.840

Table 20. Illustration of Calculations for Lognormality Test

Calculations for frequency increment $i = 13$ (80-99 cps)
 Sample size $n = 845$

k	l_k^*	u_k^*	$G(l_k)$	$G(u_k)$	\hat{P}_k	$n\hat{P}_k$	n_k	X_k^{2**}
1	2.61	∞	0.9955	1.0000	0.0045	3.80	17	45.8
2	2.25	2.61	0.9878	0.9955	0.0077	6.51	13	6.5
3	1.91	2.25	0.9719	0.9878	0.0159	13.44	27	13.7
4	1.56	1.91	0.9406	0.9719	0.0313	26.45	27	0
5	1.20	1.56	0.8849	0.9406	0.0557	47.07	26	9.4
6	0.84	1.20	0.7995	0.8849	0.0854	72.16	48	8.1
7	0.52	0.84	0.6985	0.7995	0.1010	85.34	51	13.8
8	0.17	0.52	0.5675	0.6985	0.1310	110.7	97	1.7
9	-0.18	0.17	0.4286	0.5675	0.1389	117.4	112	0.2
10	-0.55	-0.18	0.2912	0.4286	0.1374	116.1	107	0.7
11	-0.88	-0.55	0.1894	0.2912	0.1018	86.02	177	96.2
12	-1.26	-0.88	0.1038	0.1894	0.0856	72.33	123	35.5
13	$-\infty$	-1.26	0	0.1038	0.1038	87.71	20	52.3
							Total	283.9

$$* l_k = \frac{\log [a_k \times 10^{10}] - \mu}{\sigma} \quad u_k = \frac{\log [b_k \times 10^{10}] - \mu}{\sigma}$$

$$** X_k^2 = \frac{|n_k - n\hat{P}_k|^2}{n\hat{P}_k}$$

Table 21. Summary of Results for Lognormality Test

		Frequency Increments by Code Number and Range in cps									
		1	2	3	4	5	6	7	8	9	10
	5-6		7-8	9-10	11-13	14-16	17-20	21-25	26-32	33-39	40-49
Sample Size, n_i	137	34	19	13	10	9	46	51	16	40	
Number of Intervals, m_i	10	8	--	--	--	10	11	--	--	8	
X_i^2	14.9	2.3	--	--	--	16.3	14.3	--	--	18.6	
	11	12	13	14	15	16	17	18	19	20	
	50-64	65-79	80-99	100-129	130-159	160-199	200-249	250-319	320-399	400-499	
Sample Size, n_i	333	302	845	642	592	366	213	286	180	139	
Number of Intervals, m_i	11	11	13	11	9	11	10	9	7	7	
X_i^2	71.0	91.6	283.9	56.6	74.8	169.3	35.1	132.7	70.9	39.5	

$X_t^2 = 1091.8$; $m = 146$; $c = 15$

optimal for the corresponding sample size. Such problems are unavoidable, however, since the data were not collected and reduced with the intent of performing a χ^2 test.

Referring to Table 21, the value of X_t^2 , as defined in Eq. (61), is 1091.8. The total number of mean square value intervals is $m = 146$, and the number of data sets is $c = 15$. Hence, from Eq. (62), if the data in Table 17 has a lognormal distribution, then X_t^2 is distributed approximately like χ^2 with 101 degrees-of-freedom. From any table of χ^2 values, it is seen that the 1% point of χ^2 with 101 degrees-of-freedom is equal to 136. Hence, since $X_t^2 = 1091.8 > \chi_{0.01; 101}^2 = 136$, a lognormal hypothesis for the data in Table 17 is rejected at the 1% level of significance.

Technically, the foregoing results apply only to one structural zone of one aircraft group. A visual inspection of histograms (similar to Table 17) for data from various other zones and aircraft groups, however, indicates that these results may be generalized. Specifically, based upon past AFFDL vibration data, the spatial distribution for aircraft vibration levels is not lognormal in character. This fact is best illustrated by comparing the empirical density function for measured data to the lognormal density function, as is done in Figure 17. The empirical distribution in Figure 17 is calculated from data in Table 20 for the 13th frequency increment (80-99 cps) of Zone 02 for Aircraft Group 5. The results are typical of those obtained in other frequency increments. In particular, there is a definite tendency for the distribution of log values to be skewed so that the higher (but not extreme) mean square values occur with somewhat greater probability than would be predicted using the lognormal assumption.

STRUCTURAL ZONE 02
 AIRCRAFT GROUP 5
 FLIGHT CONDITION 07
 FREQUENCY INCREMENT 13

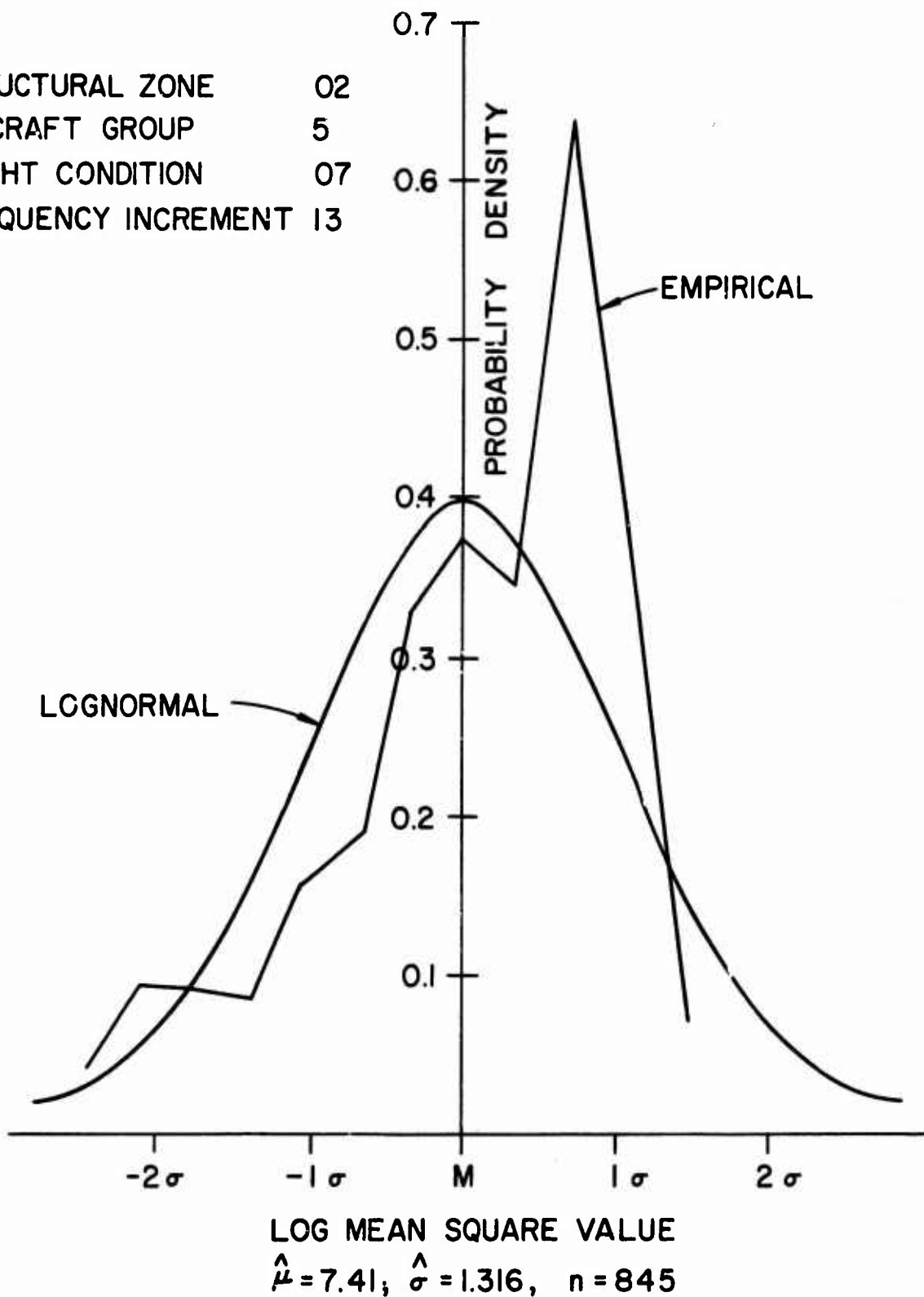


Figure 17. Illustration of Spatial Distribution for Vibration Data

The failure of the data to pass a lognormality test does not rule out the possibility that a lognormal assumption might still be acceptable for selecting test levels and design criteria. This possibility is illustrated by comparing the vibration level for some small percentage point of the actual distribution function to the level for that same percentage point of a fitted lognormal distribution function. As before, the data for frequency increment 13 of Zone 02 for Aircraft Group 5 are used. Assume a prediction at the 2% point (a 98% upper limit) is desired. From Table 17 or 20, it is seen that the 2% point for the actual data occurs at $\log [a \times 10^{10}] = 2.61 \hat{\sigma} + \hat{\mu} = 9.46$, which corresponds to a double amplitude of 0.0032 inch. From Eq. (54), the 2% point for a lognormal distribution fitted to the mean square values of the data occurs at $\log [a \times 10^{10}] = 2.056 \hat{\sigma} + \hat{\mu} = 8.73$, which corresponds to a double amplitude of 0.0023 inch. It is interesting to compare these results with those obtained by assuming the data have a simple normal distribution. First consider the case where the mean square values are assumed to be normally distributed. From Eqs. (43) and (44), the mean value and standard deviation for the mean square values are $\hat{\mu} = 0.099 \times 10^{-6} \text{ inch}^2$ and $\hat{\sigma} = 0.212 \times 10^{-6} \text{ inch}^2$. The 2% point is then 0.535×10^{-6} , which corresponds to a double amplitude of 0.0021 inches. Hence, a normal assumption for mean square values provides a poorer result than the lognormal assumption. Now consider the case where the original double amplitude values are assumed to be normally distributed. From Table 17, the mean value and standard deviations for the double amplitudes are $\bar{x} = 0.00082 \text{ inch}$ and $s = 0.00081$. The 2% point for a normal distribution fitted to the double amplitudes is then 0.0025 inch. This result is slightly better than achieved using the lognormal assumption.

The results of the spatial distribution study to this point are inconclusive. For the problem of selecting conservative test levels and design criteria, it appears that the lognormal distribution for mean square values may provide results which are no better than those obtained using a straightforward normal distribution assumption for peak or rms values. Perhaps a more accurate model for the spatial distribution of aircraft vibration should be sought out or developed. Further studies are required to resolve these issues. It is not considered appropriate, however, to pursue such studies at this time because of the limited quality of the available data. Any conclusions that might result from further studies of the currently available AFFDL vibration data would be subject to later confirmation and/or modification based upon similar studies of future data which properly represent the random contributions in the vibration environment. Hence, it is suggested that AFFDL defer studies of this problem until such future data are available in quantity.

8. PREDICTION MODEL STUDIES

Attention is now directed to the primary purpose of this effort: namely, the development of a general extrapolation model for predicting aircraft vibration environments. As a first step, it is appropriate to review the information needed to develop such a model, and to assess the progress made thus far towards acquiring this information.

From the discussions in Section 2, the development of an aircraft vibration prediction model of the general extrapolation type requires four preliminary steps, as follows.

1. Approximate relationships between fundamental source parameters and the resulting vibration environment must be developed. This step is required to define the structural, engine, and flight parameters which should be measured and recorded with the vibration data, and to provide an initial model for regression studies.

2. A large collection of accurate vibration data for representative locations in various aircraft must be obtained and identified with the fundamental parameters defined in step 1. This step provides the basic data required for the regression studies.

3. Each aircraft type of interest must be divided into appropriate structural zones, where each zone will be the basis for a single prediction model. This step is necessary to reduce the complexity and redundancy of the resulting prediction model.

4. The general form of the spatial distribution function for the vibration within each zone must be approximated. This step is needed to provide a firm statistical basis for predicting conservative limits for test specifications and design criteria.

Step 1 is dealt with in Section 3. Vibration sources are identified and relationships are developed for all aircraft groups. However, since the design of propeller type aircraft (Groups 1 and 2) is unlikely in the future, these aircraft will not be considered further. Attention will be restricted to jet powered aircraft, as represented by Groups 3, 5, and 10. The results in Section 3 indicate that, for jet powered aircraft, the critical source parameters which should be recorded and identified with measured vibration data are ρ (air density), A (jet exit area), V_e (exhaust gas velocity), c (speed of sound), c_e (local speed of sound in jet exhaust), q (dynamic pressure), w (average surface weight density), and the rpm for all rotors, gears, and other rotating equipment. The suggestions in Section 3 for analytical relationships between these various source parameters and the resulting vibration environments should provide an adequate basis for initial regression studies. It should be emphasized, however, that the relationships might be modified on a trial and error basis as required to obtain good correlation coefficients in the regression analyses.

Concerning step 2, AFFDL has collected considerable quantities of vibration data on many different aircraft, as summarized in Section 4. The data are well documented and properly identified with the pertinent source parameters indicated in step 1. In most cases, however, the quality of the data is not sufficient for use in the development of a vibration prediction model. The reasons for this are detailed in Section 5.

Recent revisions in AFFDL data acquisition and analysis procedures should provide suitable data for this application in the future, but at this time, such data are not available in quantity. Data of reasonable quality are available for one aircraft only; namely, an RF-4C (Code No. 63). Hence, the data for this aircraft will be used to illustrate the desired developments.

Step 3 is pursued in Section 6. Proper zoning of aircraft is investigated based upon homogeneity studies of past AFFDL vibration data. Because of the limited quality of the data, firm conclusions cannot be drawn. Tentative conclusions, however, are as follows. Separate prediction models are not required for the vibration along the three orthogonal axes, or for the vibration of different aircraft within a group. On the other hand, separate prediction models should be developed for the vibration in each structural zone designated by AFFDL, and for the vibration of each aircraft group. To facilitate further developments, it will be assumed that the above conclusions are valid.

Step 4 is considered in Section 7. A lognormal hypothesis for the spatial distribution of mean square vibration levels over a structural zone is tested using past AFFDL vibration data. As in step 3, firm conclusions are not possible because of the data quality. The tentative conclusion, however, is that the lognormal distribution does not provide an acceptable description for the spatial distribution of aircraft vibration. In fact, it appears that a simple normal distribution for peak or rms values might estimate the vibration levels at small percentage points with as much accuracy as a lognormal distribution for mean square values. Neither distribution function, however, produces desirable results. To facilitate further developments, the normal distribution will be assumed for the spatial distribution of peak or rms vibration levels within a given structural zone.

8.1 MODEL FORMULATION FOR JET BOMBERS AND FIGHTERS

Separate prediction models probably will be required for jet bombers (Group 3) and jet fighters (Group 5). The general form of the models, however, will be similar since the primary vibration sources for these two aircraft groups are the same. Hence, they will be considered together.

From Table 6 in Section 3, there are five sources of vibration for jet bombers and fighters which are considered sufficiently significant to include in a prediction model. In review, these sources are as follows.

- R-1 — jet acoustic noise
- R-2 — aerodynamic boundary layer noise
- R-6 — wake turbulence caused by aerodynamic devices
(lift devices, drag devices, and spoilers)
- D-3 — jet engine shaft rotation
- D-10 — gunfire

From the viewpoint of test specifications and design criteria, the ultimate requirement is to predict the most severe vibration levels which occur during the aircraft service life. This requirement permits the prediction model to be segmented and simplified. For example, the maximum vibration induced by jet noise clearly occurs during takeoff when the contribution of boundary layer noise is negligible. Corresponding, the maximum vibration induced by boundary layer noise occurs during high speed flight when the effects of jet noise are small. The contributions of jet noise can also be neglected when wake turbulence is predicted since the engine power is usually low when the various aerodynamic

devices are deployed. Guns are not used at takeoff. Hence, the worst case for gunfire induced vibration is probably at high speeds when jet noise contributions are small. Based upon these considerations, it is suggested that the power spectrum for jet bomber and fighter vibration environments be predicted in four segments, as follows.

1. For Takeoff

$$G(f)_{to} = G(f)_{r1} + G(f)_{d3} \quad (63a)$$

2. For High Speed Flight

$$G(f)_{hs} = G(f)_{r2} + G(f)_{d3} \quad (63b)$$

3. For Deployment of Aerodynamic Devices

$$G(f)_{ad} = G(f)_{r2} + G(f)_{d3} + G(f)_{r6} \quad (63c)$$

4. For Gunfire

$$G(f)_{gf} = G(f)_{r2} + G(f)_{d3} + G(f)_{d10} \quad (63d)$$

Note that a separate set of predictions will apply to each structural zone of each aircraft group.

Suggested techniques for determining each of the contributing power spectra terms in Eq. (63) are now outlined.

8.1.1 Jet Noise Contribution

From Eqs. (26) and (28), the initial model for the vibration induced in a specific zone by jet noise is

$$\hat{G}_a(\Omega)_{rl} = \hat{A}(\Omega)_{rl} X_{rl} \quad (64)$$

where

$\hat{G}_a(\Omega)_{rl}$ = average power spectral density for the acceleration response versus dimensionless frequency

$\hat{A}(\Omega)_{rl}$ = regression coefficient (estimated weight) versus dimensionless frequency

$X_{rl} = \rho A V_e^n / c^5 w^2$ (independent variable)

$\Omega = f d c_e / V_e c$ (dimensionless frequency)

ρ = atmospheric density

A = jet exit area

V_e = exhaust gas velocity

w = surface weight density of structure

c = ambient speed of sound

c_e = local speed of sound in jet

$d = A/\pi$

n = constant between 6 and 8

f = frequency in cps

Equation (64) is written in terms of dimensionless frequency to account for frequency shifts of the jet noise spectrum due to variations in the parameters which define the dimensionless frequency. A specific prediction may be readily converted to power spectral density versus frequency in cps using the definition for Ω .

The weight, $A(\Omega)_{r1}$, in Eq. (64) is estimated by a conventional regression analysis of "appropriate data," as discussed in Section 2.2 (the definition of "appropriate data" is discussed later). For the problem at hand, only one independent variable is involved. Hence, the estimation is accomplished using Eq. (10). With the estimation of the weight, Eq. (64) can then be applied to predict the average power spectrum for the jet noise induced vibration in a similar structural zone of a similar future aircraft.

The final goal, of course, is to predict some conservative upper limit for the vibration. The regression program will calculate any desired prediction limit for the data, given a distribution function for the data about the regression line, as detailed in Section 8.3 to follow. Note that, because of the w^2 term, the distribution function of concern here is not the spatial distribution discussed in Section 7. It is a more complex function dependent upon the spatial distribution of both the vibration levels and the surface mass density. For convenience, the function will be assumed normal.

Equation (64) provides an acceptable model for regression analysis, assuming the relationships in the independent variable X_{r1} are valid. If there is some uncertainty about any terms forming X_{r1} , however, the model could be expanded to evaluate these terms separately. For example, there is uncertainty concerning the proper value for n in the V_e^n term. Hence, it might be interesting to study the model written in the following form

$$\log \left[\hat{G}_a(\Omega)_{r1} \right] = \log \left[\hat{A}(\Omega)_{r1} \right] + \log \left[\frac{\rho A}{c w} \right] + n \log \left[V_e \right] \quad (65)$$

Equation (65) constitutes a regression equation of the form $y = a_0 + a_1 x_1 + a_2 x_2$ where $a_0 = \log \left[\hat{A}(\Omega)_{r1} \right]$, $a_1 = 1$ and $a_2 = n$. Hence, the regression analysis will calculate the values for both $\log \left[A(\Omega)_{r1} \right]$ and n which provide the best fit to the data. The procedure could be extended to solve for the power of every term in X_{r1} , but such a procedure is not suggested. As the number of terms in the regression model is increased, the variance for the calculated coefficients is also increased. It is desirable to restrict the model as much as can be justified by known facts.

The next problem is the selection of "appropriate data" for the regression analysis. The data used should represent as closely as possible the vibration due only to jet acoustic noise. Such data may be obtained from sample records of the vibration during takeoff, preferably at the start of takeoff after the engine has reached full power but before significant speed has been achieved. The sample records should be reduced to power spectra with all periodic components removed. Since the vibration produced by jet noise is random, any periodic components that might be present must represent other sources (principally engine shaft rotation). See Section 8.1.6 for further discussion of data reduction procedures.

The final problem is the determination of surface weight densities (w) for the measurement locations. For the basic structural zones, measurements will generally be made on frames, stringers, truss sections, or other structures with clearly defined widths. The surface weight density for such structures should be calculated as follows. Compute the weight per unit length of the structure and divide by the width. If the structure is attached to a skin section, add in the surface weight density of the skin.

If a component is attached to the structure at the measurement location, add in an effective surface weight density of the component given by

$$w_e = \frac{w_c}{N_a A_s} \quad (66)$$

where

w_c = total weight of component

N_a = number of attachment points

A_s = area of the structure in the general region
where the component is attached

8.1.2 Aerodynamic Noise Contribution

From Eqs. (26) and (30), the initial model for the vibration induced in a specific zone by aerodynamic noise is

$$\tilde{G}_a(f)_{r2} = \hat{A}(f)_{r2} X_{r2} \quad (67)$$

where

$\tilde{G}_a(f)_{r2}$ = average power spectral density for the acceleration response versus frequency

$\hat{A}(f)_{r2}$ = regression coefficient (estimated weight) versus frequency

$X_{r2} = q^2/w^2 = \rho^2 V^4/4w^4$ (independent variable)

ρ = atmospheric density

V = aircraft velocity

w = surface weight density of the structure

f = frequency in cps

The procedures for calculating the coefficient $\hat{A}(f)_{r2}$, for arriving at a conservative prediction limit for the vibration, and for determining proper values for the surface weight density w , are the same as discussed in Section 8.1.1.

Now consider the problem of selecting appropriate data for the regression analysis. The data should represent as closely as possible the vibration due only to boundary layer turbulence. The best source of data would be from sample records collected during clean dives with low engine power. However, sample records collected during any clean cruise condition should be acceptable. Care must be exercised to exclude all data obtained during those flight conditions when lift, drag, or spoiler devices are deployed, or during climb, acceleration, or other flight conditions where the engine power is high compared to the resulting airspeed. The sample records should be reduced to power spectra with all periodic components removed. As for jet noise, the vibration induced by boundary layer noise is random. Thus, any periodic components which might be in the data must represent other sources. See Section 8.1.6 for further discussions of data reduction procedures.

8.1.3 Wake Turbulence Contribution

The most straightforward approach to establishing the contribution of wake turbulence is to compare the vibration measured at similar points under similar flight conditions with and without various lift, drag, and spoiler devices deployed. By reducing the data in terms of power spectra with all periodicities removed, the contribution of wake turbulence due to the deployment of a given device would be

$$G_a(f)_{r6} = G_a(f)_w - G_a(f) \quad (68)$$

where

$G_a(f)_w$ = measured power spectrum with wake turbulence
producing device deployed

$G_a(f)$ = measured power spectrum without wake turbulence
producing device deployed

The above procedure should be repeated using data collected for different values of q to determine if $G_a(f)_{r6}$ displays a q dependence. If it does, a conservative prediction limit for $G_a(f)_{r6}$ should be established by a regression analysis of the following model.

$$\log \left[\hat{G}_a(f)_{r6} \right] = \log \left[\hat{A}(f)_{r6} \right] + B \log \left[q \right] \quad (69)$$

If it is found that $B = 2$, then the q dependence is the same as suggested in Eq. (67). Note that a weight term (w) is not suggested in Eq. (69). Since wake turbulence is predominately a low frequency phenomenon, the structural response is primarily controlled by stiffness rather than mass.

If a q dependence is not detected in the calculated values for $G_a(f)_{r6}$, then a conservative prediction limit should be established as follows. For the measurements in each structural zone, pool together the values of $G_a(f)_{r6}$ determined for all flight conditions. Calculate the mean value and standard deviation of the spectra versus frequency for each zone. Fit an appropriate distribution function (unknown at this time) using the calculated mean and standard deviation at each frequency. Determine a prediction limit by selecting the spectral density level at any desired percentage point of the fitted distribution. Further discussions of the statistical aspects of selecting prediction limits are presented in Section 8.5.

It should be mentioned that an effort was made to evaluate the contribution of wake turbulence using currently available AFFDL data. Histograms for the vibration data measured in various zones of jet bombers and fighters during clean flight conditions were compared to similar data measured during those flight conditions when various wake turbulence producing devices were deployed. In many cases, the comparisons did not reveal any significant difference in the average vibration levels for the two situations. This failure to detect the contributions of wake turbulence is probably due to the limited quality of the available data. On the other hand, wake turbulence may not be as significant as originally believed. These issues must be resolved by applying Eq. (68) to future data obtained in the manner specified.

8.1.4 Jet Engine Shaft Rotation Contribution

The vibration induced by jet engine shaft rotation is one contribution that is fully represented and described by past AFFDL vibration data. Jet engine shaft vibration is periodic with principal frequency components below 500 cps. Hence, past AFFDL data reduction techniques, as summarized in Section 5, tended to emphasize the vibration from this source. This fact is confirmed by an inspection of the shot gun data plots in [19] - [25]. It is seen in these references that the vast majority of data points are clustered at the frequencies of shaft rotation and their harmonics.

It was previously concluded in Section 3.3.6 that attempts to correlate engine shaft induced vibration with engine or flight parameters other than rpm would probably not be productive. This conclusion is supported by a review of histograms for the vibration data measured in jet bombers and fighters during various different flight conditions. The review

indicates that variations in the vibration levels at shaft frequencies and their harmonics from one flight condition to another are generally small compared to the variations from one point to another for a given flight condition. In other words, the variance of the spatial distribution within a zone is much larger than the variance caused by changing flight conditions. This point is illustrated in Table 22, which summarizes data measured in Zone 02 (center half of fuselage) of aircraft Group 5 (Century series fighters) during four widely varying flight conditions (takeoff, climb, normal cruise, cruise with afterburner). The data are presented for the frequency interval from 80 to 129 cps, which includes the fundamental of shaft rotation (high speed shaft) for the flight conditions in question. It is seen in Table 22 that the average vibration levels for the different flight conditions vary less than 1.5 to 1 while the vibration levels for any one flight condition vary up to 75 to 1. These results are typical of the data for all zones and flight conditions.

If the past AFFDL data is accepted as a valid representation of the periodic vibration environment below 500 cps, there is no need for further data collection or analysis to define the engine shaft induced vibration in jet bombers and fighters. The desired results are given directly for each structural zone of jet bombers by Figure 11 (c), and for each structural zone of jet fighters by Figure 11 (d). The results are presented as mean values and standard deviations for displacement amplitudes versus frequency for each zone. A conservative limit for a prediction may be obtained from these results by assuming a specific spatial distribution function for the data. If a normal distribution for peak values is assumed, a $(1 - \alpha)$ prediction limit for the i th frequency increment is given by

$$L_{i; (1-\alpha)} = z_{\alpha} s_i + \bar{x}_i \quad (70)$$

Table 22. Comparison of Vibration Induced by Jet Engine Shaft Rotation for Various Flight Conditions

Aircraft Group 5 (Century Series Fighters)
 Structural Zone 02 (Middle Half of Fuselage)
 Frequency Increments 13 and 14 (80 to 129 cps)

Vibration Double Amplitude 10^{-3} in.	Number of Data Points Measured for Various Flight Conditions			
	Condition 05 (assisted takeoff)	Condition 06 (normal climb)	Condition 07 (normal cruise)	Condition 48 (cruise with afterburner)
8.07-9.99		1	1	
6.40-8.06				1
5.07-6.39				1
4.02-5.06	1		2	7
3.20-4.01	9	2	14	8
2.53-3.19	28	1	13	7
2.02-2.52	24	10	30	9
1.60-2.01	39	11	39	28
1.27-1.59	34	8	37	24
1.00-1.26	27	17	80	57
0.81-0.99	30	21	81	66
0.64-0.80	31	20	159	61
0.51-0.63	50	28	179	70
0.40-0.50	63	34	243	92
0.32-0.39	71	33	286	143
0.25-0.31	73	28	223	138
0.20-0.24	35	16	84	45
0.13-0.19	4	3	16	12
Mean Value 10^{-3} in.	0.92	0.77	0.65	0.71

where

z_{α} = 100 α percentage point of standardized normal distribution

\bar{x}_i = mean value for i th frequency interval from Figure 11

s_i = standard deviation for i th frequency interval from Figure 11

Further discussions of the statistical aspects of selecting prediction limits are presented in Section 8.5.

For example, assume a 0.975 (97.5%) prediction limit is desired for the fundamental shaft vibration in Zone 02 (middle half of fuselage) for aircraft Group 5 (Century series fighters). The fundamental shaft frequency for the high speed shaft is usually in the frequency increment from 80 to 99 cps. From Figure 11(d), for the 13th frequency increment, $\bar{x} = 0.82 \times 10^{-3}$ inch and $s = 0.81 \times 10^{-3}$ inch. For a 97.5% limit, $z_{\alpha} = 1.96$. Hence, $L_{13;0.98} = 0.0024$ inch ≈ 1 g.

8.1.5 Gunfire Contribution

The vibration induced by gunfire is basically periodic with a fundamental frequency equal to the firing rate. Hence, the contribution of gunfire is easily extracted from the power spectra for aircraft vibration data collected during the operation of guns. Unfortunately, the currently available AFFDL vibration data do not include any measurements obtained during gunfire. Such data should be acquired in the future. The contributions of gunfire should be extracted from the data measured at all locations. Mean values and standard deviations should then be computed for the data in each structural zone at the firing rate frequency and its harmonics. A conservative limit for future predictions may be obtained by the procedures outlined in Section 8.1.4.

8. 1. 6 Suggested Data Reduction Procedures

The prediction models suggested in this section for jet bomber and fighter vibration environments are presented in terms of power spectra. Theoretically, the data used to develop the models should then be reduced in terms of power spectra. In practice, however, this is not always necessary or even desirable.

First consider the periodic contributions in the vibration environment (jet engine shaft rotation and gunfire). The power spectrum for a periodic vibration is theoretically a series of delta functions. Conventional analog and digital power spectral density analysis procedures, however, will display each periodic component (sinusoid) as a peak with finite density and bandwidth. These peaks must then be converted to a mean square value at a given frequency by taking the product of the indicated density and the analysis bandwidth. The data may be further reduced to rms or peak values, as desired. From the data reduction viewpoint, the only requirement is that the analysis bandwidth be sufficiently narrow to distinguish between adjacent periodic components and to extract the periodic components from the background random contribution. From the prediction model viewpoint, the data pooling operations (zoning) will produce periodic components in each zone at numerous frequencies. Hence, the predictions must be made in terms of components in predetermined frequency increments covering the frequency range of the pooled periodic data. The selection of these predetermined frequency increments need not be influenced in any way by the bandwidth used for the data reduction. The increments used for the studies in Sections 6 and 7 (see Table 17) are acceptable. The actual calculations to establish a conservative prediction level should be performed using

the data in a format compatible with the assumed spatial distribution function for the data. For example, if a lognormal distribution for mean square values is assumed, the data should be evaluated in terms of the mean square values for the periodic components; if a normal distribution for peak values is assumed, the data should be evaluated in terms of the peak values for the components, etc.

Now consider the random contributions in the vibration environment (jet noise, aerodynamic noise, wake turbulence). The usual procedure in random data analysis is to compute power spectra using relatively narrow analysis bandwidths to obtain highly resolved spectral plots. For many applications (for example, transfer function analysis), highly resolved power spectra are required. Furthermore, a highly resolved power spectrum provides the only adequate practical method of detecting and eliminating periodic components in the data spectrum. Hence, it appears reasonable that the data should be analyzed using relatively narrow analysis bandwidths, as is currently done by AFFDL (see Section 4). This does not mean, however, that the highly resolved spectral data should be used directly in the regression studies to establish a vibration prediction model.

It is wise at this point to recall the ultimate goal of the regression analysis; namely, the development of a general extrapolation procedure for predicting aircraft vibration environments. High resolution in the final predictions is not believed to be warranted by this goal since considerable frequency blurring will already have been introduced by the data pooling operations required to develop the prediction model. It is believed that predictions with relatively coarse resolution, say 1/3 octave or even 1/1 octave bandwidths, would be suitable. This prediction resolution fixes the resolution bandwidth for the power spectra data to be used for the regression analysis. Hence, for this application,

the highly resolved power spectra should be converted to average power spectral densities in 1/3 or 1/1 octave bands. This may be done by estimating the area under the power spectrum between the frequency limits of the 1/3 or 1/1 octave band in question, excluding the area under peaks due to periodic components. This procedure is illustrated for the 1/1 octave case in Figure 18.

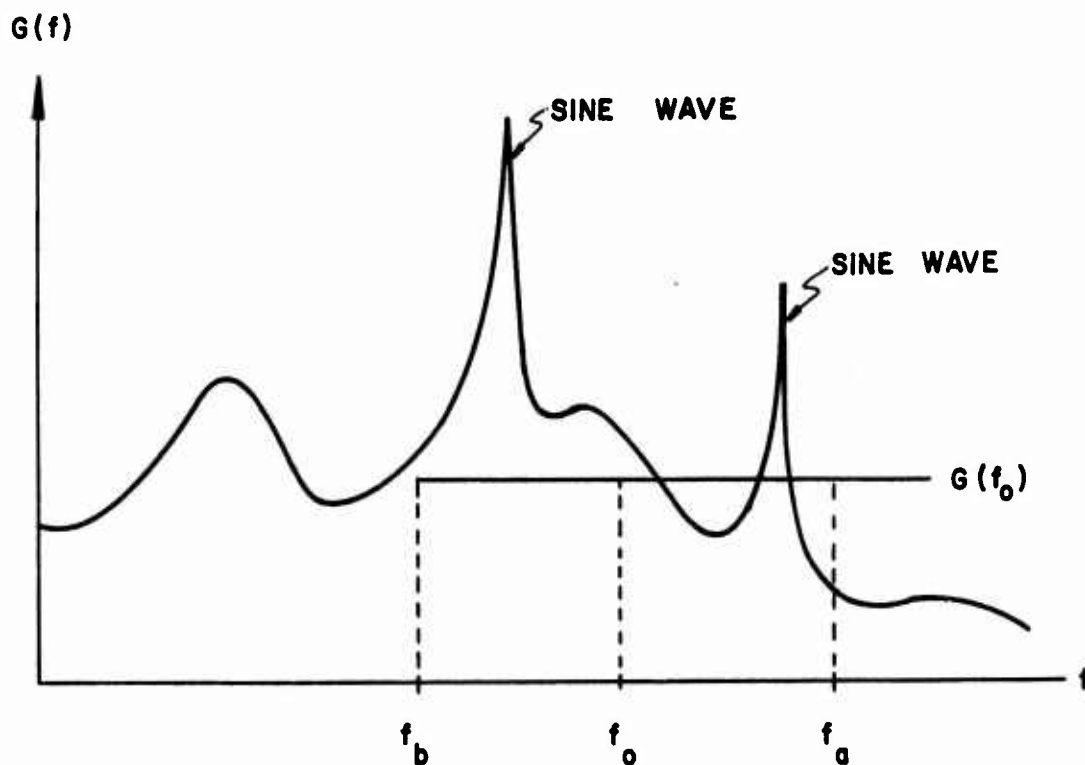


Figure 18. Illustration of Random Data Analysis Procedures

One problem is introduced by the above suggested data reduction procedures. Since the data and, hence, the resulting predictions are in

terms of average power spectra in 1/3 or 1/1 octave bands, they may well underpredict peaks in the power spectra for the actual random vibration environment. This possibility may be accounted for by adding a general correction term to the resulting predictions. The correction term would be determined empirically by noting the ratio of the highest peak to average density for each 1/3 or 1/1 octave of each power spectrum during the data evaluation illustrated in Figure 18. Of course, peaks due to periodic components would be ignored. The mean value and standard deviation for these observed peak to average ratios would then be computed. The correction factor would be determined by selecting the ratio corresponding to some small percentage point on a normal distribution with the calculated mean and standard deviation. The determination of a correction term of this type for missile vibration predictions is reported in [6]. The results suggest a correction factor of 3 dB for 1/3 octave predictions and 5 dB for 1/1 octave predictions.

8.2 MODEL FORMULATION FOR HELICOPTERS

The available AFFDL data cover both reciprocating and jet engine powered helicopters (one of each). Since the design of future reciprocating engine powered helicopters is unlikely, jet powered helicopters are of primary interest. However, the principal sources of vibration for the two are similar. Hence, data from both types may be used as a basis for predicting the vibration environment of the jet powered type.

From Table 6 in Section 3, there are seven sources of vibration for helicopters which are considered sufficiently significant to include in a prediction model. In review, these sources are as follows.

1. D-1 — rotor blade passage
2. D-2 — rotor rotation
3. D-3 — jet engine shaft rotation (jet engine powered only)
4. D-4 — reciprocating engine exhaust (reciprocating engine powered only)
5. D-6 — engine accessory equipment
6. D-8 — gear box noise
7. D-10 — gunfire

In attempting to develop a practical prediction model for the above sources, two problems quickly evolve. First, from the discussions in Section 3.3, many of these sources are poorly defined in terms of tractable analytical models. Second, all of the sources, except gunfire, occur simultaneously. That is, it is difficult to isolate the contributions of individual sources as is done for jet bombers and fighters in Section 8.1. For these reasons, an attempt to develop a prediction model for helicopter vibration based upon individual contributing sources is not considered worthwhile. Instead, the problem should be approached by evaluating the vibration environment from all sources measured for various pertinent flight conditions. Currently available AFFDL data should be acceptable for this task, at least in the frequency range below 500 cps, since the principal sources of vibration are periodic.

Histograms for the vibration levels measured by AFFDL in the three basic structural zones of helicopters during takeoff, climb, cruise, and hover are presented in Section 5 of Appendix A. An inspection of these data reveals that the vibration levels for the four different flight conditions are surprisingly similar. This fact is illustrated in Table 23, which summarizes the mean values in various frequency increments for

Table 23. Comparison of Average Helicopter Vibration Levels for Various Flight Conditions

Aircraft Group 10 (Helicopters)

Frequency Increment cps	Mean Value of Data Points Measured for Various Flight Conditions							
	Condition 04 (Takeoff)		Condition 06 (Normal Climb)		Condition 07 (Normal Cruise)		Condition 48 (Hover)	
	Number of Points	Mean Value 10^{-3} in.	Number of Points	Mean Value 10^{-3} in.	Number of Points	Mean Value 10^{-3} in.	Number of Points	Mean Value 10^{-3} in.
14-16	40	12	38	10	229	21	126	19
17-20	91	13	81	11	645	23	249	26
50-64	124	1.8	113	1.7	554	1.9	235	2.3
80-99	117	0.98	105	0.81	659	0.80	263	0.88
100-129	73	0.29	33	0.29	207	0.33	80	0.31
130-159	68	0.38	74	0.46	455	0.42	314	0.46
160-199	107	0.53	76	0.49	388	0.49	101	0.53
200-249	57	0.24	62	0.23	443	0.21	249	0.23
250-319	131	0.23	102	0.17	483	0.15	204	0.14
320-399	86	0.13	64	0.14	322	0.11	101	0.10
400-499	51	0.087	30	0.078	160	0.064	82	0.061

Zone 02 (middle half of fuselage). Note that results are presented only for those frequency increments where a significant number of data values occur. It is seen from Table 23 that the mean values for the vibration levels measured during the four flight conditions differ very little in most frequency increments. Considering the sample size for the mean value calculations, many of the indicated differences are not even statistically significant. These results are typical of those for the other zones and flight conditions. Hence, if the past AFFDL data are accepted as a valid representation of the periodic vibration environment below 500 cps, it must be concluded that the variation of helicopter vibration levels for different flight conditions is negligible compared to the variation with structural location. This means that the vibration environment for helicopters (similar to those surveyed by AFFDL) can be predicted by a single spectrum for each structural zone, independent of flight condition. The desired statistical information is given directly by Figure 11(e). By fitting an appropriate spatial distribution function to the mean values and standard deviations in Figure 11(e), a prediction for helicopter vibration amplitudes versus frequency may be determined at any desired percentage point. Such prediction curves for the three basic structural zones of helicopters, based upon the 2.5% point of a normal distribution, are presented in Figure 19.

Note that the predictions in Figure 19 do not include the contribution of gunfire. No measurements obtained during gunfire are included in the currently available AFFDL vibration data. Such data should be obtained in the future, and analyzed to generate prediction curves similar to those presented in Figure 19. These new curves would apply to those flight phases when guns are used. Further note that the predictions in Figure 19

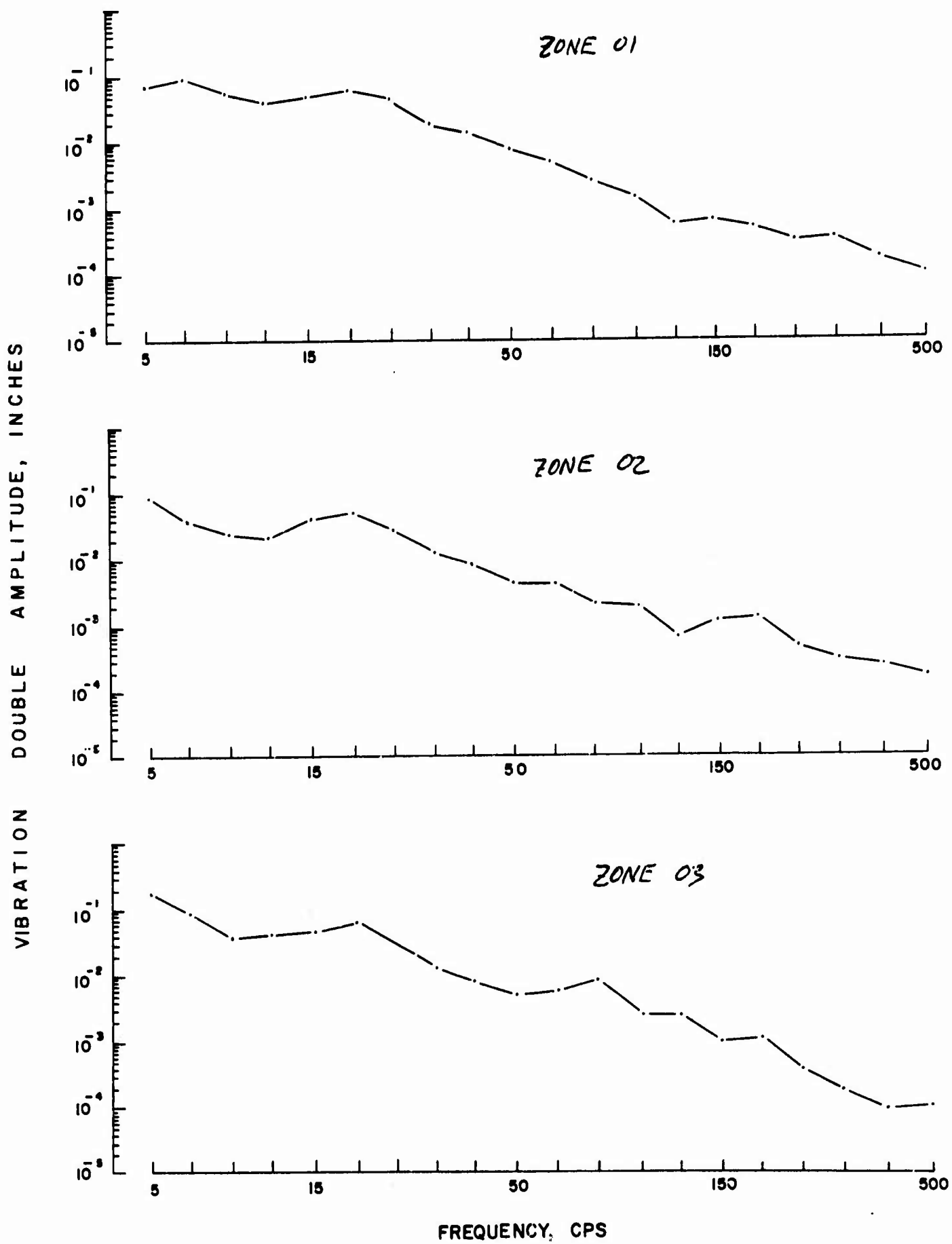


Figure 19. 97.5% Prediction Limits for Helicopter Vibration Levels

probably do not reflect the vibration induced by "blade slap" during high forward speed flight or sharp maneuvers. These conditions should be analyzed and predicted separately, as discussed in Section 3.1.

8.3 REGRESSION ANALYSIS PROCEDURES

From Section 8.1, there are two contributing sources of vibration for jet bombers and fighters which must be evaluated by a regression analysis of appropriate flight vibration data. These sources are jet noise and aerodynamic boundary layer noise. The suggested regression models for these two sources are given by Eqs. (64) and (67), respectively. In both cases, the model is of the same general form and involves only one independent variable. For simplicity, the model will be written in the form

$$y = Ax \tag{71}$$

where $y = G(f)$ and $x = X$. The problem now is to establish a $(1 - \alpha)$ upper prediction limit for y given x , based upon a collection of measured values for x and y .

Let y_i denote the i th measurement and x_i denote the independent variable associated with the i th measurement, where $i = 1, 2, 3, \dots, n$. The required calculations are as follows [34], [35].

$$A = \frac{\sum_{i=1}^n x_i y_i}{\sum_{i=1}^n x_i^2} \tag{72a}$$

$$\Phi = \frac{A^2 \sum_{i=1}^n (x_i - \bar{x})^2 (n-1)}{\sum_{i=1}^n (y_i - Ax_i)^2} \quad (72b)$$

$$\gamma = A \frac{s_x}{s_y} \quad (72c)$$

where

$$s_x = \left[\sum_{i=1}^n (x_i - \bar{x})^2 / (n-1) \right]^{1/2}$$

$$s_y = \left[\sum_{i=1}^n (y_i - \bar{y})^2 / (n-1) \right]^{1/2}$$

$$Z = 0.5 \left[n-3 \right]^{1/2} \log_e \frac{1+\gamma}{1-\gamma} \quad (72d)$$

$$L_{A;\alpha} = A \pm t_{n-1;\alpha/2} s_{y \cdot x} \left[\sum_{i=1}^n x_i^2 \right]^{-1/2} \quad (72e)$$

where

$t_{n-1;\alpha/2}$ = the $\alpha/2$ percentage point of a student's "t" distribution with $n-1$ degrees-of-freedom

$$s_{y \cdot x} = \left[\sum_{i=1}^n (y_i - Ax_i)^2 / (n-1) \right]^{1/2}$$

$$E[y_k] = Ax_k \quad ; \quad k = 1, 2, 3, \dots, N \quad (72f)$$

where

x_k = fixed value for x

$$L_{y_k; \alpha} = E[y_k] + t_{n-1; \alpha} s_{y \cdot x} \left[1 + \frac{x_k^2}{\sum_{i=1}^n x_i^2} \right]^{1/2} \quad (72g)$$

where

$t_{n-1; \alpha}$ = the α percentage point of a student's t distribution with $n - 1$ degree-of-freedom

$s_{y \cdot x}$ is defined in (72e)

The regression coefficient A is given by Eq. (72a). The other calculations are used to evaluate the model and select prediction limits, as follows.

8.3.1 Evaluation of Model Linearity

It is initially assumed that the relationship between x and y is linear. The validity of the assumption should be checked. This may be done using the value of Φ given by Eq. (72b). If the model is nonlinear, the value of Φ will be distributed like the variable, F with degrees-of-freedom given by $df_1 = 1$ and $df_2 = n - 1$ [35]. Hence, a hypothesis of non-linearity may be tested by comparing the value of Φ with the tabulated value for $F_{1, n-1; \alpha}$ at any desired level of significance α . If $\Phi < F_{1, n-1; \alpha}$, the model is nonlinear. If $\Phi > F_{1, n-1; \alpha}$, there is no reason to question that the model is linear.

8. 3. 2 Evaluation of Model Efficiency

The efficiency of the model may be evaluated in terms of the correlation coefficient γ given by Eq. (72c). The quantity $(1 - \gamma^2)$ is a measure of the power contributed to y by variables other than x . If the model provided a perfect description for y given x , γ would equal unity. On the other hand, if there were no relationship between y and x , γ would equal zero. It is clearly desirable to establish if γ is significantly different from zero. This is accomplished using the Fisher "Z" transformation given by Eq. (72d). If $\gamma = 0$, the value of Z will be normally distributed with a mean of zero and a variance of unity. Hence, a hypothesis of significant correlation may be tested by comparing the value of Z with the tabulated value of the standardized normal distribution at any desired percentage point α . If $Z < z_{\alpha}$, the correlation coefficient is not significantly different from zero. If $Z > z_{\alpha}$, the correlation coefficient is significantly different from zero. Note that the foregoing interpretations of γ are valid only if the assumption that $A_0 = 0$ is valid.

The efficiency of the model can also be evaluated in terms of the $(1 - \alpha)$ confidence interval for A , as given by Eq. (72e); if the lower confidence limit is less than zero, the interpretation is the same as for the case where the correlation coefficient is not significantly different from zero.

8. 3. 3 Selection of Prediction Limits

The final prediction limit is selected at any desired percentage point using Eqs. (72f) and (72g). The term $L_{y_k; \alpha}$ provides a $(1 - \alpha)$ prediction limit for each value of y_i for a given value, x_k , of the independent variable. Further discussions of the statistical aspects of selecting prediction limits are presented in Section 8. 5.

8.4 ILLUSTRATION OF REGRESSION ANALYSIS PROCEDURES

The procedures outlined in Section 8.3 are now illustrated using data collected by AFFDL during the flight vibration survey of aircraft Code No. 63 (RF-4C) [26]. Since data from only aircraft is available, the illustration is limited to a study of the suggested model for aerodynamic noise induced vibration, as given by Eq. (67). A study of the suggested model for jet noise induced vibration is not practical because a single aircraft provides data for only one value of the independent variable X_{r1} in Eq. (64).

Numerous sample records of the vibration at various locations in Zone 02 of the RF-4C were provided by AFFDL for analysis. The sample records were reviewed based upon the structural locations and flight conditions for the measurements. Only those records which represented measurements on basic structure during normal cruise flight were retained. Since the independent variable in Eq. (67) is proportional to $\rho^2 V^4$, every effort was made to select records covering a wide range of airspeeds and altitudes. However, sample records for flight at Mach numbers around 0.8 were omitted because the RF-4C aircraft displays unique and unrepresentative vibration characteristics around this Mach number [31]. The sample records which passed the review were then carefully edited for data quality. Only those sample records with an acceptable signal to noise ratio over most of the frequency range of interest (10 to 3000 cps) were retained. The review and editing procedures produced a total of 20 acceptable sample records covering three transducer locations and nine combinations of airspeed and altitude. This information along with estimates for the average surface weight density at each measurement location are detailed in Table 24.

The sample records for the measurements summarized in Table 24 were reduced to average power spectra in 1/1 octave bands. The results are presented in Table 25. Note that data at frequencies below 22 cps are

Table 24. Measurement Locations for RF-4C Vibration Data

Code No.	Location	Direction	Flight No.	Recess	$\frac{d}{c}$	Altitude (feet)	Indicated Air Speed (knots)	w (lbs/ft ²)	q (lbs/ft ²)
1	Power Supply Basic Structure	Lateral	5	3	12	1000	200	4.0	137.3
2	Power Supply Basic Structure	Lateral	5	4	12	1000	300	4.0	308.9
3	Power Supply Basic Structure	Lateral	5	5	12	1000	400	4.0	549.2
4	Power Supply Basic Structure	Lateral	5	6	12	1000	500	4.0	847.0
5	Power Supply Basic Structure	Lateral	5	7	12	1000	600	4.0	1222.3
6	Power Supply Basic Structure	Lateral	5	8	12	1000	700	4.0	1650.9
7	Power Supply Basic Structure	Lateral	5	9	12	1000	740	4.0	1840.4
8	Power Supply Basic Structure	Vertical	6	2	3	1000	200	4.0	137.3
9	Power Supply Basic Structure	Vertical	6	3	3	1000	300	4.0	308.9
10	Power Supply Basic Structure	Vertical	6	4	3	1000	400	4.0	549.2
11	Power Supply Basic Structure	Vertical	6	6	3	1000	600	4.0	1222.3
12	Power Supply Basic Structure	Vertical	6	7	3	1000	700	4.0	1650.9
13	Power Supply Mounting Plate	Lateral	6	2	12	1000	200	2.25	137.3
14	Power Supply Mounting Plate	Lateral	6	3	12	1000	300	2.25	308.9
15	Power Supply Mounting Plate	Lateral	6	4	12	1000	400	2.25	549.2
16	Power Supply Mounting Plate	Lateral	6	5	12	1000	500	2.25	847.0
17	Power Supply Mounting Plate	Lateral	6	6	12	1000	600	2.25	1222.3
18	Power Supply Mounting Plate	Lateral	6	7	12	1000	700	2.25	1650.9
19	Power Supply Mounting Plate	Lateral	6	19	12	15,000	400	2.25	521.7
20	Power Supply Mounting Plate	Lateral	6	33	12	30,000	400	2.25	466.8

w = surface weight density of the noted structural location

q = dynamic pressure for the noted flight condition

Table 25. Average Power Spectra for RF-4C Vibration Data

Code No.	X_{r2} $\times 10^5$	Average Power Spectral Densities in g^2/cps for 1/1 Octave Bands in cps						
		22-44	44-88	88-177	177-354	354-707	707-1414	1414-2828
1	.0118	.0016	.0010	.00071	.00036	.00023	.000036	.000032
2	.0596	.0016	.0009	.0011	.0004	.00018	.000045	.000023
3	.189	.0026	.018	.032	.0018	.0008	.00007	.000028
4	.449	.001	.0014	.0008	.013	.013	.013	.0057
5	.934	.0064	.071	.50	.04	.013	.0016	.00028
6	1.703	.0018	.00079	.0008	.04	.040	.050	.020
7	2.117	.0036	.00079	.0005	.025	.032	.057	.025
8	.0118	--	.00063	.0002	.00016	.00025	.00008	.000023
9	.0596	.00073	.0004	.0003	.0002	.0004	.00028	.00025
10	.189	.0008	.0004	.00018	.0010	.0018	.0018	.0004
11	.934	.0013	.00071	.00089	.0113	.018	.022	.0040
12	1.703	.0014	.0007	.0005	.013	.023	.036	.0063
13	.037	.0016	.00089	.00028	.00023	.00007	.000028	.000018
14	.189	.0032	.0013	.0004	.00057	.0029	.0025	.00028
15	.596	.0018	.0010	.00045	.004	.011	.014	.0008
16	1.417	--	.0016	.0014	.014	.013	.029	.0028
17	2.95	.115	.079	.090	.102	.10	.14	.023
18	5.38	.58	.29	.18	.18	.13	.16	.051
19	.538	.0020	.00089	.0004	.0036	.011	.016	.00036
20	.43	.0020	.0010	.00036	.0028	.008	.011	.00025

$$X_{r2} = \frac{g^2}{w}$$

not included because most records did not provide an adequate signal to noise ratio below this frequency. Also note that the contributions of periodic components were not removed from the data, as suggested in Section 8.1.2. Periodic components due to jet engine shaft rotation were apparent in the 88 to 177 cps octave. They were not removed to illustrate a point, which is discussed later.

The data in Table 25 are now analyzed using the procedures outlined in Section 8.3. The detailed results of the regression analysis are presented in Section 6 of Appendix A and summarized in Table 26. It is seen from Table 26 that the model is linear and provides significant correlation at the 1% level of significance for all octave bands except the 88 to 177 cps band. This is the frequency band which included periodic components due to jet engine shaft rotation. Hence, the results in this band clearly illustrate the necessity for removing periodic contributions from the data. They further illustrate the ability of the analysis procedures to detect the presence of contributing vibration sources other than aerodynamic boundary layer noise.

The results in Table 26 confirm that the prediction model for aerodynamic noise induced vibration, as suggested in Eq. (67), is acceptably linear and efficient. The indicated correlation coefficients for all octaves (excluding the 88 to 177 cps octave) are from 0.68 to 0.90. This is relatively high considering the simplicity of the model. The efficiency of the model is further confirmed by the fact that the lower confidence limits for the coefficient A are all greater than zero. Of course, when these analysis procedures are ultimately applied to data from many different aircraft, the results may not be as good as achieved here using data from only one aircraft. Nevertheless, it is believed that they will be meaningful and provide an acceptable basis for establishing conservative vibration prediction limits.

Table 26. Summary of Regression Analysis Results

Frequency Interval	Estimate for Coefficient A $\times 10^{-7}$	97.5% Confidence Interval for A $\times 10^{-7}$		Test for Linearity at 1% Level of Significance	Correlation Coefficient r_y	Test of Correlation Coefficient for Significant Difference from Zero at 1% Level of Significance
		Lower Limit	Upper Limit			
22- 44	6.857	4.468	9.246	accept	.68	accept
44- 88	3.545	2.415	4.675	accept	.70	accept
88- 177	3.245	.041	6.449	reject	.37	reject
177- 354	2.825	2.350	3.300	accept	.84	accept
354- 707	2.347	2.043	2.650	accept	.90	accept
707-1414	3.090	2.679	3.501	accept	.90	accept
1414-2828	.854	.723	.986	accept	.86	accept

The 97.5% upper prediction limits calculated for this illustration are presented in Figure 20. Curves of this type represent the ultimate goal of the analysis. Note that the predictions are in terms of average power spectral densities in 1/1 octave bands. If it is desired to have predictions which will envelop anticipated narrow band peaks in the vibration power spectra, a correction must be applied to the curves in Figure 20, as discussed in Section 8.1.6. It should be emphasized that the prediction curves in Figure 20 are presented for illustrative purposes, only. Because of the limited amount of data used to arrive at the curves, they do not represent a valid tool for predicting the vibration environment of future aircraft.

8.5 STATISTICAL CONSIDERATIONS IN THE SELECTION OF PREDICTION LIMITS

As used in this report, a $(1 - \alpha)$ prediction limit is that level calculated from past vibration measurements which hopefully will exceed $100(1 - \alpha)\%$ of all future vibration levels. In rigorous terms, such a prediction limit should be based upon a statistical tolerance limit [36]. A tolerance limit is defined as that level calculated from past observations which will exceed at least $100(1 - \alpha)\%$ of all future observations with a probability of P . For n observations of a normally distributed random variable y , the tolerance limit for future observations is given by

$$L_{P; \alpha} = \bar{x} + s_x K_{n; P; \alpha} \quad (73)$$

where \bar{x} and s_x are the sample mean and standard deviation, respectively,

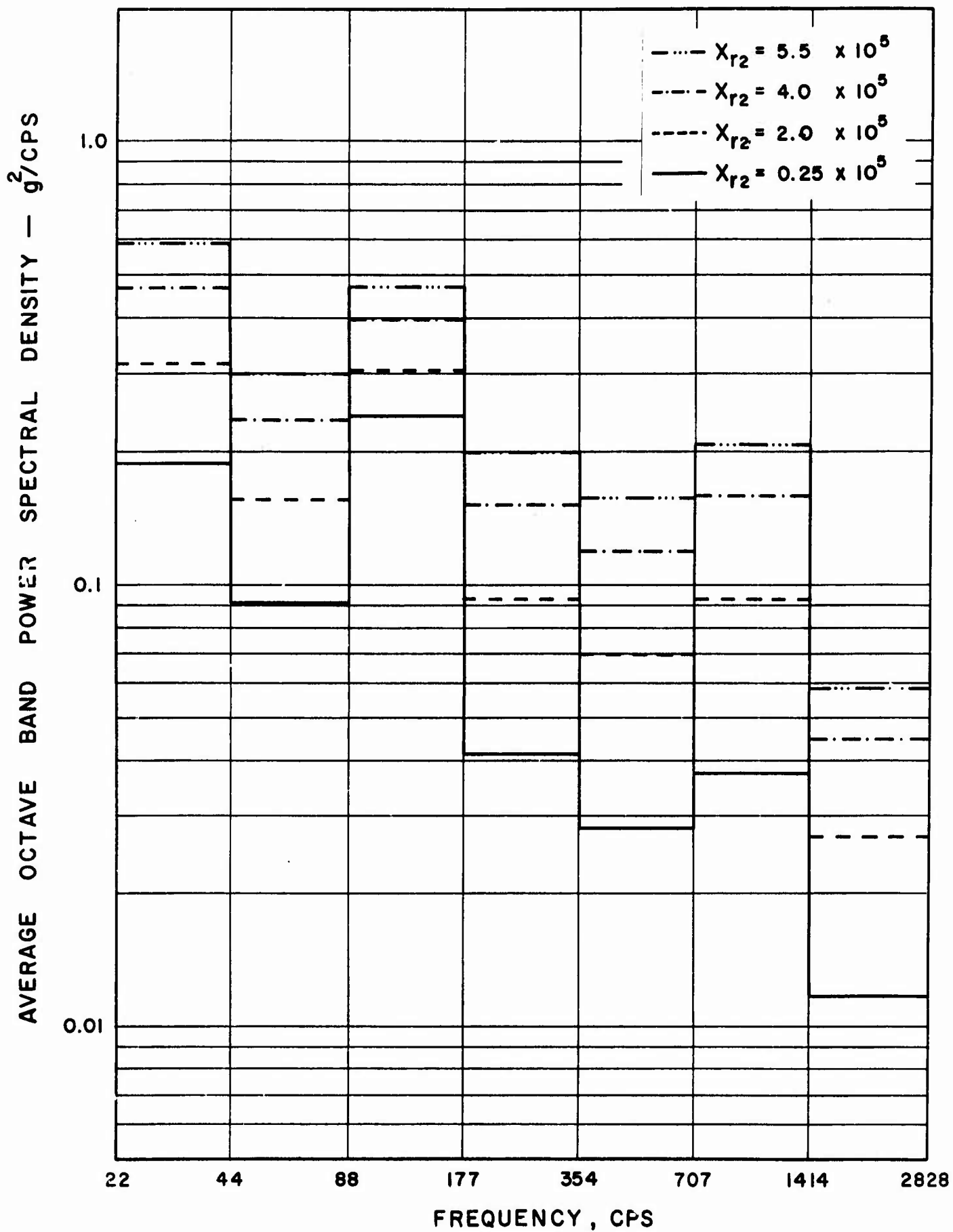


Figure 20. 97.5% Prediction Limits Calculated from RF-4C Vibration Data

and K is the tolerance factor. Tolerance factors for various values of n , P , and α are widely tabulated in the statistical literature.

The prediction limits arrived at by the procedures suggested in this report are not, rigorously speaking, statistical tolerance limits. For the case of the regression analysis procedures described in Section 8.3, the prediction limit given by Eq. (72g) is similar to a tolerance limit [34]. For the other cases, however, a $(1 - \alpha)$ prediction limit is arrived at by fitting an assumed distribution function to the data, and determining the α percentage point of the fitted distribution. The resulting prediction limit would be equivalent to a tolerance limit only if the fitted distribution were in fact the actual distribution function for the data. This, of course, is not the case. Nevertheless, the use of the percentage point procedure for selecting prediction limits is believed justified for the following two reasons.

1. Tolerance factors are well tabulated only for the case of normally distributed data. The data of interest here are not normally distributed, as discussed in Section 7.
2. The potential error introduced by using percentage points of fitted distributions, rather than tolerance factors, to establish prediction limits is negligible compared to the potential errors associated with the other steps needed to arrive at vibration predictions.

9. SELECTION OF VIBRATION TEST LEVELS AND DURATIONS

Having predicted an aircraft vibration environment, it remains to convert the predictions into practical specifications for aircraft component vibration tests. Procedures for selecting appropriate test levels and durations based upon environmental predictions are investigated in this section.

Historically, there have been two basic approaches to the design of vibration test specifications, the environmental simulation approach and the damage simulation approach. The environmental simulation approach involves the design of a vibration test specification which will conservatively simulate the environmental vibration levels and exposure times to be expected in actual service. This approach is clearly most suitable for missiles and spacecraft applications where the total duration of the service vibration environment is relatively short and, hence, can be reasonably simulated by a laboratory test. The damage simulation approach involves the design of a vibration test specification which conservatively simulates the damaging potential of the environment, as opposed to the actual environmental levels. The use of this approach permits long environmental exposure times in actual service to be replaced by short duration vibration tests. This particular property makes the damage simulation approach highly desirable for aircraft component vibration test specifications. The use of the damage simulation approach, however, does pose one serious problem. Specifically, it is necessary to establish a model for the mode and mechanism of failure to be anticipated in the component to be tested. Only on the basis of some assumed mode of failure can proper tradeoffs between vibration level and vibration duration be established.

There is an additional problem associated with the selection of vibration test durations which applies to test specifications based upon either the environmental simulation or damage simulation approach. This problem evolves from the fact that laboratory vibration tests are usually performed using a stationary vibration input, while the vibration environment of flight vehicles in actual service is generally nonstationary. Hence, the following question arises: How long should the duration for the stationary vibration test be to properly simulate a nonstationary vibration environment? For the case of missile and spacecraft component testing where an environmental simulation approach is used, the general procedure is to establish the test levels based on the maximum vibration levels which are anticipated during service, and to base the test duration upon the total exposure time in service. This approach often produces an overly conservative test, but avoids the problem of establishing equivalences between nonstationary and stationary vibration. For the case of test specifications based upon a damage simulation approach, the nonstationary-stationary equivalence problem can be dealt with more directly. In fact, it can be handled by exactly the same procedures used to make tradeoffs between test levels and test durations to compress long service exposure times into short test durations. This fact constitutes a significant advantage of the damage simulation approach over the environmental simulation approach.

9.1 FAILURE CRITERIA

The possible modes of failure for aircraft components are numerous and generally quite complex [37], [38]. For the problem at hand, however, it is necessary to hypothesize that failures will be due to some

specific mechanism which can be described by a tractable mathematical model. Two different types of failure criteria will be assumed and used independently. The first is a fatigue damage criterion and the second is a peak value criterion.

9.1.1 Fatigue Damage Criterion

The exact mechanics of structural fatigue are not well defined. However, a number of models for describing fatigue damage have been proposed over the years which produce reasonable fatigue life predictions. One of the earliest and simplest of these models is Miner's hypothesis [39], which may be stated as follows. If N_1 stress cycles with a peak stress level of S_1 will cause a fatigue failure of a given material, then $n_1 < N_1$ stress cycles with that same peak stress level will expend n_1/N_1 fractional portion of the material's useful fatigue life. Hence, if stress cycles are applied at various different peak stress levels ($S_1, S_2, \dots, S_i \dots$), a measure of fatigue damage is given by

$$D = \sum_i \frac{n_i}{N_i} \quad (74)$$

where failure is assumed to occur when $D = 1$. The relationship between the peak stress level, S_i , and the number of cycles to failure, N_i , is given by an S - N curve for the material.

S - N curves for common aircraft materials vary widely depending upon the alloy, heat treatment, mean stress, stress raisers, and other factors. For many materials, however, the S - N curve can be crudely

approximated by two straight line segments when presented on a log-log plot, as illustrated in Figure 21. The stress level which corresponds to the level of the horizontal segment in Figure 21 is called the endurance limit. The S - N curves for aluminum alloys do not generally break as abruptly as indicated in Figure 21; that is, the endurance limit is not so ideally defined. Nevertheless, there is a stress limit where stress cycles with peak values below that limit are unlikely to produce a fatigue failure, even as the number of stress cycles becomes very large.

For the moment, let the break in the S - N curve at the endurance limit be ignored. The S - N curve for stress levels above the endurance limit can be approximated analytically by

$$A|S|^b = \frac{1}{N} \quad (75)$$

where A and b are material constants. Substituting Eq. (75) into Eq. (74) yields

$$D = A \sum_i n_i |S_i|^b \quad (76a)$$

which may be applied directly to approximate the fatigue damage of a material due to sinusoidal stress loads with various different peak levels. For the case of random stress data, Eq. (76a) reduces to

$$D = nA \int_0^{\infty} |S|^b p(S) dS \quad (76b)$$

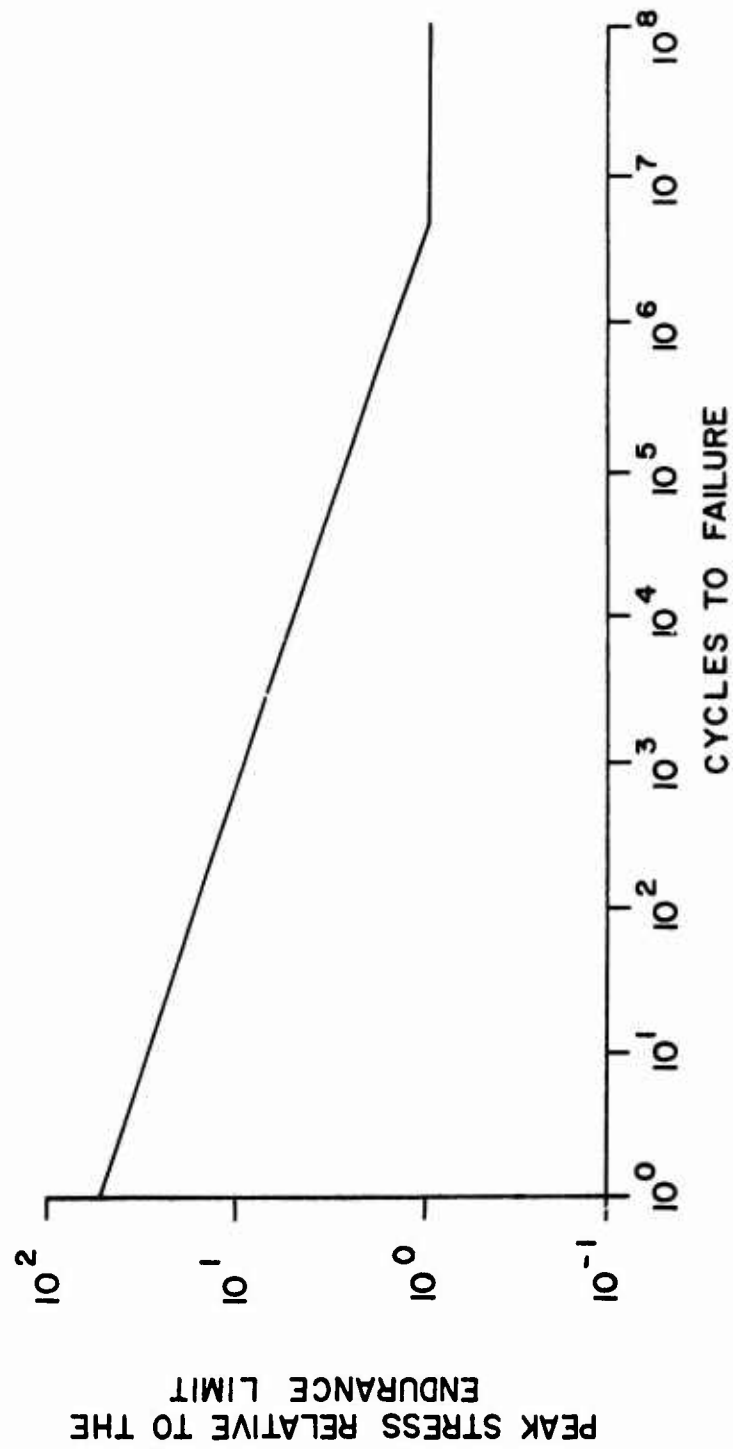


Figure 21. First Order Approximation for a S - N Curve

where $p(S)$ is the probability density function for peak values of stress, and n is some equivalent total number of cycles.

9. 1. 2 Peak Value Criterion

Consider now those failures which are due to a single extreme value of strain, stress, velocity, or acceleration. Included would be failures due to a stress level beyond the ultimate strength of the material, a displacement beyond a physical space limit (a collision or misalignment), or an acceleration beyond a functional performance limit. For the case of periodic vibration environments, such peaks are easy to define since they occur repeatedly with the same magnitude for each cycle of vibration. For random vibration environments, however, the problem is more complicated since random data generally have no clearly defined peak value. Hence, the possibility that a random vibration will or will not exceed any given level must be specified by a probability statement. The probability that a given level will be exceeded is a function of the power spectrum and probability density function for the vibration, and the total observation time. An exact closed form solution for the probability of exceeding a given level is not known to exist. However, for the case of vibration with a Gaussian probability density function, it can be shown [40] that an upper bound on the probability of exceeding a level $K = L/\sigma > 3$ is given by

$$P \leq \frac{\Omega T}{\pi} e^{-K^2/2} \quad (77)$$

where K is the ratio of the peak to rms vibration, T is the total

observation time, and Ω is π times the expected number of zero crossings per unit time. In terms of the power spectrum $G(f)$ for the vibration

$$\Omega = 2\pi \left[\frac{\int_0^{\infty} f^2 G(f) df}{\int_0^{\infty} G(f) df} \right]^{1/2} \quad (78)$$

There are other approximations for the probability of exceeding a given level which have been proposed and studied by various people. Included are those suggested by MacNeal, Barnoski, and Bailie [41], and Mark [42], which apply to the response of simple oscillators to random excitation. The result in Eq. (77), however, is generally simpler in form than other suggestions and is considered to be satisfactory for the application of interest herein.

9.2 APPLICATION TO COMPONENT MODEL

The failure criteria discussed in Section 9.1 must now be applied to a specific mechanical model which approximates the dynamics of aircraft components. The model to be used will be the simple mechanical oscillator illustrated in Figure 22, where m is the mass, k is the spring constant, c is the viscous damping coefficient, and $a(t)$ is the acceleration of the foundation.

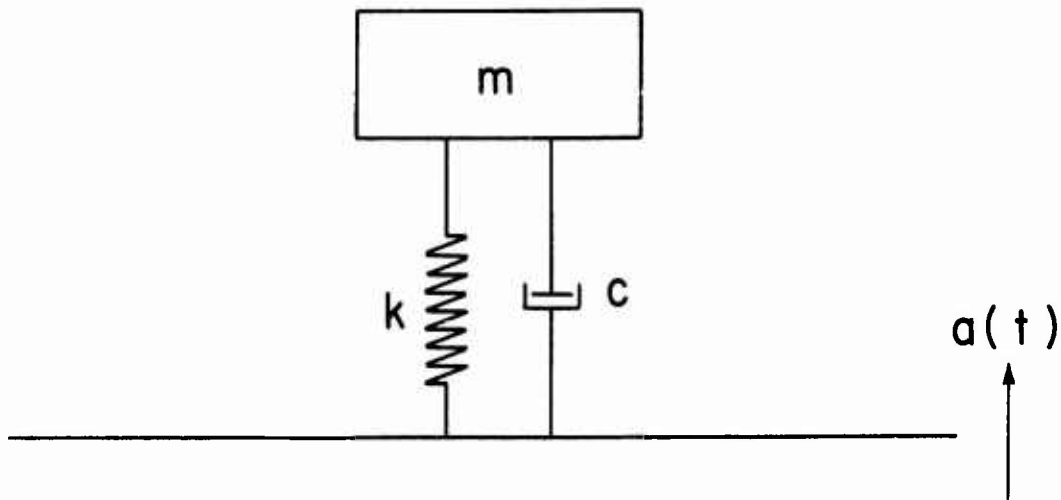


Figure 22. Mechanical Oscillator with Foundation Motion

The simple model in Figure 22 is clearly a gross oversimplification for the complex dynamic characteristics of most aircraft components. However, it must be remembered that the model is required only as a basis for comparing the damaging effects of two different environments on the same component. Furthermore, if it is assumed that sinusoidal tests will be used to simulate periodic vibration environments and random tests will be used to simulate random vibration environments, the environmental differences of interest will be principally differences in level and duration, and not differences in the basic characteristics of the vibration. For these reasons, it is believed the model in Figure 22 will provide an acceptable basis for the desired comparisons.

For either the fatigue damage or peak value criterion, the response function of interest for the model in Figure 22 is the displacement of the mass relative to the foundation (the strain in the spring). It can be readily shown [43] that the magnitude of the frequency response function for this system which relates an acceleration input to a strain response is

$$|H(f)| = \frac{1}{4\pi^2 f_n^2 U(f)} \quad (79)$$

where

$$U(f) = \sqrt{\left[1 - (f/f_n)^2\right]^2 + \left[2\zeta f/f_n\right]^2} \quad (79a)$$

$$f_n = \frac{1}{2\pi} \sqrt{\frac{k}{m}} \quad (79b)$$

$$\zeta = \frac{c}{2\sqrt{km}} \quad (79c)$$

9.2.1 Application of Fatigue Damage Criterion

Consider first the case where the vibration environment is a sinusoidal acceleration given by $a(t) = a \sin 2\pi ft$. Further assume that stress is related to strain by a constant C ; that is, $s(t) = Cz(t)$. From Eq. (79), the magnitude of the peak stress response of the model is given by

$$|s| = \frac{Ca}{4\pi^2 f_n^2 U(f)} \quad (80)$$

and the number of stress cycles is given by

$$n = fT \quad (81)$$

where T is the total exposure time. Hence, the fatigue damage to the model is approximated by Eq. (76a) as

$$D = fTA \left[\frac{Ca}{4\pi^2 f_n^2 U(f)} \right]^b \quad (82)$$

For the worst case where resonant vibration occurs, Eq. (82) becomes

$$D = f_n TA \left[\frac{CQa}{4\pi^2 f_n^2} \right]^b \quad (83)$$

where $Q = 1/2\zeta$.

Now consider the case where the vibration environment is a Gaussian random acceleration with a uniform power spectrum of G , at least over those frequencies in the region of resonance. Assuming the system Q is high (greater than 10), it can be shown [44] that the fatigue damage is approximated by

$$D = f_n TA \left[\frac{C^2 QG}{16\pi^3 f_n^3} \right]^{b/2} \Gamma \left(1 + \frac{b}{2} \right) \quad (84)$$

where $\Gamma()$ is the Gamma function.

9.2.2 Application of Peak Value Criterion

For the case where the vibration environment is a sinusoidal acceleration, the peak value criterion is of no use since any given level either will or will not be exceeded on the first cycle of vibration (after transients have subsided). In other words, the probability of a failure is not dependent upon the observation time beyond one vibration periodic.

For the case where the vibration environment is a Gaussian random acceleration, π times the expected number of zero crossings for the response, as defined in Eq. (78), becomes $\Omega = 2\pi f_n$. Hence, from Eq. (77), the probability of exceeding any given level $K = L/\sigma$ is bounded by

$$P \leq 2f_n T e^{-K^2/2} \quad (85)$$

9.3 RELATIONSHIPS BETWEEN VIBRATION LEVEL AND EXPOSURE TIME

Assume it is desired to substitute a short duration vibration test for a long duration service vibration environment. The following question arises: How much should the test level be increased to produce the same damaging potential as the service environment? This question will now be answered using the results in Section 9.2.

9.3.1 Fatigue Damage Criterion

For the case of sinusoidal vibration with a fatigue damage criterion, the relationship between the test and service environmental levels and

durations is obtained by equating damage for the two cases using Eq. (82). Since the same component is involved in both cases, it follows that

$$T_t a_t^b = T_s a_s^b \quad (86)$$

For random vibration with a fatigue damage criterion, the relationship is given by Eq. (84) as

$$T_t G_t^{b/2} = T_s G_s^{b/2} \quad (87)$$

Assuming that the power spectrum for the test and the service environments are similar in shape, Eq. (87) reduces to

$$T_t \sigma_t^b = T_s \sigma_s^b \quad (88)$$

where σ is the rms value of the random vibration. Noting that the amplitude of a sine wave is proportional to its rms value, it is seen that Eqs. (86) and (88) provide the same result, which may be written as

$$\ln \left[\frac{T_s}{T_t} \right] = b \ln \left[\frac{\sigma_t}{\sigma_s} \right] \quad (89)$$

It remains to establish an appropriate value for b .

The value of b for aircraft materials varies over a wide range depending upon the alloy, mean stress, etc. For standard alloys like 7075-T6 subjected to a stress load with zero mean, the value of b usually falls between 5 and 8 [45]. A plot of the service to test exposure time ratio versus the test to service level ratio is presented for these bounding values of b in Figure 23.

It is appropriate at this time to reconsider a basic assumption used to arrive at Eq. (76). Specifically, Eq. (76) and, correspondingly, the relationship in Eq. (89), ignore the existence of an endurance limit for the material being tested. In practice, it is quite possible that the environmental levels in service, indicated by σ_s , would be below the endurance limit. This means that the service environment would produce far less fatigue damage than would be predicted by Eq. (76). If Eq. (87) were then applied to arrive at a test level with reduced exposure time, the test level σ_t might be above the endurance limit. This could feasibly cause a failure which would not occur in service. However, the opposite is not true; that is, the use of Eq. (89) will not eliminate a failure in test which would actually occur in service. Hence, the fact that the endurance limit has been ignored should cause Eq. (89) to always produce conservative results.

9.3.2 Peak Value Criterion

For the case of random vibration with a peak value criterion, the relationship between the test and service levels and durations is obtained by equating the probability of exceeding a specific level $L = K\sigma$ using Eq. (85). Since the same component is involved in both cases, it follows that

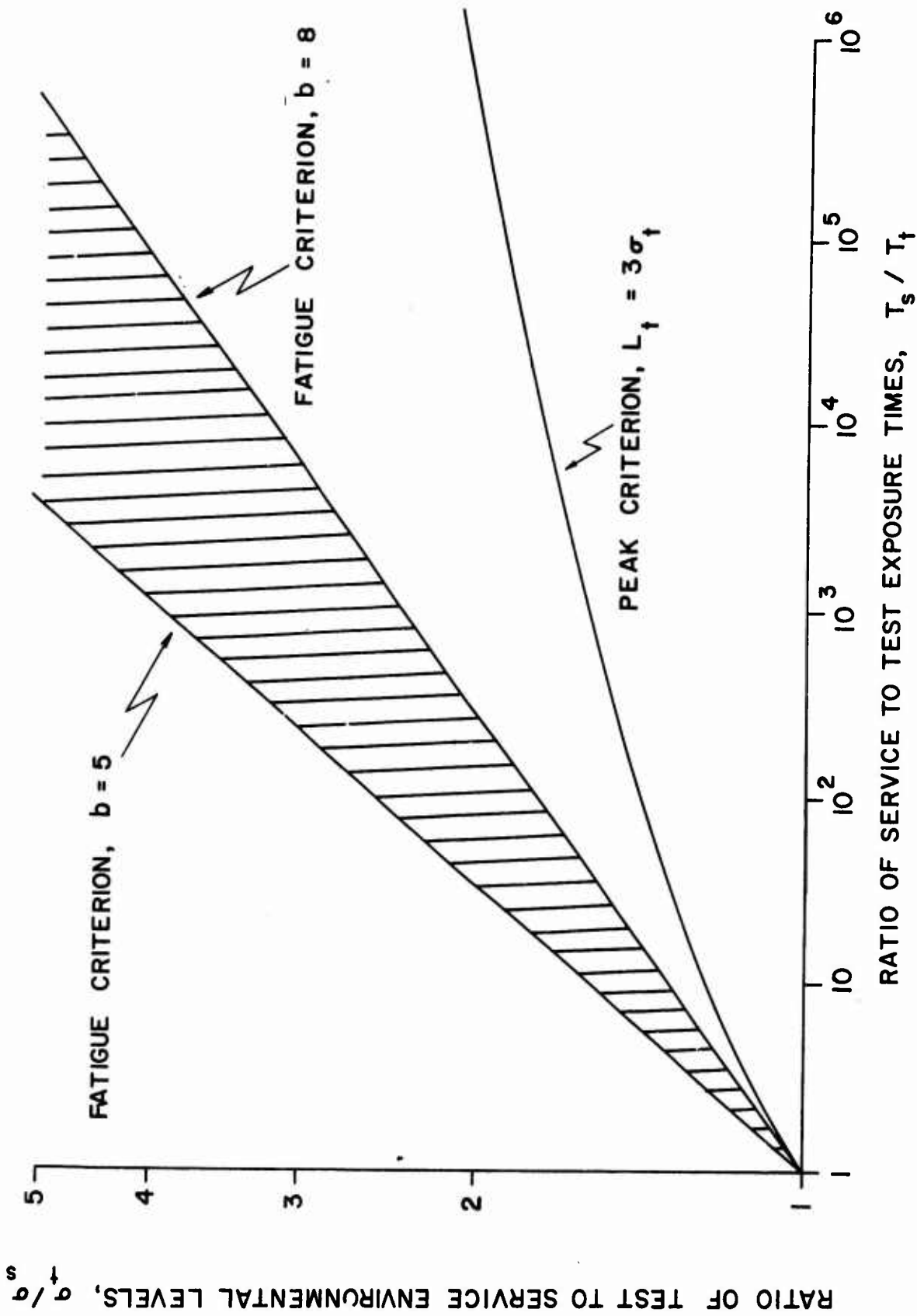


Figure 23. Test Level and Duration Tradeoffs for Fatigue Damage and Peak Criteria

$$T_t e^{-L^2/2\sigma_t^2} = T_s e^{-L^2/2\sigma_s^2} \quad (90)$$

which reduces to

$$2 \ln \left[\frac{T_s}{T_t} \right] = \frac{L^2}{\sigma_s^2} - \frac{L^2}{\sigma_t^2} \quad (91)$$

The problem now is to establish an appropriate value for L .

The vibration machines used for random vibration tests are usually equipped with limiting circuits to protect the vibration machines from damaging loads. These limiting circuits restrict the peak accelerations delivered by the machines to no more than 3 times the rms value of the vibration. Hence, in test, the value of L is fixed at $L = 3\sigma_t$. Substituting this relationship into Eq. (91) yields

$$\ln \left[\frac{T_s}{T_t} \right] = 4.5 \left[\frac{\sigma_t^2}{\sigma_s^2} - 1 \right] \quad (92)$$

A plot of the service to test exposure time ratio versus the test to service level ratio using the peak value criterion in Eq. (92) is presented in Figure 23.

9. 3. 3 Comparison of Fatigue Damage and Peak Value Criteria

It is clear from Figure 23 that the fatigue damage criterion requires a greater increase in level to account for reduced exposure time than does the peak value criterion. For example, if a 1000 hour service environment were to be simulated by a 1 hour test, the fatigue damage criterion indicates the test level should be from 7.5 to 12 dB higher than the service level, while the peak value criterion calls for a test level that is only 4 dB higher. Hence, if the peak criterion were used to select the test level, the test would be less likely to produce a fatigue failure than the service environment. On the other hand, if the fatigue damage criterion is used to select the test level, the test would be more likely to cause an extreme value failure than the service environment. To assure that the test will be conservative, it appears desirable to use the fatigue damage criterion for selecting appropriate test levels and durations. See Section 9.7 for further comments on this subject.

9. 4 APPLICATION TO NONSTATIONARY ENVIRONMENTS

Now consider the problem of simulating a nonstationary vibration service life with a stationary vibration test. Assume the vibration service life, whether random or periodic, can be described by a probability distribution function for rms values, as illustrated in Figure 24. Note that the abscissa of Figure 24 can represent the rms value of the vibration in any desired narrow frequency increment. Hence, the total vibration profile would be described by a family of distribution functions covering the frequency range of interest.

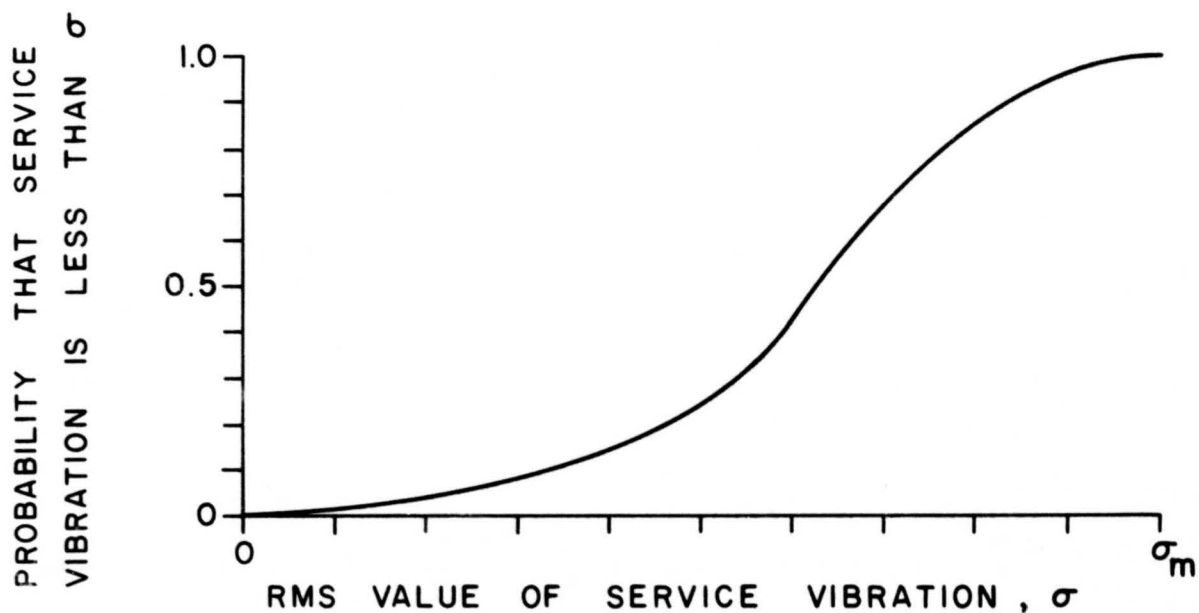


Figure 24. Illustration of Distribution Function for Aircraft Service Vibration Environment

Let $P(\sigma)$ denote the distribution function for the vibration profile. The probability density function for the vibration profile is then given by

$$p(\sigma) = \frac{d P(\sigma)}{d\sigma} \quad (93)$$

and will appear as illustrated in Figure 25.

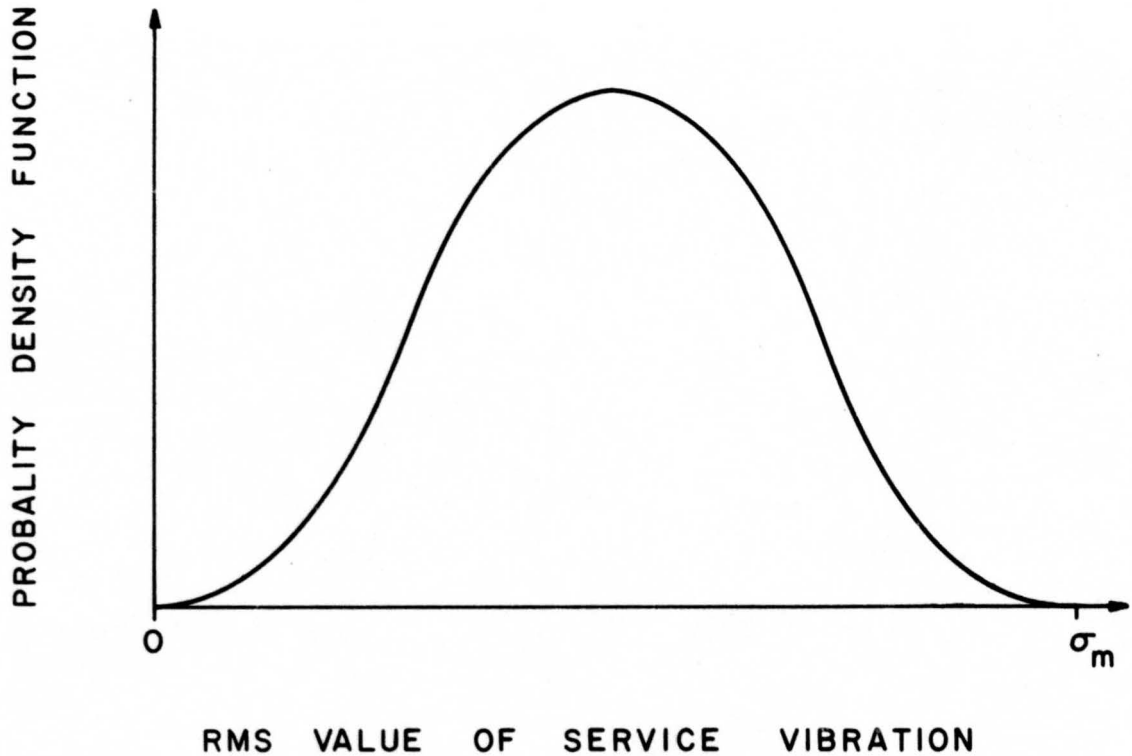


Figure 25. Illustration of Density Function for Aircraft Service Vibration Environment

In Figures 24 and 25, σ_m denotes the maximum rms vibration which occurs during the service environment. In practice, the maximum level will correspond to the highest level predicted for the various flight conditions.

Let T_m denote the exposure time at the maximum level σ_m (or some other arbitrary level) to produce the same fatigue damage as the total service vibration environment. Then, by equating damage based upon the definition in Eq. (88).

$$T_m \sigma_m^b = \sum_i \Delta t_i \sigma_i^b \quad (94)$$

where σ_i is the rms level and Δt is the time duration at the i th vibration level. Using Eq. (93),

$$\Delta t_i = T_s \Delta P(\sigma_i) = T_s p(\sigma_i) \Delta \sigma_i \quad (95)$$

where T_s is the total environmental exposure time in service. Substituting Eq. (95) into Eq. (94), and letting the increments become very small, it follows that

$$T_m = \frac{T_s}{\sigma_m^b} \int_0^{\sigma_m} \sigma^b p(\sigma) d\sigma \quad (96)$$

Equation (96) gives the desired exposure time T_m for vibration with the maximum service level σ_m that will produce the same damage as the nonstationary service environment. For example, assume that $b = 8$ and that the vibration occurs during service with equal probability at any given level between 0 and σ_m . The density function for this case would be uniform with a density of $1/\sigma_m$ between 0 and σ_m . From Eq. (96)

$$T_m = \frac{T_s}{\sigma_m^b} \int_0^{\sigma_m} \sigma^b d\sigma = \frac{T_s}{9} \quad (97)$$

Hence, the required exposure time at the maximum level would be only 1/9 the total service exposure time. Note that once T_m has been determined, the exposure time can be further reduced for testing purposes using Eq. (89), where T_m and σ_m are substituted for T_s and σ_s .

9.5 DEVELOPMENT OF VIBRATION PROFILE DATA

The task of developing vibration profile information for aircraft of concern to AFFDL should be accomplished in two steps. The first step is to estimate the fractional portion of the total aircraft service life spent in various pertinent flight conditions. The second step is to predict a conservative limit for the vibration environment during each of the pertinent flight conditions. By ranking the various flight conditions in the order of increasing vibration level, the distribution of service vibration levels is obtained directly, as illustrated in Figure 26.

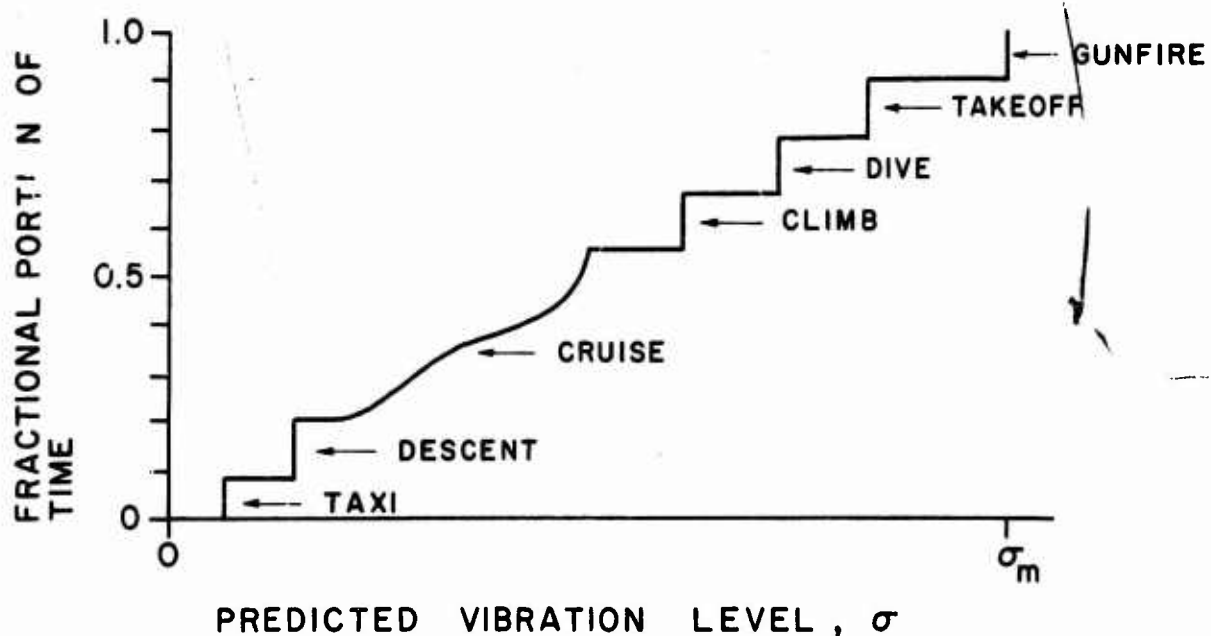


Figure 26. Illustration of Flight Vibration Profile

Given the design service life T_s , the total time required to produce equivalent damage with a stationary vibration at the maximum service vibration level is given by Eq. (96).

Consider now the problem of estimating the fractional portion of time spent in various flight conditions. This should be done for each new aircraft of interest based upon analytical evaluations of design mission requirements. Guidance may be obtained from empirical flight data for previous aircraft of similar design and purpose. The flight data, however, must be in a form which is compatible with the requirements of the vibration prediction model. For example, the flight vibration of jet bombers and fighters is predicted by Eq. (67) as a function of dynamic pressure, q . Hence, the empirical flight data used to establish vibration profiles must be in terms of the fractional portion of time spent at various values of q . It should be noted that the conventional aircraft flight and maneuver loads documents issued by AFFDL do not generally include this type of data. These loads documents do include distributions for the time spent below arbitrary altitudes and airspeeds, but such data cannot be extrapolated to distributions for the time spent below arbitrary dynamic pressures without making unreasonable assumptions. It is strongly recommended that AFFDL acquire and include such data in future flight loads documents.

Another approach to the estimation of times spent in various flight conditions is to use the flight condition identifications obtained during AFFDL flight vibration surveys. If it is assumed that vibration measurements are made at random during each survey flight, then the fractional portion of time spent in any given flight condition may be estimated from the ratio of the number of measurements identified with that flight condition to the total number of measurements. This is done for three

aircraft (B-58, F-101A, and H-37) representing aircraft Groups 3, 5, and 10 in Table 27. If the flights for vibration surveys are similar to the operation missions for that aircraft, then data of the type presented in Table 27 may be used to establish vibration profiles.

To illustrate the ideas in this section, assume a specification is required for the vibration testing of components to be installed in a fighter type aircraft similar to the F-101A. Further assume that the vibration levels in each frequency increment for the structural zone of interest are predicted using the models suggested in Section 8.1. Let the results for the various contributing sources in octave band centered at 250 cps (177 to 354 cps) be as follows.

$$G_{r1} = 10^{-2} g^2 / \text{cps}$$

$$G_{r2} = 10^{-9} q^2 g^2 / \text{cps}$$

$$G_{r6} = 10^{-8} q^2 g^2 / \text{cps}$$

$$G_{d3} = 0$$

$$G_{d10} = 0$$

For simplicity, it is assumed the contributions of engine shaft rotation (G_{d3}) and gunfire (G_{d10}) are negligible in this frequency increment. Noting that the bandwidth for the frequency increment is 177 cps, the rms value for the vibration during each general flight phase is given by Eq. (63) as

$$\text{Takeoff; } \sigma_{to} = \left[(177) 10^{-2} \right]^{1/2} = 1.3 g$$

$$\text{Clean Flight; } \sigma_{cf} = \left[(177) 10^{-9} q^2 \right]^{1/2} = 4.2 \times 10^{-4} q g$$

$$\text{Flight with Deployment of Aerodynamic Devices; } \sigma_{ad} = \left[(177)(10^{-9} + 10^{-8}) q^2 \right]^{1/2} = 1.4 \times 10^{-3} q g$$

Table 27. Estimated Flight Condition Profile for B-58, F-101A, and H-37 Aircraft

Flight Condition		Percent of Time Spent in Given Flight Condition		
Code No.	Description	B-58	F-101A	H-37
01	Taxi	1.1	2.0	4.0
02	Ground Runup	1.5	5.3	7.8
03	Takeoff Roll	-	-	1.6
04	Takeoff	-	3.4	5.4
05	Takeoff with Afterburner	2.6	-	-
06	Normal Climb	5.9	4.8	4.8
07	Normal Cruise	32.3	26.2	34.0
08	Cruise with Speedbrakes	3.4	6.5	0.8
09	Cruise with Extended Rocket Pot, Launcher, etc.	9.1	7.6	-
15	Cruise with Flaps Extended	-	1.2	-
16	Cruise with Gear Extended	4.0	1.2	2.4
17	Cruise with Refueling Doors Open	-	2.0	-
21	Clean Normal Descent	3.6	2.0	5.5
22	Normal Descent with Speedbrakes	-	0.4	0.9
23	Normal Approach	1.3	0.8	0.8
24	Normal Approach with Flaps, Gear, etc.	0.9	6.9	-
25	Touchdown	1.3	2.8	-
26	Landing Roll	3.4	0.5	-
27	Drag Chute or Reverse Thrust	-	0.8	-
28	Bomb, Camera, or Troop Doors Open	-	0.8	-
30	Cruise with One or More Engines Out	1.6	-	-

Table 27 (continued)

Flight Condition		Percent of Time Spent in Given Flight Condition		
Code No.	Description	B-58	F-101A	H-37
33	Auto-Rotation (Helicopters)	4.6	-	2.5
35	Hover (Helicopters)	-	-	13.9
36	Rearward Flight (Helicopters)	-	-	3.2
37	Side Flight (Helicopters)	-	-	8.7
38	High Speed Stop (Helicopters)	-	-	1.6
44	Ground Runup with One or More Engines Out	-	0.8	-
47	Climb with Afterburner	8.1	0.4	-
48	Cruise with Afterburner	12.1	11.4	-
49	Cruise with Afterburner and Speedbrakes	1.6	7.2	-
50	Cruise with Afterburner and Flaps Extended	-	2.8	-
51	Ground Runup with Afterburner	1.6	-	-
53	Cruise with Flaps and Gear Extended	-	-	2.1
55	Cruise with Speedbrakes and Gear Extended	-	0.4	-
56	Cruise with Speedbrakes, Flaps, and Gear Extended	-	1.4	-
61	Cruise with Afterburner, Speedbrakes, and Flaps Extended	-	0.4	-

From Table 27, the flight conditions which fall into each of these three flight phases, and the total fractional portion of time within each phase are as follows.

Takeoff (02, 04)	= 8.7%
Clean Flight (06, 07, 21, 23, 48)	= 45.2%
Flight with Deployment of Aerodynamic Devices (08-17, 22, 24, 28, 49, 50, 55, 56, 61)	= 38.8%

The remaining flight conditions (01, 25-27, 44) which account for 7.3% of the service life will be ignored.

A probability distribution for q during flight with and without the deployment of aerodynamic devices must now be estimated. For simplicity, assume q is uniformly distributed over the range from 0 to 1000 for clean flight, and from 0 to 300 for flight with deployment of aerodynamic devices. The maximum vibration levels then occur during takeoff where $\sigma_m = \sigma_{to} = 1.3$ g. The time duration for vibration at this level required to produce fatigue damage equivalent to the service environment is given by Eq. (96). Assuming $b = 8$,

$$T_m = \frac{T_s}{(1.3)^8} \left[0.087(1.3)^8 + 0.452(0.21)^8/9 + 0.388(0.42)^8/9 \right]$$

$$T_s (0.087 + 0.000 + 0.000) = 0.087 T_s$$

Hence, for this illustration, nearly all of the damage occurs during ground runup and takeoff, which constitute less than 9% of the total service environment.

To carry the illustration a step further, assume the aircraft is designed for a service life of 2000 hours. Based upon a fatigue damage criterion, the required duration for a vibration test at the predicted takeoff vibration level would be 174 hours to simulate the service environment. However, using Eq. (89) or Figure 23, the test duration could be reduced to 0.68 hour (41 minutes) by increasing the test level to 2 times the predicted takeoff level. Hence, a random vibration test with a level of $0.015 \text{ g}^2/\text{cps}$ in the frequency range from 177 to 354 cps, and a duration of 41 minutes would be appropriate for this illustration.

The above illustration considered the vibration environment in only one frequency increment. In practice, similar calculations would be required for all frequency increments covering the range of the data. The results in terms of the required test duration at maximum service levels may differ from one frequency increment to the next. This is clearly undesirable from the testing viewpoint. Hence, the levels in each frequency increment should be modified using Eq. (89) to produce the same required test duration for all frequencies. It follows that the resulting power spectrum for the test may not be similar to any of the power spectra for various phases of the predicted vibration environment. The power spectrum for the test will, in effect, represent a properly weighted composite for the varying power spectra of the vibration which occurs during the service life of the aircraft.

9.6 SELECTION OF TEST LEVEL PERCENTAGE POINTS

The levels specified for a vibration test should never be increased to exceed the maximum predicted service environment unless a corresponding reduction in test duration is made in accordance with Eq. (89). Specifically, no "safety factors" should be added to the test levels, as determined by the procedures suggested herein. Any "safety factor" needed to account for uncertainties in the environmental levels will have been included in the prediction procedure, as discussed in Section 8. The selection of a percentage point, α , for the predictions in effect establishes the desired degree of conservatism for the predictions and, hence, the resulting vibration test specification. The smaller the value of α , the greater the conservatism. An unresolved issue is the selection of an appropriate value for α .

In the past, the selection of percentage points for vibration predictions has been somewhat arbitrary. The percentage points recommended by various investigators [2], [5], [8], [33] have generally ranged from 1% to 5%, providing prediction limits which hopefully would exceed from 95% to 99% of the anticipated vibration levels in a given structural zone. Although percentage points in this range are intuitively reasonable, it would be desirable if the percentage point selection could be made on a more scientific basis. One method of approaching this problem is through the use of statistical decision theory ("cost" minimization procedures). Such a method is suggested in [46], and outlined below.

Consider an aircraft component which must be vibration tested as part of its qualification for service use. Assume there are only two possible test results; pass or fail. If the component passes the test,

there is a possibility that it will fail in service. The "cost" associated with this possibility is

$$C_a = C_0 P_F \quad (98)$$

where C_0 is the "cost" associated with a service failure, and P_F is the probability of a service failure. If the component fails the test, it must be redesigned to pass the test. The "cost" associated with this possibility is

$$C_f = C_1 \quad (99)$$

where C_1 is the anticipated "cost" of a redesign needed to pass the test. It follows that the total "cost" associated with the test is

$$C_t = P(L) C_a + [1 - P(L)] C_f = (C_0 P_F) P(L) - C_1 [1 - P(L)] \quad (100)$$

where $P(L)$ is the probability of passing the test at level L . Clearly, $P(L)$ is a function of the percentage point used to establish the test levels. The desired result is to select that value of α which will minimize the total "cost," C_t , in Eq. (100). From [46], a lower bound on the optimum value for α is given by the simple expression

$$\alpha = 1 - \left[1 - \frac{C_1}{C_0} \right]^{1/n} \quad (101)$$

where n is the total number of units for the component design in question to be manufactured and installed in service, and C_1/C_0 is assumed to be less than unity.

The deviation of Eq. (101) involves several assumptions which might be questionable in some cases, as discussed in [46]. Furthermore, the "cost" terms may be difficult to estimate in many if not all cases. Nevertheless, it is believed that the use of Eq. (101) with even rudimentary "cost" estimates provides a better basis for selecting a percentage point for vibration predictions than a simple intuitive guess. Note that the "cost" terms in Eq. (101) may be expressed in any units desired (dollars, relative importance, etc.). Also note that the "cost" terms appear as a ratio. This greatly simplifies the problem of estimating these terms, since absolute values are not required. For example, it might be unreasonable to estimate the "cost" of forcing a pilot to eject because of a service failure, or the "cost" of delaying a schedule for redesign because of a test failure. It may not be unreasonable, however, to estimate the relative importance of these two events.

To illustrate Eq. (101), assume a component is to be tested where the ratio of importance of a test failure to service failure is assessed to be 0.5. Further assume that 16 units are to be manufactured and installed for service use. The prediction limit used to derive the vibration test level should be

$$100(1 - \alpha)\% = 100 [1 - 0.5]^{1/16} = 95.7\%$$

If the ratio of importance had been 0.1, the test level would be

$$100(1 - \alpha)\% = 100 [1 - 0.1]^{1/16} = 99.3\%$$

Hence, as the anticipated "cost" of a service failure increases relative to the anticipated "cost" of a test failure, the required test level increases. If the ratio of importance had remained 0.5, but the number of units had been 64, the test level would be

$$100(1 - \alpha)\% = 100 [1 - 0.5]^{1/64} = 98.9\%$$

Hence, as the number of units to be manufactured and used in service increases, the required test level increases.

9.7 CONCLUDING COMMENTS ON VIBRATION TEST SPECIFICATIONS

The developments in Section 9 are presented only to provide some analytical guidelines which might be employed to develop improved procedures for the derivation of vibration test specifications. Many practical matters of considerable importance have been omitted in the developments for clarity and simplicity. For example, the endurance limit of structural materials and the nonlinear response properties of structural assemblies are ignored in the derivation of Figure 23. The fact that many types of failures may not be related to fatigue damage is also ignored. Furthermore, no consideration is given to the equipment loading

(structural impedance) problem. Finally, the suggested guidelines inherently assume that random vibration tests will be used to simulate the random portions of the environment, while sinusoidal tests will be used to simulate the periodic portions of the environment. In practice, the luxury of such simplifying assumptions may not be tolerable. Hence, a brief discussion of these matters is warranted.

9.7.1 Endurance Limit Problem

The endurance limit problem is often dealt with by assuming the service environment is limited to that duration necessary to deliver 5×10^6 stress cycles to the test item of interest. The theory behind this assumption is as follows [47], [48]. If a structural material is going to experience a fatigue failure, it will generally occur before 5×10^6 stress cycles have been accumulated. In other words, the break in the idealized S - N curve shown in Figure 21 usually occurs at about 5×10^6 cycles. Hence, if a fatigue damage criterion is to be used to trade off test levels against test durations, there is no need to consider the service duration to be longer than that time necessary to accumulate 5×10^6 stress cycles in the test item.

9.7.2 Structural Nonlinearity Problem

There is little question that the nonlinear properties of actual structures often tend to restrict the occurrence of extreme displacement values in the structural response [49]. This means that the trade-offs between test levels and test durations suggested in Figure 23, for either a fatigue damage or peak criterion, may deviate widely from the actual requirements. One suggested method for overcoming this problem is to perform all tests at the predicted environmental levels, and then limit the test duration solely on a basis of the 5×10^6 stress cycle rule [6].

9.7.3 Nonfatigue Failure Problem

Many types of aircraft component failures have little or no relation to fatigue damage [37]. It follows that vibration tests performed at elevated levels designed to simulate the service fatigue life may produce unrepresentative failures. This problem can be greatly reduced by separating the testing procedure into a "structural integrity" test and a "performance" test. The "structural integrity" test would be performed using elevated test levels to simulate the service fatigue damage with relatively short test durations. However, functional performance of the test component would not be expected or required during or after the test at elevated levels. A failure would be assessed solely on the basis of a structural failure of the component. Using a new sample component, the functional performance would then be evaluated by a second test performed at the predicted environmental levels with an arbitrary test duration. The theory here is that functional performance failures may be extremely sensitive to elevated test levels (in an unpredictable manner), but probably not very sensitive to exposure time.

9.7.4 Equipment Loading Problem

A major problem in the specification and performance of aircraft component vibration tests is the equipment loading problem. For the case of aircraft components which are relatively heavy compared to their supporting structure, there may be a significant difference between the vibration response of the unloaded structure and the vibration of the structure with the component attached. Vibration test specifications should always be based upon predictions for the structural vibration with the component of interest attached. The surface weight density term (w) in the random vibration prediction models suggested in Section 8 will partially account for the effect of component loading. The situation is further improved if the data used to arrive at the predictions are measured near equipment mounting points. Problems may still arise,

however, when heavy components with lightly damped resonances (sharply peaked impedance functions) are tested. The pooling operations used to arrive at the predictions tend to obscure the sharp notches in the structural response spectra induced by strong resonant reactions of heavy components mounted on low impedance structures [50]. A common method for dealing with this problem is to permit notching of the specified test levels at such frequencies. This may be done by permitting the vibration testing machine to react as permitted by its natural impedance function, by analytical corrections based upon mounting point impedance measurements for the supporting structure, or by specifying limits on the response of the component. See [51], [52] for further discussion of this problem.

9.7.5 Environmental Simulation Problem

As noted previously, the developments in Section 9 inherently assume that the random and periodic portions of the vibration environment will be simulated in test with random and sinusoidal excitations, respectively. At the present time, this procedure is not always employed. Specifically, random vibration tests are often omitted in the development of components for aircraft applications. Certainly an important reason for this must be the fact that MIL-STD-810B does not specify random vibration tests for aircraft components. It is strongly recommended that any future Military Standard Specification for the environmental testing of aircraft components include provisions for random vibration tests.

A second simulation problem evolves from the fact that periodic components in the environment (and sometimes the random components as well) are usually simulated in test by a "frequency sweep" type of

sinusoidal excitation, rather than by a series of steady state sine waves with fixed frequencies corresponding to the anticipated environmental frequencies. Frequency sweep sinusoidal testing introduces problems related to sweep rate and total sweep duration. Fortunately, these problems have been the subject of considerable past study, as summarized in [47], [48].

10. EXTENSIONS TO ACOUSTIC ENVIRONMENTS

The prediction of acoustic environments might be approached using the same general statistical procedures suggested for the prediction of vibration environments in Section 8. In at least two respects, the development of appropriate models is somewhat easier for the case of acoustic predictions. First, the spatial distribution of acoustic levels within a given structural compartment is considerably less dispersed than the distribution function for vibration levels over the structure. Second, because of high modal density and reverberation effects, the power spectra for random acoustic levels within a compartment are generally smoother in shape than the power spectra for the structural random vibration levels. In two other respects, however, the acoustic prediction problem is more difficult. First, the acoustic levels in a given aircraft compartment are heavily dependent upon the details of the compartment soundproofing materials and their installation. Second, a major portion of the acoustic environment is contributed by the airconditioning system, and is heavily dependent upon the details of the airconditioning system outlets.

In spite of the above noted problems, the possibility of developing an extrapolation type prediction procedure for internal acoustic noise in aircraft should be investigated. It is suggested that this effort be pursued using models of the form suggested for vibration environments in Section 8, with one exception. For the acoustic prediction problem, an additional constant term should be added to the various expressions in Eq. (63) to account for airconditioning noise. For example, the model for high speed flight should be

$$G(f)_{hs} = G(f)_{ac} + G(f)_{r2} + G(f)_{d3} \quad (102)$$

where

$G(f)_{ac}$ = A_0 regression coefficient to account for the contribution of airconditioning noise

$G(f)_{r2}$ = definition given by Eq. (67)

$G(f)_{d3}$ = definition given by Eq. (70)

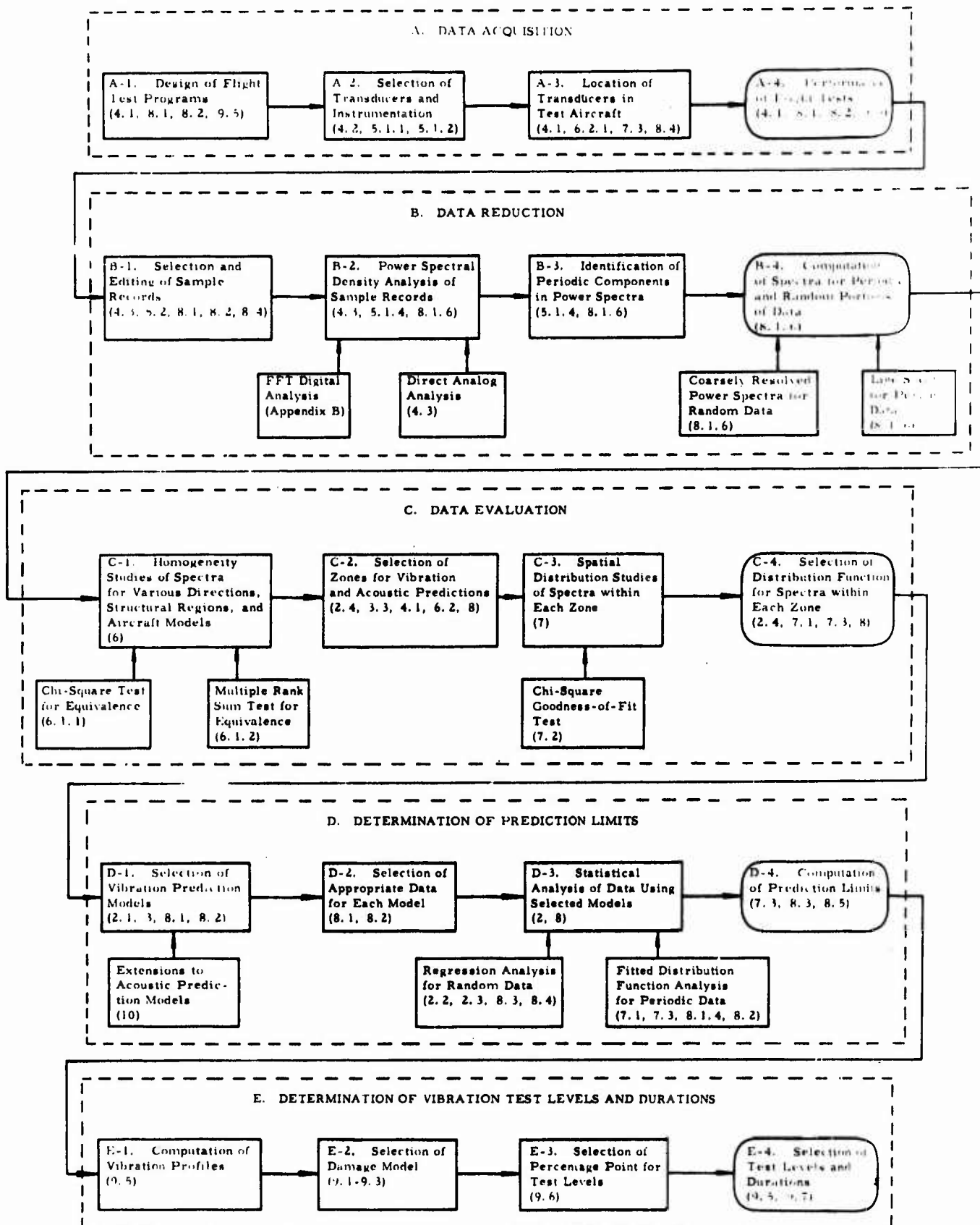


Figure 27. Flow Chart for Statistical Analysis of AFFDL Flight Vibration and Acoustic Data

11. CONCLUSIONS

The studies herein define a procedure for extrapolating data measured on previous aircraft to derive vibration and acoustic design criteria and vibration test specifications for future aircraft. The suggested procedure requires only rudimentary information concerning the future aircraft and its flight conditions. Hence, it may be used to establish preliminary specifications and/or criteria early in the conceptual design phase. The basic steps in the suggested procedure are outlined in Figure 27. Each step is identified with numbers corresponding to sections of this report which relate to the noted step.

The practicality of each suggested analysis technique in Figure 27 has been verified using currently available AFFDL vibration data. The current data, however, are not entirely adequate for all steps in the overall procedure. Further data acquisition and analysis in accordance with the techniques suggested herein will be required to fully implement the suggested procedure.

REFERENCES

1. Gray, C. L., and A. G. Piersol, "Methods for Applying Measured Data to Vibration and Acoustic Problems," AFFDL-TR-65-60, p. 32, Wright-Patterson AFB, Ohio, June 1965.
2. Condos, F. M., and W. L. Butler, "A Critical Analysis of Vibration Prediction Techniques," Proceedings of the Institute of Environmental Sciences, p. 321, 1963.
3. Barrett, R. E., "Techniques for Predicting Localized Vibration Environments of Rocket Vehicles," NASA TN D-1836, Marshall SFC, Huntsville, Alabama, October 1963.
4. Measurement Analysis Corporation, "Summary of Random Vibration Prediction Procedures," NASA CR- ____, Marshall SFC, Huntsville, Alabama, (to be published).
5. Mahaffey, P. T., and K. W. Smith, "Method for Predicting Environmental Vibration Levels in Jet-Powered Vehicles," Noise Control, Vol. 6, No. 4, July-August 1960.
6. Brust, J. M., and H. Himelblau, "Comparison of Predicted and Measured Vibration Environments for Skybolt Guidance Equipment," Shock and Vibration Bulletin No. 33, Part 3, p. 231, March 1964.
7. Eldred, K. M., Roberts, W. H., and R. White, "Structural Vibration in Space Vehicles," WADD TR 61-62, Wright-Patterson AFB, Ohio, December 1961.
8. Curtis, A. J., "A Statistical Approach to Prediction of the Aircraft Flight Environment," Shock and Vibration Bulletin No. 33, Part 1, February 1964.
9. Franken, P. A., "Sound Induced Vibrations of Cylindrical Vehicles," Journal of the Acoustical Society of America, Vol. 34, No. 4, p. 453, April 1962.
10. White, P. H., "Estimation of Structural Response to Aeroacoustic Loads," Paper No. 660721, SAE Aeronautic and Space Engineering and Manufacturing Meeting, Los Angeles, October 1966.
11. Franken, P. A., et al., "Methods of Flight Vehicle Noise Prediction," WADC TR 58-343, Wright-Patterson AFB, Ohio, November 1958.

12. Houbolt, J. C., et al., "Dynamic Response of Airplanes to Atmospheric Turbulence Including Flight Data on Input and Response," NASA TR R-199, LRC, Langley Station, Virginia, June 1964.
13. Thompson, W. T., Vibration Theory and Applications, p. 337, Prentice Hall, Inc., Englewood Cliffs, N. J., 1965.
14. von Gierke, H. E., "Types of Pressure Fields of Interest in Acoustical Fatigue Problems," University of Minnesota Conference on Acoustical Fatigue (Ed: W. J. Trapp and D. M. Forney), WADC TR 59-676, Wright-Patterson AFB, Ohio, March 1961.
15. Bies, D. A., "A Review of Flight and Wind Tunnel Measurements of Boundary Layer Pressure Fluctuations and Induced Structural Response," Bolt, Beranek and Newman Report No. 1269, January 1966.
16. Thomas, C. E., "Flight Vibration Survey of XC-123D Aircraft," ASD-TDR-62-235, Wright-Patterson AFB, Ohio, February 1962.
17. Thomas, C. E., "Flight Vibration Survey of C-130A Aircraft," ASD-TR-62-267, Wright-Patterson AFB, Ohio, March 1962.
18. Bolds, P. G., "Flight Vibration Survey of C-133 Aircraft," ASD-TDR-62-383, Wright-Patterson AFB, Ohio, April 1962.
19. Bolds, P. G., "Flight Vibration Survey of JRB-52B Aircraft," ASD-TR 61-507, Wright-Patterson AFB, Ohio, July 1961
20. Kennard, D. C., "Sonic Vibration as Exemplified by the RB-66B Airplane," WADC-TN-59-158, Wright-Patterson AFB, Ohio, May 1959.
21. Reich, H. K., "Flight Vibration Survey of B-58 Aircraft," ASD-TDR-62-384, Wright-Patterson AFB, Ohio, April 1962.
22. Thomas, C. E., "Flight Vibration Survey of F-100C-1 Aircraft," ASD-TN-61-61, Wright-Patterson AFB, Ohio, May 1961.
23. Thomas, C. E., "Flight Vibration Survey of F-101A Aircraft," ASD-TN-61-60, Wright-Patterson AFB, Ohio, May 1961.
24. Bolds, P. G., "Flight Vibration Survey of F-102A Aircraft," ASD-TDR-62-37, Wright-Patterson AFB, Ohio, January 1962.

25. Reich, H. K., "Flight Vibration Survey of F-106A Aircraft," ASD-TDR-62-504, Wright-Patterson AFB, Ohio, May 1962.
26. Wilkus, R. F., et al., "Vibration and Acoustic Measurements on the RF-4C Aircraft," AFFDL-FDDS-TM-65-53, Wright-Patterson AFB, Ohio, November 1965.
27. Thomas, C. E., "Flight Vibration Survey of H-37A Helicopter," WADD-TN-60-170, Wright-Patterson AFB, Ohio, June 1960.
28. Thomas, C. E., Holtz, E. R., and J. T. Ach, "In-Flight Acoustic and Vibration Data from UH-1F Helicopter," AFFDL-DDR-FDD-66-3, Wright-Patterson AFB, Ohio, July 1966.
29. Kennard, D. C., and C. E. Thomas, "Data Reduction Techniques for Flight Vibration Measurements," WADC TN 59-44, Wright-Patterson AFB, Ohio, February 1959.
30. Roberts, W. H., "Empirical Correlation of Flight Vehicle Vibration Response," Shock and Vibration Bulletin No. 37, Part 7, p. 77, January 1968.
31. Dreher, J. F., and W. D. Hinegardner, "RF-4C Vibration and Acoustic Environmental Study," Shock and Vibration Bulletin No. 37, Part 7 (Supplement), p. 95, January 1968.
32. Dunn, O. J., "Multiple Comparisons Using Rank Sums," Technometrics, Vol. 6, No. 3, p. 241, 1964.
33. Barrett, R. E., "Statistical Techniques for Describing Localized Vibration Environments of Rocket Vehicles," NASA D-2158, MSFC, Huntsville, Alabama, July 1964.
34. Bowker, A. H., and G. J. Lieberman, Engineering Statistics, p. 257, Prentice-Hall, Inc., Englewood Cliffs, N. J., 1959.
35. Bennett, C. A., and N. L. Franklin, Statistical Analysis in Chemistry and Chemical Industry, p. 429, John Wiley and Sons, Inc., New York, 1954.
36. Bowker, A. H., and G. J. Lieberman, op. cit., p. 224.
37. Eldred, K. M., Roberts, W. M., and R. White, op. cit., p. 394.
38. Crede, C. E., "Failures Resulting from Vibration," Ch. 5, p. 106, Random Vibration 2 (Ed. S. H. Crandall), The MIT Press, Cambridge, 1963.

39. Miner, M. A., "Cumulative Damage in Fatigue," Journal of Applied Mechanics, No. 12, p. 159, 1945.
40. Gray, C. L., "First Occurrence Probabilities for Extreme Random Vibration Amplitudes," Shock and Vibration Bulletin No. 35, Part IV, p. 99, 1966.
41. MacNeal, R. H., Barnoski, R. L., and J. A. Bailie, "Response of a Simple Oscillator to Nonstationary Random Noise," Journal of Spacecraft and Rockets, Vol. 3, No. 3, p. 441, 1966.
42. Mark, W. D., "On False-Alarm Probabilities of Filtered Noise," Proceedings of the IEEE, Vol. 54, No. 2, p. 316, 1966.
43. Crandall, S. H., and W. D. Mark, Random Vibration in Mechanical Systems, p. 62, Academic Press, New York, 1963.
44. Bendat, J. S., "Probability Functions for Random Processes: Prediction of Peaks, Fatigue Damage and Catastrophic Failures," NASA CR-33, Goddard SFC, Maryland, 1964.
45. Deneff, G. V., "Fatigue Prediction Study," WADD TR 61-153, Wright-Patterson AFB, Ohio, 1962.
46. Choi, S. C., and A. G. Piersol, "Selection of Test Levels for Space Vehicle Component Vibration Tests," Journal of the Electronics Division (ASQC), Vol. 4, No. 3, p. 3, July 1966.
47. Crede, C. E., Gertel, M., and R. D. Cavanaugh, "Establishing Vibration and Shock Tests for Airborne Electronic Equipment," WADC-TR-54-272, Wright-Patterson AFB, Ohio, June 1954.
48. Gertel, M., "Specification of Laboratory Tests," Ch. 24, Shock and Vibration Handbook (Ed. C. M. Harris and C. E. Crede), McGraw-Hill Book Co., Inc., New York, 1961.
49. Broch, J. T., "Random Vibration of Some Nonlinear Systems," Bruel & Kjaer Technical Review No. 3-1964, Naerum, Denmark.
50. Vigness, I., "Measurement of Equipment Vibrations in the Field as a Help for Determining Vibration Specifications," Shock and Vibration Bulletin No. 33, Part 3, p. 179, March 1964.
51. Piersol, A. G., "The Development of Vibration Test Specifications for Flight Vehicle Components," Journal of Sound and Vibration, Vol. 4, No. 1, p. 88, July 1966.
52. Curtis, A. J., and J. G. Herrera, "Random-Vibration Test Level Control Using Input and Test Item Response Spectra," Shock and Vibration Bulletin No. 37, Part 3, p. 47, January 1968.

UNCLASSIFIED

Security Classification

DOCUMENT CONTROL DATA - R&D		
<small>(Security classification of title, body of abstract and indexing annotation must be entered when the overall report is classified)</small>		
1. ORIGINATING ACTIVITY (Corporate author) Measurement Analysis Corporation 10960 Santa Monica Blvd. Los Angeles, California 90025		2a. REPORT SECURITY CLASSIFICATION UNCLASSIFIED
		2b. GROUP N/A
3. REPORT TITLE Statistical Analysis of AFFDL Flight Vibration and Acoustic Data		
4. DESCRIPTIVE NOTES (Type of report and inclusive dates) Final Report		
5. AUTHOR(S) (Last name, first name, initial) Piersol, Allan G. Van Der Laan, W. F.		
6. REPORT DATE June 1968	7a. TOTAL NO. OF PAGES 235	7b. NO. OF REFS 52
8a. CONTRACT OR GRANT NO. F33615-67-C-1118	9a. ORIGINATOR'S REPORT NUMBER(S) AFFDL-TR-68-	
b. PROJECT NO. 1472		
c. Task 147204		
d.	9b. OTHER REPORT NO(S) (Any other numbers that may be assigned this report) MAC Report No. 616-05	
10. AVAILABILITY/LIMITATION NOTICES This document is subject to special export control and each transmittal to foreign governments or foreign nationals may be made only with prior approval by AFFDL (FDD).		
11. SUPPLEMENTARY NOTES App. A - Tabulated Computer Results App. B - Documentation Report for Computer Program to Compute, etc.	12. SPONSORING MILITARY ACTIVITY Air Force Flight Dynamics Laboratory (FDDS) Wright-Patterson AFB, Ohio 45433	
13. ABSTRACT Techniques for predicting the vibration environments of future aircraft based upon statistical extrapolations from data measured on past aircraft are investigated. As a first step, principal sources of aircraft vibration are identified, and analytical relationships for the resulting vibration environment are approximated. Available AFFDL data are then summarized and evaluated. Extensive statistical studies are performed on the available data to investigate the average properties of aircraft vibration among the three orthogonal directions, various structural zones, various aircraft models, and various aircraft groups. The available data are also used to study the spatial distribution of vibration levels within a given structural zone. Specific prediction models are then suggested and regression analysis procedures to arrive at conservative prediction levels are detailed. The suggested techniques are illustrated using available AFFDL data. Procedures for deriving vibration test specifications based upon environmental vibration predictions are suggested. Finally, possible extension of the techniques to the prediction of internal acoustic noise are discussed. This abstract is subject to special export controls and each transmittal to foreign governments or foreign nationals may be made only with prior approval of the Air Force Flight Dynamics Laboratory, Wright-Patterson AFB, Ohio.		

DD FORM 1473
1 JAN 64UNCLASSIFIED
Security Classification

UNCLASSIFIED

Security Classification

14. KEY WORDS	LINK A		LINK B		LINK C	
	ROLE	WT	ROLE	WT	ROLE	WT
Statistical Analysis; random data; analysis of variance; power spectral density						

INSTRUCTIONS

1. **ORIGINATING ACTIVITY:** Enter the name and address of the contractor, subcontractor, grantee, Department of Defense activity or other organization (*corporate author*) issuing the report.
- 2a. **REPORT SECURITY CLASSIFICATION:** Enter the overall security classification of the report. Indicate whether "Restricted Data" is included. Marking is to be in accordance with appropriate security regulations.
- 2b. **GROUP:** Automatic downgrading is specified in DoD Directive 5200.10 and Armed Forces Industrial Manual. Enter the group number. Also, when applicable, show that optional markings have been used for Group 3 and Group 4 as authorized.
3. **REPORT TITLE:** Enter the complete report title in all capital letters. Titles in all cases should be unclassified. If a meaningful title cannot be selected without classification, show title classification in all capitals in parenthesis immediately following the title.
4. **DESCRIPTIVE NOTES:** If appropriate, enter the type of report, e.g., interim, progress, summary, annual, or final. Give the inclusive dates when a specific reporting period is covered.
5. **AUTHOR(S):** Enter the name(s) of author(s) as shown on or in the report. Enter last name, first name, middle initial. If military, show rank and branch of service. The name of the principal author is an absolute minimum requirement.
6. **REPORT DATE:** Enter the date of the report as day, month, year; or month, year. If more than one date appears on the report, use date of publication.
- 7a. **TOTAL NUMBER OF PAGES:** The total page count should follow normal pagination procedures, i.e., enter the number of pages containing information.
- 7b. **NUMBER OF REFERENCES:** Enter the total number of references cited in the report.
- 8a. **CONTRACT OR GRANT NUMBER:** If appropriate, enter the applicable number of the contract or grant under which the report was written.
- 8b, 8c, & 8d. **PROJECT NUMBER:** Enter the appropriate military department identification, such as project number, subproject number, system numbers, task number, etc.
- 9a. **ORIGINATOR'S REPORT NUMBER(S):** Enter the official report number by which the document will be identified and controlled by the originating activity. This number must be unique to this report.
- 9b. **OTHER REPORT NUMBER(S):** If the report has been assigned any other report numbers (*either by the originator or by the sponsor*), also enter this number(s).
10. **AVAILABILITY/LIMITATION NOTICES:** Enter any limitations on further dissemination of the report, other than those

imposed by security classification, using standard statements such as:

- (1) "Qualified requesters may obtain copies of this report from DDC."
- (2) "Foreign announcement and dissemination of this report by DDC is not authorized."
- (3) "U. S. Government agencies may obtain copies of this report directly from DDC. Other qualified DDC users shall request through _____."
- (4) "U. S. military agencies may obtain copies of this report directly from DDC. Other qualified users shall request through _____."
- (5) "All distribution of this report is controlled. Qualified DDC users shall request through _____."

If the report has been furnished to the Office of Technical Services, Department of Commerce, for sale to the public, indicate this fact and enter the price, if known.

11. **SUPPLEMENTARY NOTES:** Use for additional explanatory notes.
12. **SPONSORING MILITARY ACTIVITY:** Enter the name of the departmental project office or laboratory sponsoring (*paying for*) the research and development. Include address.
13. **ABSTRACT:** Enter an abstract giving a brief and factual summary of the document indicative of the report, even though it may also appear elsewhere in the body of the technical report. If additional space is required, a continuation sheet shall be attached.

It is highly desirable that the abstract of classified reports be unclassified. Each paragraph of the abstract shall end with an indication of the military security classification of the information in the paragraph, represented as (TS), (S), (C), or (U).

There is no limitation on the length of the abstract. However, the suggested length is from 150 to 225 words.

14. **KEY WORDS:** Key words are technically meaningful terms or short phrases that characterize a report and may be used as index entries for cataloging the report. Key words must be selected so that no security classification is required. Identifiers, such as equipment model designation, trade name, military project code name, geographic location, may be used as key words but will be followed by an indication of technical context. The assignment of links, rules, and weights is optional.

Security Classification